University of Glasgow

Speirs, Claire (2017) Examination of potential mechanisms linking AMPK to inhibition of IL-6 signalling. PhD thesis.

http://theses.gla.ac.uk/8185/

Copyright and moral rights for this work are retained by the author

A copy can be downloaded for personal non-commercial research or study, without prior permission or charge

This work cannot be reproduced or quoted extensively from without first obtaining permission in writing from the author

The content must not be changed in any way or sold commercially in any format or medium without the formal permission of the author

When referring to this work, full bibliographic details including the author, title, awarding institution and date of the thesis must be given

Enlighten:Theses
http://theses.gla.ac.uk/
theses@gla.ac.uk

Examination of potential mechanisms linking AMPK to inhibition of IL-6 signalling.

Claire Speirs (MRes)

Thesis submitted in fulfilment of the requirements for the Degree of Doctor of Philosophy

May 2017

School of Medical, Veterinary and Life Sciences
Institute of Cardiovascular and Medical Sciences
University of Glasgow

Supervisor: Professor T.M. Palmer
Co-supervisor: Dr I.P. Salt

Abstract

Considerable recent evidence supports the role of AMP-activated protein kinase (AMPK) as an anti-inflammatory mediator, yet the mechanisms of its anti-inflammatory actions are only starting to be unravelled. Inappropriate cytokine-stimulated Janus kinase (JAK)-signal transducer and activator of transcription (STAT) signalling is a key feature of many pro-inflammatory events, including atherogenesis. Previous unpublished studies in our group have investigated whether AMPK modifies cytokine stimulation of JAK-STAT signalling in HUVECs These preliminary investigations demonstrated that pre-treatment of HUVECs with AMPK activator, A769662, significantly inhibits both sIL-6Rα/IL-6 and IFN-α stimulation of STAT3 Tyr705 phosphorylation in HUVECs. IFN-α activates STATs via an IFNα/ß receptor 1 (IFNAR1/IFNAR2) complex which is distinct from the sIL-6Rα/IL-6/gp130 complex. The studies in this thesis therefore tested the hypothesis that AMPK was exerting its inhibitory effects at one or more common signalling loci downstream of IFNAR1/IFNAR2 and gp130 at a post-receptor level. First, it was investigated whether AMPK exerts its inhibitory effects on JAK-STAT signalling via a known regulator of JAK or STAT, or an AMPK downstream target known to either directly or indirectly impact on JAK-STAT signalling. A combination of genetic and pharmacological approaches was utilised to assess the role of each of the following AMPK targets: TC-PTP, SHP2, eNOS, PKCλ, SIRT1, CPT1 and mTOR. It was demonstrated that activation of AMPK in HUVECs inhibited sIL-6Rα/IL-6 stimulated STAT3 Tyr705 phosphorylation *via* a mechanism independent of TC-PTP, eNOS, PKC, SIRT1 and mTOR. Furthermore, inhibition of mTOR and eNOS reduced sIL-6Rα/IL-6 stimulated STAT3 Tyr705 phosphorylation, independent of AMPK activation by A769662. Next, it was investigated whether AMPK acts directly on a signalling component of the JAK-STAT pathway. Specifically, it was hypothesised that AMPK could directly phosphorylate serine or threonine residues within JAK to inhibit IL-6 signalling. siRNA-mediated downregulation of JAK isoforms demonstrated that IL-6 induced STAT3 Tyr705 phosphorylation predominantly via JAK1 in human umbilical vein endothelial cells (HUVECs). *In vitro* kinase assays of JAK1-derived peptides demonstrated that AMPK can directly phosphorylate two residues, Ser515 and Ser518, within the JAK1 SH2 domain. Subsequently, a GST-14-3-3 pull down assay of cell lysates produced from A769662 treated JAK1-defcient U4C cells transiently expressing either wild type or S515A/S518A double

mutant JAK1 demonstrated that pharmacological activation of AMPK promotes 14-3-3 binding of JAK1 via a mechanism requiring Ser515 and Ser518. Furthermore, mutation of Ser515 and Ser518 abolishes the ability of AMPK to inhibit JAK-STAT signalling by an IL-6 trans-signalling complex and from a constitutively active Val658Phe-mutated JAK1. In this study it is proposed that AMPK phosphorylation of JAK1 at Ser515 and Ser518 inhibits IL-6 stimulated JAK1 phosphorylating STAT3 by interfering with the ability of JAK1 to interact and phosphorylate the GP130 receptor and /or STAT3 and STAT1. Therefore, AMPK phosphorylation of JAK1 could potentially be a novel regulatory mechanism that could be developed as a therapy for treating chronic inflammatory diseases such as atherosclerosis.

Table of Contents

List of Tables

List of Figures

Acknowledgements

Thank you to my supervisor Professor Tim Palmer for his guidance and scientific expertise throughout this PhD project. Thank you to my co-supervisor Dr Ian Salt for his advice and supervision.

I would also like to extend a special thank you to Dr Claire Rutherford and my fellow PhD student Kirsten Munro for all their help and support in the lab, but most of all for your friendship.

Finally, I would like to thank my family. To my Mum, Dad, William, Christine, and Sam, thank you for your love, support and patience. Also, thank you to Christine and Stuart for having me as your house guest most weekends.

Funding for this project was provided by Diabetes UK.

Author's Declaration

I declare that this thesis has been written entirely by me and that all work has been performed by me unless otherwise stated. Furthermore, this work has not been previously submitted for any other degree.

Claire Speirs

May 2017

Abbreviations

ACC	Acetyl CoA carboxylase
ADP	Adenosine triphosphate
AICAR	5'-aminoimidazole-4-carboxamide ribonucleoside
AID	Autoinhibitory domain
ALL	Acute lymphoblastic leukaemia
AMBIC	Ammonium bicarbonate
AML	Acute myeloid leukaemia
AMP	Adenosine monophosphate
AMPK	AMP-activated protein kinase
Ang	Angiotensin
APS	Ammonium persulphate
ATP	Adenosine triphosphate
B-ALL	B-cell ALL
BCA	Bicinchoninic acid
BSA	Bovine serum albumin
C/EBP	CCAAT/enhancer-binding protein
CaMKK	Ca2+/calmodulin-dependent protein kinase kinase
CBM	Carbohydrate-binding module
CBP	CREB-binding protein
CBS	Cystathione-ß-synthase
CD	Circular dichroism
CHD	Coronary heart disease
CIS	Cytokine-inducible SH2-domain containing protein
COX	Cyclo-oxygenase
CPT1	Carnitine palmitoyl transferase 1
CRP	C-Reactive Protein
CTD	C-terminal domain
CVD	Cardiovascular disease
DAB	Diaminobenzidine
DAG	Diacylglycerol
DAMPs	Damage-associated molecular patterns
DMEM	Dulbecco's modified Eagle's medium
DMSO	Dimethyl sulphoxide

D-NAME	Nω-Nitro-D-arginine methyl ester hydrochloride
dNTP	Deoxyribonucleotide triphosphate
DTT	Dithiothreitol
E.coli	Escherichia coli
ECL	Enhanced chemiluminescence
ECM	Extracellular matrix
ECs	Endothelial cells
eNOS	Endothelial nitric oxide synthase
Epo	Erythropoeitin
ERK	Extracellular signal-regulated kinase
ET	Essential thrombocythemia
ET-1	Endothelin-1
FBS	Foetal bovine serum
FDA	Food and Drug Administration
FERM	band-4.1 protein, ezrin, radixin, and moesin
FOXO3	Forkhead box O3
GAPDH	Glyceraldehyde 3-phosphate dehydrogenase
G-CSFR	Granulocyte colony-stimulating factor receptor
GdnHCl	Guanidine hydrochloride
GEF	Guanine nucleotide exchange factor
GM-CSF	Granulocyte macrophage colony stimulating factor
gp130R	Glycoprotein 130 receptor
Grb2	Growth factor receptor-bound protein 2
GRO-α	Growth related oncogene-alpha
HAOECs	Human aortic endothelial cells
HASMCs	Human aortic smooth muscle cells
HEK	Human embryonic kidney
HepG2	Human hepatocellular carcinoma cell line
HRP	Horseradish peroxidase
HSCT	Haematopoietic stem cell transplant
HSVEC	Human saphenous vein endothelial cells
HUVEC	Human umbilical vein endothelial cell
ICAM-1	Intercellular adhesion molecule
IFNLR1	Interferon-λ receptor 1
IFNγ	Interferon gamma

IKK	IκB kinase
IL-	Interleukin-
iNOS	inducible NOS
IP	Immunoprecipitation
IPTG	Isopropyl b-D-thiogalactopyranoside
IRF	IFN regulatory factor
ISRE	IFN-α/ß–stimulated response element
IκBα	Inhibitor of κB
JAK	Janus Kinase
JH	JAK homology
JNK	c-Jun N-terminal kinase
KD	Kinase domain
KIR	Kinase inhibitory region
KO	Knock out
LB broth	Luria Bertani broth
LDL	Low-density lipoprotein
LKB1	Liver kinase B1
L-NAME	Nω-Nitro-L-arginine methyl ester hydrochloride
LPS	Lipopolysaccharide
MAPK	Mitogen activated protein kinase
MCP-1	Monocyte chemoattractant protein-1
M-CSF	Macrophage colony-stimulating factor
MEFs	Mouse embryonic fibroblasts
MEK	Mitogen activated protein kinase kinase
MKP-1	Mitogen-activated protein kinase phosphatase-1
MMPs	Matrix metalloproteinases
MPN	Myeloproliferative neoplasms
mTOR	Mammalian target of rapamycin
mTORC 1/2	Mammalian target of rapamycin complex 1/2
NAD^+	Nicotinamide adenine dinucleotide
NF-κB	Nuclear factor kappa B
ORF	Open reading frame
oxLDL	Oxidized LDL
PAGE	Polyacrylamide gel electrophoresis
PAMPs	Pathogen-associated molecular patterns

PBS	Phosphate buffered saline
PBST	PBS + Tween 20
PCR	Polymerase chain reaction
PIAS	Protein inhibitors of activated STAT
PKC	Protein kinase C
PMA	Phorbol 12-myristate 13-acetate
PMSF	Phenylmethylsulphonyl fluoride
PPRs	Pattern recognition receptors
PTP	Protein tyrosine phosphatase
PV	Polycythemia vera
RA	Rheumatoid arthritis
RIPA	Radioimmunoprecipitation assay
S6K	S6 kinase
SDS	Sodium dodecyl sulphate
SH2	Src homology 2
SHP	Small heterodimer partner
SHP2	SH2 domain-containing protein tyrosine phosphatase 2
sIL-6Rα	Soluble IL-6 receptor alpha
siRNA	Small interfering RNA
SIRT1	Sirtuin 1
SOCS	Suppressors of cytokine signalling
Sos	Son of sevenless
STAT	Signal transducer and activator of transcription
T2D	Type 2 diabetes
T-ALL	T-cell ALL
TBS	Tris-buffered saline
TBST	TBS + Tween 20
TC45	Nuclear 45 kDa form
TC48	Target 48 kDa form
TCA	Trichloroacetic acid
TC-PTP	T cell protein tyrosine phosphatase
TEMED	N, N, N’, N’-tetramethylenediamine
Th17	T helper type 17
TLR	Toll-like receptor
TNF-α	Tumour necrosis factor-α

Tregs	Regulatory T cells
TSC1/2	Tuberous sclerosis complex 1/2
UKDPS	United Kingdom Prospective Diabetes Study
VCAM-1	Vascular cell adhesion molecule
VEGF	Vascular endothelial growth factor
VSMCs	Vascular smooth muscle cells
WT	Wild type
ZMP	5’-aminoimidazole-4-carboxamide ribonucleoside monophosphate

Chapter 1 - Introduction

1.1 Inflammation

Inflammation is an essential immune response by the host that enables the removal of harmful stimuli as well as the healing of damaged tissue. Clinically, inflammation is characterised by heat, pain, swelling and redness, symptoms caused by increased blood flow to the affected area, leakage of fluid into tissues and the accumulation of activated leukocytes (Medzhitov, 2008). Inflammation is initiated on activation of the innate immune system by noxious stimuli and conditions, such as microbial infection and tissue injury. Innate immune cells residing in tissues, such as macrophages, mast cells, and dendritic cells, as well as circulating leukocytes, including monocytes and neutrophils, play important roles in inflammatory responses. In addition to immune cells, non-immune cells such as epithelial cells, endothelial cells and fibroblasts also contribute to inflammatory processes (Newton and Dixit, 2012). The innate immune cells immediately recognize pathogen invasion or cell damage with intracellular or surface-expressed pattern recognition receptors (PRRs) such as Toll-like receptors (TLR). These receptors detect, either directly or indirectly, pathogen-associated molecular patterns (PAMPs), such as microbial nucleic acids, lipoproteins, and carbohydrates, or damage-associated molecular patterns (DAMPs) released from injured cells (Newton and Dixit, 2012). Activated PRRs then initiate signalling cascades that triggers phagocytosis and induces changes in gene expression such as an increase in production of inflammatory cytokines (e.g. tumour necrosis factor (TNF), interleukin-1 (IL-1) and interleukin-6 (IL-6)), chemokines and vasoactive amines (Ahmed, 2011). These mediators rapidly accelerate the progression of inflammation through the modification of vascular endothelial permeability as well as the recruitment of neutrophils, lymphocytes and excess plasma (containing antibodies and complement factors) into the site of infection (Ahmed, 2011). The actions of activated innate immune cells and cytotoxic lymphocytes serve to remove pathogens and damaged tissues, clearing the way for healing and restoration of function. A successful acute inflammatory response results in the elimination of the infectious agents or injured cells followed by a resolution and repair phase (Medzhitov, 2008). The inflammatory response is normally terminated once the potential danger is eradicated. If inflammation progresses unresolved, the acute inflammation turns into a chronic stage. Whereas

acute inflammation is beneficial, chronic inflammation can result in undesirable effects and is critically involved in a variety of diseases such as atherosclerosis, rheumatoid arthritis, multiple sclerosis, and asthma (Ahmed, 2011).

1.2 Atherosclerosis

Atherosclerosis can be defined as a chronic inflammatory disease characterised by an inflammatory response of arterial wall to injuries promoted by risk factors such as dyslipidemia, diabetes, hypertension and systemic inflammation (Ross, 1999, Hadi et al., 2005). Atherosclerosis is the formation of lesions within the arterial intima due to the accumulation of lipids, macrophages, leukocytes and smooth muscle cells. Over time, these lesions may evolve to occlude the artery lumen or alternatively they may rupture, triggering thrombosis which is often followed by myocardial infarction or stroke (Langheinrich and Bohle, 2005, Glass and Witztum, 2001). Figure 1.1 outlines that formation of atherosclerotic plaque (Autieri, 2012). Endothelial dysfunction is generally accepted as the main predisposing factor towards atherosclerosis and is detected prior to the appearance of clinical symptoms (Anderson, 1999). Endothelial dysfunction is triggered in response to risk factors such as dyslipidemia, diabetes, hypertension and systemic inflammation (Hadi et al., 2005). Clinically, endothelial dysfunction is defined as impairment of endothelium dependent vasodilation but is also characterised by conversion of the endothelium to an “activated” phenotype associated with increased endothelial permeability, proliferation, leukocyte adhesion and production of pro-inflammatory cytokines (Davignon and Ganz, 2004, Anderson, 1999). Increased endothelial permeability, favours the migration of low density lipoprotein particles (LDL) through the vascular wall into the sub-endothelial intima. Trapped LDL is exposed to agents that trigger its conversion into modified forms like oxidized LDL (oxLDL). Oxidized LDL induces macrophage pro-inflammatory gene expression, including TNF-α, IL-1ß, and IL-6, to further exacerbate the endothelial dysfunctional phenotype (Malden et al., 1991, Tabas et al., 2007). Activated endothelial cells express on their luminal surface leukocyte adhesion molecules, such as E-selectin, vascular cell adhesion molecule (VCAM-1) and intercellular adhesion molecule (ICAM-1), which attracts leukocyte. Once leukocytes have attached, migration is stimulated by endothelial expressed chemokines and cytokines, such as monocyte chemoattractant protein-1 (MCP-1), macrophage colony-stimulating factor (M-CSF), IL-8 and TNF-α (Ross, 1999, Pober

and Sessa, 2007). Leukocytes adhere to the endothelial lumen and migrate through vascular wall to the sub-endothelial intima. In the arterial intima, monocytes can differentiate into macrophages under the influence of M-CSF or granulocyte-macrophage colony stimulating factor (GM-CSF). Macrophages express scavenger receptors that permit the uptake of oxLDL. Lipid loading of macrophages leads to the formation of foam cells, and ultimately leads to the mature lipid-laden macrophages of the plaque's core (Stephen et al., 2010). Also, T-lymphocytes infiltrate the atherosclerotic lesions. Activated T cells differentiate mainly into T-helper 1 cells and begin producing interferon-γ (IFN-γ), which in turn increases the process of antigen presentation by macrophages to lymphocytes and stimulates synthesis of other cytokines like TNF-α and IL-1. Growth factors and cytokines released by immune and vascular cells contribute to the formation of a fibrous cap of smooth muscle and extracellular matrix (ECM) around the lipid core, which compromises the vascular lumen (Ross, 1999, Hansson et al., 2002, Libby, 2002). Overall, atherosclerosis is not only the accumulation of fat in arterial walls but is also a complex process involving both innate and adaptive immune responses (Ross, 1999, Hansson et al., 2002).

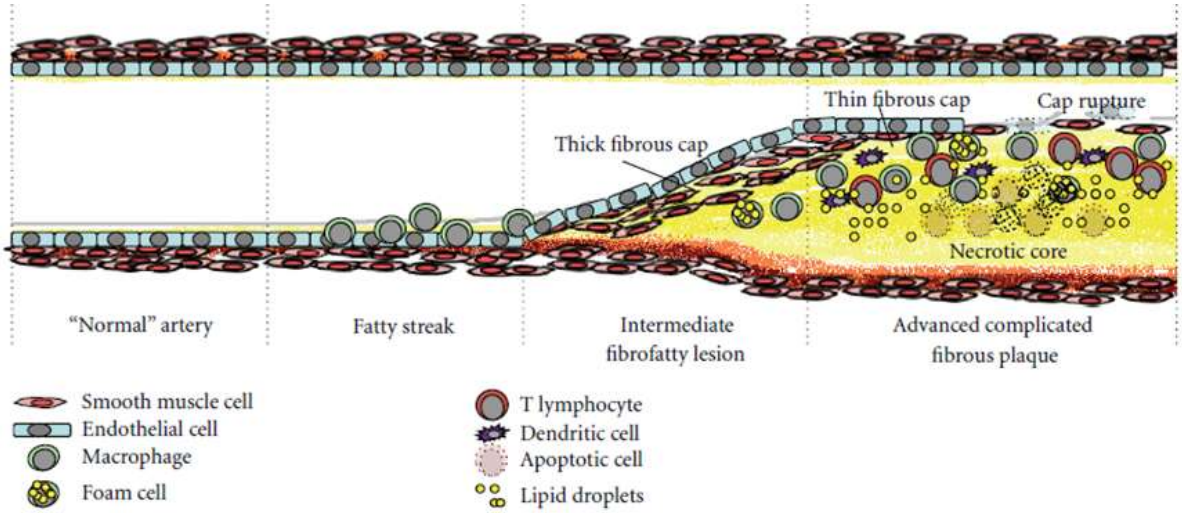

Figure 1.1: Formation of an atherosclerotic plaque.
Endothelial dysfunction is triggered in response to risk factors such as dyslipidemia, diabetes, hypertension and systemic inflammation. The endothelial monolayer becomes "leaky" allowing lipids to enter and accumulate within the intimal layer. Oxidised lipids promote the expression of leukocyte adhesion receptors and the production of chemokines by the now activated endothelial cells. Various inflammatory cells such as macrophages are recruited to this site promoting the inflammatory response and the formation of the atheromatous plaque. Smooth muscle cell migration from the media to the intima then contributes to fibrous cap formation and extracellular matrix around the lipid core. Over time, these lesions may evolve to occlude the artery lumen or alternatively vulnerable plaques, which are characterised by thin fibrous cap, rupture and may result in thrombus formation. (Figure taken from Autieri, 2012)

1.2.1 Pro-inflammatory cytokines in atherosclerosis: TNF-α, IL-1β and IL-6

The innate and adaptive immune responses in atherosclerosis are orchestrated by a range of cytokines, which regulate all stages of the disease: initiation, progression and destabilisation of atherosclerosis plaques (reviewed by Ramji and Davies, 2015). All of the major cellular constituents of plaques; macrophage/monocytes, endothelial cells (ECs), and vascular smooth muscle cell (VSMCs) are capable of producing and responding to cytokines, thus promoting a vicious cycle of pro-inflammatory signalling. Mounting evidence suggests that TNF-α, IL-1ß and IL-6 are pro-inflammatory cytokines mediating the key processes involved in atherosclerosis.

TNF-α plays a pivotal role in orchestrating the production of other pro-inflammatory cytokines, thus TNF-α is considered to be a "master regulator" of pro-inflammatory cytokine production (Maini et al., 1995). TNF-α is produced by macrophages, ECs and VSMCs of atherosclerotic arteries (Barath et al., 1990). TNF-α induces the expression of adhesion molecules ICAM-1 and VCAM-1, chemokine MCP-1 and enhances the production of cytokines such as IL-1ß, IL-8 and growth factors in a variety of cell types including lymphocytes, macrophage, ECs, and VSMCs (Bevilacqua et al., 1987, Osborn et al., 1989, Rollins et al., 1990, Libby et al., 1986) TNF-α stimulates leukocyte adhesion to endothelial cells and chemotaxis (Bevilacqua et al., 1987, Osborn et al., 1989, Ming et al., 1987). TNF-α is found in human atherosclerotic plaque and serum TNF-α levels correlate with atherosclerotic plaque burden (Skoog et al., 2002). In the atherosclerotic plaque, secretion of matrix metalloproteinases (MMPs) degrade various components of the ECM leading to instability of the plaque and rupture. Crucially, TNFα is associated with plaque rupture as it stimulates the production of several MMPs and its levels are increased in human atherosclerotic plaques (Galis et al., 1995). TNF-α deficient atherosclerosis prone mice have significantly reduced atherosclerotic lesions compared with WT atherosclerosis prone mice, which was associated with decreased expression of ICAM-1, VCAM-1, and MCP-1 (Ohta et al., 2005).

IL-1ß is produced by all the major cellular constituents of plaques; macrophage/monocytes, ECs, and VSMCs. IL-1ß also induces the expression of cytokines, adhesion molecules, and is mitogenic for VSMCs and ECs (Suzuki et al., 1989). IL-1ß –treatment of endothelial monolayers increased the adhesion of

leukocytes (Bevilacqua et al., 1985). IL-1ß is present in human atherosclerotic plaques (Frostegård et al., 1999). IL-1ß deficiency induced an approximately 30% reduction in lesions in atherosclerosis prone mice, which was associated with significantly reduced mRNA levels of VCAM1 and MCP-1(Kirii et al., 2003).

TNF-α and IL-1ß trigger pro-inflammatory effects via simultaneous activation of the canonical NF-κB (nuclear factor kappa B) pathway and MAPK (mitogen activated protein kinase) intracellular signalling cascades. Briefly, TNF-α or IL-1ß binding its cognate receptor stimulates an increase in IκB kinase (IKK) activity, which in turn phosphorylates inhibitor of κB (IκBα). Under basal conditions, IκBα is bound to the transcription factor NF-κB in the cytoplasm; however upon phosphorylation by IKK, NF-κB is released and translocates to the nucleus and initiates transcription of the target genes including cell adhesion molecules, chemokines and cytokines (Pamukcu et al., 2011). The MAPK pathway is activated in parallel following cytokine stimulation, leading to the phosphorylation and activation of c-Jun N-terminal kinase (JNK), extracellular signal-regulated kinase (ERK) and p38 MAPK. Active MAPKs can translocate to the nucleus, thereby influencing transcription by phosphorylation of transcription factors such as c-Jun, c-fos and ATF-2 (Plotnikov et al., 2011). Studies have shown that the pathways involving MAPKs regulate the proliferation and differentiation of VSMCs (ERK 1/2), expression of ECM protein in VSMCs (JNK), expression of chemokines and cytokines (p38) in ECs and macrophage foam cell formation (ERK/JNK/p38) (Muslin, 2008).

The focus of this thesis is on the IL-6/Janus kinase (JAK)-signal transducer and activator of transcription (STAT) signalling pathway. Therefore, the IL-6/JAK-STAT pathway and its role in atherosclerosis are described in detail below.

1.3 The JAK-STAT pathway

1.3.1.1 Classic IL-6 signalling vs IL-6 trans-signalling

IL-6 is a pleiotropic cytokine produced by various cell types including fibroblasts, ECs, VSMCs and immune cells such as monocytes and T-cells (Schaper and Rose-John, 2015). IL-6 can interact with either a membrane bound IL-6 receptor (IL-6Rα) or a soluble IL-6 receptor-α (sIL-6Rα), that then associates with the membrane glycoprotein 130 (gp130) receptor to initiate the JAK-STAT pathway.

gp130 is expressed ubiquitously whereas membrane bound IL-6Rα is limited to the cell surface of a few cell types including hepatocytes, monocytes, neutrophils and B-cells (Rose-John, 2012). These cells are able to respond to circulating IL-6 in what is known as classical IL-6 signalling. The sIL-6Rα is thought to be synthesised following either alternative splicing of IL6Rα mRNA or matrix metalloprotease (ADAM17 or ADAM10) shedding of a sIL-6Rα from the cell surface of IL6Rα expressing hepatocytes and monocytes (Muller-Newen et al., 1996, Mullberg et al.,1993 Matthews et al., 2003, Lust et al.,1992). The sIL-6R can bind to free IL-6 in the circulation to form a sIL-6Rα/IL-6 complex. The sIL-6R/IL-6 complex can then the interact with gp130 on cells which do not express IL-6Rα to initiate cell signalling pathways, this process is called trans-signalling. This has been demonstrated in studies using human umbilical vein endothelial cells (HUVECs) where IL-6 alone did not elicit a response, while the sIL-6Rα/IL-6 complex induced the production MCP-1 (Romano et al., 1997). Interestingly, a review of the involvement of both signalling modes in the biology of IL-6 by Scheller et al revealed that anti-inflammatory and regenerative responses are mediated by IL-6 classical signalling whereas pro-inflammatory responses of IL-6 are mediated by trans-signalling (Scheller et al., 2011).

1.3.2 IL-6 mediated JAK-STAT signalling

The gp130 signalling receptor lacks intrinsic kinase activity but is constitutively associated with JAK family tyrosine kinases. Binding of IL-6 to IL-6Rα induces dimerisation of the gp130 subunit leading to manoeuvring of receptor-associated JAKs into positions to facilitate their trans-phosphorylation and corresponding activation (Murakami et al., 1993). Subsequently, activated JAKs mediate phosphorylation of key tyrosine residues within the cytoplasmic regions of the receptor that provide docking sites for the Src homology 2 (SH2) domains of STATs, a family of latent cytoplasmic transcription factors. After docking, STATs are phosphorylated by activated JAKs, which enables them to dimerise and translocate to the nucleus where they bind to specific DNA elements, and regulate the transcription of thousands of genes (Rawlings et al., 2004, O'Shea et al., 2002, Kisseleva et al., 2002) (Figure 1.2). Studies using mutant cell lines deficient in JAK1, JAK2 or TYK2 have revealed that IL-6-mediated signalling absolutely depends on the presence of JAK1 whereas JAK2 and TYK2 are dispensable (Guschin et al., 1995). JAK1-mediated phosphorylation of gp130 at Tyr767, Tyr814, Tyr905

and Tyr915 at a pYXXQ consensus sequence enables binding of STAT3 which competes with STAT1 binding at Tyr905 and Tyr915 at a more constrained pYXLQ consensus sequence (Stahl et al., 1995, Gerhartz et al., 1996, Schmitz et al., 2000, Heinrich et al., 2003). This could account for the more potent activation and dimer formation of transcriptionally active STAT3 compared to STAT1. STATs are phosphorylated by JAKs on a single tyrosine residue: Tyr701 in STAT1 and Tyr705 in STAT3 (Shuai et al., 1994, Kaptein et al., 1996).

STATs are not the only proteins that are recruited to the activated IL-6 receptor. The SHP2 (SH2 domain-containing phosphatase 2) binds to pTyr759 on gp130 and is phosphorylated by JAK1 (Schaper et al., 1998). Activated SHP2 can then induce ERK mediated gene transcription via the recruitment of Grb2 (growth factor receptor bound protein 2) which is bound to Sos (son of sevenless). Sos serves as a guanine nucleotide exchange factor (GEF) for the Ras protein and therefore activates Ras by generating Ras-GTP. Subsequently the ERK1/2-MAPK pathway is activated, driving the expression of genes involved in proliferation, differentiation and development (Mihara et al., 2012).

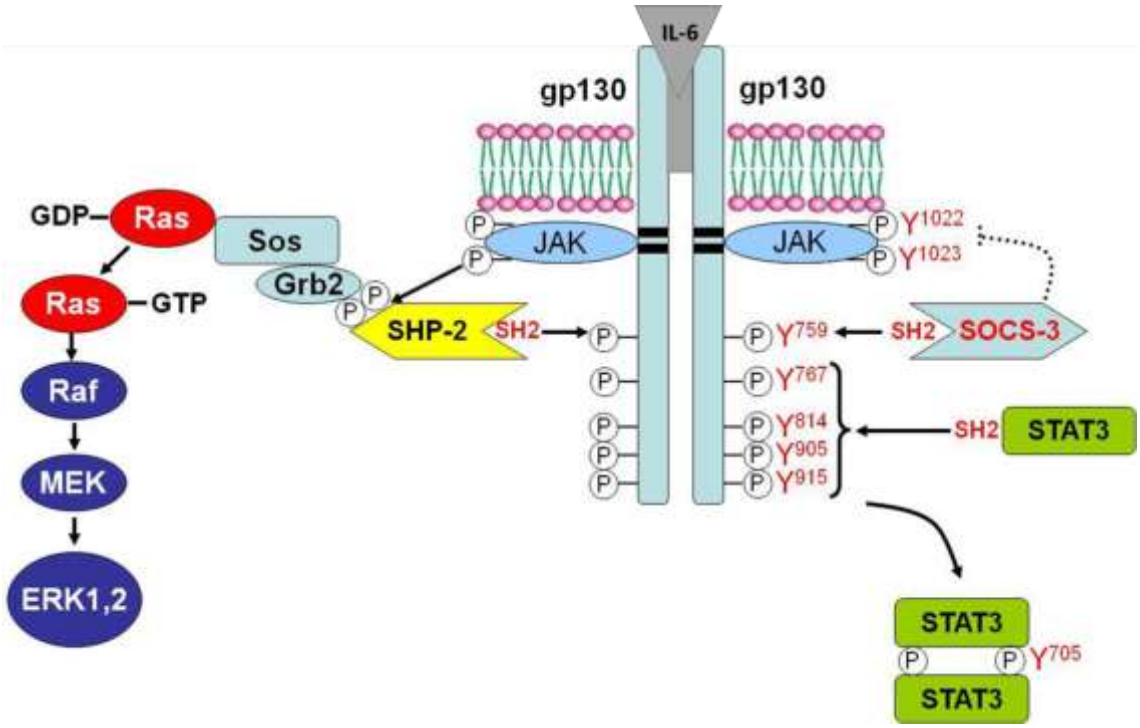

Figure 1.2: Activation of the JAK/STAT pathway by IL-6
IL-6 activates the gp130 receptor subunits, initiating their dimerization and activation (trans-autophosphorylation) of receptor associated JAK proteins. Activated JAKs phosphorylate tyrosine residues on the gp130 subunits which function as docking sites for SH2-containing proteins. STAT3 binds, is phosphorylated by JAK which induces dimer formation. SHP-2 is also phosphorylated by JAKs and initiates the Ras/Raf/MEK signalling pathway, activating ERK1/2. STAT3 dimers and ERK1/2 translocate to the nucleus where they stimulate the transcription of genes. SOCS3 may compete with SHP-2 for pY759 on the gp130R and so inhibits activation of the Ras-ERK1/2 pathway by SHP-2. (Figure taken from Rutherford et al., 2012.)

1.3.3 JAK

The JAK family consists of four mammalian members, JAK1 JAK2, JAK3 and TYK2. JAK1, JAK2 and Tyk2 are ubiquitously expressed while JAK3 is expressed predominantly in myeloid and lymphoid cells (Verbsky et al., 1996, Kisseleva et al., 2002). JAKs are relatively large kinases with a molecular weight of 130 kDa (Ihle et al., 1994). The JAK structure is characterized by the presence of seven conserved JAK homology (JH) domains. The kinase JH1 domain is at the C-terminus of JAKs, preceded by the pseudokinase JH2 domain. The N-terminal half of JAKs contains the FERM (FERM standing for: band-4.1 protein, ezrin, radixin, and moesin) domain, followed by the SH2 domain (Yamaoka et al., 2004). The unavailability of a crystal structure of a full-length JAK molecule limits our understanding on the functional roles of these domains. However biochemical and mutational studies coupled with some solved crystal structures of JAK fragments have started to unravel the basic functional roles of these domains. The kinase JH1 domain is a typical eukaryotic tyrosine kinase domain. Mutational analysis identified that the activation loop contains a conserved double tyrosine motif which is phosphorylated in response to cytokine stimulation: Y1022/Y1023 in JAK1, Y1007/Y1008 in JAK2, Y980/Y981 in JAK3 and Y1054/Y1055 in TYK2 (Liu et al., 1997, Feng et al., 1997, Leonard and O'Shea, 1998). The pseudokinase JH2 domain has been shown to play a regulatory role by suppressing kinase activity via inhibitory interactions with the C-terminal kinase JH1 domain (Lupardus et al., 2014, Shan et al., 2014, Tom et al., 2013, Ungureanu et al., 2011). Mutational analysis has indicated that the JAK SH2 domain does not function as a binding site for phosphorylated tyrosine residues, but instead interacts with the FERM domain to stabilise its conformation (Radtke et al., 2005, Haan et al., 2001). The N-terminal FERM domain binds to the cytoplasmic region of cytokine receptors and may also regulate kinase activity (Girault et al., 1998, Haan et al., 2001, Haan et al., 2008, Hilkens et al., 2001, Zhao et al., 2010). The cytoplasmic domains of the cytokine receptors contain "box1" and "box2" motifs which are required for JAK engagement. Box1 is a membrane proximal proline-rich motif while box2 consists of a single negatively-charged residue followed by several hydrophobic residues (Murakami et al., 1991, Pelletier et al., 2006, Lebrun et al., 1995, Yan et al., 1996, Tanner et al., 1995, Usacheva et al., 2002, Royer et al., 2005, Haan et al., 2002). Receptor ligation triggers a conformational change in receptor complex that brings

associated JAKs into close proximity, permitting auto-phosphorylation (Remy et al., 1999).

1.3.4 STAT

In mammalian cells seven STAT proteins exist: STAT1, 2, 3, 4, 5a, 5b and 6 (Kisseleva et al., 2002). They are ubiquitously expressed with the exception of STAT4 which is mainly found in the testis, thymus and spleen (Zhong et al., 1994). Each STAT has seven structurally and functionally conserved domains: N-terminal, coiled-coil, DNA binding, linker, SH2 and a C-terminal transcriptional activation domain (Becker et al., 1998, Chen et al., 1998, Vinkemeier et al., 1998). The STAT SH2 domain is highly conserved and is important for specific contacts with the activated receptor and the formation of STAT dimers (Greenlund et al., 1994, Heim et al., 1995, Stahl et al., 1995, Shuai et al., 1994). The sequence surrounding the receptor phosphotyrosine site specifies which STAT is recruited and activated (Stahl et al., 1995). For example, STAT3 will bind to phospho (p)YXXQ while STAT1 will only bind to pYXPQ (Stahl et al., 1995, Heim et al., 1995, Gerhartz et al., 1996). Upon cytokine stimulation, STATs are recruited to the activated cytokine receptor via their SH2 domain, where by being in close proximity of the receptor associated JAK can then be phosphorylated by JAK, leading to the STATs forming an active dimer by reciprocal SH2 phosphotyrosine interaction, which then disengages from the receptor and translocate to the nucleus (Shuai et al., 1992, Schindler et al., 1992a, Schindler et al., 1992b). STATs are phosphorylated by JAKs on a single tyrosine residue at the C-terminus end of the SH2 domain (Tyr701 in STAT1 (Shuai et al., 1994) and Tyr705 in STAT3 (Kaptein et al., 1996). STAT dimers translocate to the nucleus and bind DNA motifs known as GAS (γ-activated sequence) elements that are characterized by the consensus sequence, TTNCNNNAA. IFN-α/ß induces the formation of a heterotrimeric complex consisting of STAT1, STAT2, and IFN regulatory factor (IRF) 9 that binds to the IFN-α/ß–stimulated response element (ISRE) ($AGTTN_3TTTC$) (O'Shea et al., 2002). The STAT transcriptional activation domain is proposed to participate in modulation of transcription through interaction with additional transcription factors and co-activators such as c-Jun, BRCA1 and the cAMP-response-element-binding (CREB)-binding protein (CBP)/p300 family of histone acetyltransferases (Horvath, 2000).

In addition to canonical tyrosine phosphorylation, serine phosphorylation and acetylation has recently emerged as covalent modifications regulating STAT functions. All STATs except STAT2 are phosphorylated on at least one serine residue in their C-terminal transactivation domain: Ser727 in STAT 1 and 3, Ser721 in STAT4, Ser725 in STAT5a, Ser730 in STAT5b, Ser756 in STAT6 (Decker and Kovarik, 2000). Reporter gene studies have determined that serine phosphorylation enhances transcriptional activity of STAT1 and STAT3 (Kovarik et al., 2001). Consistent with this, mice expressing a STAT1 S727A mutant exhibit defective IFN-γ-mediated innate immunity (Varinou et al., 2003). Several serine kinases have been reported to phosphorylate STATs, for example MAPK (STATs 1, 3, 4), PKC-δ (STATs 1, 3), mTOR (STAT3) (Kojima et al., 2005). Reversible lysine acetylation has been reported for all STATs with the exception of STAT4 (reviewed by Zhuang, 2013). STAT3 is acetylated by its coactivator p300/CBP, resulting in increased DNA binding and transcriptional activity (Wang et al., 2005). Several reports have demonstrated that acetylation is required for phosphorylation of STATs, including STAT3, however acetylation has been suggested to facilitate dephosphorylation and latency of STAT1 (Kramer et al., 2009, Zhaung, 2013).

1.3.5 Negative regulation of the JAK-STAT pathway

JAK-STAT signalling is central to many biological processes and so a number of regulatory mechanisms exist to modulate the pathway at different stages. Two major mechanisms for negative regulation are dephosphorylation by protein tyrosine phosphatases (PTP) and direct inhibition by suppressors of cytokine signalling (SOCS).

1.3.5.1 Suppressors of cytokine signalling

The SOCS family members were initially discovered on the basis of their ability to bind JAK (Endo et al., 1997) and inhibit cytokine signalling (Naka et al., 1997, Starr et al., 1997). The expression of the majority of SOCS proteins is induced by activation of the JAK-STAT pathway by cytokines such as IL-6, IFN-γ, G-CSF and IL-11. They act as classical negative feedback inhibitors by inhibiting the phosphorylation of JAKs, which in turn prevents STAT activation (Chen et al., 2004). There are eight family members, SOCS1–7 and cytokine-inducible SH2-containing protein (CIS) (Starr et al., 1997, Hilton et al., 1998). All members of

the SOCS family consist of an N-terminal domain, a central SH2 domain and a C-terminal SOCS box. The majority of the SOCS family inhibit cytokine signalling by inducing the proteasome-dependent degradation of JAK-associated cytokine receptors once they are activated. The SOCS box domain interacts with elongins B and C, recruiting Cullin5, and RING-box2 to form an E3 ubiquitin ligase complex (Babon et al., 2009). The SOCS proteins therefore function as adaptors to bring the E3 ligase into proximity with its substrate, promoting the ubiquitination and subsequent proteasomal degradation of SOCS binding partners (Kamura et al., 1998, Zhang et al., 2001). In addition to their role as E3 ligases, SOCS1 and SOC3 can inhibit JAK catalytic activity via its N-terminal kinase inhibitory region (KIR), a trait peculiar to SOCS1 and SOCS3 (Sasaki et al., 1999). Kershaw et al., demonstrated that the KIR of SOCS3 sits in the substrate binding groove of the JAK kinase. This partially occludes the substrate-binding site and prevents JAK from interacting with substrates, thus inhibiting its ability to initiate downstream signalling (Kershaw et al., 2013). A crystal structure of the SOCS3-JAK2-gp130 complex demonstrated that while the SOCS3 KIR occupied the JAK substrate binding domain, the SOCS3 SH2 domain was occupied by a phosphorylated tyrosine receptor residue, thus SOCS3 binds JAK and receptor simultaneously (Kershaw et al., 2013). SOCS3 can inhibit JAK1, JAK2 and TYK2 via its KIR, but not JAK3 (Babon et al., 2012). Genetic studies have revealed that SOCS1 is particularly important in IFN-γ signalling while SOCS3 has specificity for IL-6 signalling. (Croker et al., 2003, Lang et al.,2003). SOCS3 binds to the phospho-tyrosine motif 759 within gp130 to inhibit IL-6 signalling (Schmitz et al., 2000, Nicholson et al., 2000).

1.3.5.2 Protein tyrosine phosphatases

Since tyrosine phosphorylation by kinases is a key event in the JAK-STAT signalling pathway, dephosphorylation by PTP are involved in attenuating signalling. Several PTPs have been implicated in the regulation of JAK-STAT signalling; SH2 domain-containing phosphatase (SHP) 1, SHP2, PTP 1B, T-cell PTP (TC-PTP) and CD45 (reviewed by Xu and Qu, 2008).

TC-PTP is ubiquitously expressed with the highest expression mainly in haematopoietic cells (Neel and Tonks, 1997). Phosphorylation of JAK1, STAT1 and STAT3 is enhanced in TC-PTP knockout cells (Yamamoto et al., 2002, ten Hoeve et al., 2002, Simoncic et al., 2002). TC-PTP exists as two splice variants: an

endoplasmic reticulum target 48 kDa form (TC48) and a nuclear 45 kDa form (TC45). Overexpression of TC45 in 293T cells was reported to suppress IL-6-stimulated STAT3 phosphorylation (Yamamoto et al., 2002). Furthermore, JAK1, STAT1, and STAT3 were identified as direct substrates of TC-PTP as they each co-immunoprecipitate with TC-PTP substrate trapping mutant, which is inactive but still binds to cognate substrates (Simoncic et al., 2002, Garton et al., 1996, Yamamoto et al., 2002).

SHP1 and SHP2 are phosphatases that both consist of a C-terminal phosphatase and two N-terminal SH2 domains. SHP1 is a non-transmembrane phosphatase primarily expressed by haematopoietic cells and genetic knockout mice display a range of haematopoietic abnormalities. SHP1 can directly interact with receptors for erythropoietin (Epo) and IFN-α to inhibit phosphorylation of JAK1 and JAK2 (Klingmuller et al., 1995, David et al., 1995). SHP1 can also interact with the IL-3 receptor, expression of a negative SHP-1 variant (R459M) BaF/3 cells reduced IL-3 induced tyrosine phosphorylation of STAT5 and cell proliferation (Bone et al., 1997, Paling and Welham, 2002).

In contrast with SHP1, SHP2 is ubiquitously expressed. SHP2 negatively regulates cytokine stimulation of JAK-STAT signalling, but also positively regulates IL-6 stimulation of ERK signalling (Schaper et al., 1998). SHP2 is rapidly recruited to Tyr759 in gp130 following IL-6 stimulation (Stahl et al., 1995). Disruption of SHP2 recruitment, by the substitution of Tyr757 in gp130 with phenylalanine, was shown to enhance JAK-STAT signalling but reduce ERK activation (Stahl et al., 1995, Schaper et al., 1998). In addition, IL-6 treatment of mouse fibroblasts expressing a truncated SHP2 mutant (SHP2-/-), which is unable to bind the receptors including gp130, was shown to potentiate STAT3 activation in comparison to WT fibroblasts. SHP2 also acts as a negative regulator of IFN-induced STAT activation. Treatment of SHP2-/- fibroblasts with IFN-α or IFN-γ resulted in increased phosphorylation of STAT1 and STAT2 activity, and were hypersensitive to the cytotoxic effect of both IFN-α or IFN-γ. Reintroduction of wild type SHP2 protein reversed the hypersensitivity of SHP2-/- fibroblasts to the cytotoxic effect of IFN-alpha and IFN-gamma. (You et al, 1999). Furthermore, SHP2 has been described as a dual-specificity phosphatase that dephosphorylates STAT1 at both Tyr701 and Ser727 (Wu et al., 2002).

1.3.6 Role of IL-6 and JAK-STAT signalling in atherosclerosis

1.3.6.1 Role of IL-6 in atherosclerosis

In the context of atherosclerosis, the pro-inflammatory role of IL-6 has been the most extensively studied due to substantial evidence indicating its involvement in the disease process. Studies have shown that elevated levels of IL-6 and one of its target gene products, C-reactive protein (CRP), are associated with the increased risk of cardiovascular disease (CVD) and events such as myocardial infarction (Tzoulaki et al., 2005, Ridker et al., 2000). Furthermore, both IL-6 and CRP have been detected in human atherosclerotic plaques (Torzewski et al., 2000, Schieffer et al., 2000). Importantly, human genetic studies have suggested a causal association between IL-6 receptor signalling and cardiovascular disease, and IL-6 receptor blockade is a possible therapeutic approach in these patients (Collaboration, 2012, IL6R MR, 2012). Administration of exogenous IL-6 leads to plaque development in atherosclerosis prone mice (Huber et al., 1999). Conversely, selective pharmacological inhibition of IL-6 trans-signalling reduced the development and progression of plaques in atherosclerosis prone mice, and was associated with reduced expression of adhesion molecules, ICAM-1 and VCAM-1, and consequently reduced macrophage infiltration into the vascular lesions (Schuett et al., 2012). Several *in vitro* studies have linked IL-6 stimulation of ECs and VSMCs with key mediators of atherosclerosis. In the presence of IL-6 trans-signalling complex, sIL-6Rα/IL-6, endothelial cells have been shown to produce the adhesion molecules VCAM-1, ICAM-1 and E-selectin and release the chemokines MCP-1 and IL-8 (Modur et al., 1997, Romano et al., 1997). In VSMCs, upregulation of ICAM1 and MCP-1 was also observed in the presence of a sIL-6Rα/IL-6 (Klouche et al., 1999).

1.3.6.2 Role of STAT1 and STAT3 in atherosclerosis

In the vasculature, a wide range of stimuli including cytokines and growth factors activate STAT1 and STAT3 in ECs and VSMCs. While STAT1 and STAT3 are both activated by IL-6, STAT3 is preferentially activated (Darnell et al., 1994). Leukocyte recruitment, neointima formation, and plaque angiogenesis, are key processes involved in the initiation, progression and destabilisation of atherosclerosis plaques. Several *in vitro* studies have linked activation of STAT1 and STAT3 in ECs and VSMCs with key mediators of these processes. In ECs, STAT1

and STAT3 phosphorylation up-regulates the expression of MCP-1 and ICAM-1 (Lee et al., 2003, Sikorski et al., 2011, Chatterjee et al., 2009, Jougasaki et al., 2010). STAT3 activation in endothelial cells promoted the induction of neutrophil recruitment factors; growth related oncogene-alpha (GRO-α), GM-CSF and IL-8 (Yuan et al., 2015). Endothelin-1 (ET-1), is a potent endothelium-derived vasoconstrictor, and is controlled by STAT1 activation in endothelial cells (Manea et al., 2010). Proliferation, migration and survival of VSMCs play a pivotal role in the development of neointima formation that occurs during atherosclerosis (Ross, 1999). In VSMCs, the up-regulation of expression of the proliferative gene cyclin D1 and anti-apoptotic gene surviving have been shown to be dependent on STAT3 activation (Daniel et al., 2012). STAT1 and STAT3 also upregulate expression of MCP-1 and RANTES in VSMCs (Potula et al., 2009, Kovacic et al., 2010 Singh et al., 2011). These chemokines not only cause leukocyte infiltration, but also promote the migration of VSMCs from the media to the intima where they proliferate and deposit ECM components, thereby contributing to atherosclerotic lesion formation (Ross, 1999). In ECs, STAT3 also up-regulates the expression of vascular endothelial growth factor (VEGF) and the anti-apoptotic protein survivin (Yahata et al., 2003, Cheranov et al., 2008, Mahboubi et al., 2001, Botto et al., 2011). In the late stages of atherosclerosis development, these angiogenic mediators may cause plaque angiogenesis leading to plaque growth and instability (de Vries and Quax et al., 2016).

Gomez-Guerrero and co-workers have investigated the role of STAT1 and STAT3 in the pathogenesis of atherosclerosis using atherosclerosis prone mice (Ortiz-Munoz et al., 2009, Recio et al., 2015). These studies demonstrated that knockdown of STAT3 inhibitor, SOCS3, in atherosclerotic-prone mice results in elevated levels of Tyr-phosphorylated STAT1 and STAT3 in the atherosclerotic lesion. Increased activation of STAT1/STAT3 accelerated atherosclerotic lesion size, and increased leukocyte and VSMCs intra-plaque content (Ortiz-Muñoz et al., 2009). Conversely, enforced adenoviral-vector mediated expression of SOCS1 and SOCS3 in atherosclerotic-prone mice reduced the levels of Tyr-phosphorylated STAT1 and STAT3 in the atherosclerotic lesion. Inhibition of STAT1/STAT3 activation reduced atherosclerotic lesion size in the aorta, and reduced leukocyte and chemokine MCP-1 intra-plaque content (Recio et al., 2015). Furthermore, SOCS1 and SOCS3 mediated inhibition of STAT1/STAT3 in cultured VSMCs reduced the gene

expression of chemokines (MCP-1 and RANTEs), ICAM-1 and pro-inflammatory cytokines (TNF-α and IFN-γ) (Recio et al., 2015). A pro-atherogenic role for STAT1 and STAT3 was further supported by several observations made in *in vivo* studies. Tyr701-phosphorylated STAT1 levels are elevated in aortic atherosclerotic lesions from atherosclerosis-prone mice (Koga et al., 2007) and pharmacological inhibition of STAT1 activity reduced neointimal hyperplasia *in vivo* following vascular injury (Torella et al., 20070. Tyr705-phosphorylated STAT3 levels were elevated in both the adventitial and endothelial layers of the aortic atherosclerotic lesions from atherosclerosis-prone mice (Recinos et al., 2007). These observations in experimental mice were confirmed in a study of human carotid endarterectomy specimens demonstrating that Tyr705 –phosphorylated STAT3 are elevated in endothelium from inflamed compared to non-inflamed areas of atherosclerotic regions (Gharavi et al., 2007). Loss of STAT3 expression specifically in the vascular endothelium reduces atherosclerotic lesion size in the aorta compared with WT mice following a high fat diet (Gharavi et al., 2007). Overall, these studies underscore the critical the role of STAT1 and STAT3 activation in the pathogenesis of atherosclerosis.

Given the importance of IL-6 and STAT1/STAT3 signalling in regulating key processes in atherosclerosis and that interfering with the IL-6 and STAT1/STAT3 signalling *in vivo* prevents atherosclerotic lesion formation, therapeutic strategies that inhibit the IL-6/JAK-STAT1/3 signalling pathway are likely to have a protective effect on the progression of atherosclerosis.

1.4 AMPK

1.4.1 Overview of AMPK

AMP-activated protein kinase (AMPK) is an evolutionarily conserved, heterotrimeric serine/threonine protein kinase. AMPK is ubiquitously expressed in mammalian tissues and plays a key role in regulating energy balance at a cellular and whole-body level (Hardie and Ashford, 2014). AMPK is sensitive to cellular energy levels and is activated in response to a decrease in cellular energy, and functions to switch on catabolic adenosine triphosphosphate (ATP)-producing pathways such as glycolysis and fatty acid oxidation, while switching off anabolic ATP-

consuming pathways such as fatty acid and protein synthesis in order to restore the energy balance (Hardie et al., 2012).

1.4.2 AMPK structure and regulation

The AMPK complex is a αßγ heterotrimer containing a catalytic α subunit and regulatory ß and γ subunits. In mammals, there are seven genes encoding AMPK; i.e. two isoforms of α (α1 and α2), two of ß, (ß1 and ß2), and three of γ (γ1, γ2, and γ3), thus 12 heterotrimeric complexes are theoretically possible (Kahn et al., 2005). Expression levels of the different subunit isoforms vary between tissues and may dictate the subcellular localisation of the AMPK complex; the α1, ß1 and γ1 isoforms are ubiquitously expressed, while the α2 and ß2 isoforms are predominantly expressed in striated muscle (Thornton et al., 1998, Verhoeven et al., 1995). The γ isoforms are expressed in several different tissues (Cheung et al., 2000). While endothelial cells express both the α1 and α2 subunit, the α1 subunit is predominantly expressed (Ewart and Kennedy, 2011). Figure 1.3 outlines the domain structures of the AMPK subunits. The α subunit contains an N-terminal serine/threonine kinase catalytic domain, which contains a conserved threonine residue at position 172, phosphorylation of which is essential for AMPK activity (Woods et al., 1994). The N-terminal kinase domain (KD) is immediately followed by an autoinhibitory domain (AID) (Pang et al., 2007). The three-dimensional structure shows that the AID interacts with the KD when AMP is not bound to the γ subunit and causes AMPK to be maintained in an inactive conformation (Chen et al., 2009). The AID is followed by the α-linker and the C-terminal domain (CTD). The α-linker interacts with γ subunit and is crucial in the mechanism for activation by AMP. The ß subunit contains a carbohydrate-binding module (CBM) to which oligosaccharide components of glycogen can bind and inhibit AMPK (Hudson et al., 2003, Polekhina et al., 2003, McBride et al., 2009). The ß-CTD contains an α-CTD binding site followed by a site for interacting with the γ-subunit (Crute et al., 1998, Hudson et al., 2003). The γ-subunit contains four cystathionine ß-synthetase (CBS) motifs which occur as tandem pairs, known as Bateman domains (Bateman, 1997, Kemp, 2004). An adenine nucleotide-binding pocket is located on each CBS motif. Of the four CBS motifs, only CBS1 and CBS3 can competitively bind AMP, ADP, or ATP. CBS2 always appears to be empty while CBS4 contains a tightly-bound, non-exchangeable molecule of AMP (Xiao et al., 2007, 2011).

The primary control of AMPK activity is through phosphorylation - dephosphorylation of Thr172 within the activation loop of the α subunit kinase domain (Hawley et al., 1996). Two upstream kinases that phosphorylate Thr172 are: LKB1 (liver kinase B1) and CaMKKß (Ca2+/calmodulin-dependent protein kinase kinaseß). LKB1 exists in complex with two accessory subunits, STRAD and MO25 (Hawley et al., 2003, Woods et al., 2005). This complex appears to be constitutively active, but phosphorylates AMPK more rapidly when adenosine triphosphate (ADP)/adenosine monophosphate (AMP) is bound to the AMPK γ subunit (Sakamoto et al., 2004). Alternatively, CaMKKß activates AMPK in an AMP-independent manner, in response to an increase in cytosolic calcium (Hawley et al., 2005, Woods et al., 2005, Hurley et al., 2005) (Figure 1.4).

Mammalian AMPK is activated through binding of ADP or AMP to the γ subunit. Binding of AMP has three complementary effects on AMPK: (i) promotion of Thr172 phosphorylation by upstream kinases; (ii) protection against dephosphorylation of Thr172 by protein phosphatases; (iii) allosteric activation of the phosphorylated AMPK (Gowans et al., 2013) (Figure 1.4). Of these three effects, the first two may also be triggered by ADP binding of the γ subunit, but the third, allosteric activation, is specific to AMP (Oakhill et al., 2011, Xiao et al., 2011). Binding of ATP inhibits AMPK by antagonising the binding of AM(D)P (Xiao et al., 2011) (Figure 1.4). Overall, AMPK is activated by increases in AMP and/or ADP relative to ATP, thus acting as a sensor of cellular energy status. Once activated by cellular stress it acts to restore energy homoeostasis by stimulating catabolic ATP-producing pathways, while suppressing anabolic ATP-consuming pathways.

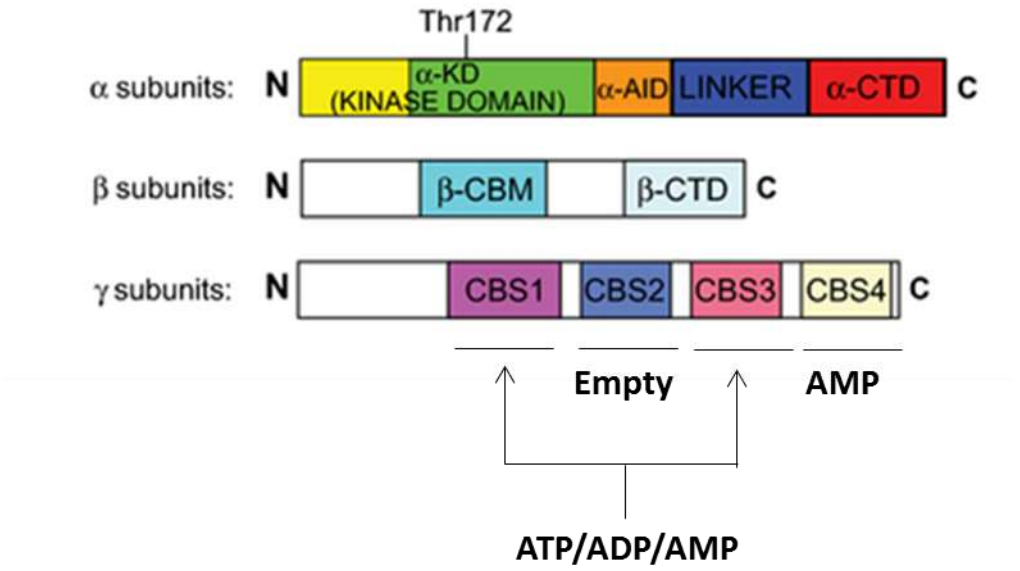

Figure 1.3: Domain structure of AMPK subunit isoforms
AMPKα subunits: kinase domain (α-KD) containing Thr-172 for the activation by upstream kinases; autoinhibitory domain (AID), α-linker and the C-terminal domain (α-CTD). AMPKβ subunits: carbohydrate-binding module (β-CBM), C-terminal domain (β-CTD). AMPKγ subunit: four cystathione-β-synthases domain (CBS 1- 4). Site 2 appears to be always empty and Site 4 to have a tightly bound AMP, whereas Sites 1 and 3 represent the regulatory sites that bind AMP, ADP or ATP in competition. (Figure adapted from Hardie, 2014)

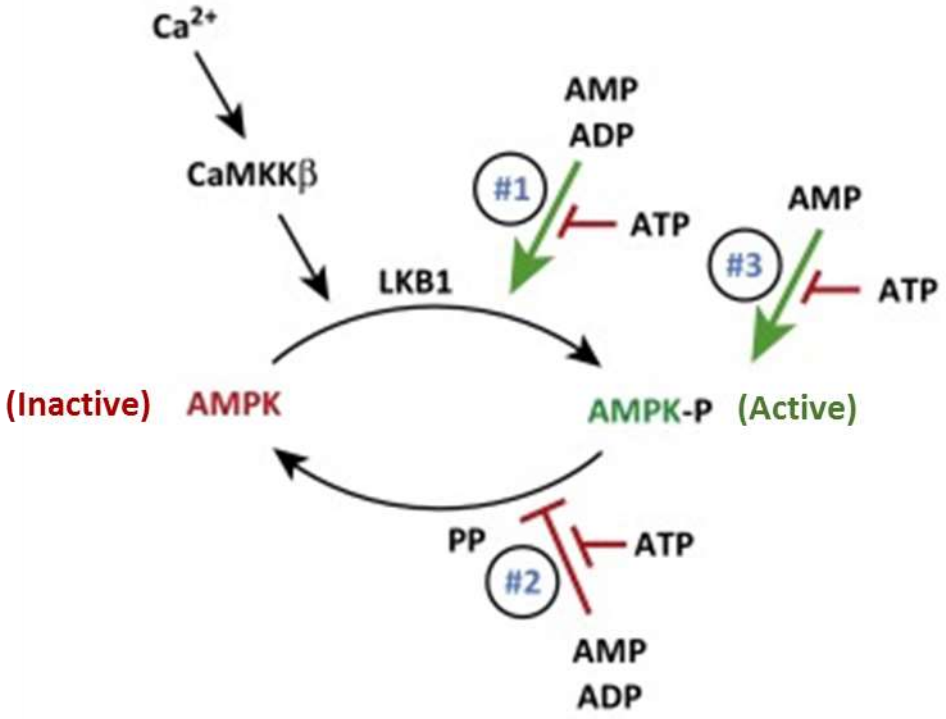

Figure 1.4: Regulation of AMPK
Mammalian AMPK is activated through binding of ADP or AMP to the γ subunit. Binding of AMP has three complementary effects on AMPK: (#1) promotion of Thr172 phosphorylation by upstream kinases; (#2) protection against dephosphorylation of Thr172 by protein phosphatases; (#3) allosteric activation of the phosphorylated AMPK (Gowans et al., 2013). Of these three effects, the first two may also be triggered by ADP binding of the γ subunit, but the third, allosteric activation, is specific to AMP. Binding of ATP inhibits AMPK by antagonising the binding of AM(D)P LKB1 appears to be constitutively active, while CaMKKβ activates AMPK in response to an increase in cytosolic calcium (Figure adapted from Hardie et al., 2016)

1.4.3 Pharmacological activators of AMPK activation

The first pharmacological AMPK activator to be developed was AICAR (5'-aminoimidazole-4-carboxamide ribonucleoside), an adenosine analogue which is taken up into cells by adenosine transporters. It is phosphorylated to the AMP mimetic ZMP (5'-aminoimidazole-4-carboxamide ribonucleoside monophosphate) by adenosine kinase, thereby activating AMPK without altering adenine nucleotide ratios (Corton et al., 1995). Similar to AMP, ZMP binds the AMPK γ subunit and activates AMPK in intact cells, tissues and animals. However, it should be noted that ZMP has the ability to regulate any enzyme which is sensitive to cellular AMP such as fructose-1,6-bisphosphate (Vincent et al., 1991).

A769662 is a member of the thienopyridine family and can directly activate AMPK, independently of AMP (Cool et al., 2006). Although, in a manner similar to AMP, A769662 caused both allosteric activation and protection against Thr172 dephosphorylation (Sanders et al., 2007, Göransson et al., 2007). A769662 selectively activates AMPK complexes containing the β1, but not β2, regulatory subunit (Scott et al., 2008). Mutation of Ser108 in β1 was reported to reduce A769662-mediated AMPK activation, suggesting that the binding site involved the β1 subunit (Sanders et al., 2007). Furthermore, when AMP and A769662 are added to AMPK together, they cause a synergistic allosteric activation of AMPK complexes (Sanders et al., 2007).

Salicylate, a derivative of aspirin, has recently been demonstrated to stimulate AMPK activation (Hawley et al., 2012). Similar to A769662, salicylate caused both allosteric activation and protection against Thr172 dephosphorylation independently of alterations in adenine nucleotide concentrations (Hawley et al., 2012). It is also likely that salicylate binds to the same site as A769962, as it was poor activator of β2-containing complexes and its effects on β1 were abolished by mutating Ser108 (Hawley et al., 2012).

Metformin is a type of biguanide, a synthetic derivative of guanide that is a natural product from the plant *Galega officinalis* (Witters, 2001). Currently, Metformin is widely used as a treatment for type 2 diabetes because of its ability to reduce hepatic glucose production (Foretz et al., 2014). Metformin activates AMPK in hepatocytes via inhibition of NADH dehydrogenase (Complex I) of the

mitochondrial respiratory chain, which blocks ATP production leading to an increased AMP/ATP ratio, thus activating AMPK. (Zhou et al., 2001, Shaw et al., 2005, Brunmair et al., 2004). Several plant-derived compounds including berberine, resveratrol and galgeine have also been reported to activate AMPK by altering adenine nucleotide ratios (Hawley et al., 2010). Interestingly, metformin and salicylate have been reported to synergistically activate AMPK to inhibit fatty acid synthesis in mouse and human hepatocytes, while little AMPK activation was observed with metformin or salicylate on their own (Hawley et al., 2012).

1.4.4 AMPK and physiological role

AMPK is activated under conditions in which cellular energy demands are increased or when fuel availability is decreased, such that intracellular ATP is reduced and AMP levels rise. Physiological stimuli which activate AMPK include metabolic stresses such as hypoxia, ischaemia, glucose deprivation and heat shock; all of which reduce ATP levels by inhibiting its production, while exercise stimulates AMPK activation in contracting muscles as it accelerates ATP consumption (Hardie, 2011). AMPK phosphorylates and inactivates many key proteins concerned with the regulation of carbohydrate and lipid metabolism, resulting in inhibition of fatty acid synthesis, cholesterol and isoprenoid synthesis, hepatic gluconeogenesis, lipolysis and mammalian target of rapamycin (mTOR)-mediated protein translation in addition to stimulation of fatty acid oxidation, muscle glucose transport, mitochondrial biogenesis and caloric intake (Hardie et al., 2012). Thus, AMPK is thought to maintain cellular energy stores and regulate whole body energy balance by stimulating ATP-producing catabolic pathways while inhibiting nonessential ATP-consuming anabolic pathways (Hardie and Ashford, 2014).

AMPK regulates a wide range of different pathways, which often involves switching off anabolic pathways by directly phosphorylating key metabolic enzymes and switching on catabolic pathways by directly phosphorylating transcription factors and co-regulators to promote expression of catabolic enzymes (Hardie et al., 2012). For example, AMPK inhibits fatty acid synthesis by directly phosphorylating and inactivating the cytosolic isoform of acetyl-CoA carboxylase (ACC1) (Davies et al., 1992). Phospho-specific antibodies that recognize the key phosphorylation site (Ser79) on ACC1 are widely used as markers for AMPK activation. AMPK directly phosphorylates several sites on the forkhead box O3 (FOXO3) transcription factor,

activating transcription of many genes, including genes involved in resistance to oxidative stresss (Greer et al., 2007). Figure 1.5 below summarises many of the well-established AMPK downstream targets and processes activated by AMPK activation.

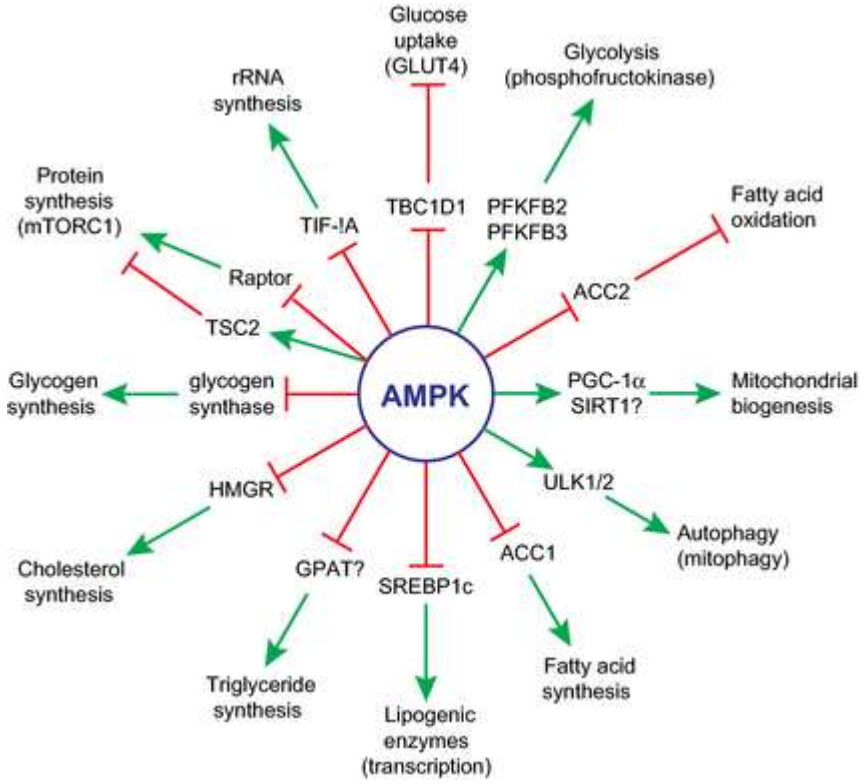

Figure 1.5: Targets for AMPK
Summary of selected protein targets and processes downstream of AMPK. A green arrow signifies activation, and a red line with a crossbar signifies inhibition. Note that if AMPK inhibits a protein that in turn inhibits a downstream process (two successive red lines with crossbars), then the overall process (e.g. glucose uptake or fatty acid oxidation) will be activated. A question mark next to a protein signifies that it is not certain that the protein is a direct target for AMPK. (Figure taken from Hardie et al., 2014)

1.4.5 Cardiovascular protective role of metformin

Coronary heart disease (CHD) is the leading cause of death in the UK (Townsend et al., 2015). Patients with diabetes are at about three times the risk of CHD compared to those without the condition (Fox et al., 2007). In part, this is explained by an accelerated development of atherosclerosis (Nicholls et al., 2008). Metformin is the first-line oral treatment option for patients with type 2 diabetes (T2D), which accounts for 90% of all diagnosed cases of diabetes (Inzucchi et al., 2015). Type 2 diabetes occurs when the beta cells of the pancreas can no longer produce enough insulin to overcome insulin resistance. Insulin resistance is associated with increased triacylglycerol content, particularly in liver and skeletal muscle. In conjunction with insulin resistance, resulting hyperglycaemia contributes to CHD risk. Metformin ameliorates hyperglycaemia by promoting glucose uptake by skeletal muscle and decreasing hepatic glucose production (Natali and Ferrannini, 2006). This drug also reduces insulin resistance in liver and skeletal muscle by promoting the oxidation of fatty acids and inhibiting synthesis of fatty acids and triacylglycerols (Natali and Ferrannini, 2006). *In vivo* studies with metformin and other pharmacological activators of AMPK has demonstrated that the anti-hyperglycaemic actions of metformin are mediated by AMPK (Zhou et al., 2001, Song et al., 2002, Iglesias et al., 2002, Cool et al., 2006). Interestingly, the United Kingdom Prospective Diabetes Study (UKPDS) demonstrated that despite similar glucose lowering effects, administration of metformin reduced all-cause mortality, myocardial infarction, and stroke more than insulin or sulfonylureas (Holman et al., 2008). This study and several other studies have concluded that treatment with metformin limits cardiovascular morbidity and mortality independent from its glucose-lowering action (Holman et al., 2008, Johnson et al., 2005, Mellbin et al., 2011, Roussel et al., 2010). Given that atherosclerosis is an inflammatory disorder, anti-inflammatory properties could contribute, at least in part, to the cardiovascular protective effects of metformin beyond glucose lowering. An increasing body of evidence suggests that metformin exhibits anti-inflammatory actions and that these actions are mediated through AMPK (reviewed by Salt and Palmer, 2012).

1.4.5.1 Inhibition of leukocyte infiltration

Of particular interest are observations that AMPK can limit leukocyte infiltration and activation in the context of cardiovascular disease. Studies using AMPKα1-/- and AMPKα2-/- mice have suggested that both isoforms contribute to AICAR-mediated inhibition of post-ischemic leukocyte adhesion to blood vessels *in vivo* (Gaskin et al., 2011). Consistent with a role for AMPK-dependent inhibition of leukocyte infiltration, aortae from AMPKα1-/- mice showed enhanced angiotensin (Ang) II-stimulated VCAM-1 expression (Schuhmacher et al., 2011). Importantly, a clinical study has shown that metformin treatment of patients with T2D was associated with decreased levels of soluble ICAM-1, VCAM-1 and E-selection, and this decrease was independent of the anti-hyperglycaemic action of the drug (De Jager et al., 2005). Furthermore, AMPK activation is associated with reduced infiltration of inflammatory cells in murine models of acute and chronic colitis (Bai et al., 2010), and rheumatoid arthritis (Guma et al., 2015) as well as a rat model of autoimmune encephalomyelitis (Prasad et al., 2006). Taken together, these studies indicate that AMPK activation in several tissues, and the vasculature in particular, impairs leukocyte infiltration by mechanisms that may involve reducing the expression of chemokines and adhesion molecules.

1.4.5.2 Regulation of pro-inflammatory signalling

Studies have linked AMPK with suppression of pro-inflammatory signalling pathways. Inhibition of cytokine-stimulated NF-κB signalling by AMPK is the most studied and has been demonstrated in several cell types including ECs, astrocytes and macrophages (Cacicedo et al., 2004, Giri et al., 2004, Yang et al., 2010). Crucially, Hattori et al., demonstrated that activation of AMPK suppressed TNF-α and interleukin-1β-induced gene expression of adhesion molecules (VCAM-1, E-selectin, ICAM-1) and MCP-1 in ECs by suppressing NF-κB activity (Hattori et al., 2006). Consistent with a role for AMPK-mediated inhibition of NF-κB signalling, aortic ECs from AMPKα2-/- mice showed increased nuclear NF-κB levels (Wang et al., 2010). Subsequently, potential mechanisms have been proposed to explain AMPK-mediated inhibition of cytokine-stimulated NF-κB signalling. First, Zhang et al reported that in ECs AMPK phosphorylates the transcriptional co-activator p300 at Ser89 to inhibit p300-mediated acetylation of NF-κB p65, leading to inhibition of TNF-α-stimulated NF-κB DNA binding (Zhang et al., 2011). Second, Bess et al

proposed that AMPK hyperphosphorylates IKKβ to inhibit subsequent phosphorylation of Iκα and p65 in COS-7 cells, resulting in suppression of TNF-α-stimulated NF-κB-mediated transcription (Bess et al., 2011). Both studies demonstrated that AMPK activation markedly reduced monocyte adhesion and adhesion molecule expression in TNF-α-stimulated endothelial cells, leading to the attenuation of the endothelial pro-inflammatory response (Bess et al., 2011, Zhang et al., 2011). A few studies have identified AMPK-dependent suppression of cytokine-stimulated MAPK phosphorylation/activation. A769662-mediated AMPK activation inhibited TNF-α/IL-1-β-stimulated phosphorylation of JNK, ERK1/2 and p38 MAPKs in adipocytes (Sarah Mancini; personal communication). Berberine was found to inhibit lipopolysaccharide (LPS)-stimulated phosphorylation of JNK, ERK1/2 and p38 MAPK in macrophages in an AMPK-dependent manner (Jeong et al., 2009). AICAR and metformin were also reported to inhibit JNK activation in HUVECs in response to TNF-α (Schulz et al. 2008). Increased JNK phosphorylation was observed not only in HUVECs following siRNA-mediated downregulation of either AMPKα1 or AMPKα2, but also in aortic endothelial cells isolated from AMPKα2-/- mice (Dong et al., 2010). A few studies have indicated that AMPK activation can inhibit JAK-STAT signalling, with two reports showing AMPK-dependent inhibition of IL-6-stimulated STAT3 phosphorylation, SOCS3 expression and expression of pro-inflammatory genes in hepatocyte cell lines (Handy et al., 2010, Nerstedt et al., 2010, Kim et al., 2012). Recently, Vasamsetti et al proposed that metformin inhibits monocyte-to-macrophage differentiation by reducing STAT3 activity due to increased AMPK activation (Vasamsetti et al., 2015). However, the effect of AMPK on JAK-STAT signalling in ECs have yet to be fully characterised. Previous unpublished studies in our group have investigated whether AMPK modifies IL-6 stimulation of JAK-STAT signalling in HUVECs (Claire Rutherford, Marie-Ann Ewart, Ian Salt, Tim Palmer, personal communication). Those studies, performed by Dr. Claire Rutherford and Dr. Marie-Ann Ewart (University of Glasgow) are described in detail in the appendix (section 6.1) and form the basis of the studies described in this thesis.

1.5 Aims

Our preliminary investigations (appendix, section 6.1) clearly demonstrated that activation of AMPK by multiple stimuli triggered a rapid and significant reduction in the ability of sIL-6Rα/IL-6 to stimulate STAT3 phosphorylation on Tyr705 (Figure

6.1). The aim of this study was to identify the mechanism of AMPK-mediated inhibition of STAT3 phosphorylation. Our preliminary experiments provided the initial step in this investigation: it is a post receptor effect. Pre-treatment of HUVECs with the direct AMPK activator, A769662, significantly inhibited both sIL-6Rα/IL-6 and IFN-α stimulation of STAT3 Tyr705 phosphorylation in HUVECs (Figure 6.5A). IFN-α activates STATs *via* an IFNα/β receptor 1 (IFNAR1/IFNAR2) complex which is distinct from the sIL-6Rα/IL-6/gp130 complex (Borden et al., 2007). The studies in this thesis therefore tested the hypothesis that AMPK was exerting its inhibitory effects at one or more common signalling loci downstream of IFNAR1/IFNAR2 and gp130 at a post-receptor level. In particular, the studies described examine whether AMPK acts:

1. Directly on a known regulator of JAK or STAT protein function.

2. On an already established AMPK downstream target which then either directly or indirectly impacts on JAK-STAT signalling.

3. Directly to phosphorylate and influence the activity/function of one or more JAK isoforms.

Chapter 2 - Methods

2.1 Cell Culture Procedures

2.1.1 Cell culture plastic ware

Human umbilical vein endothelial cells (HUVECs) were obtained from Lonza (one batch of pooled donor) and cultured in Corning T150 flasks, 10 cm diameter plates and 6 well plates.

Human fibrosarcoma cell lines 2C4 (parental cell line for U4C), U4C (JAK1-deficient) and U4C.JAK1 (stably expressing transfected human JAK1 construct) (Muller et al., 1993); a kind gift from Dr Ana P. Costa-Pereira, Imperial College London [London, UK]) were cultured in Corning T150 flasks, 10 cm plates and 6 well plates.

HEK293 cells were cultured in Corning T150 flasks, 10 cm diameter plates and 6 well plates. HEK293 cells poorly attach to cell culture plastic ware. Therefore, 10 cm diameter plates and 6 well plates were coated with poly-D-lysine prior to seeding HEK293 cells. Plastic surfaces that are coated with the poly-D-lysine possess a uniform net positive charge, which enhances the electrostatic interaction between the negatively-charged ions of the cell membrane and the coated plastic surface. Here, the culture plates were aseptically coated with 0.1 mg/ml poly-D-lysine solution. After 2-3 minutes, the excess solution was aspirated and the plates were allowed to dry before seeding cells.

2.1.2 Cell culture growth media for HUVECs

HUVECs were maintained in T150 flasks in endothelial growth medium (EGM) consisting of endothelial basal media (EBM) supplemented with 2% (w/v) fetal bovine serum, 0.04% (v/v) hydrocortisone, 0.1% (v/v) ascorbate and recombinant growth factors as recommended by the supplier (Lonza). Cells were cultured at 37 °C in a humidified atmosphere containing 5% (v/v) CO_2 in media replaced every 48 hrs.

2.1.3 Cell culture growth media for HEK293 cells

HEK293 cells were each maintained in Dulbecco's modified Eagles's medium (DMEM) supplemented with 10% (v/v) FBS, 1 mM glutamine, 100 U/ml penicillin and 100 µM streptomycin. Cells were cultured at 37 °C in a humidified atmosphere containing 5% (v/v) CO_2 in media replaced every 48 hrs.

2.1.4 Cell culture growth media for 2C4 and U4C cells

2C4 and U4C cells were each maintained in Dulbecco's modified Eagles's medium (DMEM) supplemented with 10% (v/v) FBS, 1 mM glutamine, 100 U/ml penicillin, 100 µM streptomycin and 400 µg/ml G418 to maintain selection pressure. Cells were cultured at 37 °C in a humidified atmosphere containing 10% (v/v) CO_2 in media replaced every 48 hrs.

2.1.5 Cell culture growth media for U4C.JAK1 cells

U4C.JAK1 cells were each maintained in Dulbecco's modified Eagles's medium (DMEM) supplemented with 10% (v/v) FBS, 1 mM glutamine, 100 U/ml penicillin, 100 µM streptomycin, 400 µg/ml G418 and 0.5 µg/ml puromycin to maintain selection pressure. Cells were cultured at 37°C in a humidified atmosphere containing 10% (v/v) CO_2 in media replaced every 48 hrs.

2.1.6 Passaging of HUVECs

Cells were passaged on reaching ~80% confluence, which was approximately once a week. EGM was aspirated and the cell monolayers were washed twice with sterile PBS before 2 ml of sterile endothelial grade trypsin-EDTA solution (5 U/ml porcine trypsin, 1.8 % (w/v) EDTA) was added to each T150 flask. Cells were then incubated at room temperature for 5 minutes until the cells began to detach from the flask surface. Gentle tapping of the flask dislodged all of adherent cells from the flask surface. Addition of fresh EGM neutralises the trypsin and cells were pelleted by centrifugation (200 g, 5 mins, RT). Cell pellets were resuspended in a volume of EGM determined to give a suitable cell density for counting using a haemocytometer, typically 6 ml per T150 flask. Wells were then seeded at an appropriate level according to the experiment performed. HUVECs were used for experiments between passages 2 and 5. Beyond passage 5, HUVECs rapidly alter

in culture conditions (Muller et al., 2002), therefore the cells were discarded at this stage.

2.1.7 Passaging of HEK293, 2C4, U4C, U4C.JAK1cells

Cells were passaged on reaching ~80% confluence, which was approximately twice a week. DMEM growth medium was aspirated and the cells were washed briefly with sterile PBS before 2 ml of sterile trypsin (0.05% (v/v) in diaminothanetetra-acetic acid, disodium salt [EDTA]) was added to each T150 flask. Cells were then incubated at 37 °C for 2-3 minutes until the cells began to detach from the flask surface, which was further facilitated by gentle tapping of the flask to dislodge all of the adherent cells from the surface. Fresh DMEM growth medium was then asdded to neutralise the trypsin and cells were pelleted by centrifugation (200 g, 5 mins, room temperature [RT]). Cell pellets were resuspended in a volume of DMEM growth medium determined to give a suitable cell density for counting using a haemocytometer, typically 10 ml per T150 flask. Wells were then seeded at an appropriate level according to the experiment performed.

2.1.8 Transfection of HUVECs with short interfering RNA (siRNA)

Target-specific short interfering RNAs (siRNAs) designed to knockdown individual specific JAK isoforms; JAK1, JAK2 or TYK2 (Qiagen), and control non-targeting siRNA were introduced into HUVECs using HiPerFect transfection reagent (Qiagen) as per manufacturer's instructions. Briefly, 24 hrs prior to transfection, HUVECs were seeded at a density of 2 x 10^5 cells/well in 6 well plates. For each well, 300 ng siRNA was mixed with 100 µl Opti-MEM serum-free media followed by the addition of 12 µl HiPerFect and mixed by slowly pipetting up and down. The siRNA/HiPerFect mixture was incubated for 10 minutes at room temperature to allow formation of transfection complexes. Meanwhile, cells were washed twice with 2 ml Opti-MEM which was then replaced with 700 µl fresh Opti-MEM. The siRNA/HiPerFect mixture was added drop-wise over the surface of the cells. Cells were incubated for 3 hours at 37°C and 1500 µl EGM was added to each well. 24 hours after transfection, the medium was replaced. siRNA transfected cells were subsequently incubated for an additional 24 hours and were treated as described in the figure legends.

2.1.9 Transient transfection of HEK 293, 2C4, U4C and U4C.JAK1 cells

The appropriate plasmid DNA was introduced into HEK 293, 2C4, U4C or U4C.JAK1 cells for transient expression using PolyFect transfection reagent (Qiagen) as per manufacturer's instructions. Briefly, HEK 293, 2C4, U4C or U4C.JAK1 cells were seeded in 10 cm plates and grown until approximately 70% confluent. For each 10 cm plate, 2.5 µg of plasmid DNA was mixed with 400 µl Opti-MEM followed by the addition of 40µl PolyFect transfection reagent and mixed by slowly pipetting up and down. The DNA/PolyFect mixture was incubated for 10 minutes at room temperature to allow formation of transfection complexes. Meanwhile, 7 ml fresh DMEM growth medium was added to the 10 cm plate. 1 ml DMEM growth medium was then mixed with each DNA/PolyFect mixture prior to being added drop-wise over the surface of the cells. 24 hrs after transfection, each 10 cm plate of transfected cells was split between 4 wells of a 6 well plate in order to minimise variation in transfection efficiency between wells. Cells were subsequently incubated for an additional 24 hours prior to treatment as described in the figure legends.

2.1.10 Cell treatments and subsequent incubations performed under serum-free conditions

Unless otherwise indicated in the figure legends, cell treatments and subsequent incubations were performed in serum-free conditions. Experiments on HUVECs were performed using serum-free Basal medium 199 (HEPES modification) supplemented with 1 mM glutamine, 100 U/ml penicillin, and 100 µM streptomycin. Experiments on HEK 293, 2C4, U4C and U4C.JAK1 cells were performed using serum-free DMEM supplemented with 1 mM glutamine, 100 U/ml penicillin and 100 µM streptomycin. Prior to cell treatments, cells were incubated in the appropriate serum-free media for 3 hours.

2.2 Preparation of lysates from cultured cells

Confluent cells grown on 6-well plates were first treated as described in figure legends and subsequently lysates were prepared as follows. Reactions were terminated by placing dishes on ice and washing twice with 1ml of ice-cold PBS prior to the addition of 100µl of RIPA buffer (50 mM HEPES pH7.4, 150 mM sodium chloride, 1% (v/v) Triton x100, 0.5% (v/v) sodium deoxycholate, 0.1% (w/v) SDS,

10m M sodium fluoride, 5 mM EDTA, 10 mM sodium phosphate, 0.1 mM PMSF, 10µg/ml benzamidine, 10 µg/ml soybean trypsin inhibitor, 2% (w/v) EDTA-free complete protease inhibitor cocktail). The cells were then scraped off using a cell lifter and pipetted into 1.5 ml microcentrifuge tubes. Lysates were mixed for 30 minutes at 4°C with rotation to aid solubilisation before centrifugation (21 000 g, 15 mins, 4°C) to pellet insoluble debris. 80µl of supernatant was collected and stored at -20°C. To compensate for the low protein content of HUVECs, only 65 µl of RIPA buffer was added to each well of HUVECs and 50µl of the supernatant collected. The supernatant was subsequently assayed for protein concentration using a bicinchoninic acid assay (BCA) as described below.

2.3 Determination of protein concentration using the bicinchoninic acid (BCA) assay

The BCA assay was performed by preparing the following bovine serum albumin (BSA) standards in the appropriate lysis buffer: 2.0, 1.8, 1.6, 1.4, 1.2, 1.0, 0.8, 0.6, 0.4, 0.2 and 0.0 mg/ml. Protein samples were diluted (1:3 – HUVEC and 1:5 – HEK 293, 2C4, U4C and U4C.JAK1 cells lysates) in the appropriate lysis buffer. 10µl of each BSA standard and protein sample were added to each well in duplicate to a 96-well plate. 200µL of BCA working solution (1% (w/v) 4,4 dicarboxy-2,2, biquinoline disodium salt, 2% (w/v) sodium carbonate, 0.16% (w/v) sodium potassium tartrate, 0.4% (w/v) sodium hydroxide, 0.95% (w/v) sodium bicarbonate [pH 11.25], 0.08% (w/v) copper (II) sulphate) was added to each well of the plate. The plate was then incubated at room temperature until a linear standard curve (r^2 ~0.98) was produced. Absorbance was measured at 495 nm using a POLARstar OPTIMA (BMG LabTech) microplate reader. Upon mixing with protein, Cu^{2+} ions in the BCA reagent are reduced to Cu+ which then reacts with BCA to produce a colour change from blue to purple which is detectable at 495 nm. The extent of the colour change is directly proportional to the amount of protein in a sample. The absorbance measurements obtained for the BSA standards were used to derive a straight line graph from which the concentrations of the protein samples were quantified using POLARstar OPTIMA MARS data analysis package v.1.20 and GraphPad Prism v.4.

2.4 Immunoprecipitation

2.4.1 Preparation of lysates from cultured cells for immunoprecipitation

Confluent cells grown on 10 cm plates were first treated as described in figure legends and subsequently lysates were prepared. Reactions were terminated by placing dishes on ice and washed twice with ice-cold PBS. Using a cell lifter, cells were scraped into 500 µl of ice-cold PBS and pipetted into 1.5 ml microcentrifuge tubes. Cells were pelleted by centrifugation (1000 g, 5 mins, 4 °C) and resuspended in 250 µl immunoprecipitation (IP) buffer (50 mM HEPES pH7.4, 120 mM sodium chloride, 5 mM EDTA, 10% (v/v) glycerol, 1% (v/v) Triton x100, 5 mM sodium fluoride, 1 mM sodium orthovanadate, 0.1 mM PMSF, 10 µg/ml benzamidine, 10 µg/ml soybean trypsin inhibitor and 2% (w/v) EDTA-free complete protease inhibitor cocktail). Lysates were mixed for 30 minutes at 4°C with rotation to aid solubilisation before centrifugation (21 000 g, 15 mins, 4°C) to pellet insoluble debris. Without disturbing the pellet, 220µl of supernatant was collected and stored at -20°C. The supernatant was assayed for protein concentration using a BCA assay as described above.

2.4.2 Immunoprecipitation of JAK1 and phosphotyrosine proteins

25 µl packed volume (per sample) of protein G-Sepharose beads were washed 3 times (300 g, 1 min at 4°C) with 1 ml IP buffer and resuspended in 50µl IP buffer (50% [v/v] slurry). Cell lysate (500 µg) and 6 µl mouse anti-JAK1 antibody or 10 µl mouse 4G10 (anti-phosphotyrosine antibody) were added to 50 µl of 50% slurry (v/v) of protein G beads. The volume of the protein G/lysate/antibody mixture was made up to 500 µl with IP buffer and was mixed for overnight at 4°C with rotation. The immobilized immune complexes were isolated from the lysate by centrifugation (1000 g, 1 min at 4°C) and the immunodeplete retained. The beads were then washed three times (21 000 g, 1 min at 4°C) with 1 ml IP buffer. Immunocomplexes were resuspended in 40 µl 12% (w/v) SDS sample buffer (section 2.5) and eluted by vortexing and incubating samples at 67°C at 30 minutes. Samples were then boiled at 95° C for 5 minutes to denature and dissociate antibody heavy and light chains. Beads were pelleted by brief centrifugation (10 000 g, 15 secs, RT) and supernatants were transferred to fresh 1.5 ml microcentrifuge tubes using a Hamilton syringe, prior to loading on sodium dodecyl sulphate-polyacrylamide gel electrophoresis (SDS-PAGE) for analysis.

2.4.3 Immunoprecipitation of FLAG-tagged JAK1 from U4C cell lysates

JAK1-deficient U4C cells were seeded in 10 cm dishes and transfected with human FLAG-tagged JAK1 DNA plasmid (section 2.1.9). Subsequently, confluent U4C cells expressing FLAG-tagged JAK1 were treated as described in figure legends and cell lysates were prepared for immunoprecipitation (section 2.4.1.) Immunoprecipitation of FLAG-tagged JAK1 was performed as described above (section 2.4.2) with the exception that 35µl packed volume (per sample) of pre-conjugated anti-FLAG M2 agarose beads were used in place of protein G-Sepharose beads and primary antibodies.

2.5 SDS-PAGE

Equal quantities of soluble protein lysates (10-20 µg/sample) were denatured in an equal volume of 12% (w/v) SDS sample buffer (12% (w/v) SDS, 50 mM Tris, pH 6.8, 10% (v/v) glycerol, 10 mM dithiothreitol (DTT), bromophenol blue). Samples were fractionated by SDS-PAGE on 8 - 10% (w/v) resolving gels (Table 2-1). To allow size estimation of immunoreactive protein bands, Biorad Rainbow molecular weight markers were fractionated alongside protein samples. Electrophoresis was performed in 1% (w/v) SDS running buffer (0.1% (w/v) SDS, 192 mM glycine, 25 mM Tris, pH 8.3) at a constant voltage of 150 V for approximately 1.5 hours until good separation of the molecular weight markers had been achieved.

Table 2-1: 10% resolving gel

Chemical component	Volume required
dH2O	3.4 ml
buffer 1 (1.5M Tris, pH 8.8, 0.4% (w/v) SDS)	2.5 ml
50% (v/v) glycerol	0.65 ml
ammonium persulphate (APS, 0.3mg/ml)	0.032 ml
TEMED	0.008 ml
30% (w/v) acrylamide/bis-acrylamide	3.3 ml

The percentage of the resolving gel was altered by adjusting the volumes of distilled deionised water (dH2O) and acrylamide/bis-acrylamide as follows:
8% resolving gel: 4.07 ml dH20, 2.64 ml 30% (w/v) acrylamide/bis-acrylamide
12% resolving gel: 2.74 ml dH20, 3.96 ml 30% (w/v) acrylamide/bis-acrylamide

Table 2-2: Stacking gel

Chemical component	Volume required
dH2O	3.4 ml
buffer 2 (0.5M Tris-HCl, pH 6.8, 0.4% (w/v) SDS)	1.34 ml
ammonium persulphate (APS, 0.3mg/ml)	0.054 ml
TEMED	0.007 ml
30% (w/v) acrylamide/bis-acrylamide	0.63 ml

2.6 Immunoblotting for proteins

2.6.1 List of Antibodies used for immunoblotting

Table 2-3: Primary antibodies used for immunoblotting

All membranes were incubated overnight at 4 °C.

Antibody Reactivity	Host Species	Dilution	Diluent	Supplier	Catalogue No.
Phospho-STAT3 (Tyr705)	Mouse	1:1000	5% BSA	Cell Signalling Technology	9145
STAT3	Rabbit	1:1000	5% milk	Cell Signalling Technology	9132
Phospho-STAT1 (Tyr701)	Rabbit	1:1000	5% BSA	Cell Signalling Technology	9171
STAT1	Mouse	1:1000	5% milk	Cell Signalling Technology	9176
Phospho-ACC (S79)	Rabbit	1 :1000	5% BSA	Cell Signalling Technology	3661
JAK1	Mouse	1 :1000	5% BSA	BD transduction laboratories	610232
JAK2	Rabbit	1:1000	5% BSA	Cell Signalling Technology	3230S
TYK2	Mouse	1:1000	5% BSA	BD transduction laboratories	610173
Phospho-JAK1 (Y1022/1023)	Rabbit	1:200	5% BSA	Santa Cruz Biotechnology	SC-16773
Phospho-JAK1 (Y1022/1023)	Rabbit	1:200	5% BSA	Invitrogen	44-422G
Phospho-tyrosine (clone 4G10)	Mouse	1:1000	5% BSA	Merck Millipore	05-321
GAPDH	Mouse	1: 80000	5% milk	Abcam	4300
p70 S6 kinase phospho-S371	Rabbit	1:1000	5% BSA	Cell Signalling Technology	9208

Table 2-4: Secondary antibodies used for immunoblotting

All membranes were incubated for 1 hr at room temperature.

Linked molecule	Antibody Reactivity	Host Species	Dilution	Diluent	Supplier	Catalogue No.
HRP	Mouse IgG	Goat	1:1000	5% milk	Sigma-Aldrich	A4416
HRP	Rabbit IgG	Goat	1:1000	5% milk	Sigma-Aldrich	A9169
HRP	Goat IgG	Rabbit	1:2000	5% milk	Sigma-Aldrich	A5420

2.6.2 Electrophoretic transfer

Proteins were electrotransferred from the gel on to a nitrocellulose membrane (0.2 mm pore size) for 75 min at a constant current of 400 mA in a transfer buffer (192 mM glycine, 25 mM Tris, pH 8.3 and 20% (v/v) methanol).

2.6.3 Blocking of membranes and probing with primary antibodies

Non-specific protein-binding sites on nitrocellulose membranes were blocked by incubation in immunoblotting buffer (10 mM Tris, pH 7.6, 150 mM NaCl, 0.1% (v/v) Tween 20, 5% (w/v) milk proteins) for 1 hr at room temperature with shaking. After washing (3 x 5 min) the membrane in Tris-buffered saline -Tween (TBST; 10 mM Tris, pH 7.6, 150 mM NaCl, 0.1% (v/v) Tween 20), the membrane was incubated in a specific primary antibody overnight at 4°C with shaking. Antibodies used during this study are listed in Table 2-1. Primary antibodies were diluted in either immunoblotting buffer or 5% (w/v) BSA in TBST.

2.6.4 Secondary antibodies and immunodetection of proteins using western blotting and the ECL detection system

Following an overnight incubation in primary antibody, the membranes were washed (3 x 5 min) in TBST prior to incubation for 1 hr at room temperature with the corresponding horseradish peroxidase (HRP)-conjugated secondary antibody diluted 1:1000 in immunoblotting buffer (Table 2-2). Membranes were then washed (2 x 5 min) with shaking in immunoblotting buffer followed by washing (3 x 5 min) in TBST. Following this, immunoreactive proteins were visualised using Perkin-Elmer enhanced chemiluminescence (ECL) detection reagents, according to the manufacturer's instructions. Briefly, the membrane was incubated in 2 ml

ECL reagent for 1 minute and blotted onto paper towel to remove excess liquid. Membrane was mounted onto an autoradiography cassette for exposure to Medical X-ray Blue/MXBE Film (Carestream Health, 7710783) and developed using a X-OMAT 2000 processor (Kodak).

2.6.5 Stripping of antibodies from nitrocellulose membranes

The stripping solution removes antibodies bound to the membrane without removing SDS-PAGE fractionated proteins. In order to re-probe the membrane with a different primary antibody, the membrane was washed (2 x 10 min) in stripping buffer (0.75% (w/v) glycine, 0.87% (w/v) NaCl [pH 2]) at room temperature with shaking. After washing the membrane (2 x 5 min) in TBST and re-blocking in immunoblotting buffer for 1 hour, membranes were then incubated with another primary antibody.

2.6.6 Densitometric quantification of protein bands

Immunoreactive protein bands on the developed film were scanned, Quantification was by densitometric scanning of non-saturating exposed films using TotalLab imaging software v2.0 (Phoretix, UK).

2.7 Molecular Biology

2.7.1 Plasmid DNA constructs

Table 2-5: Plasmid DNA constructs

Donor/Supplier	cDNA	Vector	Tag	A^R
Origene (Rockville, MD)	Human JAK1 (Cat.RC213878)	pCMV6	FLAG	K
In-house	Human S515518A JAK1	pCMV6	FLAG	K
In-house	Human V658F JAK1	pCMV6	FLAG	K
In-house	Human V658F S515518A JAK1	pCMV6	FLAG	K
In-house	Human JAK1 SH2 domain	pGEX-2T	FLAG, His_6	A
Grahame Hardie, University of Dundee	Rat ACC1, amino acid residues 60-94	pGEX-20T	His_6	A

Antibiotic Resistance (A^R): A = Ampicillin, K = Kanamycin

2.7.2 Transformation of competent *E. coli* cells

Circular DNA plasmids were maintained and propagated by transforming XL1-Blue E.coli. Briefly, 50 µl XL1-Blue E.coli cells were aliquoted into pre-chilled 1.5ml microcentrifuge tubes prior to the addition of 30-50 ng DNA and incubated on ice for 15 minutes. Meanwhile Luria Bertani (LB) broth (1% (w/v)) bactotryptone, 0.5% (w/v) yeast extract, 1% (w/v) sodium chloride, pH7.4) was heated to 37°C. The cell/DNA mixture was heat shocked for 90 seconds in 42°C water bath followed by immediate recovery on ice for 2 minutes. 450 µl LB-broth with no antibiotic selection was added to each tube and incubated for 1 hr at 37°C with shaking. Cells were gently pelleted by centrifugation (1000 g, 5 mins, RT) and resupended in a reduced volume of 100 µl LB-broth. 100 µl transformed cell suspension was spread onto dry LB-agar (1.5% (w/v) agar in LB-broth) plate supplemented with the appropriate selection antibiotic (ampicillin, 50µg/ml; kanamycin, 25µg/ml) and incubated overnight in a 37°C to allow growth of bacterial colonies. The following day, a single colony was picked for small scale liquid bacterial culture and subsequent plasmid DNA purification.

2.7.3 Purification of plasmid DNA

A single colony picked from a fresh bacterial transformation plate was used to inoculate 5 ml selection LB-broth and incubated for 8 hrs at 37°C with shaking. The plasmid DNA was isolated and purified from the 5ml culture (starter culture) using a Promega Wizard Plus Miniprep DNA purification system as per the manufacturer's instructions, specifically the centrifugation protocol. For large-scale preparations of plasmid DNA, the 5 ml starter culture was used to inoculate 250 ml selection LB-broth and incubated for 16 hrs at 37°C with shaking. The plasmid DNA was isolated and purified from the 250ml culture using a Qiagen EndoFree Plasmid Maxi Kit as per the manufacturer's instructions. The plasmid DNA concentration was determined at A260 using a NanoDropTM 1000 Spectrophotometer prior to storage at -20°C.

2.7.4 Preparation of glycerol stocks

Glycerol stocks were prepared for long-term storage of plasmid DNA. For each glycerol stock, 1 ml overnight (250 ml) culture was added to 0.4 ml sterile 50% (v/v) glycerol in a sterile cryovial. The mixture was by pipetted up and down to

ensure even dispersal of glycerol. Glycerol stocks were then rapidly frozen by immersion in dry ice before storage at -80°C freezer. To culture plasmid DNA from a glycerol stock, 5 ml selection LB-broth is inoculated with a scraping of the glycerol stock and incubated for 8 hrs at 37°C with shaking.

2.7.5 Determination of DNA concentration using NanoDropTM 1000 Spectrophotometer

The purified plasmid DNA concentration was determined at A260 using a NanoDropTM 1000 Spectrophotometer prior to storage at -20°C. DNA absorbs ultraviolet light most strongly at 260nm. A NanoDropTM 1000 Spectrophotometer spectrophotometer measures the amount of light that DNA absorbs at A260 and the number generated is an estimation of the sample concentration. The NanoDropTM 1000 Spectrophotometer software also calculates the A260/A280 and A260/A230 ratio of each DNA sample, which can be used as an indication of protein contamination and salt contamination, respectively. Good-quality DNA will have an A260/A280 ratio of 1.7–2.0 and an A260/230 ratio greater than 1.5.

2.7.6 Sequencing

The generation of new DNA constructs or mutated DNA plasmids was confirmed by DNA sequencing, performed by the University of Dundee Sequencing Service.

2.7.7 Site Directed Mutagenesis

Table 2-6: Primers and DNA templates for site-directed mutagenesis reactions

Mutant Plasmid	S515518A JAK1
DNA template	JAK1
Forward Primer	5’CGGTTCGGACCGC GCC TTCCCC GCC TTGGGAGACCTC3’
Reverse Primer	5’GAGGTCTCCCAA GGC GGG GAA GGC GCGGTCCGAACCG3’

Mutant Plasmid	V658F JAK1
DNA template	JAK1
Forward Primer	5’CTCTATGGCGTCTGT TTC CGCGACGTGGAG3’
Reverse Primer	5’CTCCACGTCGCG GAA ACAGACGCCATAGAG3’

Mutant Plasmid	V658F S515518A JAK1
DNA template	S515518A JAK1
Forward Primer	5’CTCTATGGCGTCTGT TTC CGCGACGTGGAG3’
Reverse Primer	5’CTCCACGTCGCG GAA ACAGACGCCATAGAG3’

Primers were synthesised by Biomers.net.

Site-directed mutagenesis is a method that uses custom designed oligonucleotide primers to introduce a desired mutation(s) in a double-stranded DNA plasmid. The oligonucleotide primers listed in the table above (Table 2-4) were used to introduce a desired mutation(s) in a pCMV6-JAK1 plasmid by following the instructions of the Agilent Technologies QuikChange Lightning site-directed mutagenesis kit. Briefly, each polymerase chain reaction (PCR) reaction was prepared on ice in thin walled

PCR tubes as follows:

10× reaction buffer	5 µl
dsDNA template (50 ng/µl)	1 µl
Forward primer (125 ng/µl)	1 µl
Reverse Primer (125 ng/µl)	1 µl
dNTP mix	1 µl
QuikSolution reagent	1 µl
Sterile dH_2O final volume of	50 µl
QuikChange Lightning Enzyme	1µl

PCR reactions were carried out in a thermocycler using the following standard conditions:

PCR step	**Temp.(^{0}C)**	**Time**	**No. of cycles**
Initial	95	2 mins	1
Denaturation	95	20 Secs	
Primer Anneal	60	10 Secs	18
Extension	68	30Secs/Kb	
Final Extension	68	5 mins	1
Hold	4	hold	1

After the reaction was complete, 1 µl of DpnI was added to each PCR reaction and incubated at 37 °C for 5 minutes to digest the parental supercoiled dsDNA. 4 µl of the reaction mix was then transformed into XL10-Gold ultracompetent cells and successful mutants were selected on antibiotic agar plates as per manufacturer's instructions. The mutant DNA was amplified, isolated, purified and quantified as previously described in sections 2.7.2 - 2.7.5 and the mutation was confirmed by DNA sequencing (section 2.7.6).

2.7.8 Preparation of GST JAK1 SH2 construct

The GST-fusion construct of the SH2 domain of human JAK1 (aa 439 – 544) was generated in house. In brief, oligonucleotide primers complementary to the boundaries of the SH2 domain (based on its assignment in the human JAK1 Uniprot entry (P23458)) within the human JAK1 were synthesised for PCR (section 2.7.8.1). These oligonucleotide primers, as shown in the Table 2-5, were designed to amplify the SH2 domain within pCMV6/human JAK1 while introducing an in-frame C terminal (His)6 tag and a stop codon, as well as BamHI and EcoRI compatible ends for subcloning. The resultant PCR product was then digested (section 2.7.8.2) with BamHI and EcoRI and ligated into similarly digested pGEX-2T bacterial expression plasmid (Section 2.7.8.5). The recombinant plasmid was transformed into XL10-Gold ultracompetent E. coli and the transformants analyzed for the presence of insert by BamHI/EcoRI restriction digestion and DNA sequencing.

2.7.8.1 DNA amplification by Polymerase Chain Reaction (PCR)

Table 2-7: Primers and DNA template for PCR reactions

Plasmid Name	GST JAK1 SH2
DNA Template	Human WT JAK1 or S515518A JAK1
Vector	pGEX-2T
DNA insert	JAK1 SH2: aa 439 - 544
Forward Primer	5'-TAAGCT *GGATCC* GGCTGTCATGGTCCAATCTG-3'
Reverse Primer	5'-AGCTTA *GAATTC* **TTA** GTGATGGTGATGGTGATG GCAGCAGCGTTTTAGCATG-3'

His tag underlined, stop codon in bold type, and restriction site italicise. Primers were synthesised by Biomers.net.

PCR reactions were prepared on ice in thin walled PCR tubes as follows:

Promega Pfu DNA polymerase 10X Buffer with MgSO4	5 µl
NEB dNTP mix (dATP, dCTP, dGTP and dTTP; 10mM each)	1 µl
Forward primer	25pmol
Reverse primer	25pmol
DNA template (10 ng/µl)	1 µl
Promega Pfu DNA polymerase (2-3 U/µl)	0.42 µl
Sterile dH2O	final volume of 50 µl

PCR reactions were carried out in a thermocycler using the following conditions:

PCR step	Temp.(°C)	Time	No. of Cycles
Initial Denaturation	95	2 mins	1
Denaturation	95	1 min	35
Primer Anneal	55	Tm - 5 °C	
Extension	72	2mins/Kb	
Final Extension	72	5 mins	1
Hold	4	hold	1

The optimal annealing temperature is generally calculated as 5 °C lower than the lowest melting temperature (Tm) of the two primers. The extension time for Promega pfu DNA polymerase was calculated as per manufacturer's instruction at approximately 2 minutes for every 1 kb to be amplified. After the PCR reaction was complete, the resultant PCR product was then digested (section 2.7.8.2) with BamHI and EcoRI.

2.7.8.2 Restriction endonuclease digestion

Restriction enzymes were purchased from Promega and digestions were performed in accordance with the manufacturer's instructions. The appropriate pair of enzymes was chosen to cut plasmids or PCR product in a 10x buffer compatible with both enzymes. Reactions were set up in 1.5 ml microcentrifuge tubes, for example:

Restriction Enzyme 10X Buffer	3 µl
Acetylated BSA (10µg/ul)	0.2 µl
Plasmid(100ng/µl)/PCR product	10 µl/20 µl
Restriction Enzyme #1 (10 U/µl)	1 µl
Restriction Enzyme #2 (10 U/µl)	1 µl
Sterile dH_2O	final volume of 30 µl

Samples were mixed and spun briefly before incubation at 37 °C for 3-4 hrs. After the digestion was complete, the product was analysed using agarose gel electrophoresis. Both digested plasmid and digested PCR products were run on either a 0.5% or a 2% (w/v) agarose gel to confirm the size and digestion of the plasmid DNA or PCR product.

2.7.8.3 DNA agarose gel electrophoresis

Plasmid DNA and PCR products (DNA samples) were analysed by agarose gel electrophoresis using 0.5% (w/v) and 2% (w/v) gels respectively. To prepare the gels, 1 g or 4 g of agarose was dissolved in 200 ml TAE buffer (40 mM Tris, 1 mM EDTA, 40 mM glacial acetic acid) by boiling in a microwave. Once the solution had cooled to hand-warm, 0.5 µg/µl ethidium bromide was mixed with the solution and poured into a gel casting cassette containing the appropriate loading comb. Once the gels sets, the gel was transferred to a horizontal gel tank filled with TAE buffer. 6x loading dye (Promega) was added to each DNA sample and a 100 bp or 1 kb DNA ladder (Promega) prior loading each sample into the wells of the gel. Electrophoresis was performed at a constant voltage of 100 V for approximately 1 hour until good separation of the DNA ladder had been obtained. Ethidium bromide is a nucleic acid stain which allows DNA bands to be visualised on a UV light box (254 nm wavelength). The DNA bands were visualised and recorded using a BioRad Molecular Imager ChemiDoc XRS+ System.

2.7.8.4 Gel extraction

DNA bands of the appropriate size were extracted and purified from agarose gels using the Qiagen QIAquick Gel Extraction Kit as per the manufacturer's instruction, specifically the centrifugation protocol. DNA was eluted in nuclease free water and stored at -20°C. The DNA concentration was determined at A260 using a NanoDropTM 1000 Spectrophotometer prior to storage at -20°C (section 2.7.5).

2.7.8.5 Ligation reactions

DNA ligase was purchased from Promega and ligation reactions were performed in accordance with the manufacturer's instructions. The insert DNA fragment (PCR product) and the target plasmid vector were digested with the appropriate

restriction enzymes (section 2.7.8.2) and subsequently isolated by gel extraction (section 2.7.8.3-4) prior to ligation.

Ligation reactions were carried out in thin-walled PCR tubes and set up on ice:

DNA insert: WT or S515518A JAK1 SH2	75ng
Vector: pGEX-2T	25ng
Ligase 10X Buffer	1µl
T4 DNA Ligase	1µl
Sterile dH_2O	final volume of 10 µl

Vector only, insert only, and DNA-free controls were also set up. The reactions were incubated at 15°C overnight. The reaction mixture was the transformed into XL10 cells and plated with appropriate selection antibiotic. The plasmid DNA concentration was determined at A260 using a NanoDropTM 1000 Spectrophotometer prior to storage at -20°C (section 2.7.5). The generation of new DNA constructs was confirmed by DNA sequencing, performed by the University of Dundee Sequencing Service (section 2.7.6).

2.7.9 GST fusion protein expression in E.coli

E.Coli BL21 (Agilent) cells were transformed with pGEX-2T, pGEX-WT JAK1 SH2, pGEX S515A/S518A JAK1 SH2 or pGEX-ACC1-His_6 and cultured shaking overnight in 10mls of LB-broth (ampicillin, 50 µg/ml) at 37 °C. This culture was used to inoculate a large culture of 400mls in a 1 litre conical flask (1:50 dilution, 8 mls into 400mls) which was grown (shaking, 37 °C) until optical density readings at 600 nm (OD600) reached 0.3. At this point GST-fusion protein expression was induced by the addition of isopropyl-ß-D-thio-galactopyranoside (ITPG, final concentration 1 mM achieved by a 1:100 dilution from 100 mM stock solution). Bacteria were allowed to grow for four hours when cells were collected by centrifugation (6700 x g, 15 mins, 4°C). Broth was removed, and cell pellets were frozen overnight at -80 °C.

To monitor protein expression, hourly 1ml samples were removed from the broth during IPTG induction. These samples were pelleted and the pellet re-suspended

in 12 % (w/v) SDS sample buffer. Samples were probe sonicated on ice for 3 x 20 seconds with 1 minute intervals to prevent build-up of heat followed by brief centrifugation. Samples were analysed by SDS-PAGE (section 2.5) and Coomassie Brilliant Blue R-250 (Section 2.7.12).

2.7.10 Purification of His-tagged proteins

Bacterial pellets were thawed and resuspended in 20 mls His lysis buffer (20mM Na3PO4, 500mM NaCl, 10mM imidazole, 1% (v/v) Triton-100, pH7.4) per 400mls of E.Coli broth. Samples were probe sonicated on ice for 6 x 20 seconds with 1 minute intervals to prevent build-up of heat and centrifuged (25 000 g, 30 mins, 4°C) to pellet insoluble material. The cleared lysate was mixed with 0.6 ml of a 50 % (v/v) Ni sepharose bead suspension in His lysis buffer and incubated for 1 hour at 4 °C with rotation in order to immobilise His-tagged proteins on the beads. The beads were pelleted by gentle centrifugation (500 g, 5 mins, 4 °C), washed twice in 10 ml pre-elution buffer (20mM Na3PO4, 500mM NaCl, 20mM imidazole, pH7.4) and then transferred to a microfuge tube for a final wash in 1 ml pre-elution buffer. Beads were resuspended in 0.3mls elution buffer (20mM Na3PO4, 500mM NaCl, 20mM imidazole, pH7.4) per one ml of beads and incubated on ice for 5-10 minutes with gentle agitation. Beads were pelleted (500 g, 5 mins, 4 °C) and eluate was gently removed and retained. Elution with 0.3 mls elution buffer, incubation and centrifugation was repeated twice and eluate sample two and three were retained. Pooled eluates were concentrated and buffer exchanged into kinase buffer (section 2.9.1) using Vivaspin sample concentrator (GE Healthcare). Protein concentration was assessed by BCA assay (section 2.3) Each His-tagged protein were analysed by SDS-PAGE (Section 2.5) and Coomassie Brillant Blue R-250 (section 2.7.12). His-tagged proteins were stored in aliquots as required and stored at -80 °C.

2.7.11 Purification of GST-tagged proteins

Bacterial pellets were thawed and resuspended in 20 mls GST lysis buffer (50mM Hepes, 150 NaCl, 5mM EDTA, 1% (v/v) Triton-100) per 400mls of E.Coli broth. Samples were probe sonicated on ice for 6 x 20 seconds with 1 minute intervals to prevent build-up of heat and centrifuged (25 000 g, 30 mins, 4 °C) to pellet insoluble material. The cleared lysate was mixed with 0.6 ml of a 50 % (v/v)

Glutathione Sepharose 4B beads suspension in GST lysis buffer and incubated for 1 hour at 4 °C with rotation in order to immobilise GST-tagged proteins on the beads. The beads were pelleted by gentle centrifugation (500 g, 5 mins, 4 °C), washed twice in 10 ml PBS and then transferred to a microfuge tube for a final wash in 1 ml PBS. The GST-tagged proteins were eluted from the beads by incubation with reduced Glutathione. PBS was aspirated from the tube and the beads were resuspended in 0.3 mls elution buffer (10 mM Glutathione, 50 mM Tris-HCl, pH 8.0) per one ml of beads for 5-10 minutes on ice with gentle agitation. Beads were pelleted at 500 x g (4 °C, five minutes) and eluate was gently removed and retained. Elution with 0.3mls elution buffer, incubation and centrifugation was repeated twice and eluate sample two and three were retained. Pooled eluates were concentrated and buffer exchanged into kinase buffer using Vivaspin sample concentrator (GE Healthcare). Protein concentration was assessed by BCA assay (section 2.3) Each GST-tagged protein were analysed by SDS-PAGE (section 2.5) and Coomassie Brilliant Blue R-250 (section 2.7.12). GST-tagged proteins were stored in aliquots as required and stored at -80 °C.

An alternative approach used to purify GST-JAK1 SH2 proteins was to replace the lysis buffer prepared in-house with the commercially available protein extraction reagent, BugBuster (Merk Millipore). Following induction of protein expression in the E.coli cells (section 2.7.9), the cells were pelleted and lysed in BugBuster as per manufacturer's instructions. In brief, bacterial pellets were thawed and resuspended in room temperature BugBuster reagent, using 5 ml reagent per gram of wet cell paste. The cell suspension was incubated on a rotating mixer at a slow setting for 10–20 minutes at room temperature. Insoluble cell debris was removed by centrifugation (16,000 g 20 mins, 4°C) and the supernatant was transferred to a fresh tube. For SDS-PAGE analysis, a small sample of the supernatant (25–50 µl) was combined with equal volume of 12 % (w/v) SDS sample buffer and heated for 3 minutes at 85°C. Samples were analysed by SDS-PAGE (section 2.5) and Coomassie Brilliant Blue R-250 (section 2.7.12).

A final approach to purifying GST-JAK1 SH2 proteins was to use the Rapid GST Inclusion Body Solubilization and Renaturation Kit (Cell Biolabs.), which was used as per manufacturer's instructions. Briefly, GST-tagged protein expression was induced with 0.1 mM IPTG at 37ºC for 3 hrs (section 2.7.9). Cell pellet was lysed

in STE Extraction Buffer (500 mM Tris, pH 7.5, 1.5 M NaCl, 10 mM EDTA). To solubilize and renature GST-tagged proteins, the cell lysate/inclusion body mixture was mixed with Detergent Solubilization Solution (diluted 1:2 with STE extraction buffer (2 fold dilution). The cell lysate was then separated into soluble and insoluble fractions by centrifugation (12000 g, 15 mins, 4°C). The soluble fraction was then mixed with Detergent Neutralization Solution. Soluble GST-tagged proteins were then purified from the renatured soluble protein fraction by GST-tag batch purification. Samples were analysed by SDS-PAGE (section 2.5) and Coomassie Brilliant Blue R-250 (section 2.7.12).

2.7.12 Coomassie staining

To detect proteins on an SDS PAGE gel, Coomassie Brilliant Blue R-250 (0.25 g Coomassie Brilliant Blue R in H2O: Methanol: Glacial Acetic Acid [4.5:4.5:1 v/v/v]) was used. After removal from the glass plates, the gel was immersed in Coomassie Brilliant Blue R-250 for at least 1 h with gently agitation. After this, the stain was poured off, and the gel washed in distilled water. To remove the excess stain from the gel and allow visualisation of the proteins, the gel was submerged in Destain Solution (5 % (v/v) Methanol, 10 % (v/v) Glacial Acetic Acid), typically overnight.

2.8 Peptide array

2.8.1 CelluSpot synthesis of peptide array

Peptide arrays were kindly prepared by Professor G.S. Baillie (University of Glasgow, Institute of Cardiovascular and Medical Sciences) using automatic SPOT synthesis as described (Frank, 2002). Briefly, cellulose-conjugated peptides are synthesised and spotted in duplicate onto a nitrocellulose coated microscope slide producing a 3-dimensional library of peptides.

Successive 25-mer peptides spanning the human JAK1, JAK2, JAK3 and TYK2 open reading frames were prepared and each consecutive peptide has a five amino-acid shift compared to the previous peptide (Tables 6.1-6.4).

Peptide arrays were spotted with a wild-type (WT) and Ser-Ala mutant versions of the human JAK1 25-mer peptides identified as potential AMPK substrates, R-Y-S^{508}-L-H-G-S^{512}-D-R-S^{515}-F-P-S^{518}-L-G-D-L-M-S^{524}-H-L-K-K-Q-I (Tables 6.3-6.4). The JAK2,

JAK3 and TYK2 25-mer peptides that aligned with the JAK1 25-mer peptide (Figure 4.11) identified as phosphorylated by AMPK were also spotted on the same peptide arrays to allow for direct comparison (Table 6.3-6.4).

2.8.2 Peptide array overlays with HRP-conjugated human 14-3-3ζ

14-3-3ζ belongs to the 14-3-3 family of proteins that interact with a wide variety of proteins containing phosphoserine and phosphothreonine-motifs (Bridges and Moorhead, 2005). Peptide arrays consisting of Ser phosphorylated JAK 25-mer peptide identified as potential AMPK phosphorylation sites was overlaid with HRP-conjugated recombinant human 14-3-3ζ. Briefly, prior to overlay with HRP-14-3-3ζ, the peptide arrays were washed (2 x 5 mins) in TBST (10 mM Tris, pH 7.6, 150 mM NaCl, 0.1% (v/v) Tween 20) and blocked in 5% (w/v) BSA in TBST for 1 hr at room temperature. Subsequently, peptide arrays were incubated with HRP-14-3-3ζ (1:500) in 5% (w/v) BSA in TBST overnight at 4^0C with shaking. Arrays were then washed (2 x 5 mins) in TBST. Reactive spots were visualised using Perkin-Elmer enhanced chemiluminescence (ECL) detection reagents, according to the manufacturer's instructions. Briefly, the arrays were incubated in 2 ml ECL reagent for 1 minute and blotted onto paper towel to remove excess liquid. Peptide array was mounted onto an X-ray cassette for exposure to Medical X-ray Blue/MXBE Film (Carestream Health, 7710783) and developed using an X-OMAT 2000 processor (Kodak).

2.9 In vitro AMPK phosphorylation assays

2.9.1 JAK isoform peptide arrays

In vitro AMPK phosphorylation of an immobilised library of full length human JAK1, JAK2 and TYK2, and Serine-Alanine mutated JAK1 25-mer peptides (Table 6.1-6.4) was under taken using AMPK purified from rat liver a generous gift from Prof. D.G. Hardie (University of Dundee) (Hawley et al., 1996) , and [γ-^{32}P] ATP. In brief, 0.5U/ml active AMPK and 1μCi/ml [γ-32P] ATP was diluted in kinase buffer (50mM HEPES pH7.4, 0.01% (v/v) Brij-35, 1mM DTT, 1mM ATP, 0.2mM AMP, 25mM MgCl2, 1% (w/v) BSA) and incubated with arrays at 30ºC for 30 minutes with agitation. Phosphorylation was detected by incorporation of radiolabelled 32P and signals were captured by autoradiography following exposure to Medical X-ray Blue/MXBE Film (Carestream Health, 7710783) for 2 days at -80ºC and developed using a X-

OMAT 2000 processor (Kodak). As a positive control, each peptide array contains a synthetic AMPK substrate called SAMS peptide (HMRSAMSGLHLVKRR) (Davies et al., 1989).

2.9.2 Full length human JAK1 protein

In vitro AMPK phosphorylation of full length JAK1 protein was under taken using purified active rat liver AMPK, and [γ-^{32}P] ATP. JAK1-deficient U4C cells were transfected with either a purified wild-type (WT) FLAG-tagged recombinant human JAK1 plasmid (section 2.1.9). FLAG-tagged JAK1 was immunoprecipitated (section 2.4.3) from protein equalised cell lysates by incubating with Anti-FLAG M2 affinity gel overnight at 4°C. Anti-FLAG M2 affinity gel precipitates were washed twice in RIPA buffer and twice with kinase buffer. Each precipitate was incubated for 10 minutes at 30 °C in the absence or presence of 0.5U/ml activated AMPK with or without 0.2mM AMP, and in the presence of 10μCi/ml [γ-^{32}P] ATP. JAK1 was eluted (section 2.4.2) from the immunocomplexes and subjected to SDS-PAGE on 8% (w/v) acrylamide resolving gels and transfer to nitrocellulose as described in sections 2.5 and 2.6.2. Phosphorylation of JAK1 was detected by autoradiography as described in section 2.9.1.

2.9.3 Full length human ACC protein

In vitro AMPK phosphorylation of full length ACC Ser79 was undertaken using purified active rat liver AMPK. ACC is a biotinylated enzyme; thus biotin-streptavidin affinity purification can be used to isolate ACC (Chen et al., 2000). HEK293 cells were prepared for purification as described in section 2.4.1. Purification of biotinylated proteins was performed as described in section 2.4.2 with the exception that 35μl packed volume (per sample) of streptavidin-Sepharose beads were used in place of protein G-Sepharose beads and primary antibodies. Biotin-streptavidin affinity gel precipitates were washed twice in RIPA buffer and twice with kinase buffer. Each precipitate and streptavidin-depleted lysate was incubated for 10 minutes at 30 °C in the absence or presence of 0.5U/ml activated AMPK with or without 0.2mM AMP, and in the presence of 10μCi/ml [γ-32P] ATP. Biotinylated proteins were eluted from the Sepharose beads and subjected to SDS-PAGE (section 2.5) on 8% (w/v) acrylamide resolving gels and

phosphorylation of ACC was detected by immunoblotting (section 2.6) for phospho-ACC (Ser79) and Total ACC.

2.9.4 GST-JAK1 SH2 fusion proteins

Purified GST-ACC, WT GST-JAK1 SH2 and S515A/S518A mutant GST JAK1 SH2 fusion proteins, and GST alone (section 2.7.8-11) were subjected to *in vitro* kinase assays using purified active rat liver AMPK, and [γ-^{32}P] ATP. Each GST fusion protein was incubated for 30 minutes at 30°C in the absence or presence of 0.5U/ml AMPK with or without 0.2mM AMP, and in the presence of 10μCi/ml [γ-^{32}P] ATP. *In vitro* kinase reactions were subject to SDS-PAGE (section 2.5) on 12% (w/v) acrylamide resolving gels and transfer to nitrocellulose (section 2.6.2). Phosphorylation of GST fusion proteins was detected by autoradiography (section 2.9.1.), followed by probing the immunoblot (section 2.6) with GST-HRP to detect GST-fusion proteins.

2.10 Statistical analysis

Statistical analysis was performed using the InStat software v3.6 (GraphPad, USA). Statistical significance was evaluated with one-way ANOVA analysis followed by the Bonferroni multiple comparisons test. Data are presented as mean ± SEM.
$p < 0.05$ was considered significant.

Chapter 3 - Molecular mechanism of AMPK mediated inhibition of IL-6 signalling: AMPK downstream targets

3.1 Introduction

3.1.1 IL-6 signalling via the JAK-STAT pathway

As detailed in the introduction (section 1.3.2), activation of IL-6 signal transduction involves gp130 dimerization, ligand-dependent tyrosine phosphorylation of JAKs, followed by tyrosine phosphorylation of STATs, with subsequent translocation of STAT dimers into the nucleus to regulate the transcription of target genes, including CRP (Zhang et al., 1996) and MCP-1 (Jougasaki et al., 2010), which are involved in the inflammatory response. While STAT1 and STAT3 are both activated by IL-6, STAT3 is preferentially activated (Darnell et al., 1994).

3.1.2 Regulation of the JAK-STAT pathway by AMPK

While AMPK has been found to inhibit MAPK/NF-κB pro-inflammatory pathways in endothelial cells (reviewed by Salt and Palmer, 2012), the effect of AMPK on JAK-STAT pro-inflammatory signalling in endothelial cells had yet to be fully characterised. Previous unpublished studies in our group have investigated whether AMPK modifies cytokine stimulation of JAK-STAT signalling in HUVECs (section 6.1, Claire Rutherford, Marie-Ann Ewart, Ian Salt, Tim Palmer, personal communication). These preliminary investigations demonstrated that pre-treatment of HUVECs with AMPK activator, A769662, significantly inhibits both sIL-6Rα/IL-6 and IFN-α stimulation of STAT3 Tyr705 phosphorylation in HUVECs (Figure 6.5A). IFN-α activates STATs via an IFNAR1/IFNAR2 complex which is distinct from the sIL-6Rα/IL-6/gp130 complex (Borden et al., 2007). The studies in this thesis therefore tested the hypothesis that AMPK was exerting its inhibitory effects at one or more common signalling loci downstream of IFNAR1/IFNAR2 and gp130 at a post-receptor level.

3.1.3 Potential downstream targets of AMPK mediating inhibition of IL-6 signalling

AMPK has been demonstrated to mediate its metabolic effects via a variety of downstream targets (Hardie et al., 2012). Therefore, it was important to investigate whether AMPK could act via a known downstream target to inhibit IL-6 signalling. To narrow down the list of candidates, the current literature was studied to identify whether any of the AMPK targets have been linked with inflammatory signalling. Interestingly, TC-PTP and SHP2, negative regulators of JAK-STAT signalling, were identified as AMPK downstream targets (Lam et al., 2001, Nerstedt et al., 2013). Furthermore, endothelial nitric oxide synthase (eNOS), protein kinase C λ (PKCλ), sirtuin 1 (SIRT1), carnitine palmitoyltransferase 1 (CPT1), and mammalian target of rapamycin (mTOR) were identified as either directly or indirectly having an impact on JAK-STAT signalling and have been reported to be regulated by AMPK (Morrow et al., 2003, Zhang et al., 2011, Cantó and Auwerx, 2009, Dagher et al., 2001, Inoki et al., 2003).

3.1.4 Aims

The aim of this chapter was to determine whether AMPK acts directly on a known regulator of JAK or STAT or an AMPK downstream target known to either directly or indirectly impact on JAK-STAT signalling. In order to determine whether inhibition of IL-6 signalling by AMPK was mediated by downstream targets of AMPK, a combination of genetic and pharmacological approaches was utilised to assess the role of each of the following AMPK targets: TC-PTP, SHP2, eNOS, PKCλ, SIRT1, CPT1 and mTOR.

3.2 Effect of phosphatases on AMPK-mediated regulation of IL-6 signalling

3.2.1 Effect of TC-PTP knockdown on A769662-mediated inhibition of STAT3 phosphorylation

JAK1, STAT1 and STAT3 have been reported to be direct substrates of TC-PTP (Yamamoto et al., 2002, ten Hoeve et al., 2002, Simoncic et al. 2002), while AMPK activation has been reported to alter cellular localisation of TC-PTP (Lam et al., 2001). Therefore, it was hypothesised that AMPK-mediated inhibition of STAT3 Tyr705 phosphorylation could potentially occur *via* TC-PTP.

A siRNA approach was used to specifically knockdown the expression of TC-PTP in order to determine the necessity of TC-PTP in AMPK-mediated inhibition of IL-6 stimulation of STAT3 Tyr705 phosphorylation. Control non-targeting siRNA and siRNA targeting TC-PTP were separately transiently transfected into HUVECs for 48 hours prior to pre-treatment with vehicle or 100μM A769662 for 40 minutes followed by stimulation with vehicle or 25ng/ml sIL-6Rα and 5ng/ml IL-6 (sIL-6Rα/IL-6) for a further 30 minutes as indicated.

In comparison to HUVECs treated with control siRNA, transfection of HUVECs with TC-PTP siRNA reduced TC-PTP expression by 60% (Figure 3.1). Activation of AMPK by A769662 was assessed by confirming AMPK-mediated ACC phosphorylation on Ser79 (Figure 3.1) (Davies et al., 1992).. sIL-6Rα/IL-6 treatment of HUVECs transfected with control or TC-PTP siRNA caused a significant (***p<0.001) stimulation of STAT3 Tyr705 phosphorylation, compared to the basal level (Figure 3.1). In comparison to sIL-6Rα/IL-6 stimulation of HUVECs transfected with control siRNA, siRNA mediated knockdown of TC-PTP had no (p>0.05, not significant [NS]) significant effect on sIL-6Rα/IL-6 stimulation of STAT3 Tyr705 phosphorylation. Pre-treatment with AMPK activator, A769662, caused a significant reduction of sIL-6Rα/IL-6 stimulation of STAT3 Tyr705 phosphorylation in both control and TC-PTP siRNA transfected HUVECs, relative to sIL-6Rα/IL-6 treatment alone, as STAT3 Tyr705 phosphorylation levels were significantly reduced by 67 ± 9% (***p<0.001) and 64 ± 9% (***p<0.001), respectively (Figure 3.1). Overall, siRNA mediated knockdown of TC-PTP did not attenuate the inhibitory effect of AMPK activation on STAT3 Tyr705 phosphorylation (Figure 3.1). The data shown in figure 3.1 was generated and analysed by Dr Claire Rutherford, University of Glasgow.

3.2.2 Effect of SHP2 on A769662-mediated inhibition of STAT3 phosphorylation

SHP2 has been reported to negatively regulate IL-6-stimulated STAT3 phosphorylation (Ohtani et al., 2000, Lehmann et al., 2003). Recently, it has been reported that AMPK activators, AICAR and metformin, reduced IL-6-stimulated SHP-2 phosphorylation in HepG2 cells (Nerstedt et al., 2013). Therefore, it was hypothesised that AMPK-mediated inhibition of STAT3 Tyr705 phosphorylation could potentially occur *via* SHP2.

SHP2 exon 3-deletion (SHP2−/−) 3T3 fibroblasts from mice express small amounts of a truncated SHP2 that lacks the N-terminal SH2 domain and does not localize appropriately to activated receptors (Saxton et al., 1997, Shi et al., 2000). SHP2-mediated inhibition of JAK-STAT signalling is dependent on its recruitment to the gp130 receptor (Stahl et al., 1994), therefore SHP2−/− 3T3 fibroblasts were used to assess a role for SHP2 in mediating AMPK's effects on STAT3 Tyr705 phosphorylation. SHP2+/+ 3T3 fibroblasts are SHP2-/- cells reconstituted with WT SHP2 (SHP2+/+) and SHP2-/- 3T3 fibroblasts were pre-treated with vehicle or 100μM A769662 for 40 minutes followed by stimulation with vehicle or 25ng/ml sIL-6Rα and 5ng/ml IL-6 (sIL-6Rα/IL-6) for a further 30 minutes as indicated.

Immunoblotting of cell extracts with SHP2 antibody confirmed that SHP2 was effectively depleted in SHP2 -/- 3T3 fibroblasts, relative to levels in SHP2+/+ 3T3 fibroblasts. sIL-6Rα/IL-6 treatment of SHP2 +/+ and SHP2-/- 3T3 fibroblasts caused a significant (**p<0.001) stimulation of STAT3 Tyr705 phosphorylation, compared to the basal level (Figure 3.2A). In comparison to sIL-6Rα/IL-6 stimulation of SHP2+/+ fibroblasts, depletion of SHP2 in SHP2-/- 3T3 fibroblasts had no effect on sIL-6Rα/IL-6 stimulation of STAT3 Tyr705 phosphorylation. In SHP2+/+ 3T3 fibroblasts, A769662 induced a marginal 14% reduction in STAT3 Tyr705 phosphorylation compared to sIL-6Rα/IL-6 treatment alone; however this did not reach statistical significance (p>0.05, NS) (Figure 3.2A). In SHP2-/- 3T3 fibroblasts, A769662 induced a substantial 31% reduction in STAT3 Tyr705 phosphorylation compared to sIL-6Rα/IL-6 treatment alone; however this did not reach statistical significance (p>0.05, NS) (Figure 3.2). Overall, loss of SHP2 function did not attenuate the inhibitory effect of AMPK activation on STAT3 Tyr705 phosphorylation (Figure 3.2A).

While SHP2 has been reported to negatively regulate IL-6 stimulation of JAK-STAT signalling, SHP2 positively regulates IL-6 stimulation of ERK signalling (Fukada et al., 1996). SHP2-mediated activation of ERK signalling is dependent on its recruitment to the gp130 receptor (Stahl et al., 1994). Therefore, to confirm that recruitment of SHP2 to the gp130 receptor is impaired in SHP2-/- 3T3 fibroblasts, SHP2-/- and SHP2+/+ 3T3 fibroblasts were treated with or without sIL-6Rα/IL-6 for 5, 10 and 15 minutes, followed by immunoblotting of whole cell extracts with phospho-ERK 1/2, total ERK, SHP2 antibody. As shown in Figure 3.2B, sIL-6Rα/IL-6 stimulated ERK1/2 phosphorylation in both SHP2-/- and SHP2+/+ 3T3 fibroblasts. Despite that SHP2 was effectively depleted in SHP2-/- 3T3, these cells demonstrated increased levels of ERK1/2 phosphorylation, compared to SHP2+/+ 3T3 fibroblasts (Figure 3.2B). The data shown in figure 3.2 was generated and analysed by Dr Claire Rutherford, University of Glasgow.

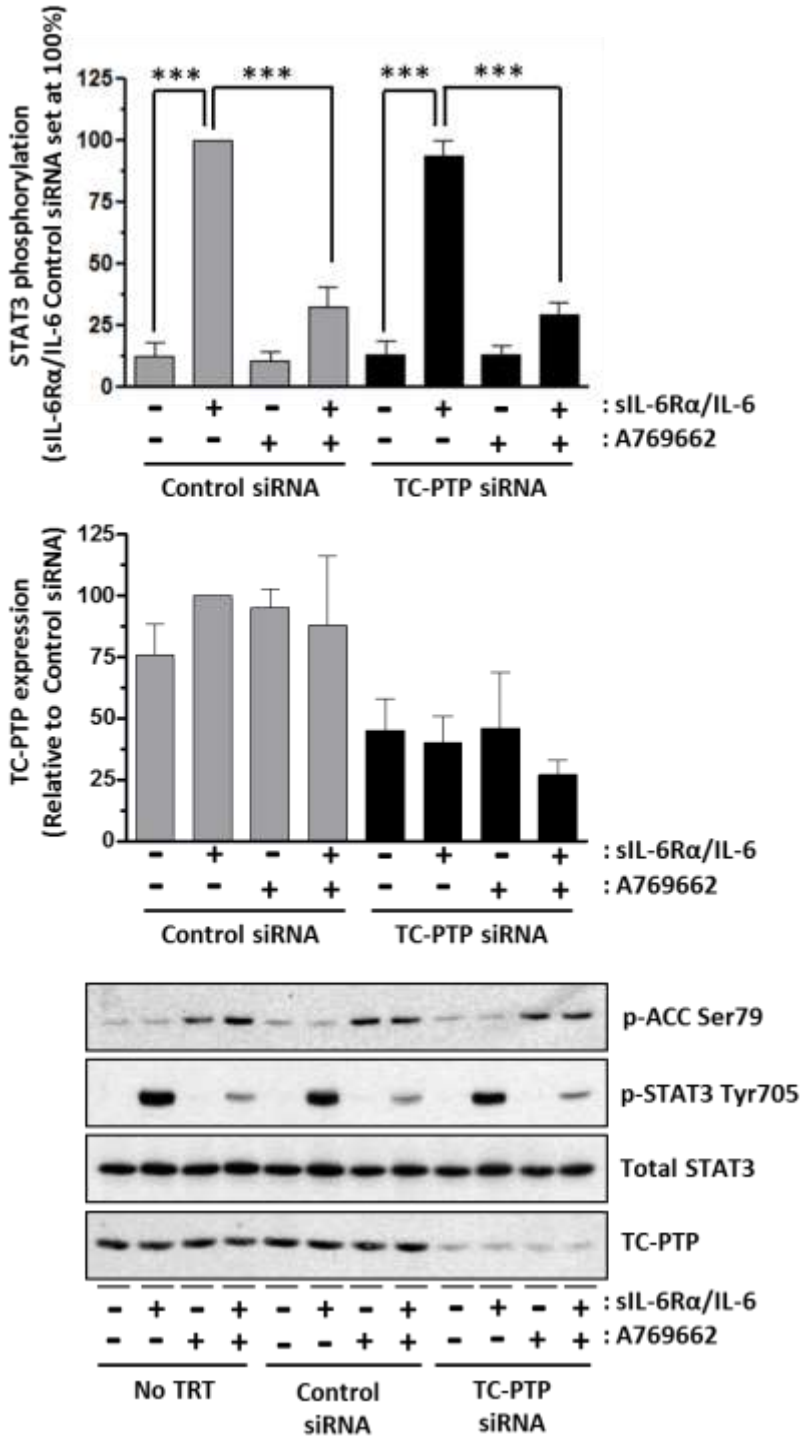

Figure 3.1: Effect of TC-PTP isoform knockdown on AMPK-mediated inhibition of sIL-6Rα/IL-6 stimulated STAT3 Tyr705 phosphorylation in HUVECs.
HUVECs were transfected with either 20nM TC-PTP or control siRNA 48hrs prior to pre-treatment with vehicle or 100μM A769662 for 40 minutes followed by stimulation with vehicle or 25ng/ml sIL-6Rα and 5ng/ml IL-6 (sIL-6Rα/IL-6) for a further 30 minutes as indicated. Control siRNA was used as a negative control. Protein-equalised cell extracts were then analysed by SDS-PAGE and immunoblotting with antibodies as indicated. STAT3 phosphorylation data were first normalized to total STAT3 levels and expressed as a percentage (%) of the maximal sIL-6Rα/IL-6 stimulation attained in vehicle pre-treated control siRNA transfected HUVECs. Total TC-PTP protein levels were first normalized to Total STAT3 levels and expressed as a percentage (%) of the maximal protein levels attained in sIL-6Rα/IL-6 stimulated control siRNA transfected HUVECs (set at 100%). Quantitative analysis from three experiments is presented. Columns are means ±SEM. *** p<0.001. A representative blot from n=3 experiments is shown. n=3 from one batch of pooled donor HUVEC (Data was generated and analysed by Dr. Claire Rutherford, University of Glasgow.)

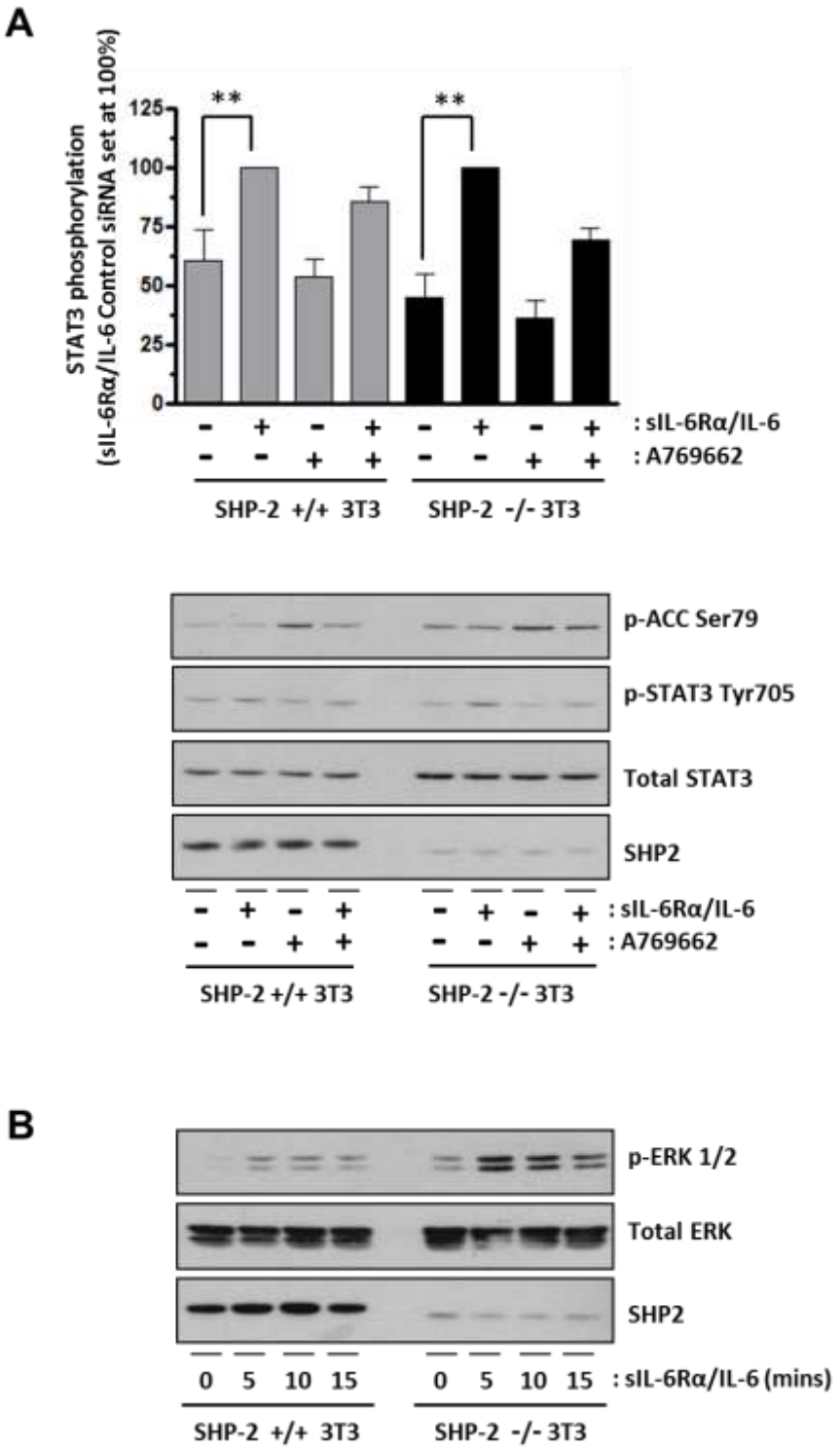

Figure 3.2: Effect of SHP2 on AMPK-mediated inhibition of sIL-6Rα/IL-6 stimulated STAT3 Tyr705 phosphorylation in 3T3 cells.
(A) SHP2+/+ and SHP2-/- 3T3 fibroblasts were pre-treated with vehicle or 100μM A769662 for 40 minutes followed by stimulation with vehicle or 25ng/ml sIL-6Rα and 5ng/ml IL-6 (sIL-6Rα/IL-6) for a further 30 minutes as indicated. Protein-equalised cell extracts were then analysed by SDS-PAGE and immunoblotting with antibodies as indicated. STAT3 phosphorylation data were first normalized to total STAT3 levels and expressed as a percentage (%) of the maximal sIL-6Rα/IL-6 stimulation attained in vehicle pre-treated SHP2+/+ or SHP2-/- 3T3 fibroblasts. Quantitative analysis from three experiments is presented. Columns are means ±SEM. A representative blot from n=3 experiments is shown. **(B)** SHP2+/+ and SHP2-/- 3T3 fibroblasts were treated with 25ng/ml sIL-6Rα and 5ng/ml IL-6 (sIL-6Rα/IL-6) for 5, 10 and 15 minutes as indicated. Protein-equalised cell extracts were then analysed by SDS-PAGE and immunoblotting with antibodies as indicated. (Data was generated and analysed by Dr. Claire Rutherford, University of Glasgow.)

3.3 Effect of eNOS inhibition on AMPK-mediated regulation of IL-6 signalling

AMPK directly phosphorylates and activates endothelial nitric oxide synthase (eNOS) to stimulate nitric oxide (NO) production in endothelial cells (Morrow et al., 2003). NO has previously been implicated in suppressing IL-6 induced STAT3 Tyr705 phosphorylation in response to shear stress (Ni et al., 2004) and subsequently shear stress was shown to induce AMPK to elevate NO production via phosphorylation and activation of eNOS (Zhang et al., 2006). Therefore, it was hypothesised that AMPK-mediated inhibition of STAT3 Tyr705 phosphorylation could potentially occur via eNOS. To test this, pharmacological and genetic approaches were utilised to assess a role for eNOS in mediating AMPK's effects on STAT3 phosphorylation in HUVECs.

3.3.1 Effect of L-NAME on A769662-mediated inhibition of STAT3 phosphorylation

NO is synthesised from L-arginine by eNOS in endothelial cells (Palmer et al., 1988). The L-arginine analogue L-NAME (Nω-Nitro-L-arginine methyl ester hydrochloride) is a competitive inhibitor of NOS and D-NAME (Nω-Nitro-D-arginine methyl ester hydrochloride) is an inactive isomer utilised as a control (Pfeiffer et al., 1996). 0.1mM L-NAME for 30 minutes has previously been shown to effectively inhibit AMPK-mediated NO production in human aortic endothelial cells (HAOECs) (Morrow et al., 2003). To determine whether pharmacological inhibition of eNOS by L-NAME altered AMPK-mediated inhibition of STAT3 phosphorylation, HUVECs were pre-treated with vehicle, 0.1mM L-NAME or 0.1mM D-NAME in endothelial cell growth medium for 30 minutes, followed by sequential treatment with A769662 and sIL-6Rα/IL-6.

Immunoblotting of whole cell extracts with phospho-ACC (Ser79) antibody confirmed AMPK activation by A769662, and that neither D-NAME nor L-NAME had any effect on A769662 activation of AMPK (Figure 3.3). sIL-6Rα/IL-6 treatment of vehicle pre-treated HUVECs caused a significant (***p<0.001) stimulation of STAT3 Tyr705 phosphorylation, compared to basal levels (Figure 3.3). A769662 significantly inhibited sIL-6Rα/IL-6 stimulation of STAT3 Tyr705 phosphorylation levels by 52 ± 7% (***p<0.01) in vehicle pre-treated HUVECs (Figure 3.3). Pre-treatment with either D-NAME and L-NAME induced a 14% and 25 ± 3% reduction

in STAT3 Tyr705 phosphorylation respectively, compared to sIL-6Rα/IL-6 treatment alone; however this did not reach statistical significance (p>0.05, NS) (Figure 3.3). In the presence of D-NAME, A769662 significantly (*p<0.05) inhibited sIL-6Rα/IL-6 stimulation of STAT3 Tyr705 phosphorylation levels by 28 ± 4 % (Figure 3.3). In the presence of L-NAME, A769662 induced a substantial 28 ± 4% reduction in STAT3 phosphorylation compared to sIL-6Rα/IL-6 treatment alone; however this did not reach statistical significance (p>0.05, NS) (Figure 3.3). Overall, pharmacological inhibiton of eNOS appeared to moderately reduce sIL-6Rα/IL-6 stimulation of STAT3 Tyr705 phosphorylation and the addition of A769662 further reduced the phosphorylation of STAT3, however this did not reach statistical significance (p>0.05, NS).

3.3.2 Effect of siRNA-mediated eNOS knockdown on A769662-mediated inhibition of STAT3 phosphorylation

An siRNA approach was used to specifically knockdown the expression of eNOS in order to determine the necessity of eNOS in AMPK-mediated inhibition of IL-6 stimulation of STAT3 Tyr705 phosphorylation. Control non-targeting siRNA and siRNA targeting eNOS were separately transiently transfected into HUVECs for 48 hours prior to pre-treatment with vehicle or 100μM A769662 for 40 minutes followed by stimulation with vehicle or 25ng/ml sIL-6Rα and 5ng/ml IL-6 (sIL-6Rα/IL-6) for a further 30 minutes as indicated.

In comparison to HUVECs treated with control siRNA, transfection of HUVECs with eNOS siRNA reduced eNOS expression by 50% (Figure 3.4). sIL-6Rα/IL-6 treatment of HUVECs transfected with control siRNA caused a significant (***p<0.001) stimulation of STAT3 Tyr705 phosphorylation, compared to the basal level (Figure 3.4). Pre-treatment of control siRNA transfected HUVECs with A769662 significantly (***p<0.001) inhibited sIL-6Rα/IL-6 stimulation of STAT3 Tyr705 phosphorylation by 62 ± 10%, compared to sIL-6Rα/IL-6 treatment alone (Figure 3.4). siRNA-mediated knockdown of eNOS significantly (***p<0.001) inhibited sIL-6Rα/IL-6 stimulation of STAT3 Tyr705 phosphorylation by 38 ± 6% compared to control siRNA transfected HUVECs treated with sIL-6Rα/IL-6 treatment alone (Figure 3.4). Pre-treatment of eNOS siRNA transfected HUVECs with A769662 significantly inhibited sIL-6Rα/IL-6 stimulation of STAT3 Tyr705 phosphorylation by 34 ± 6% (***p<0.001), compared to sIL-6Rα/IL-6 treatment alone (Figure 3.4).

Overall, siRNA-mediated knockdown of eNOS in HUVECs attenuated sIL-6Rα/IL-6 stimulation of STAT3 Tyr705 phosphorylation, but did not attenuate the inhibitory effect of AMPK activation on STAT3 Tyr705 phosphorylation (Figure 3.4). The data shown in figure 3.4 was generated and analysed by Dr Claire Rutherford, University of Glasgow.

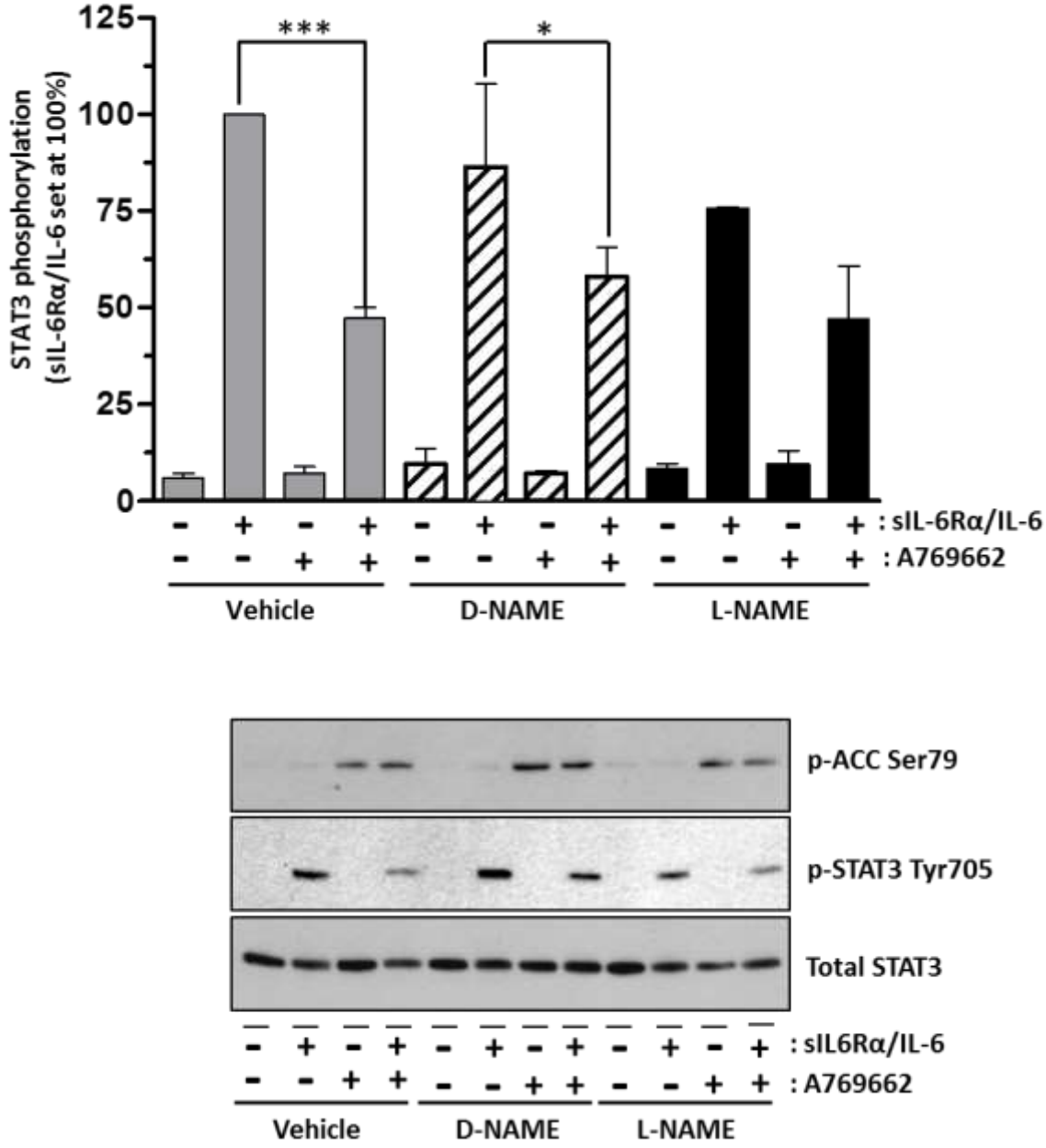

Figure 3.3: Effect of eNOS inhibitor L-NAME on AMPK-mediated inhibition of sIL-6Rα/IL-6 stimulated STAT3 phosphorylation in HUVECs

HUVECs were pre-treated with vehicle or 0.1mM L-NAME and as a negative control 0.1mM D-NAME for 30 minutes, and then treated with or without 100μM A769662 for 40 minutes prior to the addition of vehicle or 25ng/ml sIL-6Rα and 5ng/ml IL-6 (sIL-6Rα/IL-6) for a further 30 minutes as indicated. Protein-equalised cell extracts were then analysed by SDS-PAGE and immunoblotting with antibodies as indicated. STAT3 phosphorylation data were first normalized to total STAT3 levels and expressed as a percentage (%) of the maximal sIL-6Rα/IL-6 stimulation attained in vehicle pre-treated HUVECs. Quantitative analysis from three experiments is presented. Columns are means ±SEM. *** $p<0.001$, *$p>0.05$. A representative blot from n=3 experiments is shown. n=3 from one batch of pooled donor HUVEC

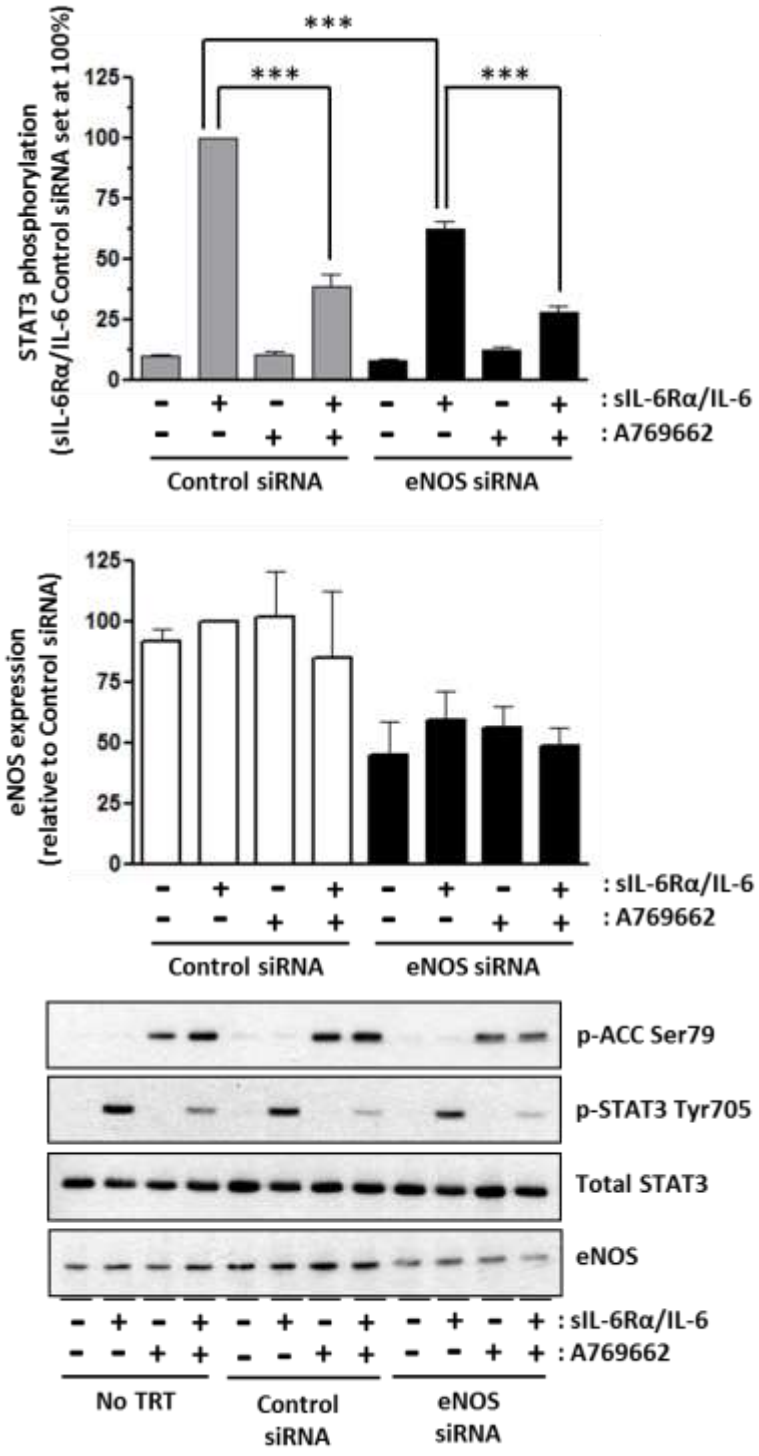

Figure 3.4: Effect of eNOS isoform knockdown on AMPK-mediated inhibition of sIL-6Rα/IL-6 stimulated STAT3 Tyr705 phosphorylation in HUVECs.
HUVECs were transfected with either 170nM eNOS or control siRNA 48hrs prior to pre-treatment with vehicle or 100µM A769662 for 40 minutes followed by stimulation with vehicle or 25ng/ml sIL-6Rα and 5ng/ml IL-6 (sIL-6Rα/IL-6) for a further 30 minutes as indicated. Control siRNA was used as a negative control. Protein-equalised cell extracts were then analysed by SDS-PAGE and immunoblotting with antibodies as indicated. STAT3 phosphorylation data were first normalized to total STAT3 levels and expressed as a percentage (%) of the maximal sIL-6Rα/IL-6 stimulation attained in vehicle pre-treated control siRNA transfected HUVECs. Total eNOS protein levels were first normalized to Total STAT3 levels and expressed as a percentage (%) of the maximal protein levels attained in sIL-6Rα/IL-6 stimulated control siRNA transfected HUVECs (set at 100%). Quantitative analysis from three experiments is presented. Columns are means ±SEM. *** p<0.001. A representative blot from n=3 experiments is shown. n=3 from one batch of pooled donor HUVEC (Data was generated and analysed by Dr. Claire Rutherford, University of Glasgow.)

3.4 Effect of PKC inhibition on AMPK-mediated regulation of IL-6 signalling

STAT3 is acetylated by its coactivator p300/CBP, resulting in increased DNA binding and transcriptional activity (Wang et al., 2005), and several reports have demonstrated that acetylation is required for phosphorylation of STATs (Zhuang, 2013). AMPK has been reported to indirectly phosphorylate p300 *via* the atypical PKCλ, resulting in inhibition of the histone acetyltransferase activity of p300 (Zhang et al., 2011). Therefore, it was hypothesised that AMPK-mediated inhibition of STAT3 Tyr705 phosphorylation could potentially occur *via* PKCλ. To test this hypothesis, pharmacological and genetic approaches were utilised to assess a role for PKC in mediating AMPK's effects on STAT3 phosphorylation in HUVECs.

3.4.1 Effect of GF109203X on A769662-mediated inhibition of STAT3 phosphorylation

GF109203X (3-[1-[3-(dimethylaminopropyl]-1H-indol-3-yl]-4-(1H-indol-3-yl)-1H-pyrrole-2,5-dione monohydrochloride), a bisindolylmaleimide, potently and selectively inhibits PKC isoforms by competing with enzyme-bound ATP (Toullec et al., 1991). phorbol 12-myristate 13-acetate (PMA) activation of novel and conventional isoforms of PKC results in activation of the ERK pathway (Schönwasser et al., 1998). 10μM GF109203X for 30 minutes abolished PMA-induced ERK activation in HUVECs, (Tim Palmer; personal communication). To determine whether pharmacological inhibition of PKC by GF109203X altered AMPK-mediated inhibition of STAT3 phosphorylation, HUVECs were pre-treated with vehicle or 10μM GF109203X for 30 minutes, followed by sequential treatment with A769662 and sIL-6Rα/IL-6.

In vehicle pre-treated cells, phospho-ACC levels were substantially increased in the presence of A769662, relative to the absence of A769662 (Figure 3.5). In contrast, A769662-mediated phosphorylation of ACC was reduced in GF109203X pre-treated cells (Figure 3.5). sIL-6Rα/IL-6 induced a significant (***p<0.001) increase in STAT3 Tyr705 phosphorylation in both the presence and absence of GF109203X, compared to the basal level (Figure 3.5). In comparison to sIL-6Rα/IL-6 stimulation of HUVECs in the absence of GF109203X, the presence of GF109203X had no significant effect on sIL-6Rα/IL-6 stimulation of STAT3 Tyr705

phosphorylation (p>0.05, NS). Sequential treatment of HUVECs with A769662 and sIL-6Rα/IL-6 in the absence or presence of GF109203X caused a significant 53 ± 6% (***p<0.001) and 61 ± 6% (***p<0.001) inhibition of STAT3 Tyr705 phosphorylation, respectively, compared to IL-6Rα/IL-6 treatment alone (Figure 3.5). Overall, pharmacological inhibition of PKC by GF109203X did not attenuate the inhibitory effect of AMPK activation on STAT3 Tyr705 phosphorylation (Figure 3.5).

3.4.2 Effect of siRNA-mediated PKCλ knockdown on A769662-mediated inhibition of STAT3 phosphorylation

An siRNA approach was used to specifically knockdown the expression of PKCλ in order to determine the necessity of PKCλ in AMPK-mediated inhibition of IL-6 stimulation of STAT3 Tyr705 phosphorylation. Control non-targeting siRNA and siRNA targeting PKCλ were separately transiently transfected into HUVECs for 48 hours prior to pre-treatment with vehicle or 100μM A769662 for 40 minutes followed by stimulation with vehicle or 25ng/ml sIL-6Rα and 5ng/ml IL-6 (sIL-6Rα/IL-6) for a further 30 minutes as indicated.

In comparison to HUVECs treated with control siRNA, transfection of HUVECs with PKCλ siRNA reduced PKCλ expression by 40% (Figure 3.6). Immunoblotting of cell extracts with phospho-ACC (Ser79) antibody confirmed AMPK activation by A769662 and siRNA mediated knockdown of PKCλ had no effect on A769662 activation of AMPK (Figure 3.6). sIL-6Rα/IL-6 treatment of HUVECs transfected with control or PKCλ siRNA caused a significant (***p<0.001) stimulation of STAT3 Tyr705 phosphorylation, compared to the basal level (Figure 3.6). In comparison to sIL-6Rα/IL-6 stimulation of HUVECs transfected with control siRNA, siRNA mediated knockdown of PKCλ had no significant (p>0.05, NS) effect on sIL-6Rα/IL-6 stimulation of STAT3 Tyr705 phosphorylation. Pre-treatment with A769662 caused a significant reduction of sIL-6Rα/IL-6 stimulation of STAT3 Tyr705 phosphorylation in both control and PKCλ siRNA transfected HUVECs, relative to sIL-6Rα/IL-6 treatment alone, as STAT3 Tyr705 phosphorylation levels were reduced by 74 ± 9% (***p<0.001) and 91 ± 11% (***p<0.001), respectively (Figure 3.6). Overall, siRNA mediated knockdown of PKCλ did not attenuate the inhibitory effect of AMPK activation on STAT3 Tyr705 phosphorylation (Figure 3.6). The data shown in figure 3.6 was generated and analysed by Dr Claire Rutherford, University of Glasgow.

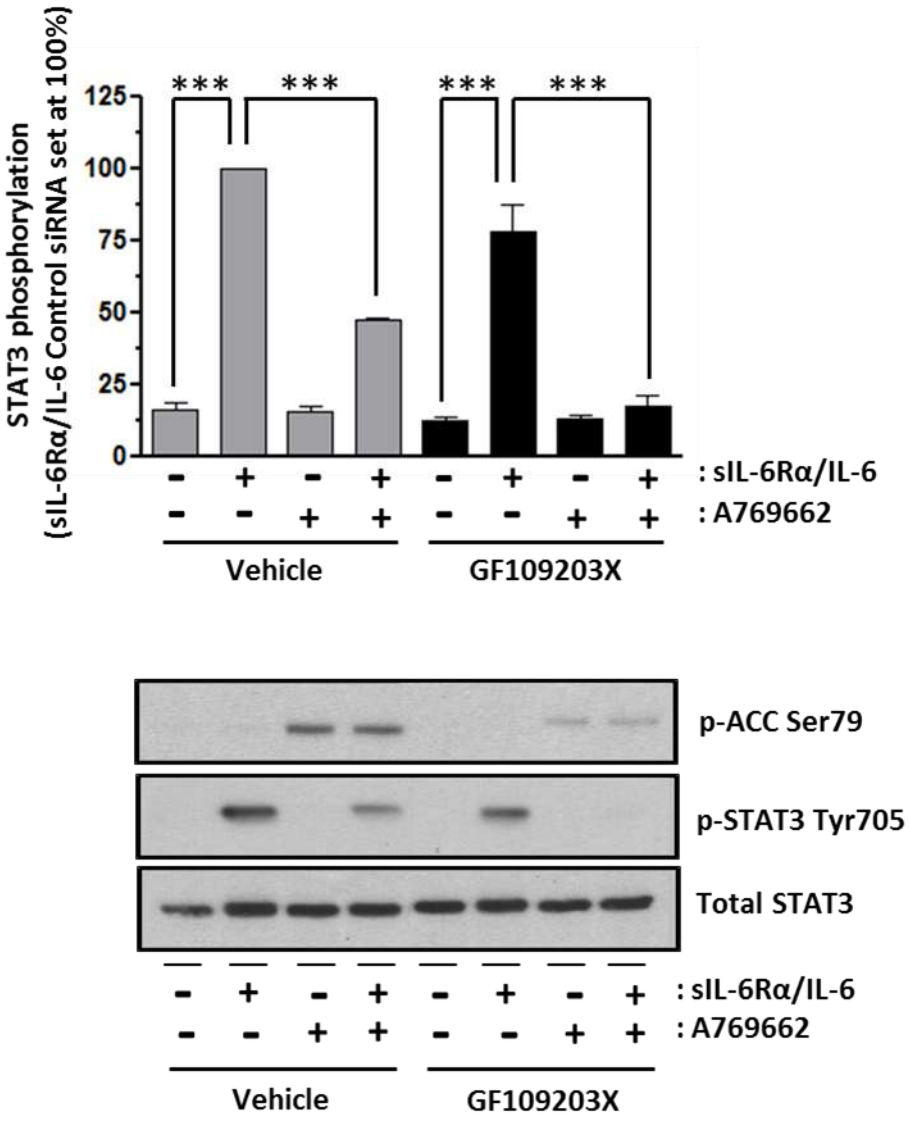

Figure 3.5: Effect of PKC inhibitor G109203FX on AMPK-mediated inhibition of sIL-6Rα/IL-6 stimulated STAT3 Tyr705 phosphorylation in HUVECs

HUVECs were pre-treated with vehicle or 10μM GF109203X for 30 minutes, and then treated with or without 100μM A769662 for 40 minutes prior to the addition of vehicle or 25ng/ml sIL-6Rα and 5ng/ml IL-6 (sIL-6Rα/IL-6) for a further 30 minutes as indicated. Protein-equalised cell extracts were then analysed by SDS-PAGE and immunoblotting with antibodies as indicated. STAT3 phosphorylation data were first normalized to total STAT3 levels and expressed as a percentage (%) of the maximal sIL-6Rα/IL-6 stimulation attained in vehicle pre-treated HUVECs. Quantitative analysis from three experiments is presented. Columns are means ±SEM. ***p<0.001 A representative blot from n=3 experiments is shown. n=3 from one batch of pooled donor HUVEC

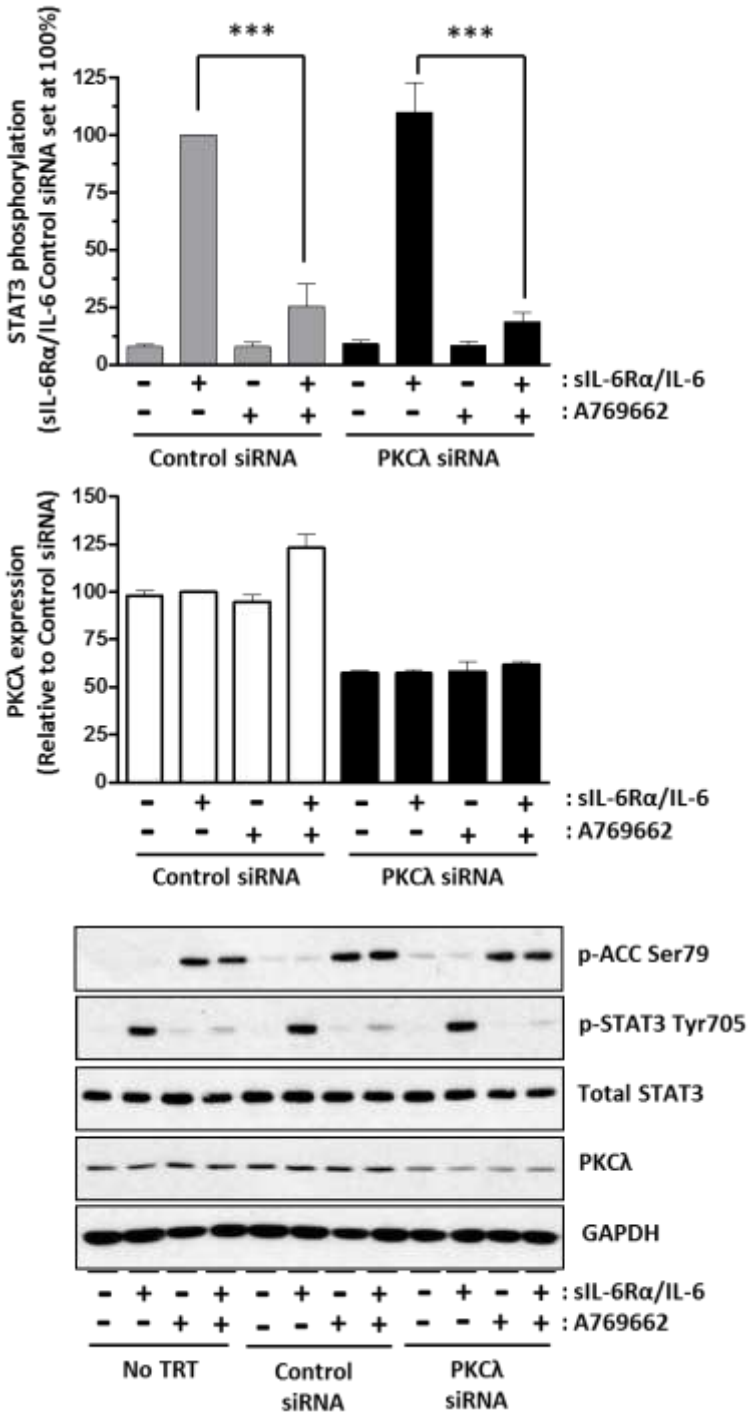

Figure 3.6: Effect of PKCλ isoform knockdown on AMPK-mediated inhibition of sIL-6Rα/IL-6 stimulated STAT3 Tyr705 phosphorylation in HUVECs.
HUVECs were transfected with either 10nM PKCλ or control siRNA 48hrs prior to pre-treatment with vehicle or 100μM A769662 for 40 minutes followed by stimulation with vehicle or 25ng/ml sIL-6Rα and 5ng/ml IL-6 (sIL-6Rα/IL-6) for a further 30 minutes as indicated. Control siRNA was used as a negative control. Protein-equalised cell extracts were then analysed by SDS-PAGE and immunoblotting with antibodies as indicated. STAT3 phosphorylation data were first normalized to total STAT3 levels and expressed as a percentage (%) of the maximal sIL-6Rα/IL-6 stimulation attained in vehicle pre-treated control siRNA transfected HUVECs. Total PKCλ protein levels were first normalized to GAPDH levels and expressed as a percentage (%) of the maximal protein levels attained in sIL-6Rα/IL-6 stimulated control siRNA transfected HUVECs (set at 100%). Quantitative analysis from four experiments is presented. Columns are means ±SEM. ***p<0.001. A representative blot from n=4 experiments is shown. n=4 from one batch of pooled donor HUVEC (Data was generated and analysed by Dr. Claire Rutherford, University of Glasgow.)

3.5 Effect of SIRT1 inhibition on AMPK-mediated regulation of IL-6 signalling

SIRT1 is a histone/protein deacetylase, whose catalytic activity is dependent on the co-substrate nicotinamide adenine dinucleotide (NAD^+) (Sauve et al., 2006). Activation of AMPK enhances SIRT1 activity by increasing production of cellular NAD^+ (Cantó and Auwerx, 2009, Yang et al., 2010). Furthermore, it has been demonstrated that SIRT1 can directly deacetylate STAT3 and that this modification is coupled with the down-regulation of STAT3 phosphorylation (Nie et al., 2009). Therefore, it was hypothesised that AMPK-mediated inhibition of STAT3 Tyr705 phosphorylation could potentially occur *via* SIRT1. To test this hypothesis, a pharmacological inhibitor of SIRT1, EX527 (6-chloro-2,3,4,9-tetrahydro-1H-carbazole-1-carboxamide), was utilised to assess a role for SIRT1 in mediating AMPK's effects on STAT3 phosphorylation in HUVECs.

3.5.1 Effect of EX527 on A769662-mediated inhibition of STAT3 phosphorylation

EX527 is a specific small molecule inhibitor of SIRT1 catalytic activity and occupies the NAD^+-binding sites of SIRT1, thereby limiting deacetylation of target proteins and histones (Napper et al., 2005, Gertz et al., 2013). 1μM EX527 for 4 hours has previously been shown to effectively inhibit SIRT1 to increase acetylation levels of its well-established substrate p53 in primary human epithelial cells and several cell lines (Solomon et al., 2006). HUVECs were pre-treated with vehicle or 1μM EX527 for 6 hours, followed by sequential treatment with A769662 and sIL-6Rα/IL-6.

This experiment was conducted under both serum-deprived (Figure 3.7) and serum-supplemented conditions (Figure 3.7). The presence of serum did not unmask any differences from the experiment conducted in the absence of serum (Figure 3.7), therefore only the results obtained in serum-deprived conditions are described below.

sIL-6Rα/IL-6 induced a significant (***$p<0.001$) increase in STAT3 Tyr705 phosphorylation in both the presence and absence of EX527, compared to the basal level (Figure 3.7). In comparison to sIL-6Rα/IL-6 stimulation of HUVECs in the absence of EX527, the presence of EX527 had no significant ($p>0.05$, NS) effect on

sIL-6Rα/IL-6 stimulation of STAT3 Tyr705 phosphorylation. Sequential treatment of HUVECs with A769662 and sIL-6Rα/IL-6 in the absence or presence of EX527 caused a significant 85 ± 5% (***p<0.001) and by 82 ± 10% (***p<0.001) inhibition of STAT3 Tyr705 phosphorylation, respectively, compared to IL-6Rα/IL-6 treatment alone (Figure 3.7). Overall, pharmacological inhibition of SIRT1 by EX527 did not attenuate the inhibitory effect of AMPK activation on STAT3 Tyr705 phosphorylation (Figure 3.7).

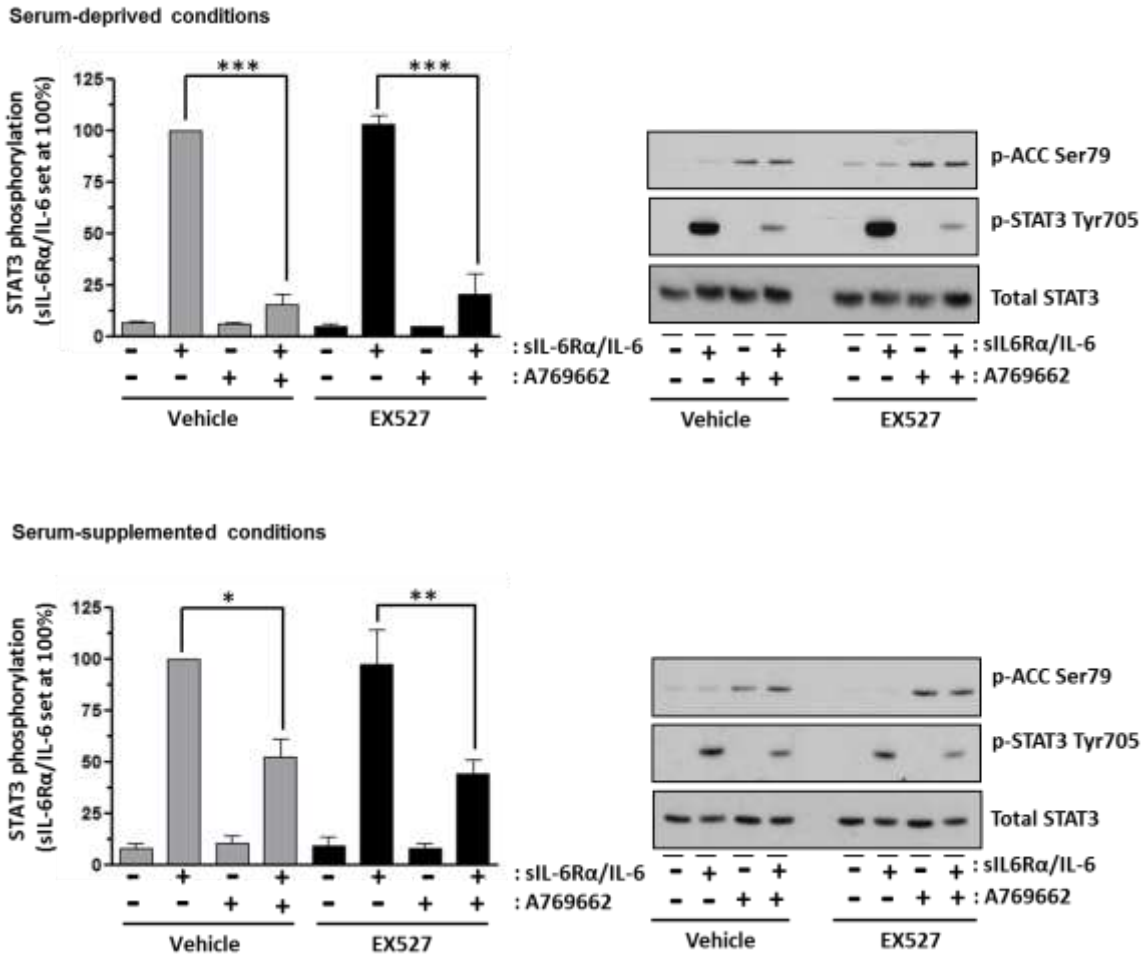

Figure 3.7: Effect of SIRT1 inhibitor EX527 on AMPK-mediated inhibition of sIL-6Rα/IL-6 stimulated STAT3 Tyr705 phosphorylation in HUVECs

HUVECs were pre-treated for 6 hours with or without 1μM EX527 in endothelial cell growth medium (serum supplemented) or basal medium 199 (serum deprived), and then treated with or without 100μM A769662 for 40 minutes prior to the addition of vehicle or 25ng/ml sIL-6Rα and 5ng/ml IL-6 (sIL-6Rα/IL-6) for a further 30 minutes as indicated. Protein-equalised cell extracts were then analysed by SDS-PAGE and immunoblotting with antibodies as indicated. STAT3 phosphorylation data were first normalized to total STAT3 levels and expressed as a percentage (%) of the maximal sIL-6Rα/IL-6 stimulation attained in vehicle pre-treated HUVECs. Quantitative analysis from three experiments is presented. Columns are means ±SEM. ***p<0.001, **p<0.01, *p<0.05 A representative blot from n=3 experiments is shown. n=3 from one batch of pooled donor HUVEC

3.6 Effect of CPT1 inhibition on AMPK-mediated regulation of IL-6 signalling

Fatty acid palmitate significantly increased levels of STAT-3 phosphorylation in HAOECs (Mugabo et al., 2011), while activation of AMPK stimulates fatty acid oxidation in HUVECs (Dagher et al., 2001). Therefore, it was hypothesised that AMPK could inhibit STAT3 Tyr705 phosphorylation by promoting fatty acid oxidation, and thereby reducing palmitate-mediated stimulation of STAT3. To test this hypothesis, a pharmacological inhibitor of CPT1, Etomoxir, was used to assess a role for fatty acid oxidation in mediating AMPK's effects on STAT3 phosphorylation in HUVECs.

3.6.1 Effect of Etomoxir on A769662-mediated inhibition of STAT3 phosphorylation

CPT1 is an enzyme found on the outer mitochondrial membrane and controls the transfer of long-chain fatty acids from the cytosol into the mitochondria for oxidation (McGarry and Brown, 1997). Etomoxir is an oxirane carboxylic acid derivative which irreversible inhibits CPT1 activity, thus decreasing fatty acid ß-oxidation (Abdel-aleem et al., 1994). Effective inhibition of fatty acid oxidation in HUVECs was achieved by our colleagues using 50μM Etomoxir for 4 hours (Ian Salt, personal communication).HUVECs were pre-treated with vehicle or 50 μM Etomoxir for 4 hours, followed by sequential treatment with A769662 and sIL-6Rα/IL-6.

This experiment was conducted under both serum-deprived (Figure 3.8) and serum-supplemented conditions (Figure 3.8). The presence of serum did not unmask any differences from the experiment conducted in the absence of serum (Figure 3.8), therefore only the results obtained in serum-deprived conditions are described below.

sIL-6Rα/IL-6 induced a significant (***p<0.001) increase, compared to the basal level, in STAT3 Tyr705 phosphorylation in both the presence and absence of Etomoxir (Figure 3.8). In comparison to sIL-6Rα/IL-6 stimulation of HUVECs in the absence of Etomoxir, the presence of EX527 had no significant (p>0.05, NS) effect on sIL-6Rα/IL-6 stimulation of STAT3 Tyr705 phosphorylation. Sequential treatment of HUVECs with A769662 and sIL-6Rα/IL-6 in the absence or presence of Etomoxir

caused a significant 66 ± 10% (***p<0.001) and by 57 ± 7% (***p<0.001) inhibition of STAT3 Tyr705 phosphorylation, respectively, compared to IL-6Rα/IL-6 treatment alone (Figure 3.8). Overall, pharmacological inhibition of fatty acid oxidation by Etomoxir did not attenuate the inhibitory effect of AMPK activation on STAT3 Tyr705 phosphorylation (Figure 3.8).

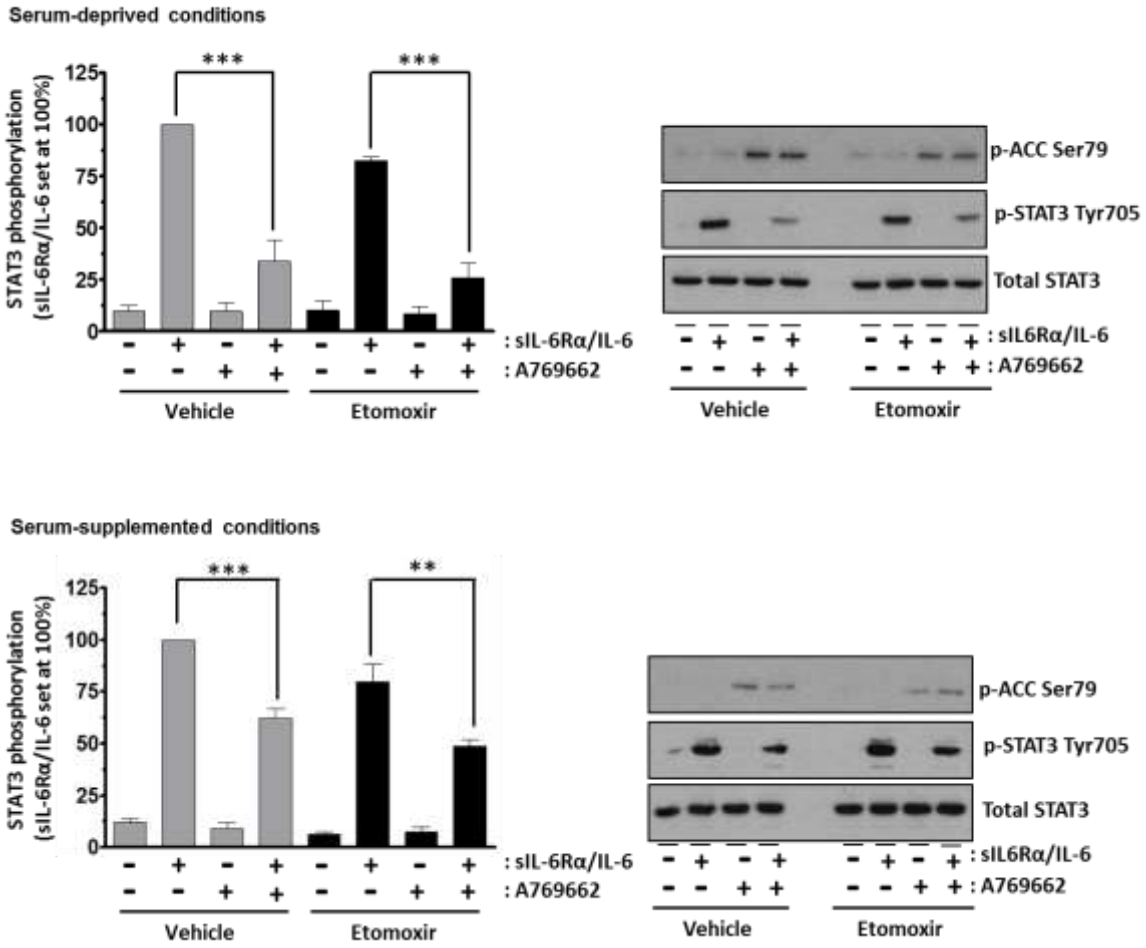

Figure 3.8: Effect of CPT1 inhibitor Etomoxir on AMPK-mediated inhibition of sIL-6Rα/IL-6 stimulated STAT3 Tyr705 phosphorylation in HUVECs

HUVECs were pre-treated for 4 hours with or without 50μM Etomoxir in endothelial cell growth medium (serum supplemented) or basal medium 199 (serum deprived, then treated with or without 100μM A769662 for 40 minutes prior to the addition of vehicle or 25ng/ml sIL-6Rα and 5ng/ml IL-6 (sIL-6Rα/IL-6) for a further 30 minutes as indicated. Protein-equalised cell extracts were then analysed by SDS-PAGE and immunoblotting with antibodies as indicated. STAT3 phosphorylation data were first normalized to total STAT3 levels and expressed as a percentage (%) of the maximal sIL-6Rα/IL-6 stimulation attained in vehicle pre-treated HUVECs. Quantitative analysis from three experiments is presented. Columns are means ±SEM. ***p<0.001, **p<0.01. A representative blot from n=3 experiments is shown. n=3 from one batch of pooled donor HUVEC

3.7 Effect of mTOR inhibition on AMPK-mediated regulation of IL-6 signalling

mTOR exists in two distinct multiprotein complexes, mTOR complex 1 (mTORC1) and mTOR complex 2 (mTORC2), which have distinct substrate specificities and are differentially regulated (Hara et al., 2002, Dos et al., 2004 Jacinto et al., 2004, Gwinn et al 2008). AMPK inhibits mTOR activity, as measured by phosphorylation of S6 kinase (S6K) (Kimura et al., 2003). Furthermore, it has been demonstrated that pharmacological inhibition of the mTOR pathway can suppress STAT3 activation (Goncharova et al., 2009). Therefore, it was hypothesised that AMPK-mediated inhibition of STAT3 Tyr705 phosphorylation could potentially occur *via* inhibition of mTOR. To test this hypothesis, a pharmacological inhibitor of mTOR, PP242, was utilised to assess a role for mTOR in mediating AMPK's effects on STAT3 phosphorylation in HUVECs.

3.7.1 Effect of PP242 on A769662-mediated inhibition of STAT3 phosphorylation

PP242 specifically inhibits both mTORC1 and mTORC2, as it binds directly to the ATP binding site of either (Feldman et al., 2009). 2μM PP242 for 3 hours has previously been shown to effectively inhibit phosphorylation of its well-established substrate S6K in mouse embryonic fibroblasts (MEFs) (Ian Salt, personal communication). HUVECs were pre-treated with vehicle or 2μM PP242 for 3 hours, followed by sequential treatment with A769662 and sIL-6Rα/IL-6.

This experiment was conducted under both serum-deprived (Figure 3.9) and serum-supplemented conditions (Figure 3.9). The presence of serum did not unmask any differences from the experiment conducted in the absence of serum (Figure 3.9), therefore only the results obtained in serum-deprived conditions are described below.

Immunoblotting of whole cell extracts with phospho-p70 S6 kinase (Ser371) antibody confirmed PP242-mediated inhibition of mTOR as phospho-p70 S6 kinase was undetectable in the presence of PP242 and AMPK had no effect on phosphorylation of p70 S6 kinase (Figure 3.9). sIL-6Rα/IL-6 treatment of vehicle pre-treated HUVECs caused a significant (***p<0.001) stimulation of STAT3 Tyr705 phosphorylation, compared to basal levels (Figure 3.9). A769662 significantly

inhibited sIL-6Rα/IL-6 stimulation of STAT3 Tyr705 phosphorylation levels by 72 ± 6% (***p<0.001) in vehicle pre-treated HUVECs (Figure 3.9). Pre-treatment with PP242 induced a 29 ± 10% (**p<0.01) reduction in sIL-6Rα/IL-6-stimulated STAT3 Tyr705 phosphorylation, compared to sIL-6Rα/IL-6 treatment alone (Figure 3.9). Sequential treatment of HUVECs with A769662 and sIL-6Rα/IL-6 in the absence or presence of PP242 caused a significant 72 ± 6% (***p<0.001) and 55 ± 3% (***p<0.001) inhibition of STAT3 Tyr705 phosphorylation, respectively, compared to IL-6Rα/IL-6 treatment alone (Figure 3.9). Overall, pharmacological inhibiton of mTOR in HUVECs attenuated sIL-6Rα/IL-6 stimulation of STAT3 Tyr705 phosphorylation, but did not attenuate the inhibitory effect of AMPK activation on STAT3 Tyr705 phosphorylation (Figure 3.9).

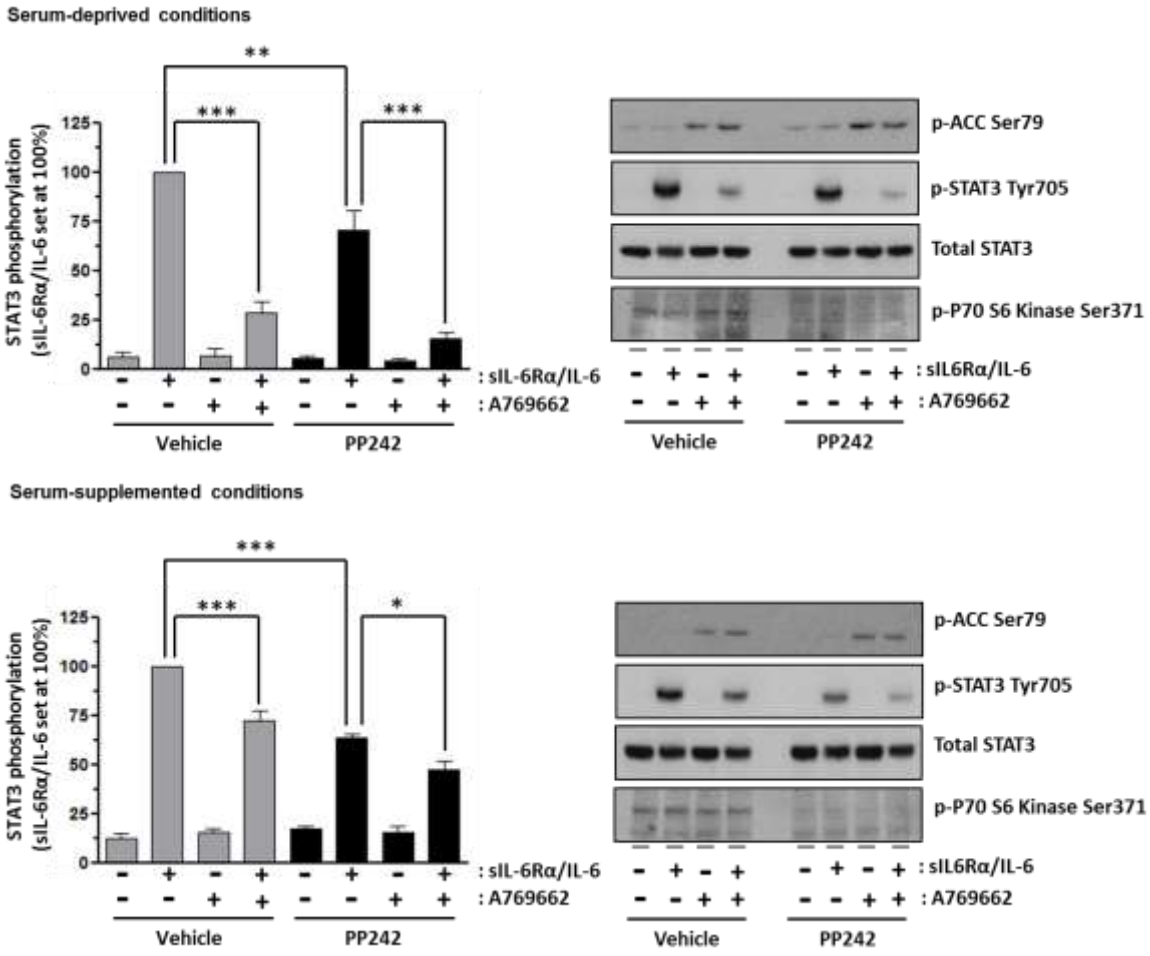

Figure 3.9: Effect of mTOR inhibitor PP242 on AMPK-mediated inhibition of sIL-6Rα/IL-6 stimulated STAT3 phosphorylation in HUVECs

HUVECs were pre-treated for 3 hours with or without 2μM PP242 in endothelial cell growth medium (serum supplemented) or basal medium 199 (serum deprived), and then treated with or without 100μM A769662 for 40 minutes prior to the addition of vehicle or 25ng/ml sIL-6Rα and 5ng/ml IL-6 (sIL-6Rα/IL-6) for a further 30 minutes as indicated. Protein-equalised cell extracts were then analysed by SDS-PAGE and immunoblotting with antibodies as indicated. STAT3 phosphorylation data were first normalized to total STAT3 levels and expressed as a percentage (%) of the maximal sIL-6Rα/IL-6 stimulation attained in vehicle pre-treated HUVECs. Quantitative analysis from three experiments is presented. Columns are means ±SEM. ***p<0.001, **p<0.01, *p<0.05 A representative blot from n=3 experiments is shown. n=3 from one batch of pooled donor HUVEC

3.8 Discussion

In this chapter, it was investigated whether AMPK exerts its inhibitory effects on JAK-STAT signalling via a known regulator of JAK or STAT, or an AMPK downstream target known to either directly or indirectly impact on JAK-STAT signalling. A combination of genetic and pharmacological approaches was utilised to assess the role of each of the following AMPK targets: TC-PTP, SHP2, eNOS, PKCλ, SIRT1, CPT1 and mTOR. The key findings of this chapter suggest that AMPK activation in HUVECs inhibited sIL-6Rα/IL-6 stimulated STAT3 Tyr705 phosphorylation *via* a mechanism independent of TC-PTP, eNOS, PKC, SIRT1 and mTOR. Furthermore, inhibition of mTOR and eNOS reduced sIL-6Rα/IL-6 stimulated STAT3 Tyr705 phosphorylation, independent of AMPK activation by A769662.

3.8.1 Role of TC-PTP

JAK-STAT signalling involves a cascade of tyrosine phosphorylation events, therefore PTPs mediating dephosphorylation of signalling components are key negative regulators of JAK-STAT signalling (Shuai and Liu 2003, Tonks and Neel 2001). Several PTPs, including SHP1, SHP2, CD45, PTP1B and TC-PTP, have been identified as regulators of JAK-STAT signalling. SHP2 and TC-PTP are ubiquitously expressed and the most studied PTPs in the JAK-STAT pathway (Xu and Qu, 2008). Therefore, it was hypothesised that AMPK-mediated inhibition of STAT3 Tyr705 phosphorylation could potentially occur *via* TC-PTP or SHP2.

JAK1, STAT1 and STAT3 have been reported to be direct substrates of TC-PTP (Yamamoto et al., 2002, ten Hoeve et al., 2002, Simoncic et al. 2002). TC-PTP exists as two splice variants: an TC48 and a TC45. Overexpression of TC45 in 293T cells was reported to suppress IL-6-stimulated STAT3 phosphorylation (Yamamoto et al., 2002). Lam et al., reported that pharmacological activation of AMPK induces the cytoplasmic accumulation of TC45 by inhibiting nuclear import (Lam et al., 2001). Therefore, it was hypothesised that AMPK-mediated inhibition of STAT3 Tyr705 phosphorylation could potentially occur *via* TC-PTP. An siRNA approach was used to specifically knockdown the expression of TC-PTP in order to determine the necessity of TC-PTP in AMPK-mediated inhibition of IL-6 stimulation of STAT3 Tyr705 phosphorylation. Figure 3.1 demonstrated that siRNA mediated knockdown of TC-PTP in HUVECs did not attenuate the inhibitory effect of AMPK

activation on STAT3 Tyr705 phosphorylation. Similar observations were made in MEFs by our colleague Sarah Mancini; IL-6-stimulated STAT3 Tyr705 phosphorylation was significantly inhibited following AMPK activation in both wild type and TC-PTP-/- MEFs (Sarah Mancini, personal communication). Overall, inhibition of IL-6 stimulated STAT3 Tyr705 phosphorylation by AMPK was not *via* TC-PTP. The data shown in figure 3.1 was generated and analysed by Dr Claire Rutherford, University of Glasgow.

3.8.2 Role of SHP2

SHP2 has been reported to negatively regulate IL-6-stimulated STAT3 phosphorylation (Ohtani et al., 2000, Lehmann et al., 2003). SHP2 is rapidly recruited to Tyr759 in gp130 following IL-6 stimulation (Stahl et al., 1995). Disruption of SHP2 recruitment, by the substitution of Tyr757 in gp130 with phenylalanine, was shown to increase STAT3-mediated gene expression (Ohtani et al., 2000, Nicholson et al., 2000, Schaper et al., 1998). Recently, Nerstedt et al., reported that both AICAR and metformin reduced IL-6 stimulated SHP-2 phosphorylation in hepatoma cell line HepG2 (Nerstedt et al. 2013). Therefore, it was hypothesised that AMPK-mediated inhibition of STAT3 Tyr705 phosphorylation could potentially occur *via* SHP2. In order to assess a role for SHP2 in mediating AMPK's effects on STAT3 Tyr705 phosphorylation, SHP2 exon 3-deletion (SHP2−/−) 3T3 fibroblasts were utilised with genetically-matched wild-type cells. SHP2 exon 3-deletion (SHP2−/−) 3T3 fibroblasts from mice are deficient in SHP2 and express small amounts of mutant SHP2 that is unable to bind to the receptor (Saxton et al., 1997, Shi et al., 2000, Lehmann et al., 2003). As shown in figure 3.2A, A769662 inhibited IL-6 stimulation of STAT3 Tyr705 phosphorylation in both SHP2-/- and SHP2 +/+ 3T3 fibroblasts, however this did not reach statistical significance. SHP2 acts to inhibit cytokine stimulated JAK-STAT signalling, but also potentiates cytokine-induced ERK signalling (Salmond et al., 2006). Mutation of the SHP2-binding site, Tyr759, in GP130 receptor abolished IL-6 stimulation of ERK activation in embryonic fibroblasts (Ohtani et al., 2000). To confirm SHP2 loss of function in SHP2 -/- 3T3 fibroblasts, sIL-6Rα/IL-6 stimulation of ERK 1/2 phosphorylation was assessed in these cells. Surprisingly, IL-6 induced ERK1/2 phosphorylation levels were minimal in SHP2 +/+ 3T3 fibroblasts, whereas phospho-ERK 1/2 levels were potentiated in SHP2 -/- 3T3 fibroblasts, compared to SHP2 +/+ 3T3 fibroblasts. In comparison to basal levels in SHP2 +/+ 3T3 fibroblasts, IL-6 has minimal effect on

STAT3 and ERK1/2 phosphorylation which suggests that overexpression of SHP2 has increased the dephosphorylation of JAK and possible other signalling proteins. Overall, our results are inconclusive on whether AMPK-mediated inhibition of sIL-6Rα/IL-6 signalling is *via* SHP2. The data shown in figure 3.2 was generated and analysed by Dr Claire Rutherford, University of Glasgow.

3.8.3 Role of NO

AMPK directly phosphorylates and activates eNOS to stimulate NO production in endothelial cells (Morrow et al., 2003). It has been reported that NO induces the inactivation of SHP-1, SHP-2, and PTP1B, but not TC-PTP (Hsu and Meng 2010). Also, AMPK activation of eNOS has been shown to inhibit TNF-α stimulation of MCP-1 expression and secretion in vascular endothelial cells (Ewart et al., 2008). Therefore, it was hypothesised that AMPK-mediated inhibition of STAT3 Tyr705 phosphorylation could potentially occur *via* eNOS. Our initial investigation into the role of eNOS in mediating AMPK's inhibitory effects on IL-6 stimulation of STAT3 Tyr705 phosphorylation utilised the eNOS inhibitor L-NAME and the negative control D-NAME. Figure 3.3 demonstrated that sIL-6Rα/IL-6 stimulation of STAT3 Tyr705 phophorylation was moderately reduced in the presence of L-NAME and the addition of A769662 further reduced the phosphorylation of STAT3. However, these changes did not reach statistical significance. Furthermore, there was no positive control for this experiment demonstrating the inhibition of eNOS by L-NAME. However, 0.1mM L-NAME has previously been shown to effectively inhibit eNOS in HAOECs (Morrow et al., 2003). Therefore, to clarify the role of eNOS in mediating AMPK's inhibitory effects on STAT3 Tyr705 phosphorylation in HUVECs a siRNA approach was utilised. Figure 3.4 demonstrated that siRNA mediated knockdown of eNOS in HUVECs significantly (***p<0.001) reduced sIL-6Rα/IL-6 stimulation of STAT3 Tyr705 phosphorylation and the addition of A769662 further significantly (***p<0.001) reduced the phosphorylation of STAT3. These data suggest that both AMPK activation and eNOS inhibition suppress sIL-6Rα/IL-6 stimulated STAT3 Tyr705 phosphorylation, and this is likely to occur *via* mutually exclusive mechanisms. Taken together, these data demonstrated that neither pharmacological inhibiton nor siRNA-mediated knockdown of eNOS attenuated the inhibitory effect of AMPK activation on STAT3 Tyr705 phosphorylation. To our knowledge, this is the first time eNOS inhibition has been linked to a reduction in STAT3 phosphorylation in endothelial cells. In contrast, Kim et al., have recently

proposed that NO produced by the inducible isoform of NOS (iNOS) inhibits STAT3 Tyr705 phosphorylation by direct S-nitrosylation of STAT3 in microglia (Kim et al., 2014). Overall, these data suggest that AMPK-mediated inhibition of STAT3 Tyr705 phosphorylation is not *via* AMPK-induced eNOS-activity. The data shown in figure 3.4 was generated and analysed by Dr Claire Rutherford, University of Glasgow.

3.8.4 Role of PKCλ and SIRT1

Acetylation of STATs is emerging as a key mechanism for regulating STAT signalling (Zhuang et al., 2013). STAT3 is acetylated by its coactivator p300/CBP, resulting in increased DNA binding and transcriptional activity (Wang et al., 2005), and several reports have demonstrated that acetylation is required for phosphorylation of STATs (Zhuang et al., 2013). Nie et al (2009) demonstrated that NAD^+-dependent deacetylase SIRT1 can directly deacetylate STAT3 and that this modification is coupled with the down-regulation of STAT3 phosphorylation (Nie et al., 2009). AMPK indirectly phosphorylates p300 *via* the atypical PKCλ, resulting in inhibition of the histone acetyltransferase activity of p300 (Zhang et al., 2011). Activation of AMPK enhances SIRT1 activity by increasing the cellular levels of its activator NAD^+ (Cantó and Auwerx, 2009, Yang et al., 2010). Therefore, it was hypothesised that AMPK-mediated inhibition of STAT3 Tyr705 phosphorylation could potentially occur *via* PKCλ mediated inhibition of p300 or SIRT1.

Pharmacological and genetic approaches were utilised to investigate whether PKCλ mediated the inhibition of STAT3 Tyr705 phosphorylation by AMPK activation. Figure 3.5 demonstrated that inhibition of PKCλ in HUVECs using a pharmacological inhibitor, GF109203X, did not attenuate the inhibitory effect of AMPK activation on STAT3 Tyr705 phosphorylation. Under the same conditions, 10μM GF109203X abolished PMA-induced ERK activation in HUVECs, thus confirming that the concentration used was sufficient to block PKC-mediated responses (Tim Palmer; personal communication). At concentrations of 10μM GF109203X is a nonselective inhibitor of PKC isoforms. As GF109203X binds to the ATP-binding site of PKC isoforms, it is perhaps unsurprising that it has been reported to inhibit other protein Ser/Thr kinases at high concentrations (http://www.kinase-screen.mrc.ac.uk/screening-compounds/341060). Indeed, at concentrations of 10μM, GF109203X has been reported to inhibit AMPK *in vitro* by 96%. This may, therefore, underlie the inhibition of A769662-stimulated ACC

phosphorylation observed in HUVECs stimulated with GF109203X (Figure 3.5). Therefore, to specifically assess the role of PKCλ in mediating AMPK's effects on STAT3 phosphorylation in HUVECs a siRNA approach was utilised. Figure 3.6 demonstrated that siRNA mediated knockdown of PKCλ in HUVECs did not attenuate the inhibitory effect of AMPK activation on STAT3 Tyr705 phosphorylation. Overall, these data suggest that inhibition of IL-6-stimulated STAT3 Tyr705 phosphorylation by AMPK was not *via* PKCλ. The data shown in figure 3.6 was generated and analysed by Dr Claire Rutherford, University of Glasgow.

A pharmacological inhibitor of SIRT1, EX527, was used to investigate whether SIRT1 mediated the inhibition of STAT3 phosphorylation by AMPK activation. Figure 3.7 demonstrated that pharmacological inhibition of SIRT1 in HUVECs did not attenuate the inhibitory effect of AMPK activation on STAT3 Tyr705 phosphorylation. It is noted that there was no positive control for this experiment demonstrating the inhibition of SIRT1 activity by EX527, therefore data should be interpreted with care. However, 1μM EX527 has previously been shown to effectively inhibit SIRT1 to increase acetylation levels of its well-established substrate p53 in primary human epithelial cells and several cell lines (Solomon et al., 2006). Overall, these data suggest that AMPK-mediated inhibition of STAT3 Tyr705 phosphorylation is not *via* AMPK-induced SIRT1-activity. These observations are based on the notion that AMPK activates SIRT1, however it has recently been demonstrated by Lee et al (2012) that activated AMPK inhibits SIRT1-mediated deacetylation of its well documented downstream target p53 tumour suppressor protein (Vaziri et al., 2001, Cantó and Auwerx, 2009, Lee et al., 2012). On the contrary, Lau et al (2014) has proposed that AMPK activates SIRT1-mediated deacetylation of p53 (Lau et al., 2014). These studies were performed in two different types of cancer cells and demonstrate that the effect of AMPK activation on SIRT1 activity needs to be further investigated, particularly in a cell specific manner. Intriguingly, Nin et al., observed that in cells incubated with AMPK activators for a short period of time (1-2hrs) AMPK modulates SIRT1 activity without any changes in NAD^+ levels, whereas Cantó and Auwerx had previously observed that in cells incubated (8-12 hrs) with AMPK activators for a long period of time (7-12hrs) AMPK modulates SIRT1 activity by altering NAD^+ levels (Nin et al., 2012, Cantó and Auwerx, 2009). In this study, AMPK-mediated inhibition of STAT3 Try705 is detected in cell lysates prepared from cells incubated with AMPK

activator A769662 for 70 minutes (Figure 3.7). Overall, these data suggest that inhibition of IL-6-stimulated STAT3 Tyr705 phosphorylation by AMPK was not *via* SIRT1.

3.8.5 Role of fatty acids

Increased levels of fatty acids have been associated with endothelial dysfunction and fatty acids have been shown to affect the activity of kinases, such as protein kinase C and AMPK (Watt et al., 2006, Egan et al., 1999, Hennig et al., 1994). Recently, it was reported that free fatty acid palmitate significantly increased levels of STAT-3 phosphorylation in human aortic endothelial cells (Mugabo et al., 2011), while activation of AMPK stimulates fatty acid oxidation in HUVECs (Dagher et al., 2001). Therefore, it was postulated that AMPK could inhibit IL-6 signalling by promoting fatty acid oxidation. AMPK stimulates fatty acid oxidation by phosphorylating and inhibiting ACC activity, thus leading to decreased formation of malonyl-CoA which inhibits CPT1 to block transfer of fatty acids into the mitochondria for oxidation (Lopaschuk et al., 1994, Merrill et al., 1997, Vavvas et al., 1997). Etomoxir, a pharmacological inhibitor of CPT1, was used to promote fatty acid oxidation in HUVECs in order to assess a role for fatty acid oxidation in mediating AMPK's effects on STAT3 phosphorylation in HUVECs. Figure 3.8 demonstrated that pharmacological inhibition of CPT1 in HUVECs did not attenuate the inhibitory effect of AMPK activation on STAT3 Tyr705 phosphorylation. Thus, these data suggest that AMPK-mediated inhibition of STAT3 Tyr705 phosphorylation was not *via* AMPK-induced fatty acid oxidation. It should be noted that CPT1 inhibition by Etomoxir and stimulation of fatty acid oxidation by AMPK was not confirmed, yet effective inhibition of fatty acid oxidation in HUVECs was achieved by colleagues using the same lot of Etomoxir (Ian Salt, personal communication). Overall, our results are inconclusive on whether AMPK-mediated inhibition of sIL-6Rα/IL-6 signalling is via fatty acid oxidation.

3.8.6 Role of mTOR

mTOR is a serine/threonine kinase found as two structurally and functionally different complexes, mTORC1 and mTORC2, and regulates cell growth and proliferation. Inoki et al., demonstrated that AMPK inhibits mTORC1 activity by directly phosphorylating and activating tuberous sclerosis protein 2 (TSC2), a

negative regulator of mTOR (Inoki et al., 2003). Alternatively, Gwinn et al., demonstrated that AMPK directly phosphorylates raptor, a component of mTORC1, which suppressed mTORC1 activity. Gwinn et al., 2008). Studies utilising TSC2-deficient cells or siRNA-mediated knockdown of TSC2 have reported an increase in STAT3 Tyr705 phosphorylation (Chen et al., 2012, Goncharova et al., 2009), whereas pharmacological inhibition of mTOR with rapamycin ameliorated STAT3 Tyr705 phosphorylation and transcriptional activity (Onda et al., 2002, Weichhart et al. 2008). It was of important, therefore, to investigate the role of mTOR in AMPK-mediated inhibition of IL-6-stimulated STAT3 phosphorylation in HUVECs using the pharmacological mTORC1/2 inhibitor PP242. Figure 3.9 demonstrated that PP242-mediated inhibition of mTOR significantly (***p<0.001) reduced sIL-6Rα/IL-6 stimulation of STAT3 Tyr705 phosphorylation, however STAT3 Tyr705 phosphorylation levels are further reduced by the addition of A769662. The same experiments performed in MEFs by our colleague Sarah Mancini demonstrated a significant reduction in IL-6 stimulated STAT3 Tyr705 phosphorylation in response to A769662, while inhibition of mTOR with PP242 induced a moderate reduction in STAT3 Tyr705 phosphorylation (Sarah Mancini, personal communication). It can be seen in figure 3.9 that PP242 successfully inhibited mTOR activity in HUVECs as indicated by p70 S6 kinase phosphorylation. However, A769662-mediated activation of AMPK was not found to reduce phosphorylation of p70 S6 kinase (Figure 3.9). This was unexpected as AMPK had been reported to inhibit mTOR phosphorylation of p70 S6 kinase (Kimura et al., 2003). To our knowledge, this is the first time mTOR inhibition has been linked to a reduction in STAT3 phosphorylation in HUVECs, and supports previous studies that reported that inhibition of mTOR with rapamycin suppressed STAT3 phosphorylation in other cell types (Weichhart et al., 2008, Onda et al., 2002, Goncharova et al., 2009, Chen et al., 2012). In HUVECs, PP242 mediated inhibition of IL-6 stimulation of STAT3 Tyr705 phosphorylation was further reduced by the addition of A769662. Taken together, these data suggest that both AMPK activation and mTOR inhibition suppress IL-6-stimulated STAT3 phosphorylation, and this is likely to occur *via* mutually exclusive mechanisms. Overall, these data suggest that inhibition of IL-6-stimulated STAT3 Tyr705 phosphorylation by AMPK was not *via* mTOR.

3.8.7 Effect of serum starvation

To examine whether performing the experiments in the absence or presence of serum could affect our results, experiments investigating the effects of CPT1 inhibitor Etomoxir, SIRT1 inhibitor EX527 and mTOR inhibitor PP242 on AMPK-mediated inhibition of IL-6 signalling were conducted under both serum-supplemented and serum-deprived conditions. It is recognised that the cell culture medium (endothelial cell growth medium and basal medium 199) used to create these conditions have additional differences other than serum, but for simplification these conditions are assigned as serum-supplemented and serum-deprived. Overall, AMPK significantly inhibits sIL-6Rα/IL-6 stimulated STAT3 Tyr705 phosphorylation in both serum-supplemented and serum-deprived conditions, though serum-deprivation appears to potentiate AMPK's ability to inhibit STAT3 Tyr705 phosphorylation (Table 3.1). It could be suggested that the serum supplements increased STAT3 Tyr705 phosphorylation or that serum-deprivation increased AMPK activation, however detailed analysis of AMPK activation or sIL-6Rα/IL-6 stimulation under these conditions was not carried out and as noted earlier serum is not the only variable between the two conditions, thus definitive conclusions could not be made. Nevertheless, we have clearly demonstrated that under serum-deprived conditions, AMPK-mediated inhibition of STAT3 Tyr705 phosphorylation is increased.

Overall, the key findings of this chapter suggest that AMPK activation in HUVECs inhibited sIL-6Rα/IL-6 stimulated STAT3 Tyr705 phosphorylation *via* a mechanism independent of TC-PTP, eNOS, PKC, SIRT1 and mTOR. Furthermore, inhibition of mTOR and eNOS reduced sIL-6Rα/IL-6 stimulated STAT3 Tyr705 phosphorylation, independent of AMPK activation by A769662. However, it is noted that due to limitations in these studies it is not possible to draw definitive conclusions. One limitation is that siRNA-mediated knockdown of TC-PTP, eNOS and PKCλ was poor as immunoblotting with the appropriate specific antibody demonstrated that TC-PTP, eNOS and PKCλ proteins levels was reduced to only 40%, 50% and 60%, respectively. A second limitation is that a positive control for pharmacological inhibition of each target, except mTOR, was not included in each study. Although, pharmacological inhibitors were used under the same conditions that had previously been shown to effectively inhibit its target (these studies are referenced in the results section). Another limitation is that in studies utilising

pharmacological inhibitors, the total levels of the target protein was not assessed. Therefore, STAT3 Tyr705 phosphorylation levels may have been effected by changes in target protein levels.

Experiment	Serum-supplemented	Serum - deprived	supplemented vs deprived (*P*-value)
	% inhibition of STAT3 Tyr705 phosphorylation by AMPK		
PP242	27 ± 5	71 ± 6	***$p<0.001$
Etomoxir	38 ± 5	66 ± 10	*$p<0.05$
EX527	48 ± 8	85 ± 5	***$p<0.001$

Table 3-1: Percentage (%) inhibition of sIL-6Rα/IL-6 stimulated STAT3 Tyr705 phosphorylation by AMPK in vehicle pre-treated HUVECs under both serum-supplemented and serum-deprived conditions.

Experiments investigating the effects of Etomoxir, EX527 and PP242 on AMPK-mediated inhibition of IL-6 signalling were conducted under both serum-supplemented and serum-deprived conditions. STAT3 phosphorylation data were first normalized to total STAT3 levels and expressed as a percentage (%) inhibition of STAT3 phosphorylation relative to maximal sIL-6Rα/IL-6 stimulation attained in vehicle pre-treated HUVECs. Data shown represent the mean ± SEM of three independent experiments

Chapter 4 - Molecular mechanism of AMPK mediated inhibition of IL-6 signalling: direct phosphorylation of JAK1

4.1 Introduction

4.1.1 Regulation of the JAK-STAT pathway by AMPK

At this point in the study, AMPK did not appear to act *via* a known regulator of JAK-STAT signalling, or an AMPK downstream target known to either directly or indirectly impact on JAK-STAT signalling. Therefore, the next line of inquiry was to assess whether AMPK could act directly on components of the JAK-STAT pathway. Preliminary investigations of the effects of AMPK on JAK-STAT signalling demonstrated that the inhibitory effect of AMPK on sIL-6Rα/IL-6 responses was not restricted to STAT3, as pre-incubation of HUVECs with AMPK activator, A769662, also abrogated sIL-6Rα/IL-6-stimulated phosphorylation of STAT1 (Figure 6.5B). A769662 also suppressed STAT3 phosphorylation in response to IFNα, which activates STATs *via* an IFNAR1/IFNAR2 complex distinct from the receptor complex formed by gp130 (Borden et al., 2007) (Figure 6.5A). These results suggested that AMPK was exerting its inhibitory effects at one or more common signalling loci downstream of IFNAR1/IFNAR2 and gp130 at a post-receptor level. AMPK is a Ser/Thr-directed protein kinase for which numerous distinct substrates continue to be identified (Schaffer et al., 2015). Thus, it was hypothesised that AMPK could directly phosphorylate serine or threonine residues within one or more JAKs to inhibit sIL-6Rα/IL-6 signalling.

4.1.2 Aims

The aims of this chapter were to determine whether or not one or more JAK isoforms were substrates of AMPK, assess whether AMPK-mediated phosphorylation of JAKs is required for inhibition of IL-6 signalling, and elucidate how AMPK phosphorylation of JAK might inhibit downstream signalling.

4.2 Results

4.2.1 Effect of JAK isoform knockdown on JAK-STAT signalling

The JAK-STAT signalling pathway can be activated in a variety of different cell types and within each cell type each cytokine activates a distinct subset of JAKs and STATs (Murray, 2007). In HUVECs, the individual components of the IFN-α or IL-6-induced JAK-STAT signalling pathway have yet to be clearly defined. Therefore, before investigating a role for JAKs as targets of AMPK's effect, the JAK isoform(s) through which IL-6 and IFN-α predominantly signal downstream in HUVECs needed to be identified.

4.2.1.1 Efficiency of JAK siRNA transfection of HUVECs

To begin testing this, a siRNA approach was used to specifically knockdown the expression of JAK1, JAK2 or TYK2 in order to investigate their individual contribution to IL-6- and IFN-α-stimulated downstream signalling. HUVECs express all four members of the JAK family, however the contribution of JAK3 was not investigated as expression levels are at a low basal level and a physiological role for JAK3 has not been shown in HUVECs (Verbsky et al., 1996). Control non-targeting siRNA and siRNA targeting each JAK isoform were separately transiently transfected into HUVECs for 48 hours prior to stimulation with either sIL-6Rα/IL-6 (25 ng/ml, 5 ng/ml) or IFN-α (25000 units/ml) for 30 or 15 minutes, respectively. In comparison to HUVECs treated with control siRNA, transfection of HUVECs with JAK1 siRNA significantly reduced JAK1 expression by 66 ± 11% (***p<0.001) (Figure 4.1). Similarly, transfection of HUVECs with JAK2 siRNA significantly reduced JAK2 expression by 60 ± 6% (***p<0.001) (Figure 4.2) and transfection of HUVECs with TYK2 siRNA significantly reduced TYK2 expression by 52 ± 7% (***p<0.001) (Figure 4.3). JAK1, JAK2 and TYK2 protein levels did not alter significantly with sIL-6Rα/IL-6 or IFN-α treatment. Overall, the siRNAs were effective in knocking down specific JAK isoforms.

4.2.1.2 Effect of JAK isoform knockdown on sIL-6Rα/IL-6 and IFN-α signalling in HUVECs.

IL-6 and IFN-α can each trigger STAT1 and STAT3 phosphorylation at Tyr701 and Tyr705, respectively, which are required for STAT1 and STAT3 activation respectively and can therefore be used as surrogate markers for their activation

(Shuai et al., 1994, Kaptein et al., 1996). Therefore, to determine the effect of JAK knockdown on sIL-6Rα/IL-6 and IFN-α signalling in HUVECs, whole-cell extracts were immunoblotted with phospho-STAT1 (Tyr701) and total-STAT1 or phospho-STAT3(Tyr705) and total-STAT3 antibodies.

In comparison to control siRNA-treated HUVECs, JAK1 siRNA treatment significantly inhibited sIL-6Rα/IL-6 stimulation of STAT3 Tyr705 phosphorylation by 61 ± 7% (***p<0.001) (Figure 4.4). In contrast, JAK2 siRNA treatment significantly inhibited sIL-6Rα/IL-6 stimulation of STAT3 Tyr705 phosphorylation by only 20 ± 5% (**p<0.01) (Figure 4.5) and TYK2 siRNA treatment produced a statistically insignificant 7 ± 2% (p>0.05, NS) inhibition of sIL-6Rα/IL-6-stimulated STAT3 Tyr705 phosphorylation (Figure 4.6). For each JAK siRNA transfection, sIL-6Rα/IL-6 stimulation of STAT3 Tyr705 phosphorylation in untreated HUVECs compared with control siRNA treated HUVECs demonstrated that control siRNA treatment did not significantly alter sIL-6Rα/IL-6 stimulation of STAT3 Tyr705 phosphorylation (Figure 4.4, 4.5 and 4.6). Altogether, these data suggest that sIL-6Rα/IL-6 stimulation of STAT3 phosphorylation on Tyr705 mainly requires activation of JAK1 with some contribution of JAK2, and no contribution of TYK2 detectable.

For both JAK1 and JAK2 siRNA experiments, IFN-α stimulation of HUVECs treated with control siRNA did not significantly stimulate STAT3 Tyr705 phosphorylation beyond the basal levels produced by unstimulated cells treated with control siRNA (Figure 4.4 and 4.5). For the TYK2 experiments, IFN-α stimulation of STAT3 Tyr705 phosphorylation was found to be variable between and within individual experiments and therefore the data was inconclusive (Figure 4.6). As IFN-α signals predominantly through STAT1, immunoblots were also probed with antibodies versus phospho-STAT1 (Tyr701) and total-STAT1 (Ramana et al., 2000) (Figure 4.8). In comparison to untreated HUVECs, transfection of HUVECs with siRNA increased total STAT1 levels. Overall, it was not possible to compare the effects of JAK knockdown on STAT1 Tyr701 phosphorylation or IFN-α signalling. However previous reports have demonstrated IFN-α signals through JAK1 and TYK2 in multiple cell types (Borden et al., 2007, Gauzzi et al., 1996). Thus in conjunction with my data, JAK1 was identified as a common post receptor intermediately downstream of both IL-6 and IFN-α signalling.

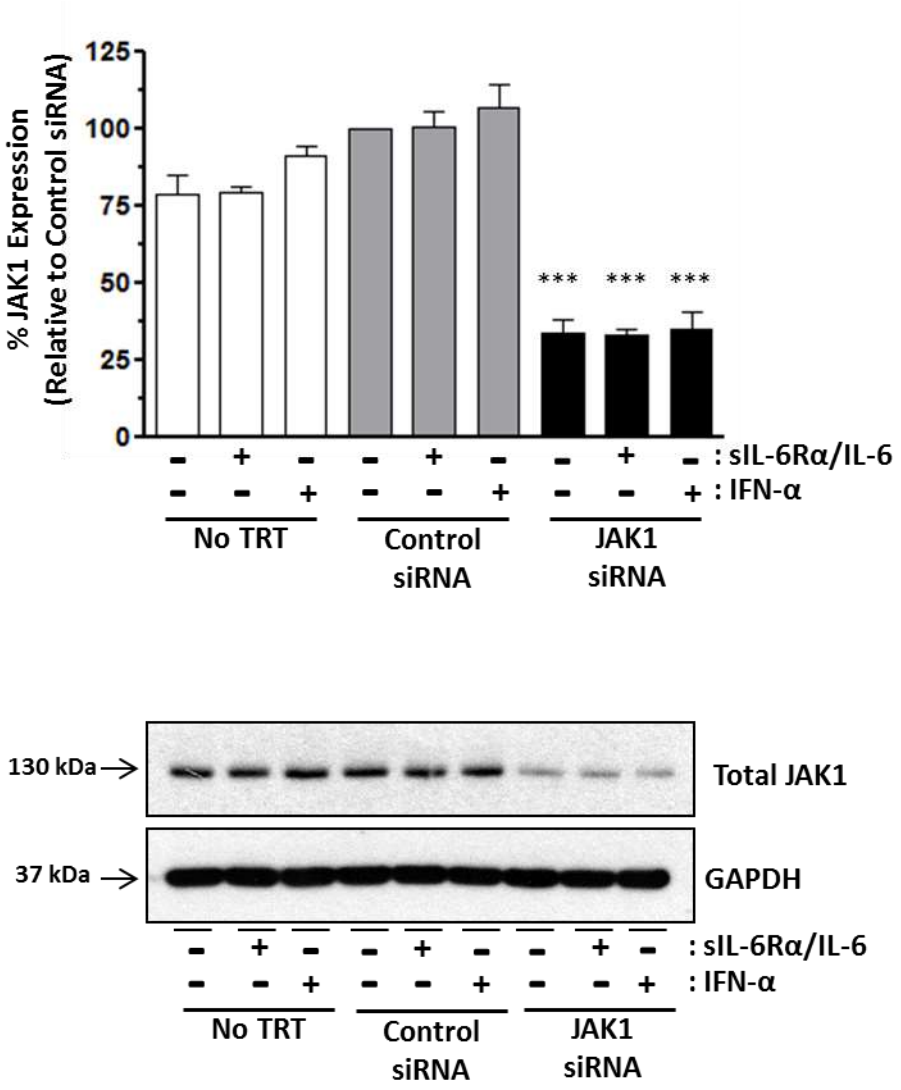

Figure 4.1: siRNA-mediated knockdown of JAK1 isoform expression in HUVECs
HUVECs were transfected with either 10nM JAK1 or control siRNA 48hrs prior to stimulation with or without 25ng/ml sIL-6Rα and 5ng/ml IL-6 (sIL-6Rα/IL-6) or 25000 units/ml IFN-α for either 30 or 15 minutes, respectively. Control siRNA was used as a negative control. Protein-equalised cell extracts were then analysed by SDS-PAGE and immunoblotting with antibodies specific for total JAK1 and GAPDH as indicated. GAPDH served as a loading control. Total JAK1 protein levels were first normalized to GAPDH levels and expressed as a percentage (%) of the maximal protein levels attained in unstimulated control siRNA transfected HUVECs (set at 100%). Quantitative analysis from three experiments is presented. Columns are means ±SEM, *** p<0.001. A representative blot from n=3 experiments is shown. n=3 from one batch of pooled donor HUVEC

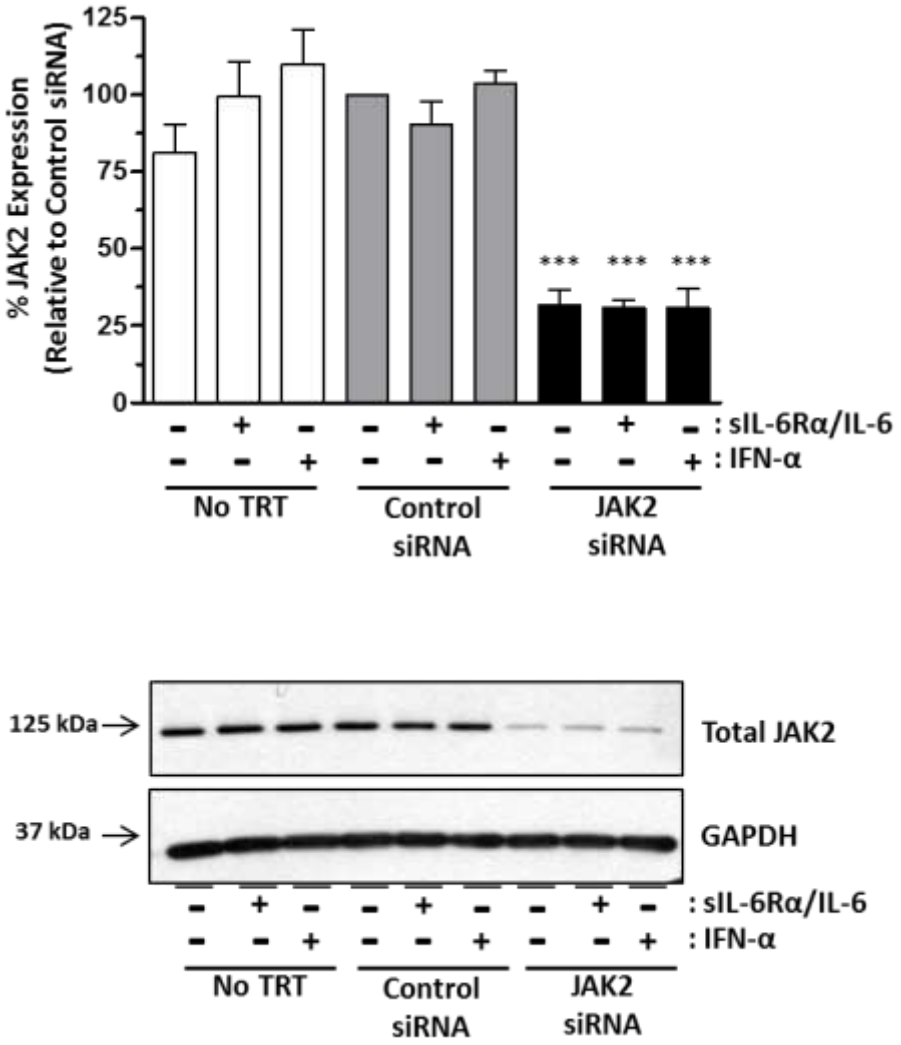

Figure 4.2: siRNA-mediated knockdown of JAK2 isoform expression in HUVECs
HUVECs were transfected with either 10nM JAK2 or control siRNA 48hrs prior to stimulation with or without 25ng/ml sIL-6Rα and 5ng/ml IL-6 (sIL-6Rα/IL-6) or 25000 units/ml IFN-α for either 30 or 15 minutes, respectively. Control siRNA was used as a negative control. Protein-equalised cell extracts were then analysed by SDS-PAGE and immunoblotting with antibodies specific for total JAK2 and GAPDH as indicated. GAPDH served as a loading control. Total JAK2 protein levels were first normalized to GAPDH levels and expressed as a percentage (%) of the maximal protein levels attained in unstimulated control siRNA transfected HUVECs (set at 100%). Quantitative analysis from three experiments is presented. Columns are means ±SEM, *** p<0.001. A representative blot from n=3 experiments is shown. n=3 from one batch of pooled donor HUVEC

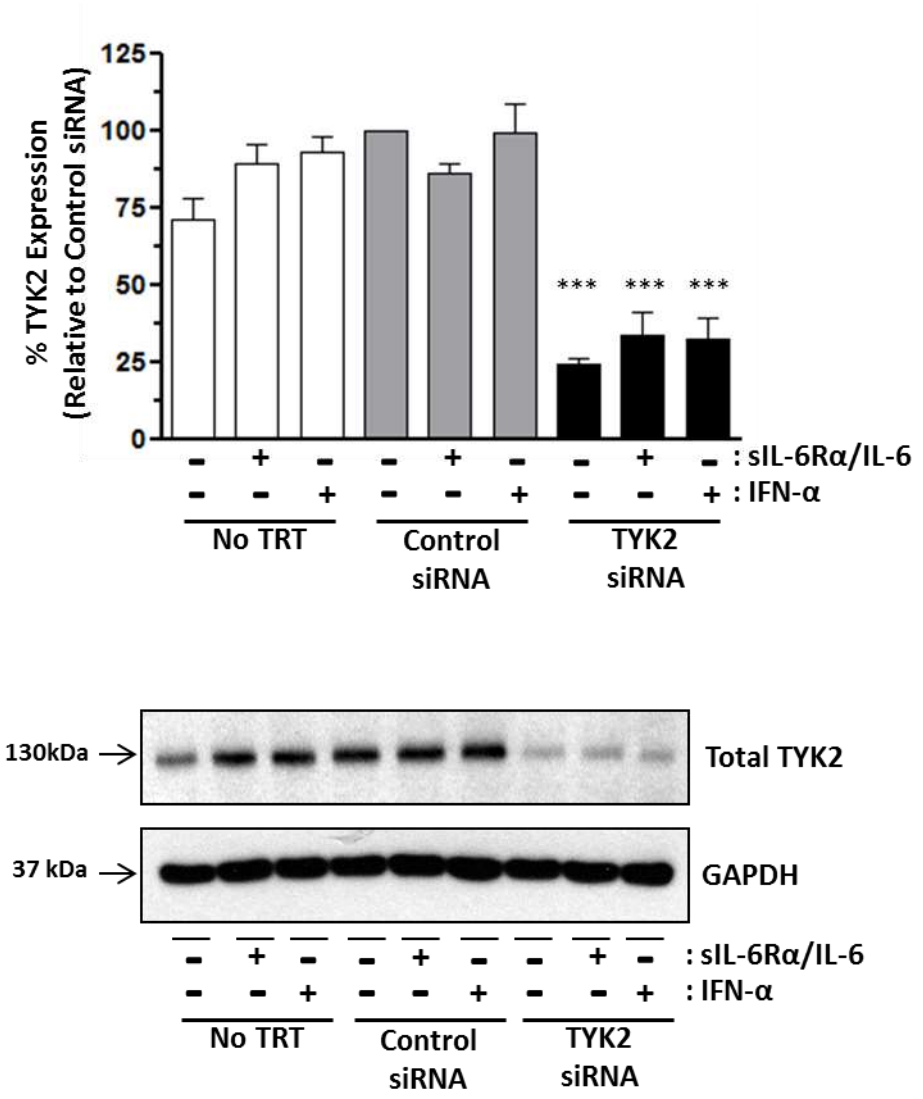

Figure 4.3: siRNA-mediated knockdown of TYK2 isoform expression in HUVECs
HUVECs were transfected with either 10nM TYK2 or control siRNA 48hrs prior to stimulation with or without 25ng/ml sIL-6Rα and 5ng/ml IL-6 (sIL-6Rα/IL-6) or 25000 units/ml IFN-α for either 30 or 15 minutes, respectively. Control siRNA was used as a negative control. Protein-equalised cell extracts were then analysed by SDS-PAGE and immunoblotting with antibodies specific for total TYK2 and GAPDH as indicated. GAPDH served as a loading control. Total TYK2 protein levels were first normalized to GAPDH levels and expressed as a percentage (%) of the maximal protein levels attained in unstimulated control siRNA transfected HUVECs (set at 100%). Quantitative analysis from three experiments is presented. Columns are means ±SEM, *** p<0.001. A representative blot from n=3 experiments is shown. n=3 from one batch of pooled donor HUVEC

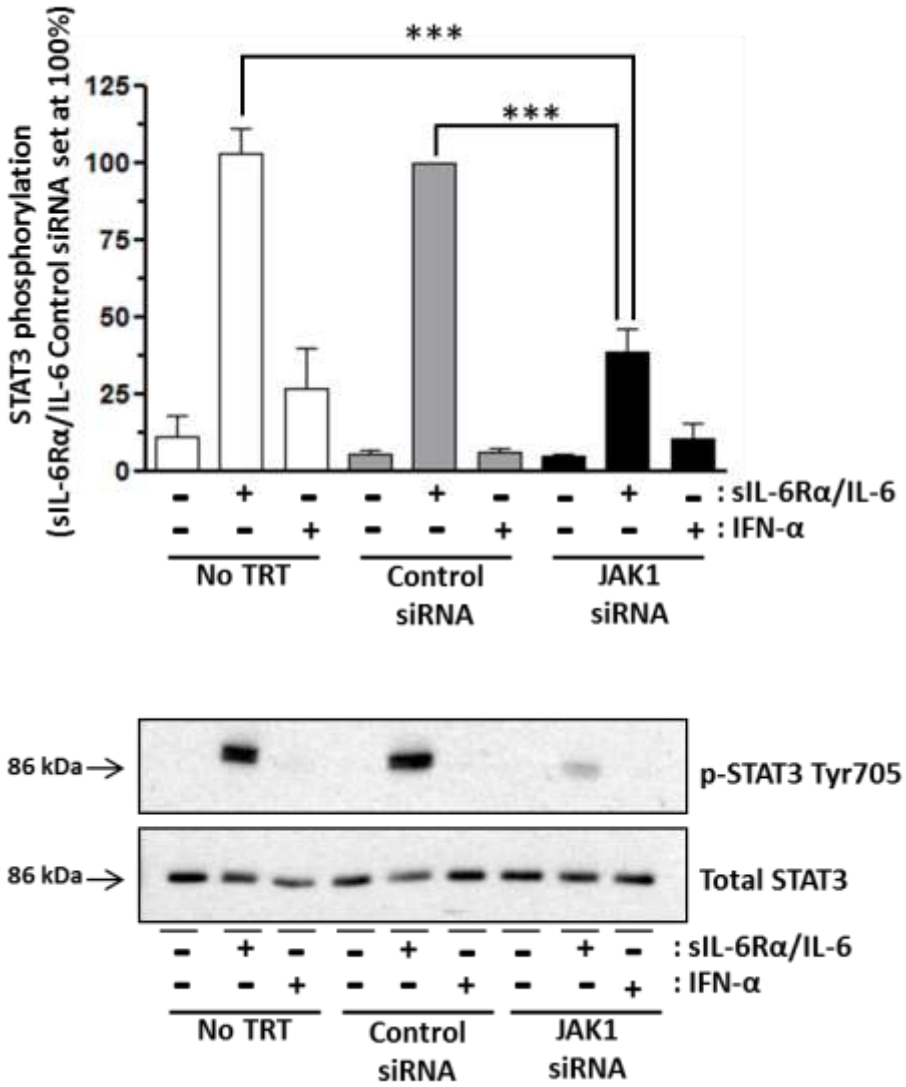

Figure 4.4: Effect of JAK1 isoform knockdown on sIL-6Rα/IL-6-stimulated STAT3 tyrosine (705) phosphorylation in HUVECs.
HUVECs were transfected with either 10nM JAK1 or control siRNA 48hrs prior to stimulation with or without 25ng/ml sIL-6Rα and 5ng/ml IL-6 (sIL-6Rα/IL-6) or 25000 units/ml IFN-α for either 30 or 15 minutes, respectively. Control siRNA was used as a negative control. Protein-equalised cell extracts were then analysed by SDS-PAGE and immunoblotting with antibodies specific for phospho-STAT3 (Tyr705) and total STAT3 as indicated. STAT3 phosphorylation data were first normalized to total STAT3 levels and expressed as a percentage (%) of the maximal sIL-6Rα/IL-6 stimulation attained in control siRNA transfected HUVECs (set at 100%). Quantitative analysis from three experiments is presented. Columns are means ±SEM, *** p<0.001. A representative blot from n=3 experiments is shown. n=3 from one batch of pooled donor HUVEC

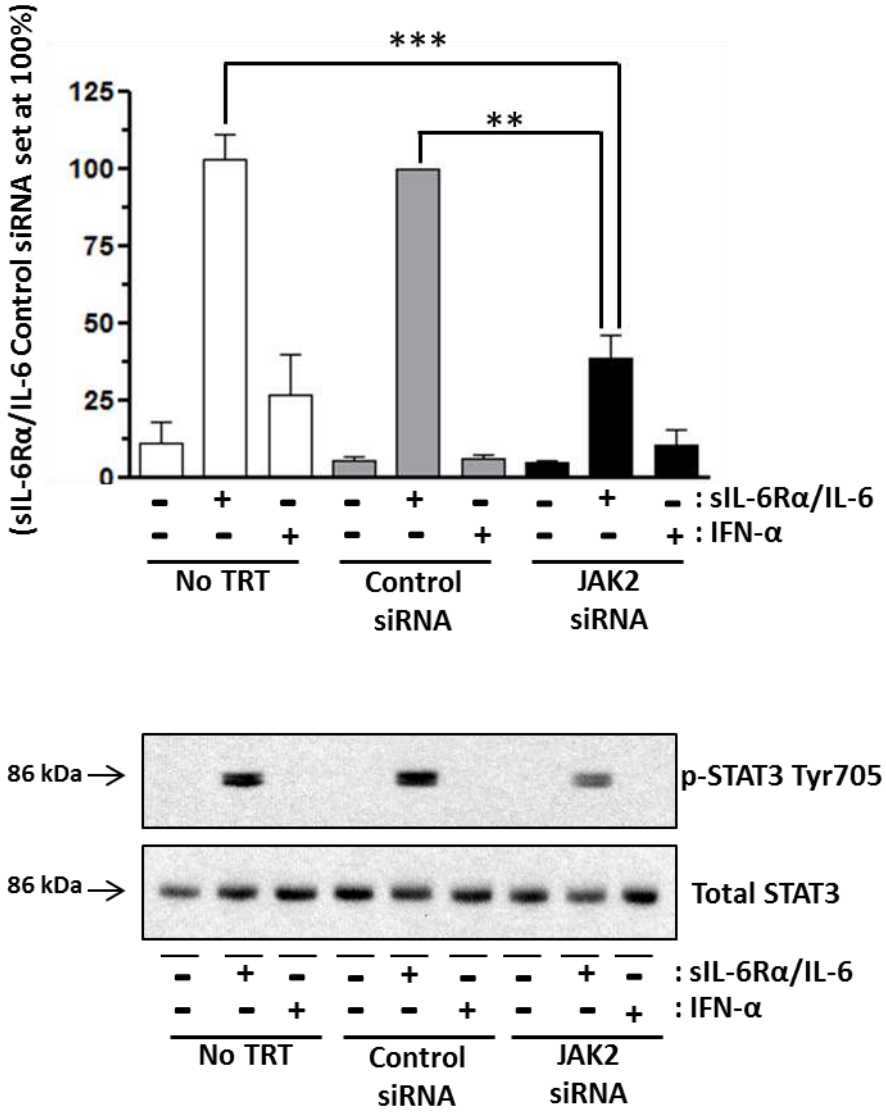

Figure 4.5: Effect of JAK2 isoform knockdown on sIL-6Rα/IL-6-stimulated STAT3 tyrosine (705) phosphorylation in HUVECs.
HUVECs were transfected with either 10nM JAK2 or control siRNA 48hrs prior to stimulation with or without 25ng/ml sIL-6Rα and 5ng/ml IL-6 (sIL-6Rα/IL-6) or 25000 units/ml IFN-α for either 30 or 15 minutes, respectively. Control siRNA was used as a negative control. Protein-equalised cell extracts were then analysed by SDS-PAGE and immunoblotting with antibodies specific for phospho-STAT3 (Tyr705) and total STAT3 as indicated. STAT3 phosphorylation data were first normalized to total STAT3 levels and expressed as a percentage (%) of the maximal sIL-6Rα/IL-6 stimulation attained in control siRNA transfected HUVECs (set at 100%). Quantitative analysis from three experiments is presented. Columns are means ±SEM, *** p<0.001, **p<0.01. A representative blot from n=3 experiments is shown. n=3 from one batch of pooled donor HUVEC

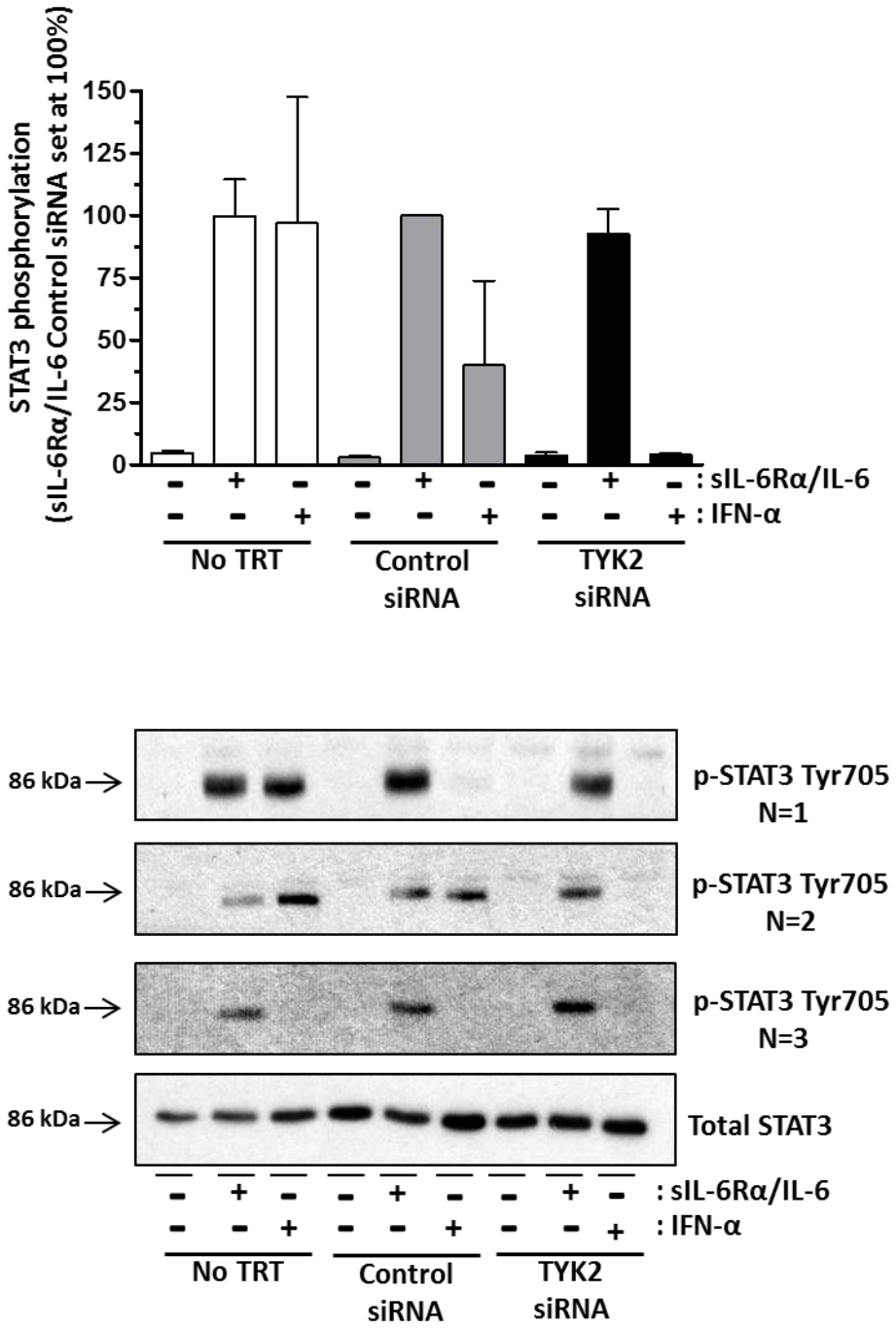

Figure 4.6: Effect of TYK2 isoform knockdown on STAT3 (705) tyrosine phosphorylation in HUVECs

HUVECs were transfected with either 10nM TYK2 or control siRNA 48hrs prior to stimulation with or without 25ng/ml sIL-6Rα and 5ng/ml IL-6 (sIL-6Rα/IL-6) or 25000 units/ml IFN-α for either 30 or 15 minutes, respectively. Control siRNA was used as a negative control. Protein-equalised cell extracts were then analysed by SDS-PAGE and immunoblotting with antibodies specific for phospho-STAT3 (Tyr705) and total STAT3 as indicated. STAT3 phosphorylation data were first normalized to total STAT3 levels and expressed as a percentage (%) of the maximal sIL-6Rα/IL-6 stimulation attained in control siRNA transfected HUVECs (set at 100%). Quantitative analysis from three experiments is presented. Columns are means ±SEM, not significant (NS), $p>0.05$ A representative blot from n=3 experiments is shown. n=3 from one batch of pooled donor HUVEC

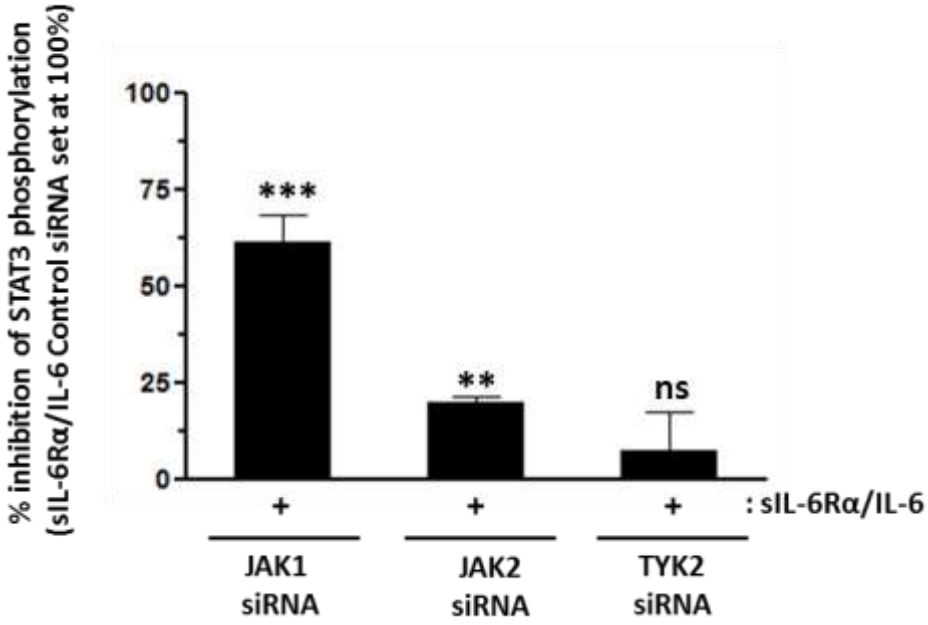

Figure 4.7: The effect of JAK isoform knockdown on STAT3 tyrosine (705) phosphorylation in HUVECs.

HUVECs were transfected with either 10nM JAK1 or 10nM JAK2 or 10nM Tyk2 siRNA 48hrs prior to stimulation with or without 25ng/ml sIL-6Rα and 5ng/ml IL-6 (sIL-6Rα/IL-6) for 30 minutes. Control siRNA was used as a negative control. Protein-equalised cell extracts were then analysed by SDS-PAGE and immunoblotting with antibodies specific for phospho-STAT3 (Tyr705) and total STAT3. STAT3 phosphorylation data were first normalized to total STAT3 levels and expressed as a percentage (%) inhibition of STAT3 phosphorylation relative to maximal sIL-6Rα/IL-6 stimulation attained in control siRNA transfected HUVECs. Quantitative analysis from three experiments is presented. Columns are means ±SEM, $p>0.05$ NS, $^{**}p<0.01$ *** $p<0.001$.

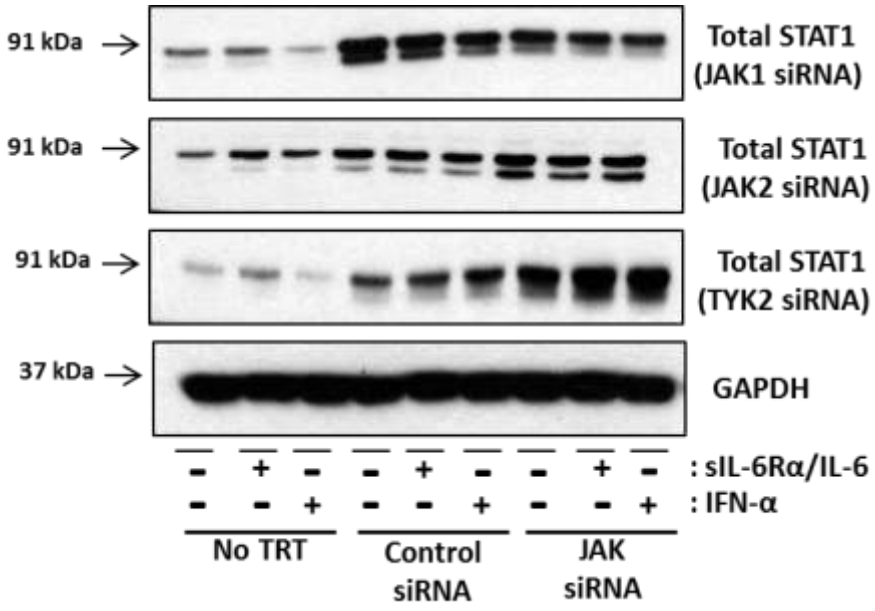

Figure 4.8: Effect of JAK isoform knockdown on total STAT1 expression in HUVECs
HUVECs were transfected with either 10nM JAK1 or 10nM JAK2 or 10nM Tyk2 siRNA 48hrs prior to stimulation with or without 25ng/ml sIL-6Rα and 5ng/ml IL-6 (sIL-6Rα/IL-6) or 25000 units/ml IFN-α for either 30 or 15 minutes, respectively. Control siRNA was used as a negative control. Protein-equalised cell extracts were then analysed by SDS-PAGE and immunoblotting with an antibody specific for total STAT1 as indicated. GAPDH served as a loading control. A representative blot from n=3 experiments is shown. n=3 from one batch of pooled donor HUVEC

4.2.2 AMPK phosphorylation of JAK-derived peptides *in vitro*

4.2.2.1 AMPK phosphorylation of full-length human JAK peptides *in vitro*

It was hypothesised that AMPK could directly phosphorylate JAK1 to inhibit both sIL-6Rα/IL-6 and IFN-α stimulation of STAT3 phosphorylation on Tyr705. To test whether AMPK could directly phosphorylate Ser or Thr residues in JAK, *in vitro* AMPK assays were carried out using immobilised libraries of 25-mer peptides overlapping by 5 residues that span the entire ORFs of human JAK1, JAK2, JAK3 and TYK2 (kindly prepared by Professor G.S. Baillie [University of Glasgow]), and using AMPK purified from rat liver (Hawley et al., 1996, a generous gift from Prof. Grahame Hardie [University of Dundee]).

Using automatic SPOT synthesis, the full length primary sequences of each of the human JAK isoforms (JAK1, JAK2, JAK3, Tyk2) were spotted onto nitrocellulose coated microscope slides in overlapping 25-mer peptides that spanned the entire open reading frames to produce immobilised libraries of peptides (Frank, 2002). Each consecutive 25-mer peptide is a 5 amino-acid shift of the previous peptide and is spotted in duplicate (schematic representation shown in Figure 4.9). Peptide arrays were then incubated in the absence or presence of purified active rat liver AMPK in the presence of [γ-^{32}P] ATP. ^{32}P-Phosphate incorporation was detected by autoradiography following exposure to X-ray film, with duplicate dark spots representing potential sites of peptide phosphorylation by AMPK.

Figures 4.10, 4.12, 4.13 and 4.14 show the autoradiogram of the full length human JAK peptide arrays subjected to *in vitro* AMPK phosphorylation; areas of interest have been highlighted and then magnified for clarity. Tables 6-1 to 6-4 found in the appendix details the layout of each peptide array and the amino acid sequences corresponding to each peptide spot. As a positive control, each peptide array slide contained a synthetic AMPK peptide substrate termed “SAMS peptide” (HMRSAMSGLHLVKRR) which is derived from residues 73- 85 on rat ACC1 which includes known AMPK site Ser79 (Davies et al., 1989). (Figure 4.10, 4.12-14, highlighted and magnified in green). In comparison to the peptide arrays incubated without active AMPK, the SAMS peptide spots on the arrays incubated with active AMPK are darker, confirming that the AMPK preparation used was catalytically active (Figure 4.10, 4.12-14, highlighted and magnified in green).

On the full length human JAK1 peptide array, a cluster of darker spots can be observed in the presence of AMPK but not in its absence (Figure 4.10, highlighted and magnified in red). These comprise four consecutive overlapping peptides; K-N-F-Q-I-E-V-Q-K-G-R-Y-S^{508}-L-H-G-S^{512}-D-R-S^{515}-F-P-S^{518}-L-G, E-V-Q-K-G-R-Y-S^{508}-L-H-G-S^{512}-D-R-S^{515}-F-P-S^{518}-L-G-D-L-M-S^{524}-H, R-Y-S^{508}-L-H-G-S^{512}-D-R-S^{515}-F-P-S^{518}-L-G-D-L-M-S^{524}-H-L-K-K-Q-I and G-S^{512}-D-R-S^{515}-F-P-S^{518}-L-G-D-L-M-S^{524}-H-L-K-K-Q-I-L-R-T-D-N, which appear to be phosphorylated by active AMPK (Figure 4.10). These overlapping peptides span five putative AMPK phosphoacceptor sites; Ser508, Ser512, Ser515, Ser518 and Ser524 (Figure 4.10).

Alignment of the primary sequences of all four JAK isoforms identified a related sequence similarly positioned within the SH2 domain of each protein (Figure 4.11). These 25-mer peptides are highlighted and magnified in red on the full length JAK2, JAK3 and TYK2 peptide arrays (Figure 4.12, 4.13 and 4.14).

On initial inspection, the full length human JAK2 peptide array incubated with active AMPK, did not appear to be detectably phosphorylated when compared with the JAK2 peptide array incubated without AMPK (Figure 4.12). However, closer inspection of the JAK2 25-mer peptide that aligns with the JAK1 25-mer peptide identified as phosphorylated by AMPK demonstrates that these spots are slightly darker when compared with the JAK2 peptide array incubated without AMPK (Figure 4.12, highlighted and magnified in red). These comprise three consecutive overlapping peptides; H-C-L-I-T-K-N-E-N-E-E-Y-N-L-S^{465}-G-T^{467}-K-K-N-F-S^{472}-S^{473}-L-K, K-N-E-N-E-E-Y-N-L-S^{465}-G-T^{467}-K-K-N-F-S^{472}-S^{473}-L-K-D-L-L-N-C, E-Y-N-L-S^{465}-G-T^{467}-K-K-N-F-S^{472}-S^{473}-L-K-D-L-L-N-C-Y-Q-M-E-T, which appear to be phosphorylated by active AMPK. These overlapping peptides span four putative AMPK phosphoacceptor sites; Ser465, Thr467, Ser472, and Ser473 (Figure 4.12).

Full length human JAK3 and TYK2 peptide arrays were also subjected to *in vitro* phosphorylation by activated AMPK. However, no phosphorylation was detectable when compared to the corresponding peptide array incubated without active AMPK despite positive AMPK-dependent phosphorylation of SAMS peptide on each array slide (Figure 4.13 and 4.14). To confirm this observation, the JAK2, JAK3 and TYK2 25-mer peptides that aligned with the JAK1 25-mer peptide identified as phosphorylated by AMPK were spotted on the same peptide arrays to allow for direct comparison (Figure 4.15). These demonstrated that AMPK only

phosphorylated the JAK2 25-mer peptide, E-Y-N-L-S^{465}-G-T^{467}-K-K-N-F-S^{472}-S^{473}-L-K-D-L-L-N-C-Y-Q-M-E-T, but not the JAK3 and TYK2 25-mer peptides, T-F-L-L-V-G-L-S^{444}-R-P-H-S^{448}-S^{449}-L-R-E-L-L-A-T^{456}-C-W-D-G-G and A-F-V-L-E-G-W-G-R-S^{523}-F-P-S^{526}-V-R-E-L-G-A-A-L-Q-GC-L, respectively (Figure 4.15). Overall, these data suggest that SH2 domain-derived peptides from JAK1 and JAK2, but not JAK3 and Tyk2, can serve as substrates for phosphorylation by AMPK *in vitro*.

4.2.2.2 Identification of AMPK phosphoacceptor sites within JAK1-derived peptides

Thus far, the data suggests that JAK1 could potentially be a substrate of AMPK as AMPK phosphorylated a 25-mer peptide of JAK1 which contains five serine residues *in vitro*. To identify whether some or all of the five serine residues are phosphorylated by AMPK, *in vitro* AMPK phosphorylation assays were conducted using peptide arrays spotted with wild-type (WT) and serine-to-alanine mutated versions of the JAK1 25-mer peptide identified as an AMPK substrate. The chemical structure of alanine is identical to serine, except it is missing the -OH group and therefore alanine is “non-phosphorylatable”. Consistent with Figure 4.10, the WT JAK1 peptide, was phosphorylated by AMPK as highlighted by the darker spots that appear in the presence of AMPK (Figure 4.16). In contrast, a mutated peptide in which all five Ser residues have been replaced by non-phosphorylatable Ala residues abolished AMPK-dependent phosphorylation (Figure 4.16). Mutant JAK1 peptides containing Ala substitutions at each individual Ser residue were also spotted on the array. It can clearly be seen that AMPK phosphorylated the mutant JAK1 peptides containing Ala substitution at Ser508, Ser512 or Ser524, whereas Ala substitution at either Ser515 or Ser518 appear to have reduced phosphorylation by AMPK (Figure 4.16). Mutant JAK1 peptides containing Ala substitutions at two or more Ser residue were also prepared. The mutant JAK1 peptide containing Ala substitutions at Ser508, Ser512 and Ser524 appears to be phosphorylated by AMPK equivalently to WT peptide, whereas Ala substitution of both Ser515 and Ser518 abolished AMPK-dependent phosphorylation similarly to the peptide in which all five Ser residues were mutated to Ala (Figure 4.16). Overall, these data indicate that AMPK can phosphorylate the identified JAK1 25-mer peptide *in vitro* at Ser515 and Ser518.

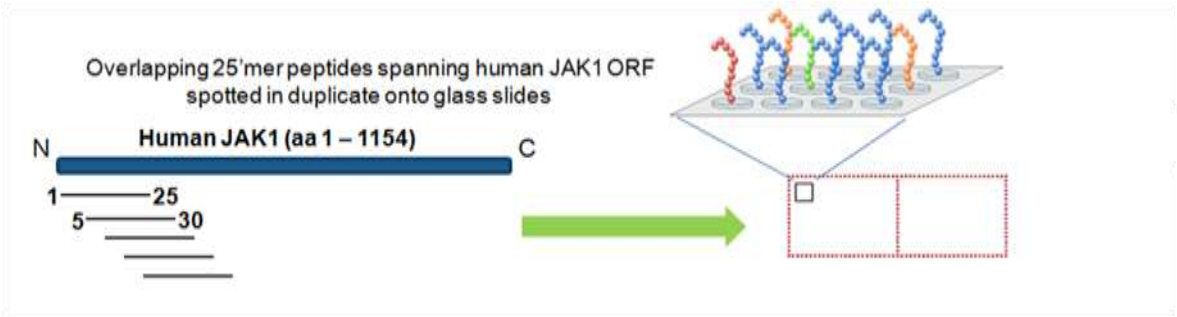

Figure 4.9: Schematic representation of full length human JAK peptide array
Using automatic SPOT synthesis, the full length primary sequences of each of the human JAK isoforms (JAK1, JAK2, JAK3, Tyk2) were spotted onto nitrocellulose coated microscope slides in overlapping 25-mer peptides that spanned the entire open reading frames to produce immobilised libraries of peptides (Frank, 2002). Each consecutive 25-mer peptide is a 5 amino-acid shift of the previous peptide and is spotted in duplicate.

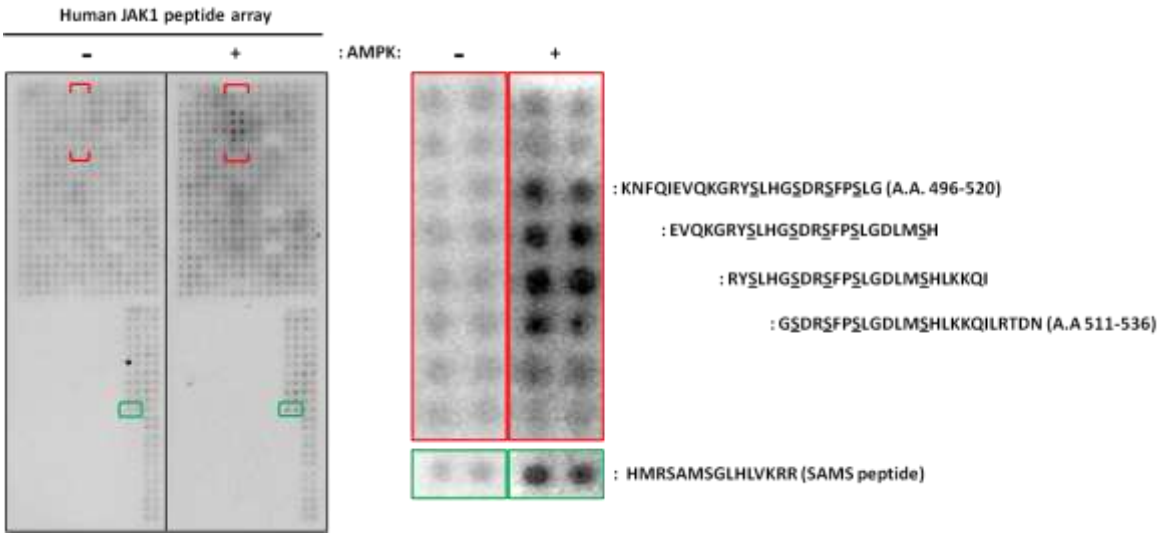

Figure 4.10: In vitro AMPK phosphorylation of JAK1 peptide arrays
Peptide arrays consisting of consecutive 25-mer peptides spanning the human JAK1 reading frame were incubated in 1µCi/ml γ-^{32}P-ATP and in the presence of 0.5U/ml activated AMPK at 30 °C for 30 minutes. As a control, a peptide array was incubated in radiolabelled γ-^{32}P-ATP alone. Phosphorylation was detected by incorporation of radiolabelled ^{32}P and radioactive signals were captured by autoradiography following exposure to Kodak X-ray film, and dark spots represent positive areas of phosphorylation by AMPK. Positive areas of phosphorylation of JAK1 peptides by AMPK are highlighted and magnified in red. As a positive control, each peptide array contains a synthetic AMPK substrate called SAMS peptide (HMRSAMSGLHLVKRR), highlighted in green. A representative autoradiogram from n=3 experiments is shown.

Human	JAK1	506	R - Y S L H G S D R **S** F P **S** L G D L M S H L K K Q I	530
Human	JAK2	460	E E Y N L S G T K K N F **S** **S** L K D L L N C Y Q M E T	485
Human	JAK3	436	G T F L L V G L S R P H **S** **S** L R E L L A T C W D G G	467
Human	TYK2	513	A - F V L E G W G R **S** F P **S** V R E L G A A L Q G C L	537

Figure 4.11: Alignment of JAK1 25-mer peptide identified as phosphorylated by AMPK with JAK2, JAK3, and TYK2

NCBI BLAST program was used to align the primary sequences all four JAK isoforms to identify the JAK2, JAK3 and TYK2 25-mer peptides that align with the JAK1 25-mer peptide identified as phosphorylated by AMPK

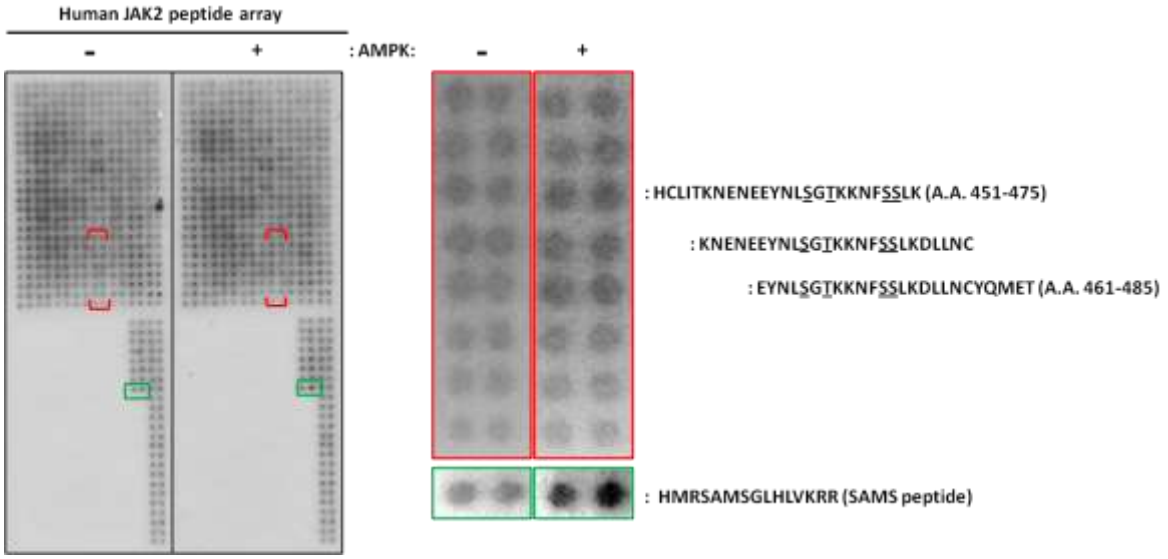

Figure 4.12: *In vitro* AMPK phosphorylation of JAK2 peptide arrays
Peptide arrays consisting of consecutive 25-mer peptides spanning the human JAK2 reading frame were incubated in 1µCi/ml γ-^{32}P-ATP and in the presence of 0.5U/ml activated AMPK at 30 °C for 30 minutes. As a control, a peptide array was incubated in radiolabelled γ-^{32}P-ATP alone. Phosphorylation was detected by incorporation of radiolabelled ^{32}P and radioactive signals were captured by autoradiography following exposure to Kodak X-ray film, and dark spots represent positive areas of phosphorylation by AMPK. Positive areas of phosphorylation of JAK2 peptides by AMPK are highlighted and magnified in red. As a positive control, each peptide array contains a synthetic AMPK substrate called SAMS peptide (HMRSAMSGLHLVKRR), highlighted in green. A representative autoradiogram from n=3 experiments is shown.

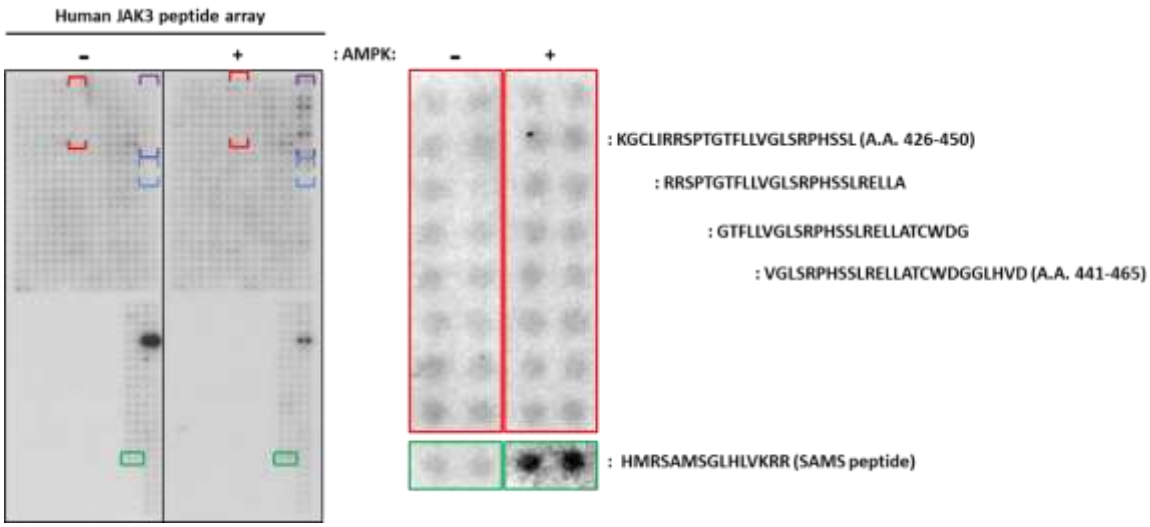

Figure 4.13: *In vitro* AMPK phosphorylation of JAK3 peptide arrays
Peptide arrays consisting of consecutive 25-mer peptides spanning the human JAK3 reading frame were incubated in 1µCi/ml γ-^{32}P-ATP and in the presence of 0.5U/ml activated AMPK at 30 °C for 30 minutes. As a control, a peptide array was incubated in radiolabelled γ-^{32}P-ATP alone. Phosphorylation was detected by incorporation of radiolabelled ^{32}P and radioactive signals were captured by autoradiography following exposure to Kodak X-ray film, and dark spots represent positive areas of phosphorylation by AMPK. Positive areas of phosphorylation of JAK3 peptides by AMPK are highlighted and magnified in red. As a positive control, each peptide array contains a synthetic AMPK substrate called SAMS peptide (HMRSAMSGLHLVKRR), highlighted in green. A representative autoradiogram from n=3 experiments is shown.

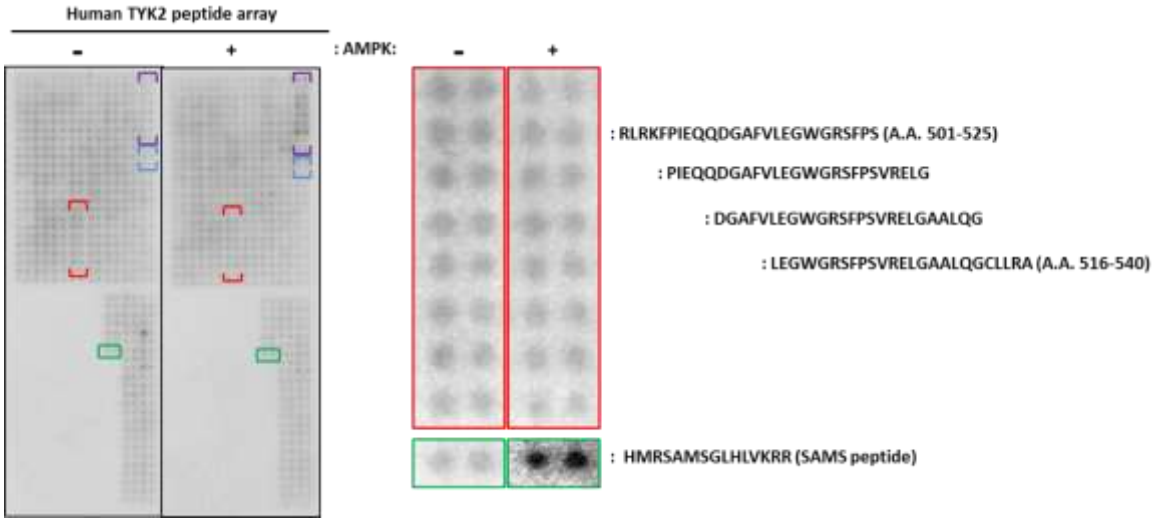

Figure 4.14: *In vitro* AMPK phosphorylation of TYK2 peptide arrays
Peptide arrays consisting of consecutive 25-mer peptides spanning the human TYK2 reading frame were incubated in 1µCi/ml γ-^{32}P-ATP and in the presence of 0.5U/ml activated AMPK at 30 °C for 30 minutes. As a control, a peptide array was incubated in radiolabelled γ-^{32}P-ATP alone. Phosphorylation was detected by incorporation of radiolabelled ^{32}P and radioactive signals were captured by autoradiography following exposure to Kodak X-ray film, and dark spots represent positive areas of phosphorylation by AMPK. Positive areas of phosphorylation of TYK2 peptides by AMPK are highlighted and magnified in red. As a positive control, each peptide array contains a synthetic AMPK substrate called SAMS peptide (HMRSAMSGLHLVKRR), highlighted in green. A representative autoradiogram from n=3 experiments is shown.

Figure 4.15: *In vitro* AMPK phosphorylation of JAK SH2 domain-derived peptides
Peptide arrays consisting of JAK2, JAK3 and TYK2 SH2 domain-derived peptides were incubated in 1µCi/ml γ-^{32}P-ATP and in the presence of 0.5U/ml activated AMPK at 30 °C for 30 minutes. As a control, a peptide array was incubated in radiolabelled γ-^{32}P-ATP alone. Phosphorylation was detected by incorporation of radiolabelled ^{32}P and radioactive signals were captured by autoradiography following exposure to Kodak X-ray film, and dark spots represent positive areas of phosphorylation by AMPK. A representative autoradiogram from n=3 experiments is shown.

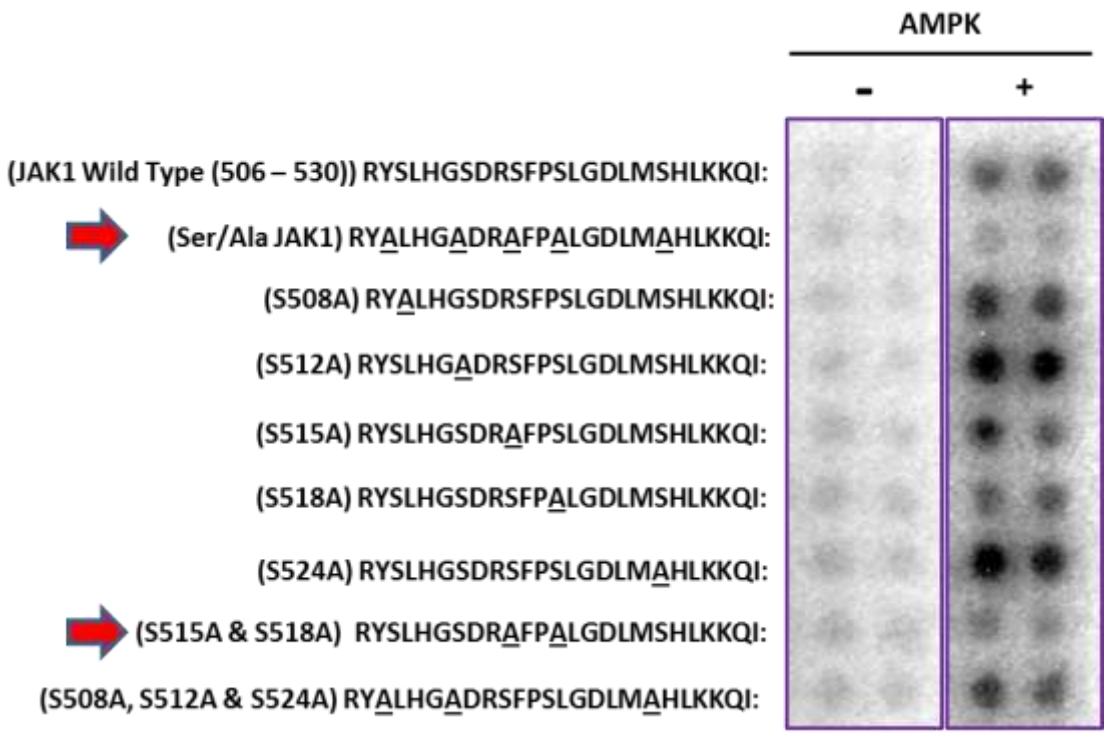

Figure 4.16: *In vitro* AMPK phosphorylation of Ser-Ala mutated JAK1 peptides
Peptide arrays consisting of WT and Ser-Ala mutated human JAK1 25-mer peptides were incubated in 1µCi/ml γ-^{32}P-ATP and in the presence of 0.5U/ml activated AMPK at 30 °C for 30 minutes. As a control a peptide array was incubated in radiolabelled γ-^{32}P-ATP alone. Phosphorylation was detected by incorporation of radiolabelled ^{32}P and radioactive signals were captured by autoradiography following exposure to Kodak X-ray film, and dark spots represent positive areas of phosphorylation by AMPK. The Ser-Ala mutated putative phosphoacceptor sites for the serine/threonine AMPK are indicated in bold and underlined in each peptide sequence. The arrows highlight the Ser-Ala mutated JAK1 peptides which have abolished AMPK phosphorylation of JAK1 peptide. A representative autoradiogram from n=3 experiments is shown.

4.2.3 Effect of AMPK activator A769662 on IL-6 signalling in human fibrosarcoma cells

JAK1-null U4C human fibrosarcoma cells were derived from parental cell 24C by Muller et al., (1993). These cells were used to investigate the role of JAK1 phosphorylation in AMPK-mediated inhibition of IL-6 signalling. First, the effects of A769662 on sIL-6Rα/IL-6 signalling in these cells had to be assessed to ensure that AMPK could inhibit JAK1-mediated phosphorylation of STAT3. To test this, 2C4, U4C and U4C.JAK1 cells (U4C.JAK1 are U4C-derived cell line in which JAK1 had been stably re-expressed (Guschin et al., 1995)) were pre-treated with vehicle or A769662 for 40 minutes followed by stimulation with vehicle or sIL-6Rα/IL-6 for 30 minutes.

JAK1, JAK2 and TYK2 levels were assessed by by immunoblotting cell extracts with total JAK1, JAK2 and TYK2 antibodies, respectively. JAK1 was expressed in parental cells 24C and JAK1 rescue cells U4C.JAK1, but JAK1 was absent in U4C cells (Figure 4.17A). JAK2 and TYK2 expression was detected in both 2C4 and U4C cells. In comparison to 2C4 cells, expression of TYK2 and JAK2 was unchanged by the loss of JAK1 (Figure 4.17B). Whole-cell extracts were also immunoblotted with phospho-STAT3 (Tyr705) and total-STAT3 antibodies. In comparison to vehicle treated 2C4 and U4C.JAK1 cells, sIL-6Rα/IL-6 substantially stimulated STAT3 Tyr705 phosphorylation (Figure 4.17A). A769662 activation of AMPK substantially inhibited sIL-6Rα/IL-6 stimulation of STAT3 Tyr705 phosphorylation in 2C4 and U4C.JAK1 cells (even in rescue cells when JAK is highly over expressed) (Figure 4.17A). sIL-6Rα/IL-6 treatment of U4C cells did not stimulate STAT3 phosphorylation (Figure 4.17A). Overall, the results were consistent with those of Guschin et al. (1995) and demonstrated that JAK1 was required for IL-6 signalling in human fibrosarcoma-derived cells. A769662 activated AMPK to inhibit IL-6 signalling in 2C4 and U4C.JAK1 cells, thus the U4C cells were a potentially a valuable tool for investigating the role of JAK1 in AMPK-mediated inhibition of IL-6 signalling.

4.2.4 Role of JAK1 Ser515 and Ser518 in AMPK-mediated inhibition of JAK1-dependent signalling

4.2.4.1 Role of JAK1 Ser515 and Ser518 in AMPK-mediated inhibition of IL-6 signalling

So far in the current study it has been demonstrated that AMPK inhibits sIL-6Rα/IL-6 signalling, which is predominantly via JAK1, and that AMPK phosphorylates JAK1 on Ser515 and Ser518 *in vitro* (Figure 4.7 and 4.16). To determine whether AMPK-mediated inhibition of sIL-6Rα/IL-6 signalling is dependent on Ser515 and Ser518, a human JAK1 expression plasmid in which Ser515 and Ser518 were mutated to non phosphorylatable Ala (S515A/S518A) was generated. The effects of AMPK activation on sIL-6Rα/IL-6 signalling in JAK1-null U4C transiently expressing S515A/S518A mutant JAK1 were then examined. U4C cells were transfected with either an empty plasmid control pcDNA3.1, WT JAK1 or S515A/S518A mutant JAK1 plasmid 48 hours prior to pre-treatment with vehicle or A769662 for 40 minutes followed by stimulation with vehicle or sIL-6Rα/IL-6 for 30 minutes.

Immunoblotting of cell extracts with Total JAK1 antibody revealed equivalent expression levels of WT and S515A/S518A mutant JAK1 (Figure 4.18). In comparison to vehicle treated WT JAK1 and S515A/S518A mutant JAK1 expressing cells, sIL-6Rα/IL-6 significantly stimulated STAT3 Tyr705 phosphorylation by 66 ± 6% (***p<0.01) in WT JAK1 expressing cells and by 67 ± 6% (***p<0.01) in S515A/S518A mutant JAK1 expressing cells, respectively (Figure 4.18) While A769662 activation of AMPK significantly inhibited sIL-6Rα/IL-6 stimulation of STAT3 Tyr705 phosphorylation by 57 ± 5% (***p<0.01) in cells expressing WT JAK1, treatment of S515A/S518A mutant JAK1 expressing cells with A769662 prior to sIL-6Rα/IL-6 stimulation had no significant effect on sIL-6Rα/IL-6 stimulation of STAT3 Tyr705 phosphorylation (Figure 4.18). Overall, these data suggested that Ser515 and Ser518 were required for effective AMPK-mediated inhibition of IL-6 signalling to STAT3.

4.2.4.2 Role of JAK1 Ser515 and Ser518 in AMPK-mediated inhibition of constitutively active Val658Phe JAK1 signalling

A constitutively active Val658Phe-mutated version of JAK1 has been identified in some patients with acute lymphoblastic leukaemia (ALL) (Staerk et al., 2005, Jeong et al., 2008). In order to study the effects of AMPK activation on signalling

independently of cytokine receptor stimulation, a human JAK1 plasmid containing a Phe substitution at Val658 (V658F) was generated. Additionally, a human JAK1 plasmid containing V658F, S515A and S518A mutations (V658F/S515A/S518A) was also generated in order to determine whether any AMPK-mediated effects on constitutively active V658F JAK1 signalling were dependent upon Ser515 and Ser518 in JAK1. The effects of AMPK activation on constitutively active V658F JAK1 signalling in JAK1-null U4C cells, transiently expressing either V658F mutant or V658F/S515A/S518A mutant JAK1 were examined. In brief, U4C cells were transfected with either an empty control plasmid, WT JAK1, V658F mutant JAK1 or V658F/S515A/S518A mutant JAK1 plasmid 48 hours prior to treatment with vehicle or A769662 for 40 minutes.

Immunoblotting of cell extracts with total JAK1 antibody detected equal expression of JAK1 in U4C cells transfected individually with WT JAK1, V658F mutant JAK1 or V658F/S515A/S518A mutant JAK1 plasmid, whereas U4C cells transfected with empty plasmid control do not express JAK1 (Figure 4.19).. Whole-cell extracts were also immunoblotted with phospho-STAT3 (Tyr705), total-STAT3, phospho-STAT1 (Tyr701), total-STAT1 and GAPDH antibodies, and subsequently protein levels were quantified by densitometry as shown in Figure 4.19. Transfection of JAK1-null U4C cells with V658F mutant JAK1 significantly increased phosphorylation of STAT1 Tyr701 and STAT3 Tyr705 by 94 ± 11% (***p<0.001) and 78 ± 9% (***p<0.001), respectively, compared to cells transfected with WT JAK1 (Figure 4.19). Treatment of V658F mutant JAK1 transfected cells with A769662 significantly reduced STAT1 Tyr701 and STAT3 Tyr705 phosphorylation by 57 ± 6% (***p<0.001) and 41 ± 5% (**p<0.01), respectively, relative to the absence of A769662 (Figure 4.19). In comparison to vehicle treated V658F mutant JAK1 transfected cells, STAT1 Tyr701 and STAT3 Tyr705 phosphorylation was significantly reduced by 64 ± 7% (***p<0.001) and 46 ± 5% (***p<0.01), respectively, in vehicle treated cells transfected with V658F/S515A/S518A mutant JAK1 (Figure 4.19). Treatment of V658F/S515A/S518A JAK1 transfected cells with A769662 had no significant effect on STAT3 Tyr705 and STAT1Tyr701 phosphorylation, relative to the absence of A769662, as STAT3 Tyr705 and STA1 Tyr701phosphorylation was reduced by only 5 ± 1% (p>0.05,NS) and 4% (p>0.05,NS), respectively (Figure 4.19). Overall, these data suggest that Ser515 and Ser518 are required for AMPK-mediated inhibition of constitutively active V658F JAK1 signalling.

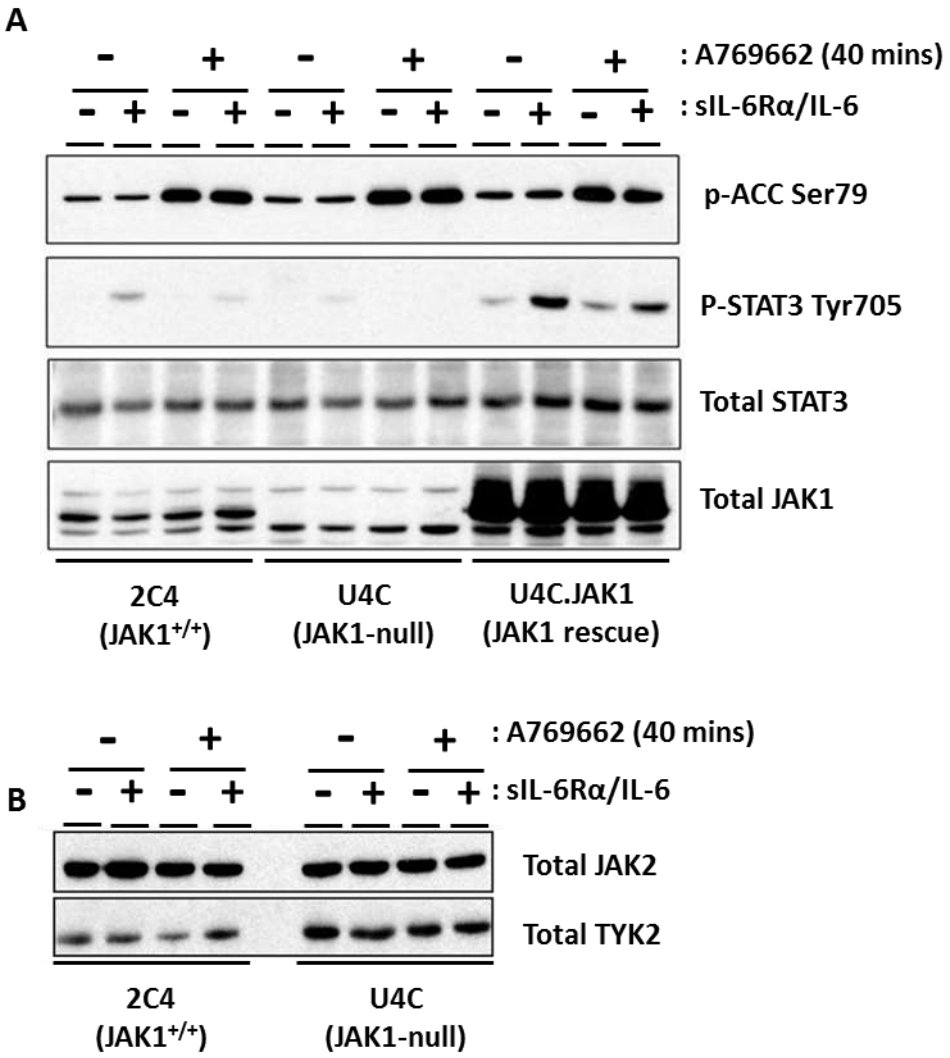

Figure 4.17: Effect of A769662 on sIL-6Rα/IL-6 stimulation of STAT3 tyrosine (705) phosphorylation in human fibrosarcoma cells.
2C4, U4C, and U4C.JAK1 cells were pre-treated with vehicle or 100µM A769662 for 40 minutes followed by stimulation with vehicle or 25ng/ml sIL-6Rα and 5ng/ml IL-6 (sIL-6Rα/IL-6) for a further 30 minutes. Protein-equalised cell extracts were then analysed by SDS-PAGE and immunoblotting with antibodies as indicated. **(A)** Immunoblotting with antibodies specific for phospho-STAT3 (Tyr705), total STAT3, phospho-ACC (Ser79) and total JAK1 as indicated. **(B)** Immunoblotting with antibodies specific for JAK2 and TYK2 as indicated.

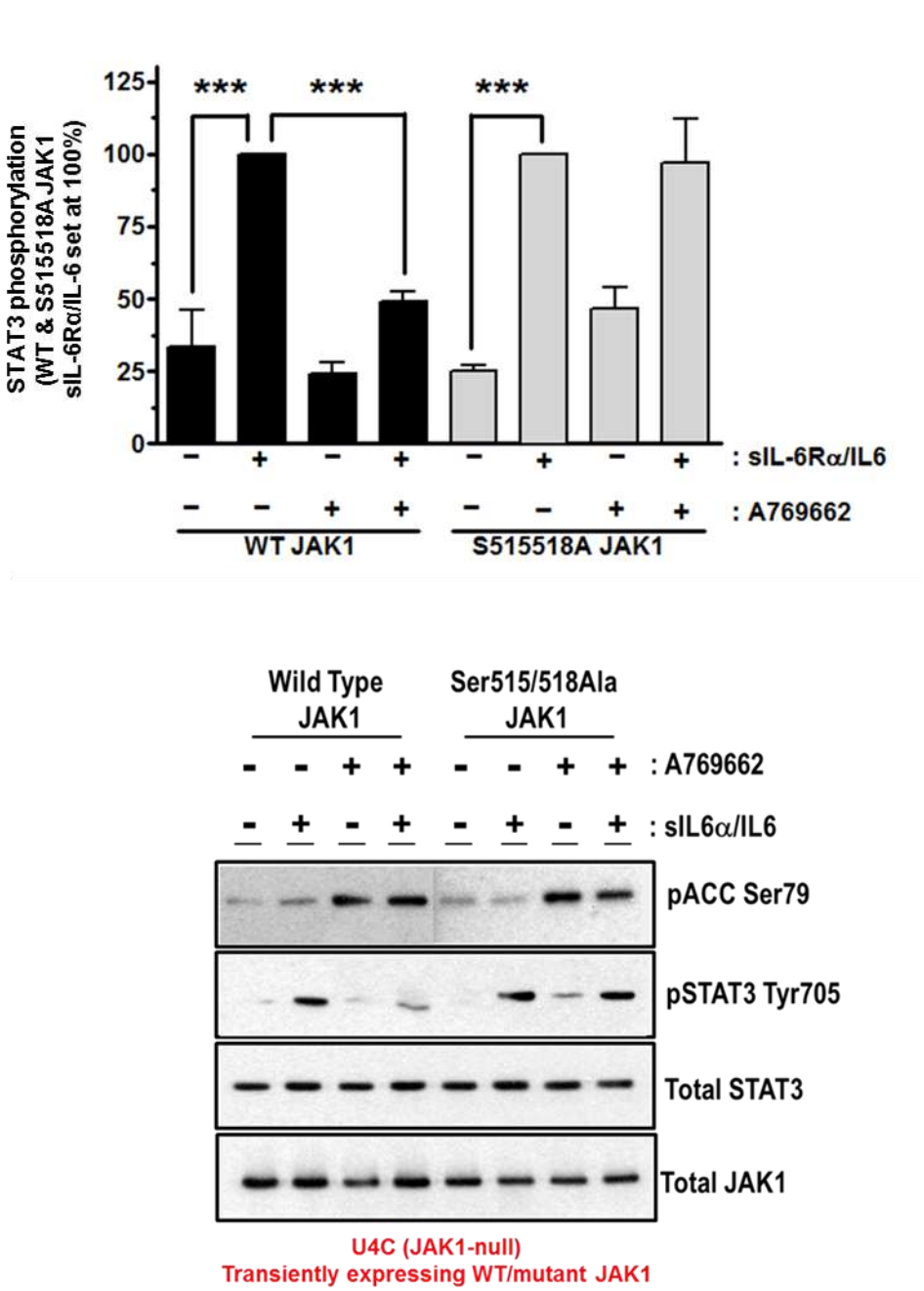

Figure 4.18: Role of JAK1 Ser515 and Ser518 in AMPK-mediated inhibition of IL-6 signalling. JAK1-null U4C cells were transfected with either wild type JAK1 or S515A/S518A mutant JAK1 48 hours prior to pre-treatment with vehicle or 100μM A769662 for 40 minutes followed by stimulation with vehicle or 25ng/ml sIL-6Rα and 5ng/ml IL-6 (sIL-6Rα/IL-6) for a further 30 minutes. Protein-equalised cell extracts were then analysed by SDS-PAGE and immunoblotting with antibodies specific for phospho-STAT3 (Tyr705), total STAT3, phospho-ACC (Ser79) and total JAK1 as indicated. Immunoblots were probed for total JAK1 to confirm equivalent expression of WT and mutated JAK1 in transfected cells. STAT3 phosphorylation data were first normalized to total STAT3 levels and expressed as a percentage (%) of the maximal sIL-6Rα/IL-6 stimulation attained in vehicle pre-treated U4C cells transiently expressing either WT JAK1 or S515518A JAK1 (Set at 100%). Quantitative analysis from three experiments is presented. Columns are means ±SEM. *** p<0.01. A representative blot from n=3 experiments is shown.

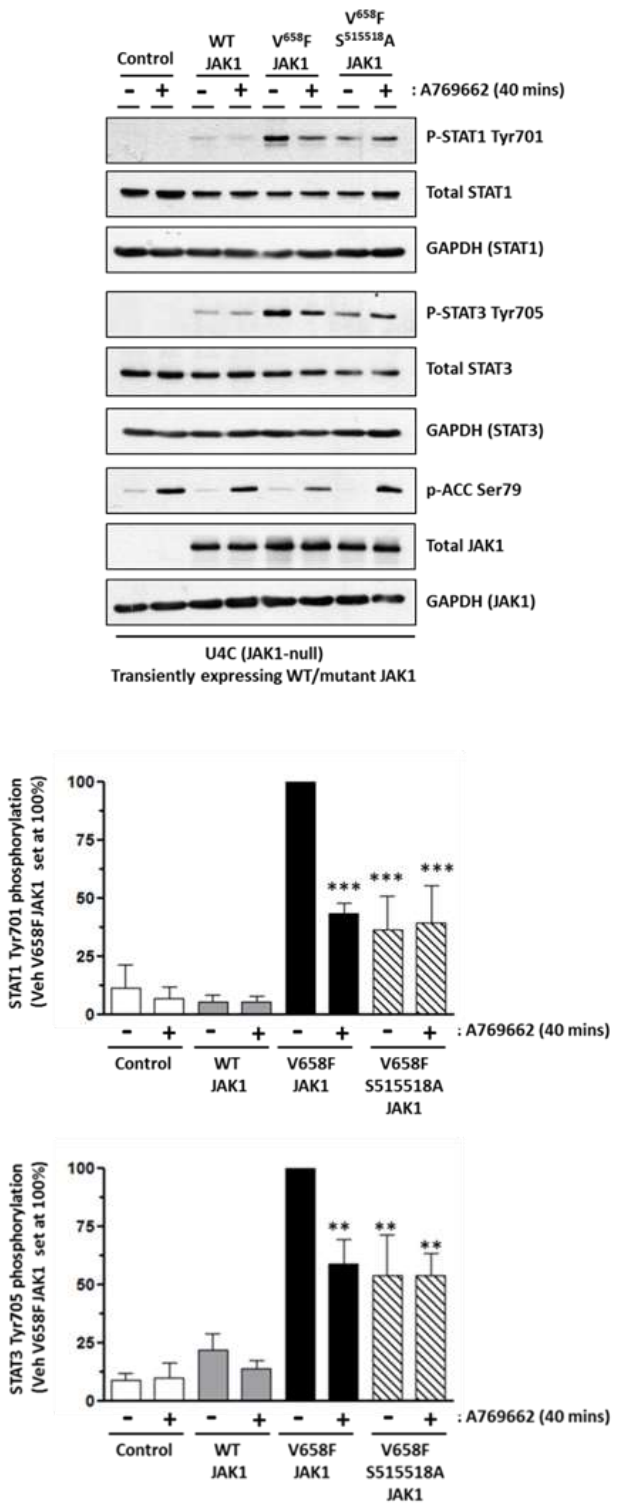

Figure 4.19: Effect of AMPK activation on constitutively active V658F-mutated JAK1-meditated STAT3 phosphorylation on Tyr705

JAK1-null U4C cells were transfected with either wild type JAK1, V658F mutant JAK1 or V658F/S515A/S518A mutant JAK1 48 hours prior to treatment with vehicle or 100µM A769662 for 40 minutes. Protein-equalised cell extracts were then analysed by SDS-PAGE and immunoblotting with antibodies specific for phospho-STAT1 (Tyr701), total STAT1, phospho-STAT3 (Tyr705), total STAT3, Phospho-ACC (Ser79), total JAK1 and GAPDH as indicated. Immunoblots were probed for total JAK1 to confirm expression of JAK1. STAT1 and STAT3 phosphorylation data were first normalized to total STAT1 and STAT3 levels respectively, and expressed as a percentage (%) of the maximal phosphorylation levels attained in vehicle pre-treated U4C cells transiently expressing V658F JAK1 (set at 100%). Quantitative analysis from three experiments is presented. Columns are means ±SEM. ** p<0.01, *** p<0.01. A representative blot from n=3 experiments is shown.

4.2.5 14-3-3 binding as a strategy to detect AMPK phosphorylated JAK1

A common mechanism for phosphorylation-mediated regulation of target protein function is phosphorylation-dependent binding to members of the 14-3-3 family of proteins (Bridges and Moorhead, 2005). The 14-3-3 family proteins bind to phosphoserine- and phosphothreonine-containing proteins and two consensus 14-3-3 binding phosphopeptide motifs, RXXpS/pTXP and RXXXpS/pTXP, have been identified (Yaffe et al., 1997). AMPK phosphorylation of either Ser515 or Ser518 within JAK1 creates a phosphopeptide motif that shares similarities with these 14-3-3 binding motifs.

4.2.5.1 14-3-3ζ binding of JAK1 phospho-peptides

To assess whether phosphorylation of Ser515 and Ser518 could facilitate JAK1 interaction with 14-3-3 protein *in vitro*, a peptide array spotted four times with the 25-mer JAK1 peptide, R-Y-S-L-H-G-S-D-R-S^{515}-F-P-S^{518}-L-G-D-L-M-S-H-L-K-K-Q-I, phosphorylated at either or both of Ser515 and Ser518 was overlaid with HRP-conjugated 14-3-3ζ. As a positive control, the peptide array was spotted four times with the high-affinity non-phosphorylated ligand of 14-3-3, P-H-C-V-P-R-D-L-S-W-L-D-L-E-A-N-M-C-L-P (termed R18), and as a negative control, the low-affinity non-phosphorylated peptide ligand of 14-3-3, R-F-T-T-Q-G-E-R-G-I-T-H-L-R-E-S-S-T-L-G (termed C01) was also spotted four times (Wang et al., 1999).

As shown in Figure 4.20, HRP-14-3-3ζ-bound positive control peptide R18 but not negative control peptide C01. On the same arrays, HRP-14-3-3ζ did not bind either the non-phosphorylated JAK1 peptide or the peptide in which both Ser515 and Ser518 were phosphorylated (Figure 4.20). However, HRP-14-3-3ζ did bind JAK1 peptide when monophosphorylated at either Ser515 or Ser518. In addition, the signal from bound HRP-14-3-3ζ was substantially stronger with the phospho-Ser515 JAK1 peptide *versus* the phospho-Ser518 JAK1 peptide (Figure 4.20). In addition, the peptide array was also spotted four times with the 25-mer JAK-2 peptide, E-Y-N-L-S^{465}-G-T-K-K-N-F-S^{472}-S^{473}-L-K-D-L-L-N-C-Y-Q-M-E-T, phosphorylated at either or all three of Ser465, Ser472 and Ser473, and overlaid with HRP-14-3-3ζ to assess whether phosphorylation of these sites could facilitate JAK2 interaction with 14-3-3 protein *in vitro*. HRP-14-3-3ζ bound to non-phosphorylated JAK2 peptide and phospho-Ser465 JAK2 peptide, and did not bind phospho-Ser472 or phospho-Ser473

JAK2 peptide (Figure 4.20). The signal from bound HRP-14-3-3ζ was stronger with the non-phosphorylated JAK2 peptide *versus* the phospho-Ser465 JAK2 peptide (Figure 4.20). Overall, these observations demonstrate that 14-3-3ζ interacts with JAK1 peptide at either phospho-Ser515 or phospho-Ser518, but not when both sites are phosphorylated. 14-3-3ζ also interacts with non-phosphorylated JAK2 peptide and phospho-Ser465 JAK2 peptide, but not with phospho-Ser472 or phospho-Ser473 JAK2 peptides.

4.2.5.2 Development of a GST/14-3-3ζ pull down assay for detecting AMPK phosphorylated JAK1 in intact cells

Having demonstrated that phospho-Ser515 and phospho-Ser518 peptides strongly interacted with HRP-14-3-3ζ *in vitro* (Figure 4.20), bacterially expressed and purified GST-tagged 14-3-3ζ was used in pull down assays to detect AMPK-mediated phosphorylation of Ser515 and Ser518 in JAK1 in intact cells. Initial experiments in JAK1-null U4C human fibrosarcoma cells stably expressing recombinant JAK1 (U4C.JAK1) demonstrated that GST-14-3-3ζ, but not GST alone, could specifically isolate JAK1 (Figure 4.21A). GST-14-3-3ζ was used in pull down assays with cell lysates produced from JAK1-null U4C cells transfected with either an empty plasmid control, WT JAK1 or S515A/S518A mutant JAK1 plasmid 48 hours prior to treatment with or without A769662. To assess levels of JAK1 protein captured by GST/14-3-3ζ, pull downs were immunoblotted with total JAK1 antibody. As shown in Figure 4.21B, GST-14-3-3ζ appears to bind basal levels of JAK1 in untreated WT JAK1 transfected cells. Upon treatment of WT JAK1 transfected cells with A769662, the amount of WT JAK1 bound by GST-14-3-3ζ was significantly (*p<0.05) increased (Figure 4.21C). In contrast, the amount of S515A/S518A mutant JAK1 bound by GST-14-3-3ζ following A769662 treatment was significantly (*p<0.05) reduced (Figure 4.21C). Whole cell extracts were probed for total JAK1 and phospho-ACC to confirm that the levels of WT and S515A/S518A mutant expression were similar in transfected cells, and that A769662 activated AMPK equally (Figure 4.21B). Overall, these data demonstrate that A769662 activates AMPK to promote 14-3-3 binding of JAK1 *in vitro*, and confirms that Ser515 and Ser518 are critical for this interaction. The data shown in figure 4.21 was generated and analysed by Dr Claire Rutherford, University of Glasgow.

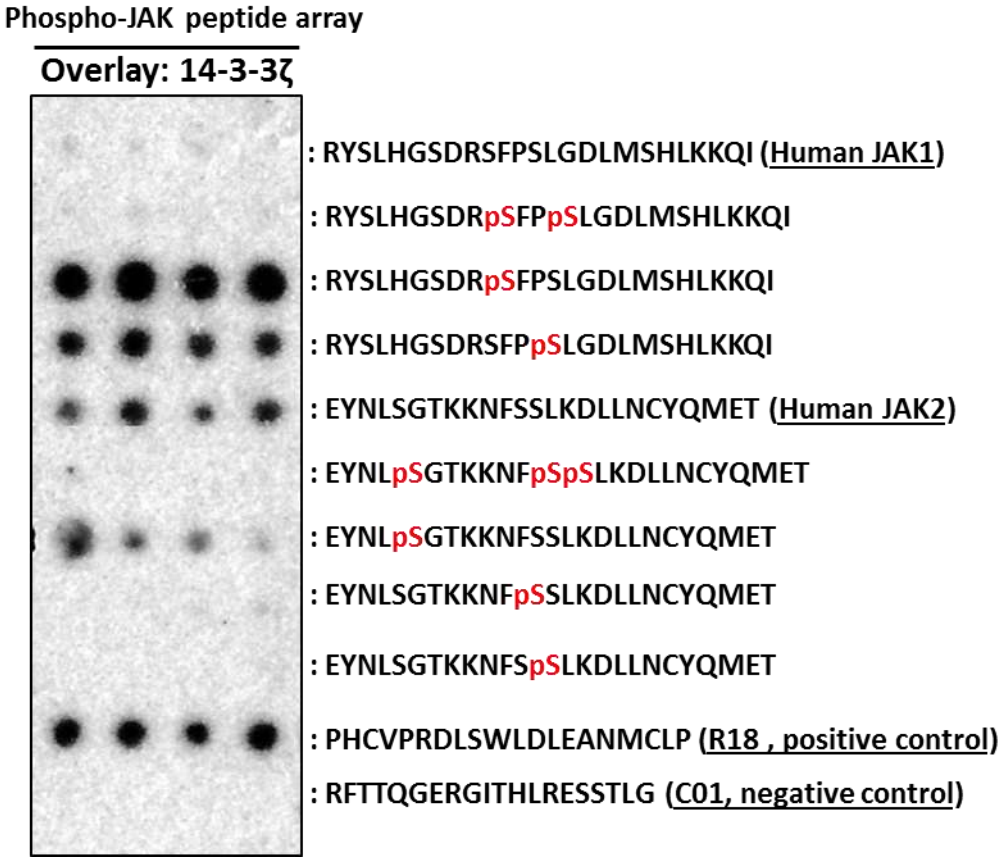

Figure 4.20: 14-3-3ζ binding of JAK1 and JAK2 phospho-peptides
Peptide arrays consisting of Ser phosphorylated JAK1 and JAK2 25-mer peptide identified as potential AMPK phosphorylation sites was overlaid with HRP-conjugated recombinant human 14-3-3ζ. Reactive spots were visualised using Perkin-Elmer enhanced chemiluminescence (ECL) detection reagents, according to the manufacturer's instructions. The positive control, R18, and negative control, C01, peptides for 14-3-3ζ interaction were taken from Wang et al. Biochemistry (1999). Each 25-mer peptide was spotted four times on the glass slide. A representative blot from n=3 experiments is shown.

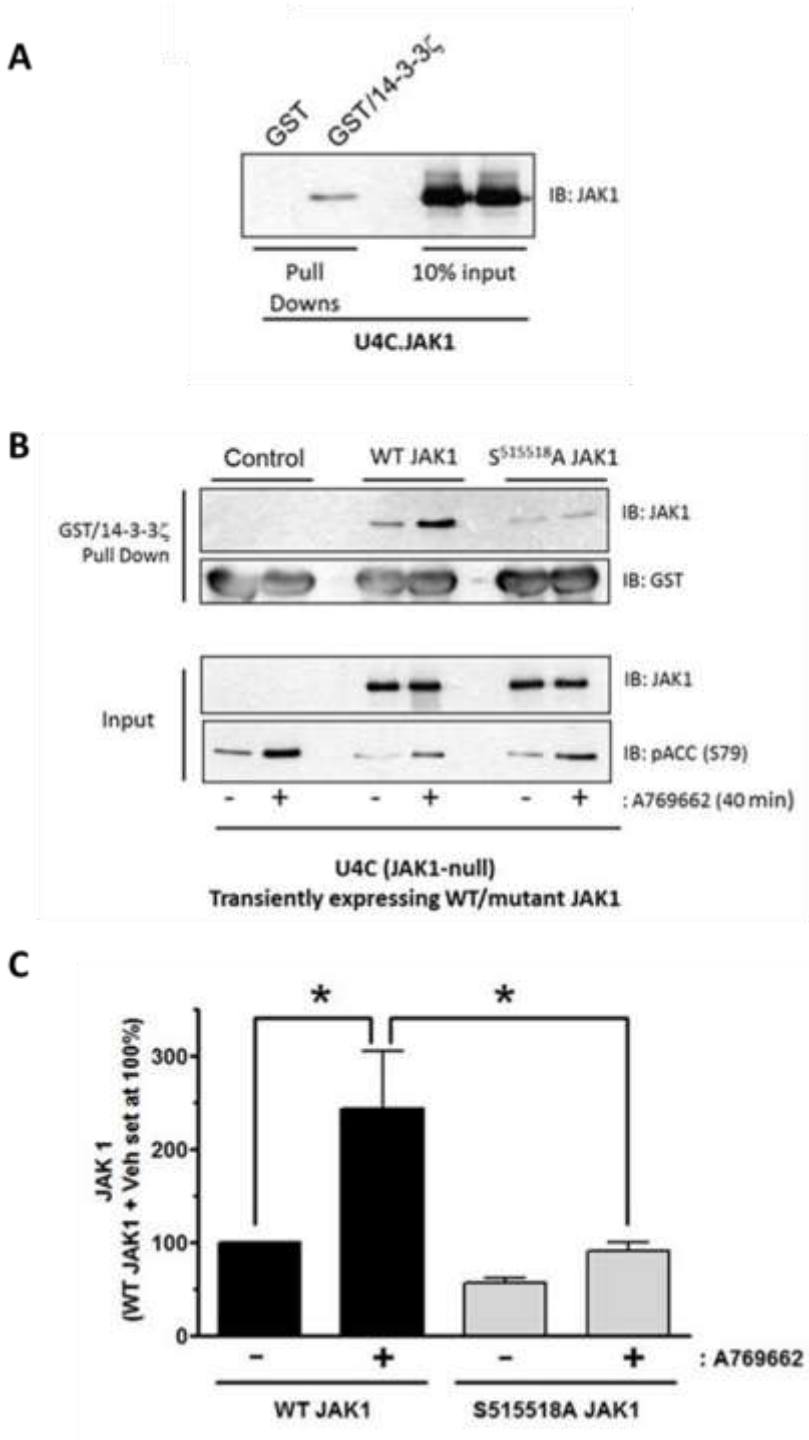

Figure 4.21: AMPK-mediated phosphorylation of JAK1 in intact cells.
(A) Untreated U4C.JAK1 extracts were prepared and used in a pull-down assay using either GST or GST-14-3-3ζ as indicated. Protein complexes eluted from beads and whole-cell extracts (input) were then fractioned by SDS-PAGE for immunoblotting with antibodies specific for total JAK1 as indicated. Blot from n=1 experiment **(B & C)** JAK1-null U4C cells were transfected with either WT JAK1, S515A/S518A mutant JAK1, or an empty control expression plasmid 48 hours prior to treatment with or without 100μM A769662 AMPK activator for 40 minutes. Protein-equalised cell extracts were prepared and used in a pull-down assay using GST-14-3-3ζ. Protein complexes eluted from beads and whole-cell extracts (input) were then fractioned by SDS-PAGE for immunoblotting with antibodies specific for total JAK, phospho-ACC (Ser79) and GST as indicated. JAK1 pull-down levels were first normalized to total JAK1 and expressed as a percentage (%) of the maximal JAK1 pull-down levels attained in vehicle pre-treated U4C cells transiently expressing WT JAK1. Quantitative analysis from three experiments is presented. Columns are means ±SEM. *p<0.05. A representative blot from n=3 experiment is shown. (Data generated and analysed by Dr Claire Rutherford, University of Glasgow)

4.2.6 Effect of A769662 on JAK1 tyrosine phosphorylation.

4.2.6.1 Effect of sIL-6Rα/IL-6 on JAK1 phosphorylation

Having established that STAT3 is predominantly activated by sIL-6Rα/IL-6 via JAK1 in HUVECs, it was hypothesised that AMPK inhibits sIL-6Rα/IL-6 stimulation of STAT3 Tyr705 phosphorylation by inhibiting tyrosine phosphorylation of its predominant upstream activator, JAK1. sIL-6Rα/IL-6 induces JAK1 phosphorylation at Tyr1022/1023, an event which is required for JAK1 activation (Liu et al. 1997).

To test this hypothesis, HUVECs were pre-treated with either vehicle or A769662, followed by stimulation with vehicle or sIL-6Rα/IL-6 for either 5 or 15 minutes. Whole-cell extracts were then immunoprecipitated with total-JAK1 antibody, fractionated by SDS-PAGE and immunoblotted with phospho-JAK1 (Tyr1022/1023) antibody and total-JAK1 antibody. Immunoblotting with total-JAK1 antibody revealed bands corresponding to approximately 130 kDa confirming that equal levels of JAK1 had been successfully immunoprecipitated (Figure 4.22). However, it was not possible to successfully detect sIL-6Rα/IL-6 stimulated JAK1 Tyr1022/1023 phosphorylation in HUVECs using Santa Cruz and Invitrogen phospho-specific antibodies against these sites on JAK1(Figure 4.22). As can be seen in Figure 4.22, phospho-JAK1 antibody typically failed to detect phospho-JAK1 either after enrichment of JAK1 by immunoprecipitation or in whole cell extracts. Thus, it was not possible to deduce any information from these experiments.

As an alternative approach to detect tyrosine phosphorylated JAK1, anti-phospho-tyrosine 4G10 monoclonal antibody was used to probe JAK1 immunoprecipitates. An initial time course of sIL-6Rα/IL-6 stimulation of JAK1 tyrosine phosphorylation was conducted (Figure 4.23). HUVECs were treated with or without sIL-6Rα/IL-6 for 5, 15 and 30 minutes. Whole-cell extracts were then immunoprecipitated with total JAK1 antibody, fractionated by SDS-PAGE and immunoblotted with anti-phospho-tyrosine 4G10 monoclonal antibody and total JAK1 antibody (Figure 4.23). Probing with 4G10 can theoretically detect multiple phosphorylated Tyr residues in different contexts and is therefore not specific for JAK1 Tyr 1022/1023. Low basal tyrosine phosphorylation levels of JAK1 were detected in HUVECs. sIL-6Rα/IL-6 stimulation of JAK1 tyrosine phosphorylation peaked at 15 minutes and remained above basal levels 30 minutes post-stimulation (Figure 4.23). The

hypothesis being tested was whether AMPK could inhibit sIL-6Rα/IL-6 stimulation of STAT3 Tyr705 phosphorylation by inhibiting tyrosine phosphorylation of its predominant upstream activator, JAK1. To test this hypothesis, HUVECs were pre-treated with either vehicle or A769662, followed by stimulation with vehicle or sIL-6Rα/IL-6 for either 5 or 15 minutes. Whole-cell extracts were immunoprecipitated with total JAK1 antibody, followed by immunoblotting with anti-phospho-tyrosine antibody 4G10. In comparison to the basal levels of JAK1 tyrosine phosphorylation detected in unstimulated HUVECs, sIL-6Rα/IL-6 stimulation of HUVECs for 5 minutes appeared to have no detectable effect on JAK1 tyrosine phosphorylation, whereas sIL-6Rα/IL-6 stimulation for 15 minutes marginally increased JAK1 tyrosine phosphorylation levels (Figure 4.24). Treatment of HUVECs with A769662 prior to sIL-6Rα/IL-6 stimulation for 15 minutes appears to slightly reduce JAK1 tyrosine phosphorylation (Figure 4.24). This would suggest that AMPK activation can inhibit sIL-6Rα/IL-6 stimulation of JAK1 tyrosine phosphorylation. Whole-cell extracts were also immunoblotted with phospho-STAT3 (Tyr705) and total-STAT3 antibodies to confirm AMPK-mediated inhibition of sIL-6Rα/IL-6 stimulation of STAT3 Tyr705 phosphorylation (Figure 4.24). Subsequently, protein levels were quantified by densitometry as shown in Figure 4.24. In HUVECs, sIL-6Rα/IL-6 significantly stimulated STAT3 Tyr705 phosphorylation after only 15 minutes, and this was significantly inhibited by the activation of AMPK by A769662.

As an alternative way to use 4G10 to detect tyrosine phosphorylated JAK1, 4G10 antibody was used to immunoprecipitate tyrosine phosphorylated proteins from treated cells followed by SDS-PAGE and immunoblotting with total anti-JAK1 antibody. Initial antibody titration experiments using 4G10 for immunoprecipitation were performed on JAK1 rescue cells (U4C.JAK1) and JAK1-null cells (U4C) pre-treated with hydrogen peroxide and sodium vanadate to inhibit cellular protein tyrosine phosphatase activity and thus increase levels of tyrosine phosphorylated proteins (Hecht et al., 1992). Whole cell extracts were then immunoprecipitated with increasing concentrations of phospho-tyrosine 4G10 antibody and total-JAK1 antibody as a positive control, followed by immunoblotting with total-JAK1 antibody to examine the effects on JAK1 tyrosine phosphorylation. Figure 4.25 demonstrates that total-JAK1 antibody detects tyrosine phosphorylated JAK1 protein in 4G10 immunoprecipitates derived from

U4C.JAK1 cell extracts only. The lack of any specific signal in 4G10 immunoprecipitates derived from U4C (JAK1 null) cell extracts confirms the specificity of this approach for specifically assessing JAK1 Tyr phosphorylation. 4G10 efficiently immunoprecipitates JAK1, with 6µl being the most efficient at immunoprecipitating JAK1 and immunoprecipitating to a similar extent as the total-JAK1 antibody (Figure 4.25). Having optimised this approach to detect tyrosine-phosphorylated JAK1, HUVECs were pre-treated with vehicle or A769662 followed by stimulation with vehicle or sIL-6Rα/IL-6 for either 2, 5, 15 or 30 minutes and immunoprecipitated with phospho-tyrosine 4G10 antibody, followed by SDS-PAGE and immunoblotting with total-JAK1 antibody. In comparison to probing JAK1 immunoprecipitates with 4G10 (Figure 4.24), this approach has substantially reduced the basal levels of tyrosine phosphorylated JAK1 detected (Figure 4.26). As shown in Figure 4.26, sIL-6Rα/IL-6 stimulation of JAK1 tyrosine phosphorylation peaked at 5 minutes, but was still above basal levels at 30 minutes. Treatment of HUVECs with A769662 for 40 minutes prior to sIL-6Rα/IL-6 stimulation for 5 minutes slightly reduced JAK1 tyrosine phosphorylation (Figure 4.26). However this effect seemed to be transient as it was not reproducibly detected at any of the later time points. Immunoblotting of cell extracts with phospho-ACC (Ser79) antibody confirmed AMPK activation by A769662 (Figure 4.26). Whole-cell extracts were also immunoblotted with phospho-STAT3 (Tyr705) and total-STAT3 antibodies to confirm AMPK-mediated inhibition of sIL-6Rα/IL-6 stimulation STAT3 (Tyr705) phosphorylation at each time point (Figure 4.26)

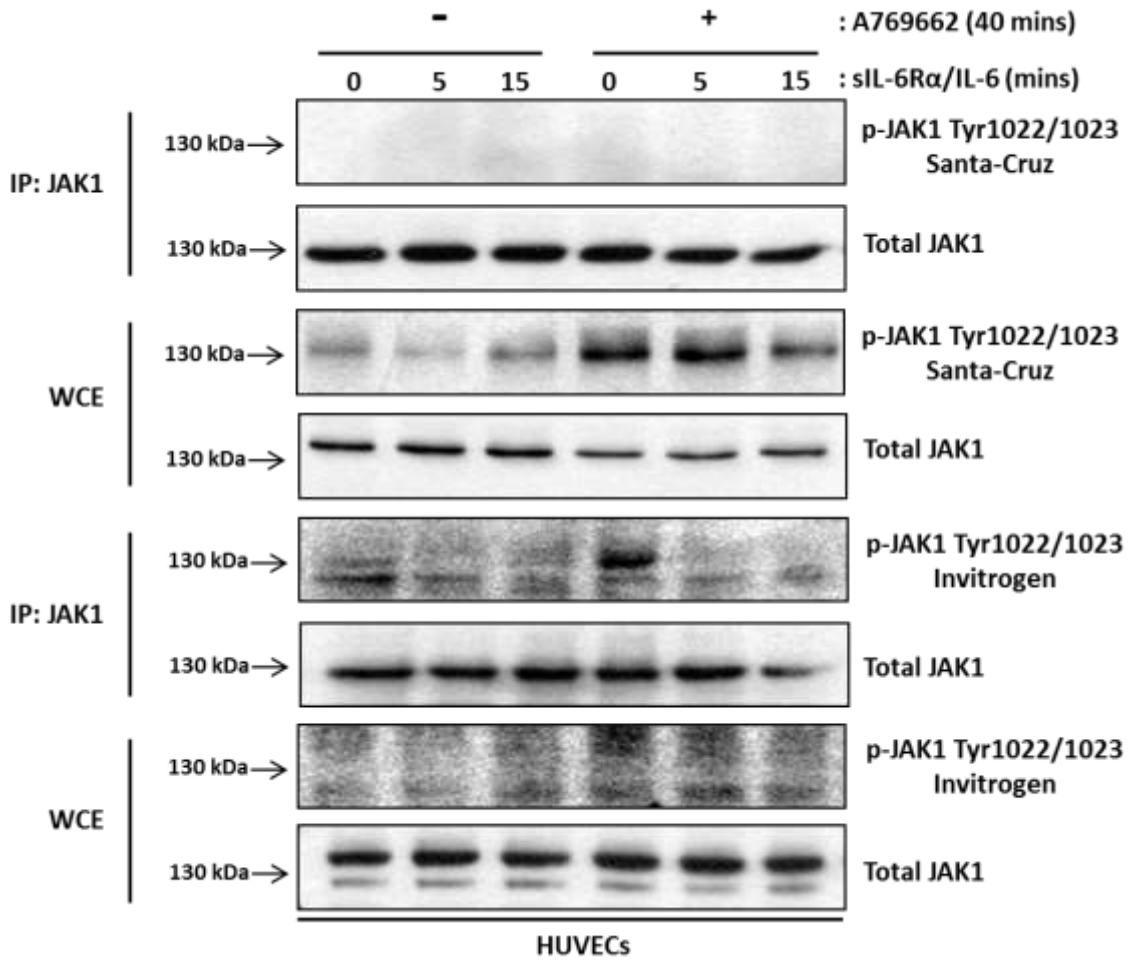

Figure 4.22: Effect of sIL-6Rα/IL-6 on JAK1 phosphorylation
HUVECs were pre-treated with vehicle or 100μM A769662 followed by stimulation with vehicle or 25ng/ml sIL-6Rα and 5ng/ml IL-6 (sIL-6Rα/IL-6) for time period indicated. Protein-equalised cell extracts were then immunoprecipitated with anti-JAK1 antibody and protein A-Sepharose beads. Eluted immunoprecipitated (IP) proteins and whole cell extracts (WCE) were analysed by SDS-PAGE and immunoblotting with antibodies specific for phospho-JAK1 (Tyr1022/1023), total JAK1, as indicated.

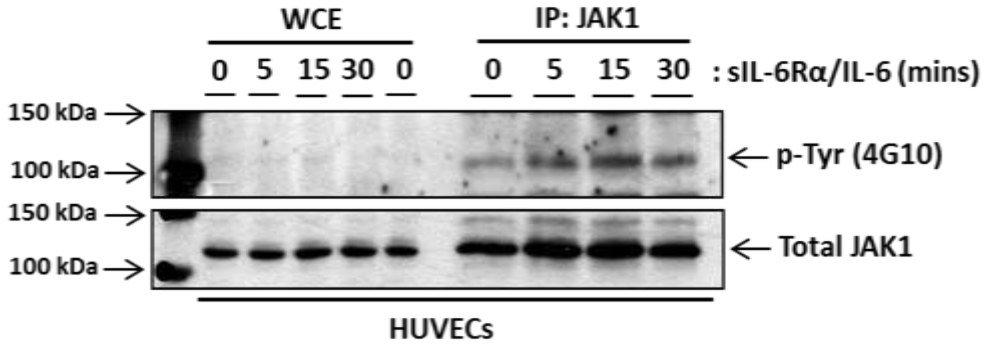

Figure 4.23: Time-course of sIL-6Ra/IL-6-stimulated Tyr phosphorylation of JAK1 in HUVECs.

HUVECs were stimulated with vehicle or 25ng/ml sIL-6Rα and 5ng/ml IL-6 (sIL-6Rα/IL-6) for the time period indicated. Protein-equalised cell extracts were then immunoprecipitated with total JAK1 antibody and protein A-Sepharose beads. Immunoprecipitated proteins were eluted from beads and fractionated by SDS-PAGE in parallel with whole cell extracts. After transfer to nitrocellulose, membranes were probed with either anti-p-Tyr 4G10 antibody or total JAK1 antibody and visualised by ECL.

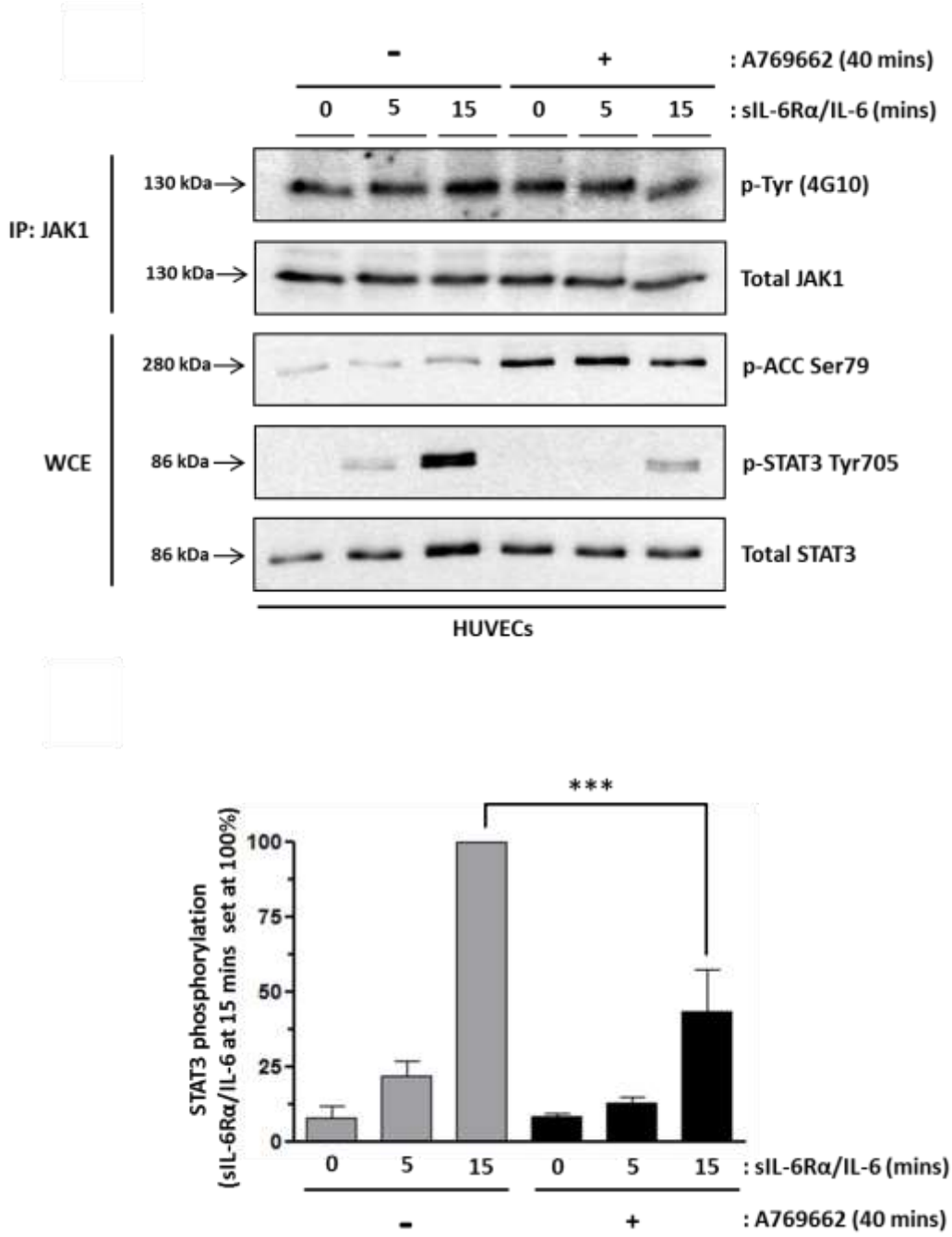

Figure 4.24: Effect of A769662 on sIL-6Rα/IL-6 stimulated JAK1 and STAT3 phosphorylation in HUVECs (JAK1 immunoprecipitates)

HUVECs were pre-treated with vehicle or 100μM A769662 for 40 minutes followed by stimulation with vehicle or 25ng/ml sIL-6Rα and 5ng/ml IL-6 (sIL-6Rα/IL-6) for time period indicated. Protein-equalised cell extracts were then immunoprecipitated with total JAK1 antibody and protein A-Sepharose beads. Eluted immunoprecipitated proteins and whole cell extracts were analysed by SDS-PAGE and immunoblotting with 4G10 anti-p-Tyr antibody and antibodies specific for total JAK1, phospho-STAT3 (Tyr705), total STAT3 and phospho-ACC (Ser79) as indicated. STAT3 phosphorylation data were first normalized to total STAT3 levels and expressed as a percentage (%) of the maximal sIL-6Rα/IL-6 stimulation attained in vehicle pre-treated HUVECs (Set at 100%). Quantitative analysis from three experiments is presented. Columns are means ±SEM. *** p<0.01.

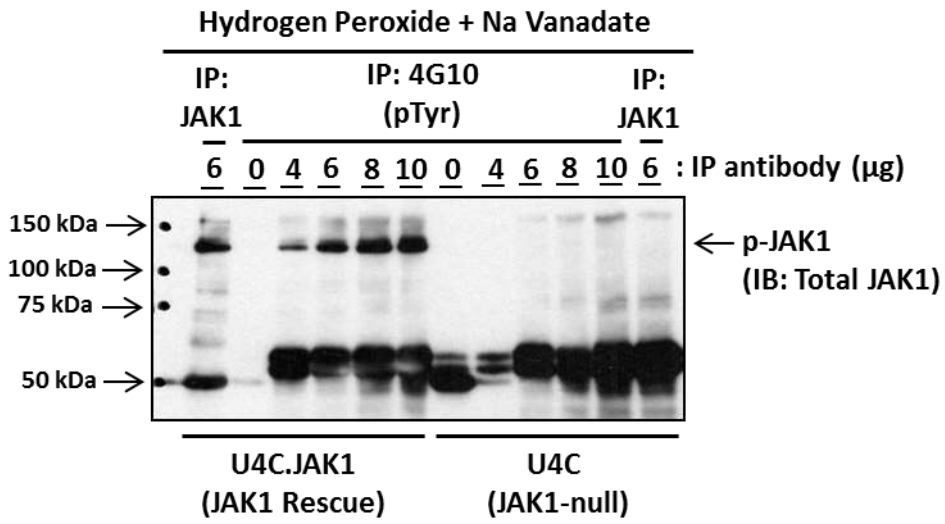

Figure 4.25: Titration of p-Tyr 4G10 antibody for immunoprecipitation of tyrosine phosphorylated JAK1

JAK1-null U4C and U4C.JAK1 cells were treated for with 1mM hydrogen peroxide for 2 hours and sodium vanadate treatment was performed for the final 30 minutes of this 2 hour period. Protein-equalised cell extracts were then immunoprecipitated with pTyr 4G10 antibody and protein A-Sepharose beads. Immunoprecipitated proteins were eluted from beads and analysed by SDS-PAGE and immunoblotting with total JAK1 antibody.

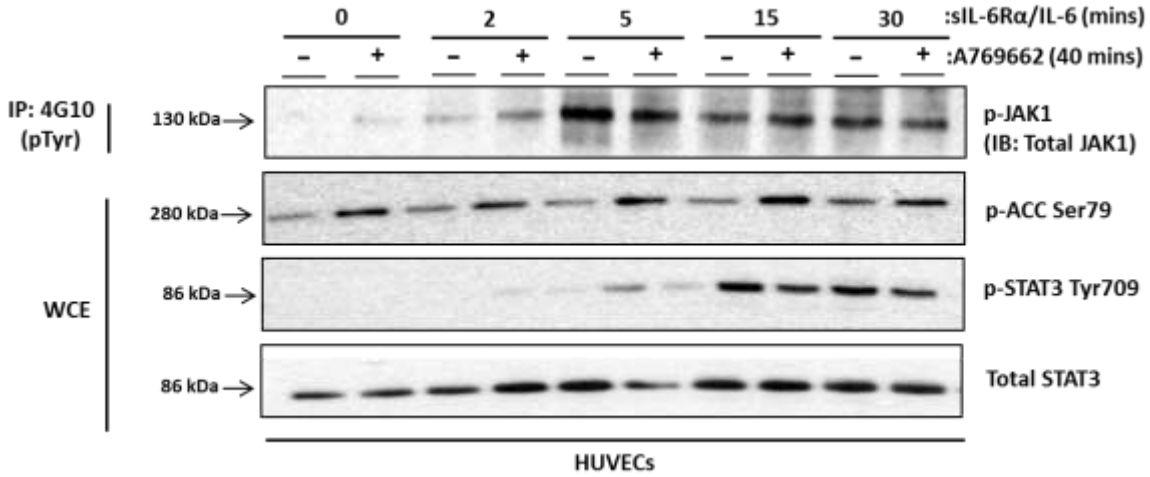

Figure 4.26: Effect of A769662 on sIL-6Rα/IL-6 stimulated JAK1 phosphorylation in HUVECs (4G10 immunprecipitates)

HUVECs were pre-treated with vehicle or 100µM A769662 for 40 minutes followed by stimulation with vehicle or 25ng/ml sIL-6Rα and 5ng/ml IL-6 (sIL-6Rα/IL-6) for time period indicated. Protein - equalised cell extracts were then immunoprecipitated with pTyr 4G10 antibody and protein A-Sepharose beads. Eluted immunoprecipitated proteins and whole cell extracts were analysed by SDS-PAGE and immunoblotting with antibodies as indicated.

4.2.7 AMPK phosphorylation of full-length human JAK *in vitro*

Having demonstrated that AMPK phosphorylates a JAK1 peptide at both Ser515 and Ser518 *in vitro*, the next step was to investigate whether full-length JAK1 protein could be phosphorylated by AMPK *in vitro*.

First, *in vitro* AMPK phosphorylation of ACC Ser79 was conducted to confirm *in vitro* kinase activity of rat liver purified AMPK. HEK293 cells were lysed and ACC was captured using streptavidin agarose beads. ACC is a biotinylated enzyme; thus biotin-streptavidin affinity purification can be used to isolate ACC (Chen et al., 2000). Streptavidin purified ACC and streptavidin depleted lysates were then incubated in the absence or presence of purified rat liver AMPK with or without AMP. AMPK phosphorylation of ACC is detected by probing with anti phospho-ACC (Ser79) antibody (Figure 4.27A). The presence of AMPK alone caused a substantial increase, compared to the basal level, in ACC Ser79 phosphorylation (Figure 4.27A). Moreover, phosphorylation of ACC (Ser79) by AMPK was further increased by the addition of AMP. Immunoblotting with total ACC antibody confirmed that ACC (265kDa) was successfully purified from cell lysates as total ACC is present in streptavidin purified lysates and absent from streptavidin depleted lysates (Figure 4.27A). Overall, this positive control experiment confirms that these *in vitro* phosphorylation events were mediated by catalytically active AMPK.

To test whether full-length JAK1 protein could be phosphorylated by purified active rat liver AMPK *in vitro*, JAK1-null U4C cells, were transfected individually with wild-type (WT) FLAG-tagged recombinant human JAK1 plasmid or an empty expression plasmid as a control. Cell lysates were then immunoprecipitated with anti-FLAG antibody, and the immunocomplexes were then incubated in the absence or presence of purified active rat liver AMPK with or without AMP, and in the presence of [γ-^{32}P] ATP. Incorporation of radiolabelled phosphate from [γ-^{32}P] ATP into a protein substrate was detected by autoradiography following exposure to X-ray film. Phosphorylated proteins are represented by dark bands on the autoradiogram which can be seen in Figure 4.27B. Phosphorylated proteins of approximately 110 and 130 kDa appear in lanes 3,4,7 and 8 which are reactions prepared from both control and JAK1 transfected U4C cells (Figure 4.27B). Immunoblotting with total-JAK1 antibody confirmed that JAK1 (130kDa) was only present in the reactions (lanes 5-8) prepared from U4C cells transfected with

FLAG-tagged JAK1 plasmid (Figure 4.27B). Therefore, it would appear that the FLAG antibody has immunoprecipitated proteins other than JAK1 from cell lysates and therefore the phosphorylated proteins detected at 130kDa were not specifically JAK1. These non-specific proteins were phosphorylated only in the presence of AMPK, which was greatly enhanced by the addition of AMP (Figure 4.27B). Overall, it was not possible to determine whether AMPK phosphorylates full-length JAK1 *in vitro* from these experiments.

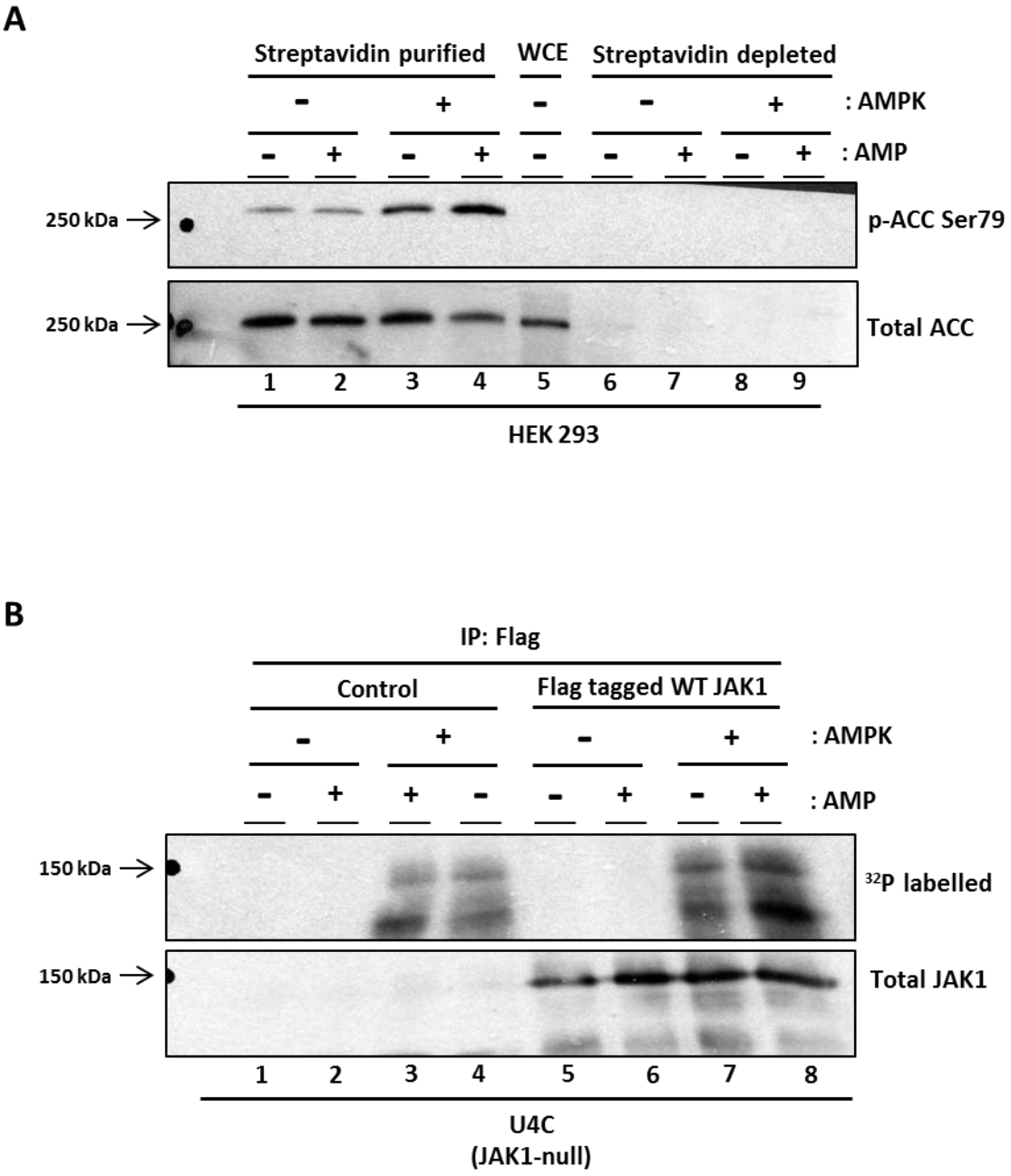

Figure 4.27: *In vitro* AMPK phosphorylation of full-length ACC and JAK1
(A) HEK293 cell lysates were equalised for protein content and ACC was captured using streptavidin agarose beads. Streptavidin purified ACC and streptavidin depleted lysates were incubated in the absence or presence of 0.5U/ml activated AMPK with or without 0.2mM AMP. ACC was eluted from beads and fractionated by SDS-PAGE in parallel with streptavidin depleted lysates and whole cell extract. After transfer to nitrocellulose, membrane was probed with phospho-ACC (Ser79) and total ACC antibody as indicated. A blot from a single experiment is shown. **(B)** U4C cells were transfected with either Flag-tagged JAK1 plasmid or an empty expression plasmid as a control. Protein equalised cell lysates were immunoprecipitated with Anti-FLAG M2 affinity gel, and then each precipitate was incubated for 30 minutes in the absence or presence of 0.5U/ml activated AMPK with or without 0.2mM AMP, and in the presence of 10μCi/ml γ-^{32}P-ATP. JAK1 was eluted from the precipitate and analysed by SDS-PAGE and immunoblotting with anti-JAK1 antibody, and phosphorylated proteins were visualised by autoradiography.

4.2.8 AMPK phosphorylation of GST-JAK1 SH2 fusion protein *in vitro*

In order to establish JAK1 protein as a *bona fide in vitro* AMPK substrate and to determine the specific site(s) of phosphorylation in JAK1 as Ser515/Ser518, this study next sought to determine the stoichiometry of phosphorylation of Ser515/Ser518 in JAK1 by AMPK *in vitro*. To determine this, human wild-type and S515A/S518A JAK1 SH2 domain, and rat ACC1 residues 60-94 were bacterially expressed as GST fusion proteins and subjected to *in vitro* kinase assays using α1- and α2-containing AMPK complexes immunoprecipitated from detergent-solubilised rat liver homogenates, and [γ-^{32}P] ATP. The incorporation of radiolabelled phosphate from [γ-^{32}P] ATP into the GST-fusion proteins was to be determined by scintillation counting of phosphorylated proteins excised from dried SDS-PAGE gels.

4.2.8.1.1 Construction of the pGEX recombinant plasmids

The construction of recombinant wild-type and non phosphorylatable S515A/S518A pGEX-JAK1 SH2 plasmids is described in the Material and Methods. Briefly, site-directed mutagenesis of pCMV6/human JAK1 plasmid was performed to change Ser515 and Ser518 residues to a non-phosphorylatable alanine residues (S515A/S518A). Oligonucleotide primers complementary to the boundaries of the SH2 domain (residues 439 –544) within human JAK1 were synthesised for amplification by PCR. These oligonucleotide primers were designed to amplify the SH2 domain within WT and S515A/S518A mutant pCMV6/human JAK1 while introducing an in-frame C terminal His_6 tag and a stop codon, as well as BamHI and EcoRI compatible ends for subcloning. The resultant PCR products were then digested with BamHI and EcoRI and ligated into similarly digested pGEX-2T bacterial expression plasmid in frame with the GST open reading frame. The pGEX-ACC1-$(His)_6$ plasmid was a kind gift from Prof. Grahame Hardie (Scott et al., 2002). This plasmid encodes residues 60-94 of rat liver ACC1, which contains the major AMPK phosphorylation site Ser79, and a C terminal $(His)_6$ tag.

4.2.8.1.2 GST fusion protein expression and purification

Bacterial expression and purification of GST alone and WT GST JAK1 SH2, S515A/S518A mutant GST JAK1 SH2 and GST-ACC fusion proteins were described in the Materials and Methods. Briefly, *E.coli* BL21 cells transformed with pGEX-2T,

pGEX-WT JAK1 SH2, pGEX S515A/S518A JAK1 SH2 or pGEX-ACC1-His_6 were grown until log phase. At this point, GST fusion protein expression was induced by the addition of 1 mM of IPTG. The cells were grown for a further 4 hours at 37°C and hourly 1ml samples were removed to monitor protein expression. These samples were pelleted and the pellet re-suspended in SDS sample buffer for analysis by SDS-PAGE and Coomassie staining (Figure 4.28). After 4 hours, the cells were pelleted and stored frozen at -80°C until ready for purification. Each GST fusion protein has a $(His)_6$ tag at the C terminus, therefore expressed GST fusion proteins were isolated from bacterial lysates by batch purification with Ni-NTA agarose followed by elution with imidiazole and exchange into substrate buffer (Figure 4.28). GST alone was isolated from bacterial lysates by batch purification with GSH, followed by elution with reduced glutathione (Figure 4.28).

Figure 4.28 shows the expression and purification of the GST fusion proteins: WT and S515A/S518A mutant GST-JAK1 SH2, and GST-ACC, and GST alone. For GST alone and each GST fusion protein, the strongest band for each IPTG induction time-point corresponds with the predicted molecular weight of the GST fusion protein, suggesting that full length products are being expressed. The predicted molecular weight of WT and S515A/S518A mutant GST-JAK1 SH2 is 38 kDa, GST-ACC is 34kDa, and GST is 26kDa. GST alone was successfully purified from the bacterial lysate as indicated by the single band in the eluted product (Figure 4.28A). GST-ACC was also successfully purified, although there are two bands present in the eluted product, one band at about 34 kDa corresponding to GST-ACC and one band at about 25 kDa suggesting that the protein is degrading to GST alone (Figure 4.28B). As shown in figure 4.28C and 4.28D, WT and S515A/S518A mutant GST JAK1 SH2 were not successfully purified by His-tag purification. GST-JAK1 SH2 proteins were also absent from the cleared lysates, which suggests that the GST-JAK1 SH2 protein was not eluted efficiently or that the GST-JAK1 SH2 protein was insoluble.

Another approach used to purify GST-JAK1 SH2 proteins was to replace the lysis buffer prepared in-house with the commercially available protein extraction reagent, BugBuster. Following induction of protein expression in the E.coli cells, the cells were pelleted and lysed in BugBuster as per manufacturer's instructions. The cell lysate was then separated into soluble and insoluble fractions by

centrifugation and each fraction was subject to SDS-PAGE analysis (Figure 4.29). Figure 4.29 shows that the expressed protein is accumulating in the insoluble pellet and thus absent from the soluble lysate. It appears that the expressed protein is insoluble and perhaps accumulating in inclusion bodies as a result of high level of protein expression. Reducing the rate of protein synthesis can help improve the solubility of the expressed protein (Rosano and Ceccarelli, 2014). Therefore, various inducing conditions were tried, such as reducing the growth temperature from 37 degrees to 25 degrees, reducing the inducer concentration from 1mM to 0.1mM IPTG, reducing the time of induction from 4 hours to 3 hours and varying the OD600 value for induction between 0.3 – 0.6. Various combinations of inducing conditions were tried, but none resulted in solubilisation of the expressed protein.

A final approach to purifying GST-JAK1 SH2 proteins was to purify the protein under denaturing conditions. Conventional denaturing and renaturing protocols use denaturing buffers containing either 6 M guanidine hydrochloride (GdnHCl) and 8 M urea, and renaturing methods such as dialysis or dilution steps (Singh and Panda, 2004). To purify GST-JAK1 SH2 proteins from inclusion bodies, the Rapid GST Inclusion Body Solubilization and Renaturation Kit (Cell Biolabs.) was used as per manufacturer's instructions. Briefly, WT GST-JAK1 SH2 expression was induced with 0.1 mM IPTG at 37ºC for 3 hrs. Cell pellet was lysed in STE Extraction Buffer (500 mM Tris, pH 7.5, 1.5 M NaCl, 10 mM EDTA). To solubilize and renature WT GST-JAK1 SH2 proteins, the cell lysate/inclusion body mixture was mixed with Detergent Solubilization Solution (diluted 1:2 with STE extraction buffer (2 fold dilution). The cell lysate was then separated into soluble and insoluble fractions by centrifugation. The soluble fraction was then mixed with Detergent Neutralization Solution. Figure 4.30 demonstrates that the WT GST-JAK1 SH2 protein was present in the renatured soluble protein fraction at this final stage of the Rapid GST Inclusion Body Solubilization and Renaturation Kit protocol. Soluble WT GST-JAK1 SH2 proteins were then purified from the renatured soluble protein fraction by GST-tag batch purification. Figure 4.30 confirms that WT GST-JAK1 SH2 is present in the eluted product following purification and concentration by buffer exchange. This method was also used to extract, solubilise, renature and purify S515A/S518A mutant GST-JAK1 SH2 protein. Figure 4.30 confirms that S515A/S518A mutant GST JAK1 SH2 is present in the eluted product following

purification and concentration by buffer exchange, however a second band is also present at about 25 kDa suggesting that the protein is degrading to GST alone.

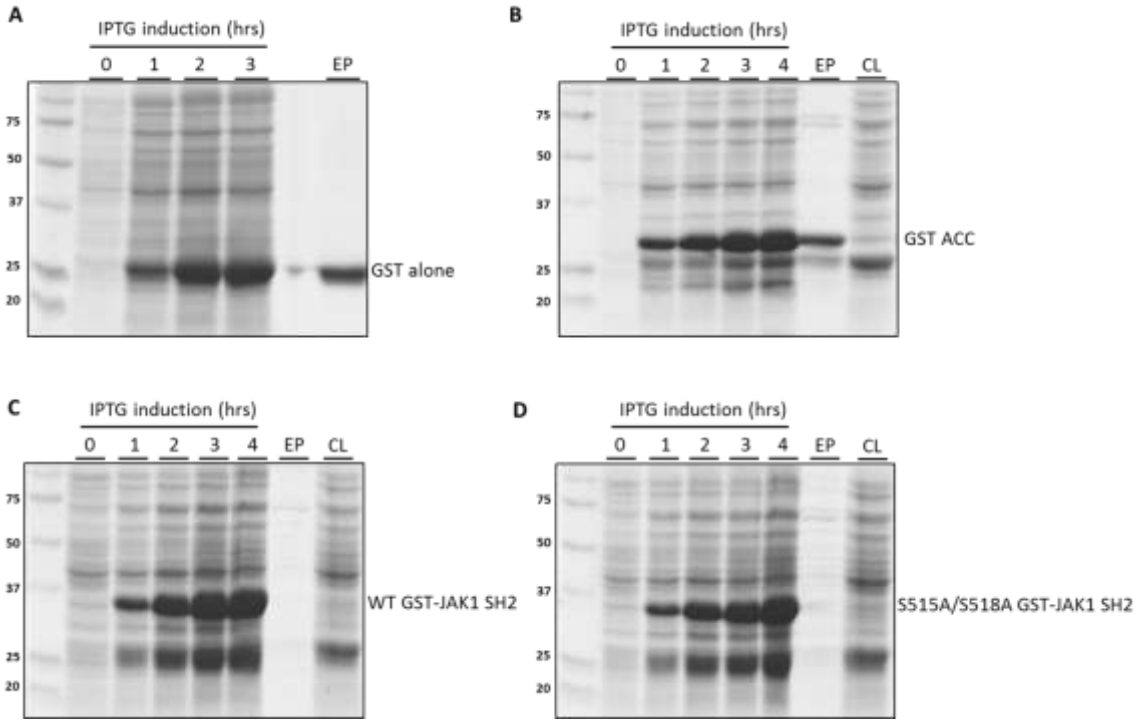

Figure 4.28: Verification of GST fusion protein expression and purification by SDS PAGE and Coomassie staining.

Bacterial expression of GST-fusion proteins were induced by IPTG for 0, 1, 2, 3 and 4 hrs. GST fusion proteins were purified by batch purification with Ni-NTA agarose, followed by elution with imidiazole. GST alone was purified by batch purification with glutathione-Sepharose, followed by elution with reduced glutathione. Samples were analysed by 12% SDS-PAGE and proteins visualised by staining with Coomassie Brilliant Blue R-250 **(A)** GST alone runs at 26 kDa **(B)** GST-ACC runs at 34kDa **(C)** WT GST-JAK1 SH2 runs at 38 kDa **(D)** S515A/S518A mutant GST-JAK1 SH2 runs at 38 kDa EP = Eluted protein and CL = clear lysate

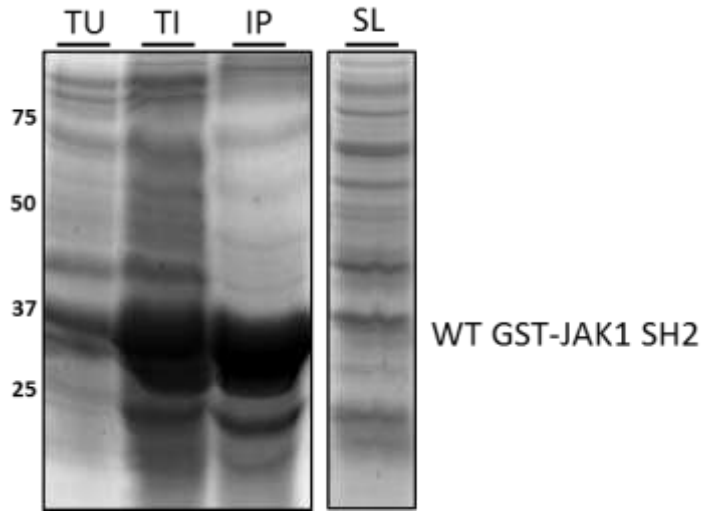

Figure 4.29: Verification of GST fusion protein expression and protein extraction using BugBuster by SDS PAGE and Coomassie staining
Bacterial expression of WT GST JAK1 SH2 fusion protein was induced by IPTG for 3 hrs. Bacterial pellet was lysed in BugBuster protein extraction reagent. Samples were analysed by 12% SDS-PAGE and proteins visualised by staining with Coomassie Brilliant Blue R-250. WT GST-JAK1 SH2 runs at 38 kDa. TU = total uninduced protein, TI = total induced protein, Insoluble pellet = IP and SL = soluble lysate.

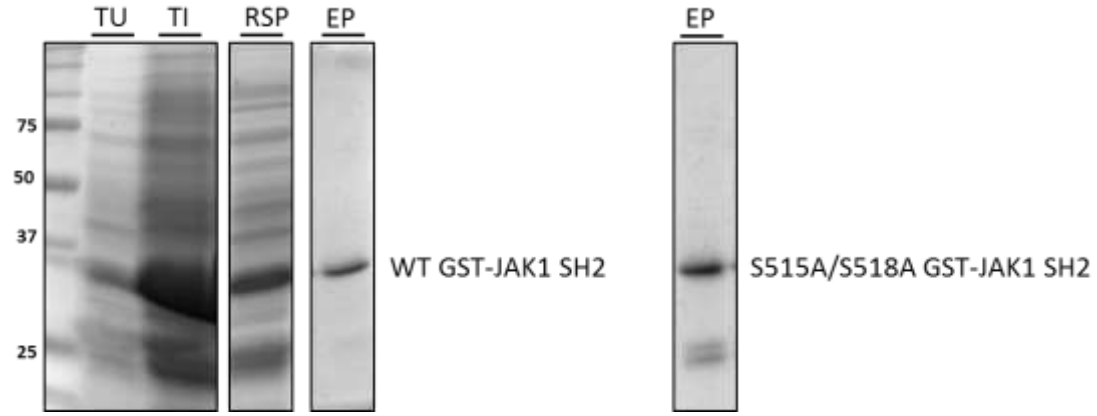

Figure 4.30: Verification of GST fusion protein expression and purification under denaturing conditions by SDS PAGE and Coomassie staining
Bacterial expression of WT GST JAK1 SH2 and S515A/S518A GST JAK1 SH2 fusion protein was induced by IPTG for 3 hrs. GST fusion proteins were purified by GST-batch purification under denaturing conditions using the Rapid GST Inclusion Body Solubilization and Renaturation Kit (Cell Biolabs.). Samples were analysed by 12% SDS-PAGE and proteins visualised by staining with Coomassie Brilliant Blue R-250 **(A)** WT GST-JAK1 SH2 runs at 38 kDa. **(B)** S515A/S518A mutant GST-JAK1 SH2 runs at 38 kDa TU = total uninduced protein, TI = total induced protein, RSP = renatured soluble protein and EP = Eluted protein.

4.2.8.1.3 *In vitro* AMPK phosphorylation of GST-JAK1 SH2 fusion protein

The hypothesis being tested was whether JAK1 protein is as a *bona fide in vitro* AMPK substrate and that the specific site(s) of phosphorylation in JAK1 are Ser515/Ser518. Thus, this study sought to determine the stoichiometry of phosphorylation of Ser515/Ser518 in JAK1 by AMPK *in vitro*. To determine this, purified GST-ACC, WT GST-JAK1 SH2 and S515A/S518A mutant GST JAK1 SH2 fusion proteins, and GST alone were subjected to *in vitro* kinase assays using purified active rat liver AMPK, and [γ-^{32}P] ATP. The incorporation of radiolabelled phosphate from [γ-^{32}P] ATP into the GST-fusion proteins was to be determined by autoradiography of phosphorylated proteins and excision of gel slices for scintillation counting after fractionation by SDS-PAGE.

Prior to stoichiometric analysis of protein phosphorylation by scintillation counting, it was important to visualise protein phosphorylation by autoradiography in order to confirm that the GST-fusion proteins of the corresponding molecular mass were phosphorylated (i.e that the GST alone contaminant was not phosphorylated). *In vitro* kinase reactions were resolved by SDS-PAGE and immunoblotted, followed by autoradiography. As shown in Figure 4.31, phosphorylated proteins are represented by dark bands on the autoradiogram. GST-ACC was potently phosphorylated in the presence, but not in the absence, of purified active rat liver AMPK, and the addition of AMP appeared to enhance AMPK phosphorylation of GST-ACC (Figure 4.31). In contrast, GST alone, WT JAK1, S515A/S518A JAK1 and the degradation products of GST-fusion protein were not phosphorylated under these same conditions, as indicated by the absence of phosphorylated protein bands of the corresponding molecular mass on the autoradiogram (Figure 4.31). Taken together, these data confirmed that AMPK is catalytically active and that AMPK phosphorylates only the ACC portion of the fusion protein. Following autoradiography, the immunoblot was probed with HRP-conjugated anti-GST antibody to confirm the presence of GST and GST fusion proteins in each reaction (Figure 4.31). Recombinant GST fusion proteins of the expected molecular weight were present in each reaction: WT and S515A518A GST-JAK1 SH2 at 38 kDa, GST alone at 26 kDa and GST-ACC at 34 kDa (Figure 4.31). Overall, phosphorylation of WT GST JAK1 SH2 by AMPK was not observed under *in vitro* conditions where GST ACC was robustly phosphorylated. Thus, these

experiments were not followed by *in vitro* AMPK kinase assays subject to stoichiometric analysis.

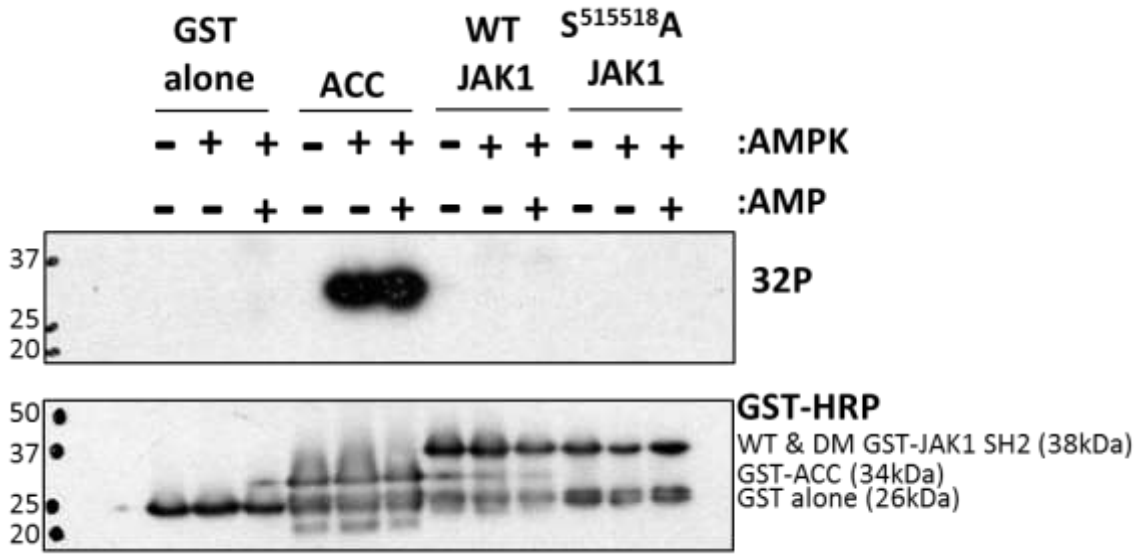

Figure 4.31: AMPK phosphorylation of GST-JAK1 SH2 fusion proteins *in vitro*
Bacterially expressed and purified GST-ACC, WT GST-JAK1 SH2 and S515A/S518A mutant GST JAK1 SH2 fusion proteins, and GST alone were incubated for 30 minutes in the absence or presence of 0.5U/ml activated AMPK with or without 0.2mM AMP, and in the presence of 10µCi/ml γ-^{32}P-ATP. *In vitro* kinase reactions were resolved by SDS-PAGE and immunoblotted, and phosphorylated proteins were visualised by autoradiography. The immunoblot was probed with GST-HRP to detect. A representative autoradiogram from n=2 experiments is shown.

4.3 Discussion

In this chapter, it was investigated whether AMPK acts directly on a signalling component of the JAK-STAT pathway. Specifically, it was hypothesised that AMPK could directly phosphorylate serine or threonine residues within JAK to inhibit IL-6 signalling. The key findings of this chapter are that *in vitro* kinase assays of JAK1-derived peptides demonstrated that AMPK can directly phosphorylate two residues, Ser515 and Ser518, within the JAK1 SH2 domain. In addition, pharmacological activation of AMPK promotes 14-3-3 binding to JAK1 *via* a mechanism requiring Ser515 and Ser518. Furthermore, mutation of Ser515 and Ser518 abolishes the ability of AMPK to inhibit JAK-STAT signalling by an IL-6 trans-signalling complex and from a constitutively active Val658Phe-mutated JAK1.

Having demonstrated that AMPK inhibits both sIL-6Rα/IL-6 and IFN-α (Figure 6.5A), the initial aim was to identify the JAK isoform(s) that mediate the actions of sIL-6Rα/IL-6 and IFN-α in HUVECs. sIL-6Rα/IL-6 has been shown to signal predominantly through STAT3 in several cell types. SiRNA-mediated downregulation of JAK isoforms in HUVECs demonstrated that sIL-6Rα/IL-6 stimulation of STAT3 Tyr705 phosphorylation does not require activation of TYK2, but mainly requires activation of JAK1 and to a lesser extent JAK2 (Figure 4.7). This is consistent with published data from Guschin et al., (1995) who reported that in JAK1-null human fibrosarcoma U4C cells, STAT3 activation is profoundly inhibited despite IL-6 activation of JAK2 and TYK2 (Guschin et al., 1995). IFN-α signals predominantly through STAT1 (Ramana et al, 2000), however in this study it was not possible to assess the effects of siRNA-mediated downregulation of JAK isoforms on IFN-α stimulation of STAT1 Tyr701 phosphorylation as transfection of HUVECs with siRNAs at levels required to knockdown JAK isoform expression resulted in an increase in total STAT1 levels (Figure 4.8). IFN-α also signals through STAT3 (Ho and Ivashkiv, 2006) but despite siRNA transfection of HUVECs appearing to have no effect on total STAT3 levels, IFN-α stimulation of STAT3 Tyr705 phosphorylation in HUVECs was found to be variable between and within individual experiments (Figure 4.4, 4.5 and 4.6). Overall, it was not possible to assess the effects of siRNA-mediated downregulation of JAK isoforms in HUVECs on IFN-α signalling. siRNAs have been shown to induce an interferon (IFN) response which may explain why the total STAT1 levels in cells transfected with siRNA increased as STAT1 is an IFN-inducible gene (Reynolds et al., 2006, Satoh & Tabunoki, 2013).

siRNA stimulation of an interferon response could also explain why IFN-α did not reproducibly stimulate STATs as the cells had been desensitised to interferon stimulation following siRNA transfection 48 hrs prior to IFN-α treatment (Whitehead et al., 2011). Previous reports have demonstrated IFN-α signals through JAK1 and TYK2 (Borden et al., 2007, Gauzzi et al., 1996).

Overall, JAK1 was identified as a post receptor intermediate of both IL-6 and IFN-α signalling. Therefore, it was proposed that AMPK could potentially directly phosphorylate Ser or Thr site(s) within JAK1 to inhibit sIL-6Rα/IL-6 and IFN-α stimulation of STAT phosphorylation. Peptide arrays consisting of overlapping 25-mer peptides spanning the entire open reading frame of human JAK1, JAK2, JAK3 and TYK2 (Figure 4.9, schematic diagram) were subject to *in vitro* phosphorylation with AMPK purified from rat liver and [γ^{32}P]ATP. No phosphorylation of TYK2 or JAK3 peptides by AMPK was observed when compared to the corresponding peptide array incubated without active AMPK (Figure 4.13 and 4.14). It was observed that SH2 domain-derived peptides from JAK1 and JAK2 can serve as substrates for phosphorylation by AMPK *in vitro* (Figure 4.10 and 4.12). Alignment of the primary sequences of JAK1 and JAK2 identified the JAK1 and JAK2 25-mer peptides phosphorylated by AMPK as related sequences similarly positioned within the SH2 domain of each protein (Figure 4.11). To confirm these observations, the JAK2, JAK3 and TYK2 25-mer peptides that aligned with the JAK1 25-mer peptide identified as phosphorylated by AMPK were spotted on the same peptide arrays to allow for direct comparison (Figure 4.15). These confirmed that SH2 domain-derived peptides from JAK1 and JAK2, but not JAK3 and Tyk2, can serve as substrates for phosphorylation by AMPK *in vitro*. The JAK1 25-mer peptide, R-Y-S^{508}-L-H-G-S^{512}-D-R-S^{515}-F-P-S^{518}-L-G-D-L-M-S^{524}-H-L-K-K-Q-I, phosphorylated by AMPK *in vitro* contains five potential phospho-acceptor sites (indicated in red). The JAK2 25-mer peptide, Y-N-L-S^{465}-G-T^{467}-K-K-N-F-S^{472}-S^{473}-L-K-D-L-L-N-C-Y-Q-M-E-T, phosphorylated by AMPK *in vitro* contains four potential phospho-acceptor sites (indicated in red).

To identify which of the five potential phospho-acceptor sites within JAK1 were phosphorylated *in vitro* by AMPK, phosphorylation assays were performed on arrays spotted with the wild-type (WT) and mutant versions of the JAK1 25-mer peptide in which each Ser residue was substituted with a non-phosphorylatable

Ala residue either individually or in combination (Figure 4.16). Consistent with Figure 4.10, the WT JAK1 peptide was phosphorylated by active AMPK (Figure 4.16). In contrast, substitution of all five Ser residues with Ala abolished AMPK phosphorylation (Figure 4.16). However, individual substitution of each Ser residue with Ala either did not alter or enhanced AMPK phosphorylation of the resulting peptides (Figure 4.16). Mutant JAK1 peptides containing Ala substitutions at two or more Ser residue were also prepared. The mutant JAK1 peptide containing Ala substitutions at Ser508, Ser512 and Ser524 was phosphorylated by AMPK, whereas Ala substitution of both Ser515 and Ser518 abolished AMPK phosphorylation similarly to the peptide in which all five Ser residues were mutated to Ala (Figure 4.16). Taken together, these observations identified Ser515 and Ser518 in human JAK1 as potential sites of phosphorylation by AMPK *in vitro*. A search of scientific literature and the PhosphoSitePlus database (Cell Signalling Technology PhosphoSitePlus) revealed that phosphorylation of Ser515 and Ser518 sites has never been previously reported therefore this study has identified a novel phosphorylation site in JAK1.

Peptide library screening, mutagenesis and molecular modelling studies (Scott et al., 2002, Gwinn et al., 2008) have all been used to identify optimal AMPK substrate motifs. Bioinformatic analysis of JAK1 orthologues revealed that phosphorylation sites equivalent to Ser518 in human JAK1 are conserved in multiple species (Figure 4.32). Importantly, residues at positions +3 and +4 downstream of the phospho-acceptor sites which are known to be critical for substrate recognition are well conserved (Figure 4.32). In contrast, Ser515 is unique to human JAK1 and would only form a weak consensus for AMPK substrate recognition if Ser518 became negatively charged via prior phosphorylation. However other examples of AMPK substrates that only loosely follow the optimized consensus have also been documented (e.g. eNOS phosphorylation at Ser633) (Chen et al., 2009b). Thus, the potential role for both Ser515 and Ser518 were examined in more detail.

Ser515 and Ser518 are found within SH2 domain of JAK1 (Figure 4.33). The SH2 domain is preceded by the N-terminal FERM domain (FERM standing for: band-4.1 protein, ezrin, radixin, and moesin) and immediately upstream of the pseudokinase JH2 domain (Figure 4.33). The unavailability of a crystal structure

of a full-length JAK1 molecule limits our understanding on the functional roles of these domains. However biochemical and mutational studies coupled with some solved crystal structures of JAK fragments have started to unravel the basic functional roles of these domains. The JH2 domain has been shown to play a regulatory role by suppressing kinase activity via inhibitory interactions with the C-terminal JH1 tyrosine kinase catalytic domain (Lupardus et al., 2014, Shan et al., 2014, Tom et al., 2013, Ungureanu et al., 2011). The N-terminal FERM domain binds to the cytoplasmic region of cytokine receptors and may also regulate kinase activity (Girault et al., 1998, Haan et al., 2001, 2008, Hilkens et al., 2001, Zhao et al., 2010). The cytoplasmic domains of the cytokine receptors contain “box1” and “box2” motifs which are required for JAK engagement. Box1 is a membrane proximal proline-rich motif while box2 consists of a single negatively-charged residue followed by several hydrophobic residues (Murakami et al., 1991, Pelletier et al., 2006, Yan et al., 1996, Tanner et al., 1995, Usacheva et al., 2002, Royer et al., 2005, Haan et al., 2002). A classical SH2 domain typically contains a conserved arginine residue that coordinates phosphotyrosine binding (Liu et al., 2012). However the JAK1 SH2 domain is not believed to maintain the phosphotyrosine-binding function of classical SH2 domains as an in depth study by Radtke and co-workers found no phenotype associated with mutation of the highly conserved arginine residue at position 466 to lysine within the SH2 domain (Radtke et al., 2005). In contrast, a recent study suggested that the SH2 domain is required for full activation of JAK (Gorantla et al., 2010). They demonstrated that mutation of a highly conserved arginine residue at position 426 within the SH2 domain of JAK2 had no effect on receptor and membrane association, but reduced cytokine-induced JAK2 and STAT5 phosphorylation. Sequence analysis suggested that the SH2 domain interacts with the FERM domain to stabilise its conformation to allow it to associate with cytokine receptors (Radtke et al., 2005). Recently, Lupardus and co-workers have presented a crystal structure of the FERM-SH2 region of TYK2 and JAK1 which confirms and provides structural details of such an interaction (Wallweber et al., 2014, Ferrao et al., 2016). These crystal structures revealed that the FERM subdomains (F1, F2 and F3) and SH2 domain are intimately linked to form a tightly integrated structural module. The TYK2 and JAK1 FERM-SH2 crystal structures were determined in complex with a peptide derived from cytokine receptors interferon-α receptor 1 (IFNAR1) and interferon-λ receptor 1 (IFNLR1), respectively (Figure 4.34 is a cartoon representation of these structures

adapted from Wallweber et al., 2014 and Ferrao et al., 2016). These crystal structures revealed that binding of receptor box1 motif is mediated by the FERM F2 subdomain and receptor box2 binding is primarily mediated by the SH2 domain. Previous studies have demonstrated that both box1 and box2 motifs are required for gp130 mediated JAK1 activation (Murakami et al., 1991, Haan et al., 2002). Lupardus also demonstrated that the receptor box1 is the primary binding site of JAK1 and box2 further stabilises the JAK1-receptor complex (Ferrao et al., 2016). The crystal structure of the FERM-SH2 region of TYK2 in complex with a fragment of IFNAR1 showed that the box2 motif of IFNAR1 binds to the SH2 domain in a manner that mimics a classical SH2-phosphopeptide interaction (Wallweber et al., 2014). In this structure, a glutamic acid residue (Glu497) of the IFNAR1 box2 motif resides in the phosphotyrosine-binding pocket of the SH2 domain and a hydrophobic box2 segment C-terminal to the glutamic acid lies in a hydrophobic βG1-EF groove of the SH2 domain (Figure 4.35). Reciprocal His and GST pull-down assays confirmed that Glu497 is required for IFNAR1 peptide binding to the TYK2 FERM-SH2 module. Thermal stability assays also demonstrated that simultaneous mutation of the glutamic acid residues at positions 497 and 496 in the IFNAR1 peptide reduced the melting temperature of the interaction with Tyk2 FERM-SH2 by more than 5^{o}C indicating that Glu497 is important for the stability of the TYK2 FERM-SH2 module (Wallweber et al., 2014). In summary, these studies indicate that the SH2 domain is an integral part of the JAK-receptor complex which serves to interact with the cytokine receptor and structurally support the FERM domain in order to stabilise the JAK-receptor complex. Mapping of the AMPK phosphorylation sites Ser515 and Ser518 of JAK1 to their analogous locations on the TYK2 FERM-SH2 crystal structure revealed that these residues lie beside the hydrophobic βG1-EF groove in the SH2 domain (Wallweber et al., 2014) (Figure 4.35). The hydrophobic box2 segment of IFNAR1 is buried in the hydrophobic groove formed by the βG1 strand and EF loop of the SH2 domain. TYK2 Ser522/525, analogous to JAK1 Ser515/518, are C-terminal residues of the EF loop preceding the αB helix, which is followed by the βG1 strand (Figure 4.35). Preceding TYK2 Ser522 and Ser525 are residues, Leu516, Glu517, Gly518 and Tryp519, which interact with the IFNAR1 hydrophobic box2 segment (Wallweber et al., 2014). The introduction of a negatively charged phosphate group may affect the orientation and stability of the αB helix and EF loop to disrupt the SH2 hydrophobic βG1-EF groove and its interaction with the receptor hydrophobic box2 segment. Taken

together with the current study, it is proposed that AMPK phosphorylation of Ser515 and Ser518 within the SH2 domain of JAK1 disrupts the cytokine receptor box2-JAK1 SH2 binding site to destabilise the JAK1-cytokine receptor complex leading to impaired JAK1 signalling.

In addition to receptor association, studies have demonstrated that the FERM domain may also participate in regulation of kinase activity (Haan et al., 2008, Zhao et al., 2010). The TYK2-IFNAR1 crystal structure highlights the critical scaffolding function of the SH2 domain to structurally support the FERM domain (Wallweber et al., 2014). Altogether, this information suggests that AMPK phosphorylation of Ser515 and Ser518 at the cytokine receptor box2-JAK1 SH2 binding site could also potentially restrain the kinase activity of JAK1 by destabilising the JAK1 FERM association with its cytokine receptor. There is growing evidence suggesting that the regulation of catalytic activity involves a complex interplay of the JAK domains (Haan et al., 2010). Therefore, it is conceivable that the cytokine receptor box2-JAK1 SH2 interface may enforce allosteric interactions essential for optimal enzymatic activity. In a previous study, Haan et al., (2002) demonstrate that alanine substitution of Tryp652 within the transmembrane region of gp130 has no effect on JAK1 association but abrogates JAK1 activation (Haan et al., 2002). It was postulated that the activation of JAKs involves structural re-organisation of the JAK/receptor binding interface, and that residues, such as W652 of gp130, are involved in the activation process and allosteric regulation of kinase activity (Haan et al., 2006). Thus, AMPK phosphorylation of Ser515 and Ser518 at the cytokine receptor box2-JAK1 SH2 interface disrupts this interaction to abolish the allosteric capacity of the cytokine receptor box2-JAK1 SH2 interface to promote optimal enzymatic activity. It is likely that JAK-receptor interactions at multiple sites within the complex dictates the JAK position in a defined orientation. Therefore, it is also conceivable that AMPK phosphorylation of Ser515 and Ser518 at the cytokine receptor box2-JAK1 SH2 binding site may alter the positioning of the kinase domain in the receptor complex, impairing the phosphorylation of substrates (e.g. gp130 cytoplasmic tyrosine residues and/or STAT1/3).

The JAK SH2 domain might be a part of the machinery that activates JAK in response to cytokine engagement of its cognate receptor. The sequence of events

that lead to JAK activation within the JAK-receptor complex remain largely elusive. However, it is proposed that cytokine binding to the receptor induces a conformational change which relieves the inhibitory JH1-JH2 interaction to allow autophosphorylation of the JAKs and their activation and progression of signal transduction (Babon et al., 2014). The crystal structure of the TYK2 pseudokinase JH2 –kinase JH1 region revealed an extensive interface between the two domains and an interdomain linker connecting the SH2 domain to the JH2 domain bridges the two domains (Lupardus et al., 2014). Activating mutations located in the JH2 domain and the SH2-JH2 linker suggest that this complex represents a physiological autoinhibitory conformation (Shan et al., 2014). A mutational study of the JAK2 SH2-JH2 linker by Zhao and co-workers demonstrated that the linker plays a crucial role in both autoinhibition and cytokine stimulated JAK2 activation (Zhao et al., 2009). This study also demonstrated that activating mutations are located within the C-terminal end of the SH2-JH2 linker, whereas mutation of residues located within the N-terminal end of the linker are essential for the interaction of JAK2 with the Epo receptor. Taken together, these studies propose that the cytokine-induced conformational changes in the JAK-receptor complex are propagated through the SH2-JH2 linker to relieve the autoinhibitory interaction, leading to JAK activation (Zhao et al., 2009). The crystal structure of the TYK2 FERM-SH2 region indicates that the FERM-SH2 interface also plays a key role in communicating cytokine receptor engagement to the kinase domain (Wallweber et al., 2014). The crystal structure reveals that the N-terminal end of the SH2-pseudokinase linker, labelled as L3, is sandwiched between the FERM and SH2 domains and lies in close proximity to the SH2 domain–receptor interface. This region appears to play a crucial role in facilitating effective communication between the FERM and SH2 domains as the SH2-JH2 linker interacts with each domain and other interdomain linkers (Wallweber et al., 2014). Thus, mutations within the N-terminal end of the SH2-JH2 linker are predicted to destabilise the FERM-SH2 interface and disrupt its interaction with the receptor. Overall, the crystal structure suggests that both the FERM-SH2 interface and SH2-JH2 linker play a key role in communicating cytokine receptor engagement to JAK activation. Taken together with the current study, these data suggest that AMPK phosphorylation of Ser515 and Ser518 in the SH2 domain could inhibit JAK1 activation by destabilising the JAK1 FERM –SH2 interface, thus disrupting the

communication between the activated receptor and kinase domain resulting in partially activated JAK.

Mutation of serine 512 for leucine in the SH2 domain was identified as a somatic JAK1 mutation in adult acute lymphoblastic leukaemia (ALL) (Flex et al., 2008). Interestingly, TYK2 Tryp519, analogous to JAK1 Ser512, is located within the SH2 EF loop and lies within the SH2 hydrophobic βG1-EF groove to interact with the IFNAR1 hydrophobic box2 segment (Wallweber et al., 2014). Presumably, mutation of a polar residue serine to a hydrophobic residue leucine in Ser512 enhances the cytokine receptor box2-JAK1 SH2 interaction leading to aberrant JAK1 signalling and gives rise to ALL. Taken together with the current study, these data indicate that structural re-organisation of the cytokine receptor box2-JAK1 SH2 interface plays a key role in the regulation of JAK signalling.

Potential functional roles of the JAK1 SH2 domain have been described: mediating and structurally supporting receptor association, dictating JAK orientation for efficient phosphorylation of substrates, facilitating JAK activation and allosterically regulating kinase activity. Interestingly, the JAK SH2 domain may not necessarily only function as a "passive" structural element of the JAK-receptor signalling complex, but “actively” influence JAK signalling via the the cytokine receptor box2-JAK1 SH2 interface. It is proposed that AMPK phosphorylation of Ser515 and Ser518 within the SH2 domain of JAK1 disrupts the cytokine receptor box2-JAK1 SH2 interface to affect one or a more of the potential functions of the SH2 domain, leading to impaired JAK1 signalling. Therefore, studying the effects of AMPK activation on each proposed functional role of the SH2 domain is crucial to establishing the mechanism of the inhibitory effect of AMPK. Structural studies of full-length JAK are also required to better establish the functional role of the SH2 domain, as it not clear if and how the FERM-SH2 module may interact with the JH2 and JH1 domains to participate in JAK activation and regulation of tyrosine kinase activity. Crucially, structural studies of full length JAKs bound to receptor chains, in both active and inactive states, will be required to address whether the JAK-receptor interface “actively” contributes to JAK signalling.

So far this study indicates that AMPK phosphorylates JAK1 at Ser515 and Ser518 *in vitro*, therefore the next step was to determine whether AMPK-mediated inhibition of sIL-6Rα/IL-6 signalling is dependent on the phosphorylation of JAK1

by AMPK at Ser515 and Ser518. JAK1-null human fibrosarcoma U4C cells and a stable rescue form U4C.JAK1 were mutated from there parental cell 24C by Muller et al. (1993) (Muller et al., 1993). These cells were used to investigate the role of JAK1 in AMPK-mediated inhibition of sIL-6Rα/IL-6 signalling. First, the effects of AMPK activator A769662 on sIL-6Rα/IL-6 signalling in these cells had to be assessed (Figure 4.17). sIL-6Rα/IL-6 stimulated STAT3 Tyr705 phosphorylation in 24C and U4C.JAK1 cells. In contrast, sIL-6Rα/IL-6 stimulation of STAT3 Tyr705 phosphorylation was almost completely abolished in JAK1-null U4C cells (Figure 4.17). This result is consistent with previous work by Guschin et al., (1995) and the siRNA experiments discussed earlier in the current study (Guschin et al., 1995). Taken together, these data demonstrate that JAK1 is required for IL-6 signalling in HUVECs and, human fibrosarcoma cells and its mutants. A769662 activates AMPK to inhibit sIL-6Rα/IL-6 signalling in 2C4 and U4C.JAK1, thus U4C cells are a valuable tool for investigating the role of JAK1 in AMPK-mediated inhibition of IL-6 signalling. In order to determine whether AMPK-mediated inhibition of sIL-6Rα/IL-6 signalling is dependent on Ser515 and Ser518, a human JAK1 plasmid containing non phosphorylatable alanine substitution at these sites (S515A/S518A) was generated. The effects of AMPK activation on sIL-6Rα/IL-6 signalling in JAK1-null U4C cells transiently expressing WT and S515A/S518A mutant human JAK1 were examined (Figure 4.18). sIL-6Rα/IL-6 treament of U4C cells transiently expressing WT or S515A/S518A mutant JAK1 significantly stimulated STAT3 Tyr705 phosphorylation. While A769662 activation of AMPK significantly inhibited sIL-6Rα/IL-6 stimulation of STAT3 Tyr705 phosphorylation in cells expressing WT JAK1, treatment of S515A/S518A JAK1 expressing cells with A769662 prior to sIL-6Rα/IL-6 stimulation had no substantial effect on sIL-6Rα/IL-6 stimulation of STAT3 phosphorylation (Figure 4.18). Overall, these data demonstrate that Ser515 and Ser518 of JAK1 are required for effective AMPK-mediated inhibition of IL-6 signalling.

The effects of AMPK activation on signalling downstream of a constitutively active mutant V658F mutant JAK1 was also examined (Jeong et al., 2008). The V658F mutation in the JAK1 has been identified in some patients with ALL (Staerk et al., 2005) and is analogous to the V617F mutation in JAK2 responsible for several myeloproliferative neoplasms (MPN) (James et al., 2005). The V658F mutation within the JAK1 JH2 pseudokinase domain is thought to relieve an auto-inhibitory

interaction with the catalytic JH1 domain, thereby increasing Tyr kinase activity independent of cytokine stimulation (Lupardus et al., 2014, Shan et al., 2014, Toms et al., 2013, Ungureanu et al., 2011). The effects of AMPK activator A769662 on U4C cells transiently expressing either WT, V658F mutant or V658F S515A/S518A mutant JAK1 were examined. In contrast to WT JAK1, transient expression of V658F JAK1 in U4C cells was sufficient to trigger detectable Tyr phosphorylation of STAT1 and STAT3 in the absence of added cytokine (Figure 4.19). Importantly, treatment with A769662 significantly inhibited STAT1 and STAT3 phosphorylation. Expression of the triple mutant V658F/S515A/S518A JAK1 also resulted in increased basal STAT1 and STAT3 phosphorylation, although this was significantly less than with single mutant V658F JAK1 (Figure 4.19). However, A769662 treatment failed to significantly further inhibit the response despite increasing ACC phosphorylation (Figure 4.19). Overall, mutation of Ser515 and Ser518 abolishes the ability of AMPK to inhibit JAK-STAT signalling from a constitutively active Val658Phe mutated JAK1. Together, these observations suggest that Ser515 and Ser518 are required for effective AMPK-mediated inhibition of JAK-STAT signalling by an IL-6 *trans*-signalling complex and from a constitutively active Val658Phe-mutated JAK1. Intriguingly, mutation of Ser515 and Ser518 to Ala within the SH2 domain of WT JAK1 had no substantial effect on sIL-6Rα/IL-6 stimulated STAT3 Tyr705 phosphorylation (Figure 4.18), whereas the addition of these mutations into the SH2 domain of V658F JAK1 significantly inhibits V658F JAK1-mediated phosphorylation of STAT3 (Figure 4.19). These results support the findings reported by Gorantla and co-workers (2010), who proposed that the SH2 domain is critical for V617F JAK2-mediated constitutive signalling (Gorantla et al., 2010) . Mutation of Arg426 to Lys (R426L) within the SH2 domain of WT human JAK2 reduced IL-3 stimulated STAT5 phosphorylation, whereas the incorporation of this mutation into the SH2 domain of V617F JAK2 abolished V617F JAK2-mediated phosphorylation of STAT5 (Gorantla et al., 2010) (Gorantla et al., 2010). Crucially, it was also reported that the SH2 domain in V617F JAK2 is critical for the induction of a myeloproliferative neoplasm-like disease. Myeloproliferative disease was only induced in mice transplanted with bone marrow cells expressing single mutant V617F JAK2 and not in induced in mice transplanted with bone marrow cells expressing double mutant V617F/R426L JAK2 (Gorantla et al., 2010). These data suggest that the SH2 domain is critical for both V658F-JAK1 and V617F-JAK2 mediated constitutive signalling. The ability of AMPK to inhibit V658F JAK1

mediated phosphorylation of STATs via a mechanism requiring Ser515/Ser518 in the SH2 domain would support clinical studies to evaluate AMPK activators such as metformin as potential treatment options for ALL caused by activating JAK1 mutations. These clinical studies could be expanded to include myeloproliferative neoplasms induced by V617F JAK2 as activated AMPK was also shown to phosphorylate SH2 domain-derived peptides and the SH2 domain is critical V617F-JAK2 mediated constitutive signalling (Gorantla et al., 2010). However the effects of AMPK activation on signalling downstream of an endogenous ligand activated JAK2 or a constitutively active V617F mutant JAK2 have still to be examined.

A common mechanism for phosphorylation-mediated regulation of target protein function is phosphorylation-dependent binding to members of the 14-3-3 family of proteins (Bridges & Moorhead, 2005). The 14-3-3 family proteins bind to phospho-serine and phospho-threonine-containing proteins, and two consensus 14-3-3 binding phospho-peptide motifs, RXXpS/pTXP and RXXXpS/pTXP, have been identified (Yaffe et al., 1997). AMPK phosphorylation of either Ser515 or Ser518 within JAK1 creates a phospho-peptide motif that shares similarities with the 14-3-3 binding motifs. AMPK has been shown to induce binding of 14-3-3 to many *in vivo* substrates of AMPK, including Raptor, ULK1, BRAF, and Atg9, although JAK1 has never been identified before (Gwinn et al., 2008, Mack, Zheng, Asara, & Thomas, 2012, Shen et al., 2013, Weerasekara et al., 2014). Recently, the expression of 14-3-3ε in microglia cells has been reported to be induced by IL-6 through the JAK-STAT3 pathway (Eufemi et al., 2015). To assess whether phosphorylation of Ser515 and Ser518 could facilitate JAK1 interaction with 14-3-3 protein *in vitro*, a peptide array spotted with the 25-mer JAK1 peptide, R-Y-S-L-H-G-S-D-R-S^{515}-F-P-S^{518}-L-G-D-L-M-S-H-L-K-K-Q-I, phosphorylated at either or both of Ser515 and Ser518 was overlaid with HRP-conjugated 14-3-3ζ. 14-3-3ζ strongly interacted with the JAK1 peptides individually phosphorylated at Ser515 and Ser518, but did not interact with either the non-phosphorylated JAK1 peptide or the peptide phosphorylated at both Ser515 and Ser518 (Figure 4.20). The signal from bound 14-3-3ζ was substantially stronger with the phospho-Ser515 JAK1 peptide than the phospho-Ser518 JAK1 peptide (Figure 4.20). This was surprising as Ser518 is highly conserved among a wide variety of species, while Ser515 is not highly conserved (Radtke et al., 2005). Phospho-Ser518 may play a redundant role in the binding of 14-3-3, therefore binding 14-3-3 when phospho-Ser515 is not

available structurally or conservatively. The peptide array was also spotted with the 25-mer JAK-2 peptide, E-Y-N-L-S^{465}-G-T-K-K-N-F-S^{472}-S^{473}-L-K-D-L-L-N-C-Y-Q-M-E-T, phosphorylated at either or all three of Ser465, Ser472 and Ser473, and overlaid with 14-3-3ζ-HRP to assess whether phosphorylation of these sites could facilitate JAK2 interaction with 14-3-3 protein *in vitro*. 14-3-3ζ bound to non-phosphorylated JAK2 peptide and phospho-Ser465 JAK2 peptide, and did not bind phospho-Ser472 or phospho-Ser473 JAK2 peptide (Figure 4.20). The signal from bound 14-3-3ζ was stronger with the non-phosphorylated JAK2 peptide than the phospho-Ser465 JAK2 peptide (Figure 4.20). These interactions are possible as 14-3-3 binding of non-phosphorylated motifs, and divergent phospho-Ser/Thr motifs have been reported to occur between 14-3-3 and several proteins (Yaffe, 2002).

To assess the role of AMPK activation on JAK1 phosphorylation in intact cells, WT and Ser515A/S518Ala mutated human JAK1 were transiently expressed in U4C cells prior to treatment with A769662 and preparation of cell extracts for pull down assays with GST-14-3-3ζ and immunoblotting with anti-JAK1 antibody (Figure 4.21B and 4.21C). These demonstrated that A769662 treatment increased 14-3-3ζ interaction with JAK1 but not Ser515A/S518Ala mutated JAK1 despite equivalent activation of AMPK and expression of WT and mutated JAK1 proteins in transfected cells (Figure 4.21B). Overall, these data demonstrate that pharmacological activation of AMPK promotes 14-3-3 binding of JAK1 *via* a mechanism requiring Ser515 and Ser518. The data shown in figure 4.21 was generated and analysed by Dr Claire Rutherford, University of Glasgow.

IL-6 induces phosphorylation of Tyr1022/1023 in the activation loop of the JAK1 kinase domain, which is required for catalytic activation of JAK1 (Liu, 1997). Recently, Nerstedt et al (2013) used the phospho-JAK1 Tyr1022/1023 antibody from Cell Signalling Technology (#3331) to investigate the effect of AMPK activation on IL-6 stimulation of JAK1 activation in the human hepatocellular carcinoma cell line (HepG2) (Nerstedt et al., 2013). It was demonstrated that AMPK agonists, AICAR and metformin significantly inhibited IL-6 stimulation of JAK1 Tyr1022/1023 phosphorylation and STAT3 Tyr705 phosphorylation (Nerstedt et al., 2013) . With exception of the work recently published by Nerstedt and co-workers (Nerstedt et al., 2013), there was no additional evidence in the literature regarding the effect of AMPK on JAK1 activity at the time of conducting this study.

It was hypothesised that AMPK inhibits sIL-6Rα/IL-6 stimulation of STAT3 Tyr705 phosphorylation by inhibiting tyrosine phosphorylation of its predominant upstream activator, JAK1. Confirmation of AMPK-mediated inhibition of IL-6 stimulated JAK1 tyrosine phosphorylation in HUVECs would suggest that this is the primary event which subsequently leads to inhibition of STAT3 Tyr705 phosphorylation and the data presented in this study would further suggest this was achieved by AMPK directly phosphorylating and presumably inhibiting JAK1 catalytic activation. However, it was not possible to successfully detect sIL-6Rα/IL-6 stimulated JAK1 Tyr1022/1023 phosphorylation in HUVECs using Santa Cruz or Invitrogen phospho-specific antibodies against these sites on JAK1. As can be seen in Figure 4.22, phospho-JAK1 antibody typically failed to detect phospho-JAK1 either after enrichment of JAK1 by immunoprecipitation or in whole cell extracts. Thus, it was not possible to deduce any information from these experiments. As an alternative approach to detect tyrosine phosphorylated JAK1, anti-phospho-tyrosine 4G10 monoclonal antibody was used to probe JAK1 immunoprecipitates. Probing with 4G10 can theoretically detect multiple phosphorylated Tyr residues in different contexts and is therefore not specific for JAK1 Tyr 1022/1023. HUVECs were pre-treated with AMPK activator A769662, followed by stimulation with sIL-6Rα/IL-6 and then whole-cell extracts were immunoprecipitated with total JAK1 antibody, followed by immunoblotting with anti-phospho-tyrosine antibody 4G10. In comparison to the basal levels of JAK1 tyrosine phosphorylation detected in unstimulated HUVECs, sIL-6Rα/IL-6 stimulation of HUVECs for 15 minutes slightly increased JAK1 tyrosine phosphorylation levels (Figure 4.24). Treatment of HUVECs with A769662 prior to sIL-6Rα/IL-6 stimulation for 15 minutes appears to slightly reduce JAK1 tyrosine phosphorylation (Figure 4.24). However, the changes of JAK tyrosine phosphorylation observed with sIL-6Rα/IL-6 and A769662 treatment were modest; it is possible that the high basal level of JAK1 tyrosine phosphorylation is masking the inhibitory effects of A769662 on phosphorylation of Tyr 1022/1023. These data indicate that AMPK activation can inhibit sIL-6Rα/IL-6 stimulation of JAK1 tyrosine phosphorylation. As an alternative way to use 4G10 to detect tyrosine phosphorylated JAK1, 4G10 antibody was used to immunoprecipitate tyrosine phosphorylated proteins from treated cells followed by SDS-PAGE and immunoblotting with total anti-JAK1 antibody. In comparison to probing JAK1 immunoprecipitates with 4G10 (Figure 4.24), this approach has substantially

reduced the basal levels of tyrosine phosphorylated JAK1 detected (Figure 4.26). As shown in Figure 4.26, sIL-6Rα/IL-6 stimulation of JAK1 tyrosine phosphorylation peaked at 5 minutes, but was still above basal levels at 30 minutes. Treatment of HUVECs with A769662 prior to sIL-6Rα/IL-6 stimulation for 5 minutes slightly reduced JAK1 tyrosine phosphorylation (Figure 4.26). Despite the low basal levels of JAK1 tyrosine phosphorylation, AMPK-mediated inhibition of JAK1 tyrosine phosphorylation remained modest. Furthermore, this effect seemed to be transient as it was not reproducibly detected at any of the later time points. Overall, these data indicate that inhibition of JAK1 tyrosine phosphorylation may not be the primary mechanism which subsequently leads to AMPK-mediated inhibition of STAT3 phosphorylation. AMPK may have no substantial effect on activation of JAK1 via tyrosine phosphorylation, but AMPK could still act via JAK1 to inhibit IL-6 signalling by interfering with the ability of JAK1 to interact and phosphorylate the GP130 receptor and /or STAT3.

Having demonstrated that AMPK phosphorylates a JAK1 peptide at both Ser515 and Ser518 *in vitro*, the next step was to investigate whether full-length JAK1 protein could be phosphorylated by AMPK *in vitro*. In a positive control experiment, *in vitro* AMPK phosphorylation of ACC purified from cell lysates confirmed that purified rat liver AMPK was catalytically active and phosphorylated full-length ACC Ser79 *in vitro* as detected by immunoblotting with phospho-ACC Ser79 antibody (Figure 4.27A). Subsequently FLAG-tagged JAK1 immunoprecipitates from cell lysates were subjected to *in vitro* AMPK reactions, however AMPK phosphorylation of JAK1 could not specifically be detected by incorporation of radiolabelled ^{32}P as phosphorylation of a 130 kDa protein, the same molecular weight as JAK1, was detected in both JAK1 -deficient and –enriched reactions (Figure 4.27B). Thus, [γ-^{32}P] ATP was not selective for the detection of AMPK phosphorylated JAK1, unless JAK1 can be immunoprecipitated without binding non-specific proteins, a phospho-JAK1 Ser515/518 antibody is required for probing the *in vitro* AMPK reactions. Currently, a phospho-JAK1 Ser515/518 antibody is not available. Once *in vitro* phosphorylation of full-length JAK1 was demonstrated, the next step was to conduct an *in vitro* AMPK phosphorylation of full-length S515A/S518A mutant JAK1 to demonstrate that alanine substitution of Ser515 and Ser518 abolishes AMPK phosphorylation of full-length JAK1. Overall, the investigation of whether full-length JAK1 could be phosphorylated by AMPK at Ser515 and Ser518 *in vitro* is

inconclusive as the method for immunoprecipitating JAK1 and detecting *in vitro* AMPK phosphorylation of full-length JAK1 requires further optimisation.

In order to establish JAK1 protein as a bona fide *in vitro* AMPK substrate and to determine the specific site(s) of phosphorylation in JAK1 as Ser515/Ser518, this study next sought to determine the stoichiometry of phosphorylation of Ser515/518 in JAK1 by AMPK *in vitro*. To determine this, human wild-type and S515A/S518A mutant JAK1 SH2 domain, and rat ACC1 residues 60-94 were bacterially expressed as GST fusion proteins and subjected to *in vitro* kinase assays using purified active rat liver AMPK, and [γ-^{32}P] ATP. Prior to stoichiometric analysis, phosphorylated proteins were visualised by autoradiography. As shown in Figure 4.31, this experiment demonstrated that catalytically active AMPK phosphorylates only the ACC portion of the GST fusion protein, while phosphorylation of WT GST JAK1 SH2 by active AMPK was not observed under *in vitro* conditions. GST-ACC was purified under native conditions (Figure 4.28B) whereas GST-JAK1 SH2 proteins were purified under denaturing conditions (Figure 4.30). Denaturing conditions were used to purify GST-JAK1 SH2 as the protein had become insoluble during bacterial expression (Figure 4.30). It is possible that AMPK may have not been able to phosphorylate WT GST-JAK1 SH2 protein as a result of the denaturing conditions of its purification. Denaturing and renaturing of GST-JAK1 SH2 proteins has likely misfolded the protein, which has hidden the phosphorylation sites, Ser515 and Ser518, from AMPK. The secondary structural composition of a purified protein can be used as an indicator of the folding state of a protein. This information can be obtained by performing circular dichroism (CD) spectroscopy (Kelly et al., 2005). Unfortunately, the GST-fusion proteins were not analysed by CD before the end of this project. Following visual confirmation of *in vitro* AMPK phosphorylation of WT and S515A/S518A mutant GST JAK1 SH2, and GST-ACC, phosphorylation for each GST fusion protein was to be measured by scintillation counting and the stoichiometry of phosphorylation calculated. It was predicted that AMPK phosphorylates WT GST-JAK1 SH2 and GST-ACC proteins, but not S515A/S518A GST JAK1 SH2 protein. The stoichiometry of phosphorylation of WT GST-JAK1 SH2 by AMPK would be similar to that of GST-ACC, suggesting that JAK1 SH2 protein is a good *in vitro* substrate of AMPK (Scott et al., 2002). Mutation of Ser515 and Ser518 with alanine would abolish the phosphorylation of GST-JAK1 SH2 by AMPK, suggesting that these sites are phosphorylated by AMPK *in vitro*.

Overall, this study has demonstrated that AMPK phosphorylates a JAK1 peptide at both Ser515 and Ser518 *in vitro*. Unfortunately, it remains undetermined whether AMPK phosphorylates full length JAK1 *in vitro*, and whether JAK1 is a bona fide *in vitro* AMPK substrate. *In vitro* phosphorylation assays were used for these experiments. However, this assay has limitations in that the phosphorylation *in vitro* may differ from what takes place physiologically. Thus, it is crucial that AMPK phosphorylation of JAK1 is confirmed *in situ* and most importantly *in vivo*.

Taken together, the key findings of this chapter suggest that active AMPK can directly phosphorylate two residues, Ser515 and Ser518, within the JAK1 SH2 domain. Pharmacological activation of AMPK promotes 14-3-3 binding of JAK1 *via* a mechanism requiring Ser515 and Ser518. Furthermore, mutation of Ser515 and Ser518 abolishes the ability of AMPK to inhibit JAK-STAT signalling by an IL-6 *trans*-signalling complex and from a constitutively active Val658Phe-mutated JAK1.

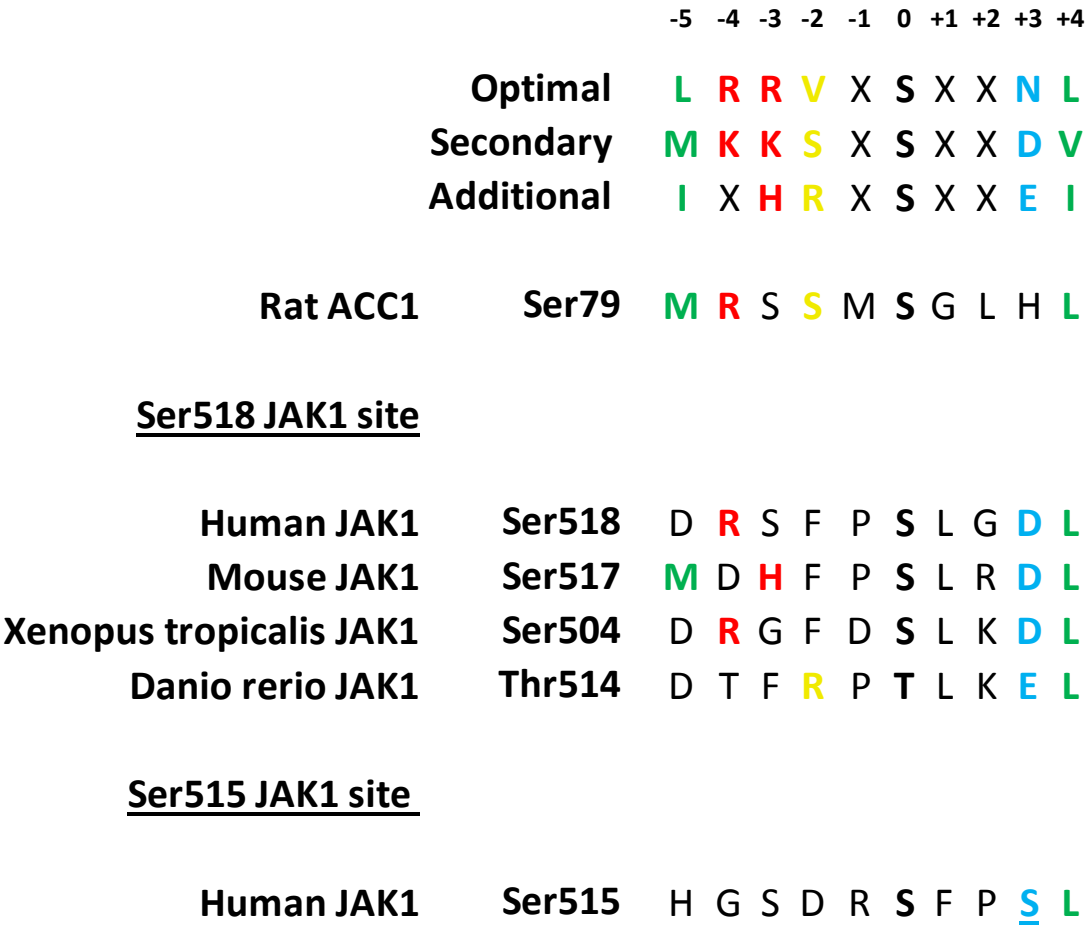

Figure 4.32: Alignment of *in vitro* AMPK phosphorylation sites Ser515 and Ser518 in JAK1 with the AMPK optimal phosphorylation motifs

(A) Optimal and secondary selections for AMPK substrate recognition taken from Gwinn et al., 2008. AMPK phosphorylates Ser/Thr residues (indicated in bold) in the context of hydrophobic residues (green) at P-5 and P+4, basic residues (red) at P-4, P-3, or both, and polar or negatively charged residues (blue) at P+3. Strong selection for either Val (V), Arg (R) or Ser (S) (yellow) at P-2 was also noted. The sequence from rat ACC1 known to be phosphorylated by AMPK at Ser79 is shown for comparison (Davies et al., 1992) The conformity of the sequence surrounding Ser518 on human JAK1 to the AMPK consensus, and its evolutionary conservation, are shown. The sequence surrounding the Ser515 site on human JAK1 is also shown. The underlined Ser residue (equivalent to Ser518) indicates that this sequence would potentially conform to a weak AMPK consensus site following the acquisition of negative charge upon its phosphorylation.

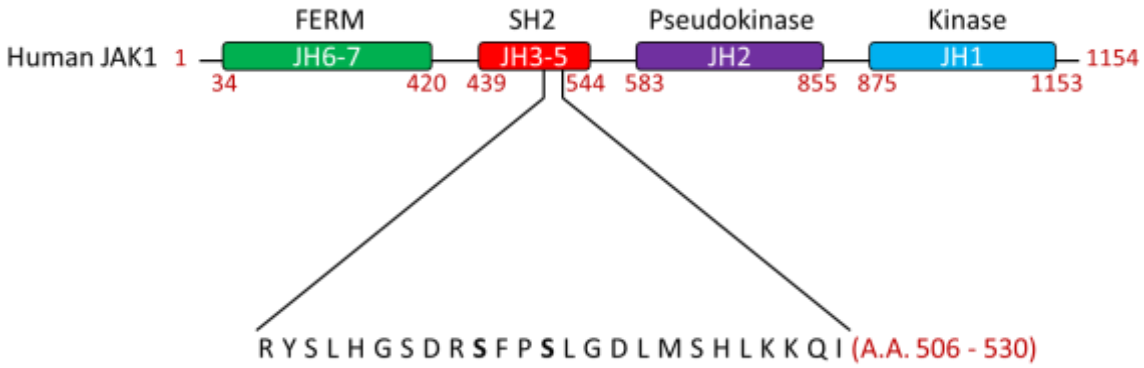

Figure 4.33: *In vitro* AMPK phosphorylation sites Ser515 and Ser518 are found within the SH2 domain of human JAK1

(A) A schematic representation of the primary structure of JAK1. JAKs consist of a FERM, SH2, pseudokinase and kinase domains. An alternative nomenclature for the putative domains is a series of Janus homology (JH) domains (Yamaoka et al., 2004). The location of the JAK1 25-mer peptide phosphorylated *in vitro* by AMPK is indicated. Ser515 and Ser518 (indicated in bold) are shown to be found in the JAK1 SH2 domain.

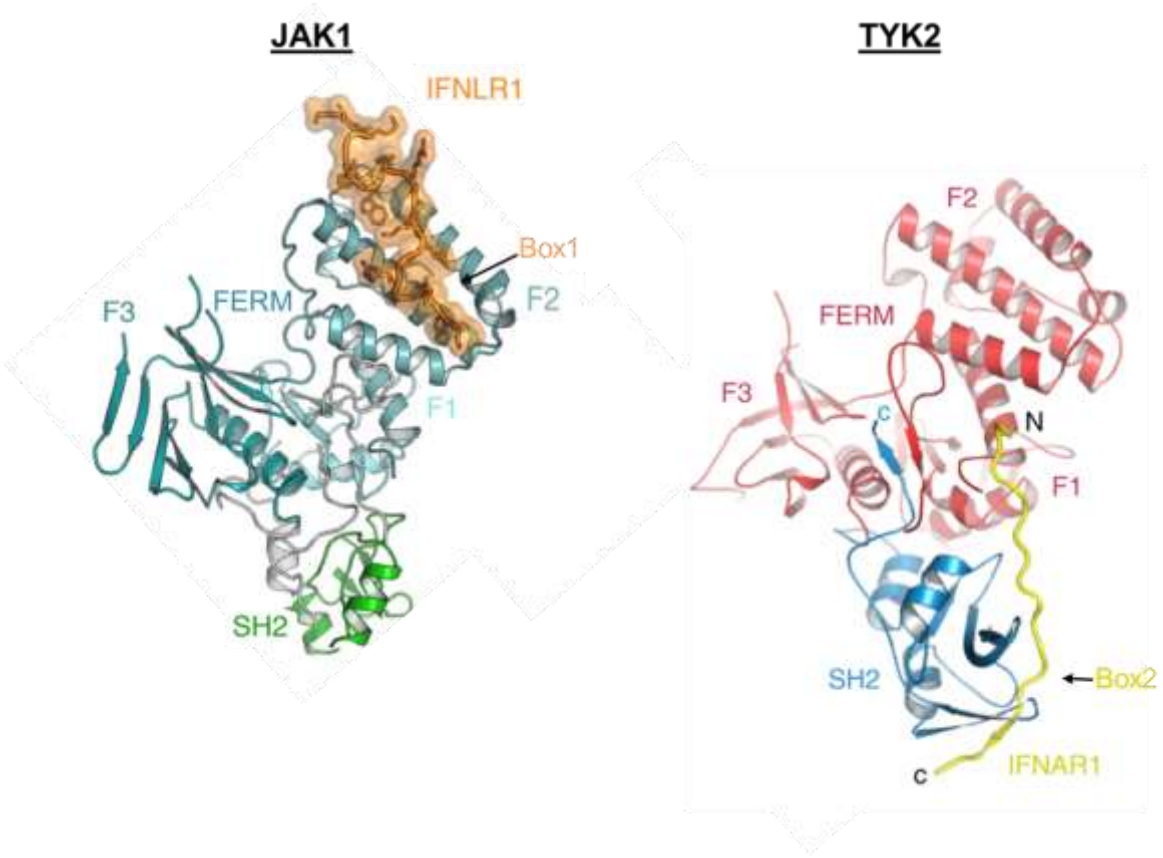

Figure 4.34: JAK interacts with cytokine receptor box1 and box2 motifs via distinct binding sites

Cartoon representation of JAK1 FERM-SH2 domain bound to the box1 motif of IFNLR1 is shown on the left (adapted from Ferrao et al., 2016) and TYK2 FERM-SH2 domain bound to the box2 motif of IFNAR1 is shown on the right (adapted from Wallweber et al., 2014) The cytokine receptor fragment (IFNLR1 box1 or IFNAR1 box2), FERM subdomains (F1, F2, and F3) and SH2 domain are indicated. The box1 (orange) interaction is mediated by the FERM F2 subdomain (teal) and box2 (yellow) binding is primarily mediated by the SH2 domain (blue).

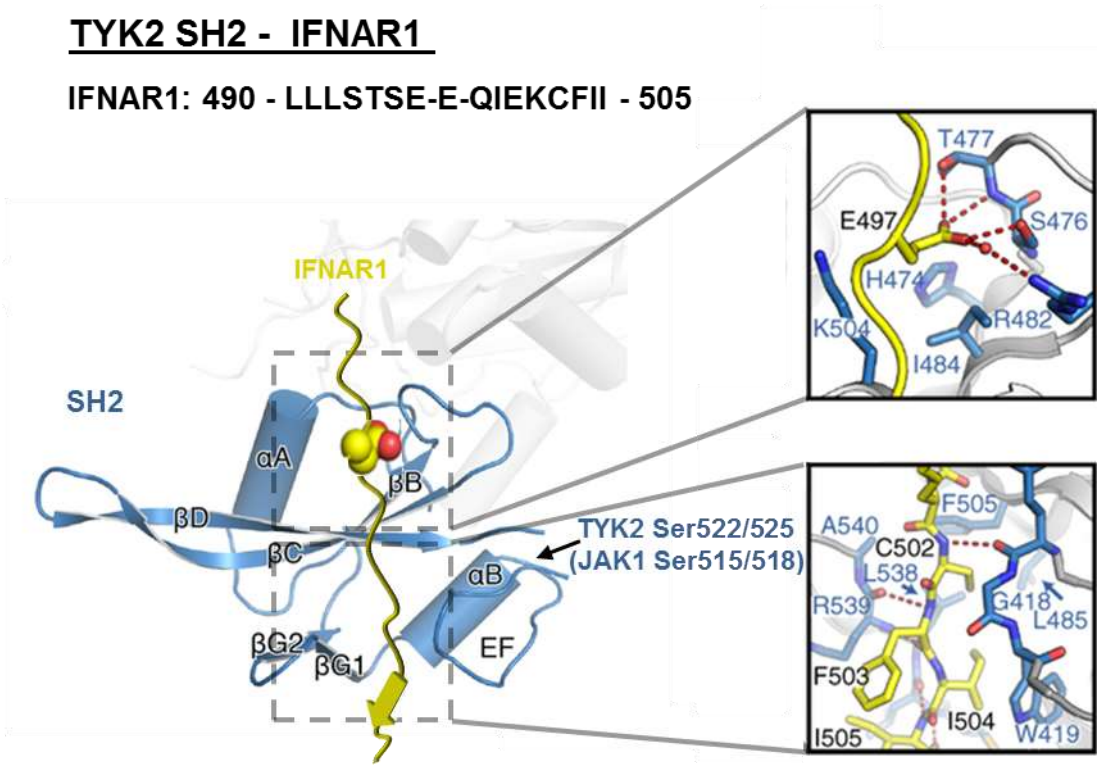

Figure 4.35: TYK2 Ser522/Ser525, analogous to JAK1 Ser515/Ser518, lie beside the receptor box2 binding site.
Cartoon representation of TYK2 SH2 domain (blue), annotated with secondary structure elements, bound to the box2 motif of IFNAR1 (yellow) is shown on the left. Detailed views of the IFNAR1 E497 (top panel) and hydrophobic box2 segment interactions (bottom panel) with TYK2 SH2 are shown on the right. Key residues are shown as stick models, and polar contacts are shown as dashed lines (adapted from Wallweber et al., 2014). IFNAR1 E497 interacts with the TYK2 SH2 domain *via* polar contacts with TYK2 S476 and T477, and a water-mediated hydrogen bond with TYK2 R482 (top panel). The hydrophobic box2 segment of IFNAR1, starting five residues C-terminal to E497 at C502, lies in a hydrophobic groove formed by the βG1 strand and EF loop of the SH2 domain. C502, F503 and I504 form a short β-sheet with the βG1 strand (bottom panel). TYK2 Ser522/525, analogous to JAK1 Ser515/518, are C-terminal residues of the EF loop preceding the αB helix, which is followed by the βG1 strand.

Chapter 5 - Final Discussion

Preliminary investigations of the effects of AMPK on JAK-STAT signalling demonstrated that AMPK can rapidly and profoundly inhibit activation of the JAK-STAT pathway in response to multiple stimuli in vascular endothelial cells and in the current study the underlying molecular mechanism of this phenomenon was investigated. The current study has demonstrated that active AMPK can directly phosphorylate two residues, Ser515 and Ser518, within the JAK1 SH2 domain. Furthermore, mutation of Ser515 and Ser518 abolishes the ability of AMPK to inhibit JAK-STAT signalling by an IL-6 trans-signalling complex and from a constitutively active Val658Phe-mutated JAK1.

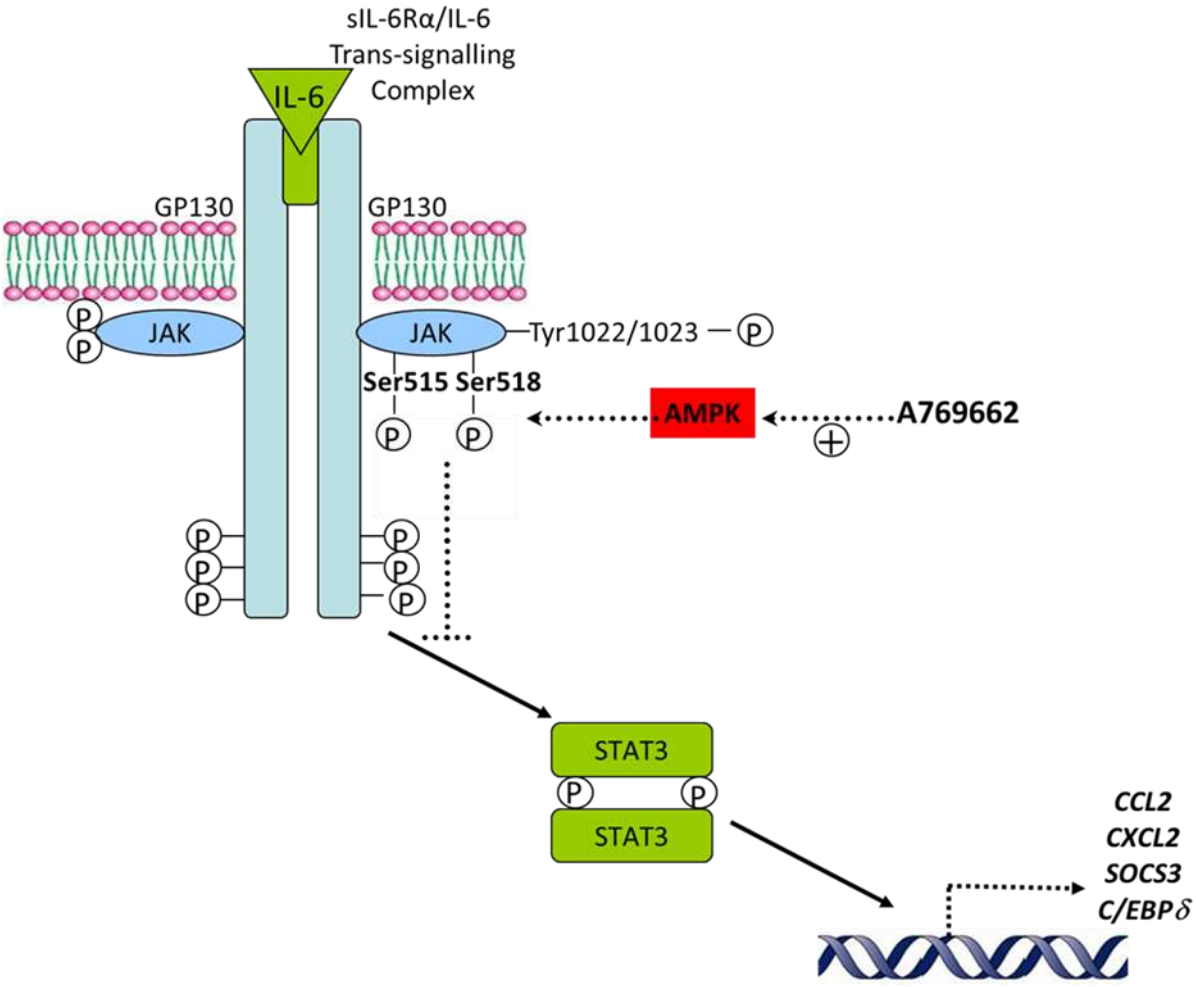

Figure 5.1: A schematic model of AMPK-mediated inhibition of IL-6 signalling via JAK1. Active AMPK directly phosphorylate two residues, Ser515 and Ser518, within the JAK1 SH2 domain to inhibit JAK-STAT signalling by an IL-6 trans-signalling complex. Figure adapted from Rutherford et al., 2012

During the course of this study, only a small number of groups have reported an AMPK-mediated reduction in IL-6-stimulated STAT3 phosphorylation (Nerstedt et al., 2010, Kim et al., 2012, Nerstedt et al., 2013, Cansby et al., 2014). However, these studies were conducted in either liver-derived HepG2 hepatocellular carcinoma cells or primary hepatocytes. In contrast to endothelial cells, and indeed the majority of cells, hepatocytes do not require the presence of a soluble IL-6 receptor as IL-6 elicits its effects via binding a membrane-bound IL-6 receptor complexed with the co-receptor gp130 (classical signalling) (Rose-John, 2012). Work in the current study demonstrated that A769662-mediated AMPK activation inhibited STAT3 Tyr705 phosphorylation stimulated by a sIL-6Rα/IL-6 trans-signalling complex in HUVECs. This finding was corroborated in adipocytes by our colleagues who demonstrated that A769662 inhibited sIL-6Rα/IL-6 stimulated STAT3 Tyr705 phosphorylation in 3T3-L1 adipocytes (Mancini et al., 2017). Kim et al (2012) and Nerstedt et al (2013) also investigated the molecular mechanism(s) underlying AMPK-mediated inhibition of IL-6 signalling in liver cells. Kim and co-workers suggested that the mechanism by which long-term AMPK activation may suppress IL-6 signalling in the liver is via induction of the orphan nuclear receptor small heterodimer partner (SHP) (Kim et al., 2012). It was shown that chronic AMPK activation in hepatocytes with metformin for 12 hours can increase levels of SHP which can interact with the DNA binding domain of STAT3, thereby blocking its recruitment to target gene promoters such as the SOCS3 promoter following IL-6 stimulation. However, this mechanism does not clarify the AMPK-mediated inhibition of STAT3 phosphorylation because SHP could interact with both phospho-STAT3 and STAT3 (Kim et al., 2012). Nerstedt and co-workers reported that chronic AMPK activation in hepatocytes with AICAR inhibits IL-6 signalling by suppressing IL-6 stimulated phosphorylation of Tyr1022/1023 of JAK1 and its downstream targets STAT3 and SHP2. It was proposed that the reduction in phosphorylation of key sites (Tyr1022/1023) regulating the activity of JAK1 is the primary event which subsequently leads to inhibition of phosphorylation of its downstream targets SHP2 and STAT3 (Nerstedt et al., 2013). In the current study, acute AMPK activation in endothelial cells with A769662 inhibited JAK1 tyrosine phosphorylation only slightly and was not statistically significant (Figure 4.24 and 4.26). Finally, He and co-workers reported during the course of writing this thesis that AICAR activated AMPK inhibits both IFN-γ and angiotensin (Ang)-II stimulation of STAT1 Tyr701 phosphorylation in human aortic smooth muscle cells (HASMCs) (He et al., 2015).

Furthermore, activated AMPK diminished Ang-II-induced production of IL-6 and MCP-1 (He et al., 2015). Mechanistically, it was shown that chronic AMPK activation in HASMCs with AICAR for 4 hours can enhance mitogen-activated protein kinase phosphatase-1 (MKP-1) protein levels and siRNA-mediated knockdown of MKP-1 prevented AICAR-reduced STAT1 phosphorylation. (He et al., 2015). MKP-1 is a dual specificity phosphatase that dephosphorylates phospho-Ser/Thr and phospho-Tyr residues within the same substrate (Sun et al., 1993). MKP-1 has previously been shown to be involved in dephosphorylation of Ang-II-activated STAT1, but not in the dephosphorylation of STAT3 (Venema et al., 1998, Liang et al., 1999). In contrast, the current study proposes that acute activation of AMPK directly phosphorylates JAK1 to rapidly inhibit JAK-STAT signalling by an IL-6 trans-signalling complex. The existence of several inhibitory mechanisms by which AMPK can suppress JAK-STAT signalling mirrors the multifaceted impact of AMPK on the mTOR signalling pathway, which it inhibits through direct phosphorylation of two components TSC2 on Ser1387 and Raptor on Ser722 and Ser792 (Inoki et al., 2003, Shaw et al., 2004, Gwinn et al., 2008). These observations suggest that, like the mTOR pathway, AMPK-mediated regulation of JAK-STAT signalling has also evolved, such that multiple mechanisms and targets are used to limit its activation.

As discussed in Chapter 1 (1.3.6), a number of studies have described the critical role of IL-6 and STAT1/STAT3 signalling in regulating key processes in atherosclerosis and that interfering with the IL-6 and STAT1/STAT3 signalling *in vivo* prevents atherosclerotic lesion formation. As described (section 6.1), preliminary investigations demonstrated that activation of AMPK in HUVECs reduced sIL-6Rα/IL-6 induction of STAT3 target genes and STAT3-mediated monocyte chemotaxis (Figure 6.3 and 6.4). Similarly, He and co-workers demonstrated that activated AMPK reduced Ang-II induction of STAT1 target genes, including MCP-1, in HASMCs (He et al., 2015). Utilising AMPKα2 knockout mice, He and co-workers investigated the role of AMPK in the suppression of vascular inflammation and for the first time investigated whether AMPK suppresses inflammation through inhibition of STAT1 signalling *in vivo* (He et al., 2015). Compared to WT mouse aortas, deletion of AMPKα2 increased the expression of pro-inflammatory mediators and amplified Ang-II induction of these mediators (He et al., 2015). Administration of a STAT1 inhibitor, fludarabine, attenuated the

expression of pro-inflammatory mediators in AMPKα2 knockout mice in the absence and presence of Ang-II infusion (He et al., 2015). He and co-workers propose that AMPK suppression activates STAT1 signalling, resulting in aberrant inflammation in the vasculature and establishing an essential role for AMPK in promoting an anti-inflammatory phenotype that is vital for protection against the formation of atherosclerotic lesions (He et al., 2015). Taken together with the current study, these findings suggest that AMPK-mediated phosphorylation of JAK1 may be a valid pharmacological target for the prevention and treatment of vascular inflammation. Importantly, preliminary investigations demonstrated that sIL-6Rα/IL-6 stimulation of STAT3 Tyr705 phosphorylation was significantly inhibited in HUVECs pre-treated with a combination of clinically utilized AMPK activators metformin and salicylate (the active metabolite of aspirin) (Figure 6.1). Overall, these findings provide a mechanistic rationale for the clinical evaluation of AMPK activators such as metformin or salicylate, as a potential therapeutic agent in the prevention and treatment of vascular inflammation, which could slow down the process of atherosclerosis and therefore decrease the incidence of cardiovascular events.

In patients with type 2 diabetes, several observational studies have reported that treatment with metformin limits cardiovascular morbidity and mortality independent from its glucose-lowering action (Holman et al., 2008, Johnson et al., 2005, Mellbin et al., 2011, Roussel et al., 2010). This finding has led researchers to investigate whether metformin might potentially improve cardiovascular outcome in non-diabetic patients at risk for CVD. However, small short-term randomized controlled trials in non-diabetic patients suffering from coronary heart disease showed that treatment with metformin on top of optimal statin therapy did not improve cardiovascular risk profile or intima-media thickness (Lexis et al., 2015, Preiss et al., 2014). Further large long-term randomised controlled clinical trials of metformin monotherapy are necessary to definitively conclude about the cardiovascular protective effects of metformin treatment in non-diabetic CVD. With interest, we await the results of ongoing Glucose Lowering In Non-diabetic hyperglycaemia Trial (GLINT; ISRCTN34875079), in which 12 000 patients with high cardiovascular risk and dysglycaemia but without diabetes, will be assigned to metformin or placebo for 5 years. Until then, the role of metformin for improving cardiovascular outcomes in non-diabetic

patients has promise, but is still largely unproven. Aspirin is an acetylated form of salicylate, which is rapidly broken down to salicylate within the bloodstream (Higgs et al., 1987). Aspirin is well recognized as an effective anti-platelet drug for secondary prevention in patients at high risk of cardiovascular events (Hennekens and Dalen, 2013). The mechanism of this treatment is through the transfer of aspirin's acetyl group to a serine side chain at the cyclo-oxygenase (COX) active site which irreversibly inhibits the COX1 and COX2 enzymes and subsequently inhibit blood clotting caused by platelets (Vane et al., 1998). Interestingly, it has recently been shown that salicylate directly activates AMPK in a mechanism similar to A-769662 (Hawley et al., 2012), therefore activation of AMPK by salicylate may provide another mechanism in which aspirin is able to treat CVD. However, it remains to be fully determined whether the cardiovascular protective effects are directed through AMPK and also to what extent. The widespread use of metformin and salicylate suggests that AMPK-activating drugs could be relatively safe for the long-term management of chronic inflammatory conditions such as atherosclerosis. Given that metformin (indirect) and salicylate (direct) activate AMPK via distinct mechanisms (Hawley et al., 2012), the preliminary data suggests that metformin and salicylate may exert vascular protection through synergistic activation of AMPK-mediated inhibition of JAK-STAT signalling (Figure 6.1). However, future work is required to determine whether this inhibitory effect is evident at low doses as a very high dose of salicylate was used to treat HUVECs in these experiments and prolonged exposure to such high doses of aspirin used would have unacceptable side effects, especially potentially serious gastrointestinal bleeding. Interestingly, lower (clinically-relevant) doses of metformin and salicylate synergistically activate AMPK to inhibit lipogenesis in primary hepatocytes from mice and humans (Ford et al., 2015).

Despite numerous reports suggesting that AMPK activators may be beneficial for the treatment of cardiovascular disease and a number of human pathologies (Hardie, 2014), no direct AMPK activators have reached clinical use. Therefore, it remains unknown whether a safe AMPK activator can be developed. While the AMPK subunits (α,ß,γ) are expressed more or less ubiquitously and the AMPK heterotrimeric complex can come in twelve different possible combinations, the individual AMPK subunit isoform in humans and mice display considerable variation in tissue-specific expression and subcellular localisation (Ross et al., 2016). Thus,

the development of tissue-selective AMPK activators could offer a safety advantage. The discovery that A769662 could selectively target ß1-containing AMPK complexes revealed that it may be feasible to design AMPK activators that are targeted to specific tissues, such as the vasculature, by exploiting tissue-specific variation of subunit isoforms (Scott et al., 2008). Compound 2 ([C2] [5-(5-hydroxyl-isoxazol-3-yl)-furan-2-phosphonic acid]) is another allosteric AMPK activator and activates AMPK by binding to the γ subunit Gómez-Galeno et al., 2010, Hunter et al., 2014). C2 is an AMP-mimetic compound similar to AICAR (Gómez-Galeno et al., 2010, Hunter et al., 2014). Importantly, a crystal structure of the C2: AMPK complex revealed that the two C2-binding sites in the γ-subunit are distinct from nucleotide sites (Langendorf et al., 2016). Numerous small molecule direct AMPK activators have been identified from high throughput screens such as PF-06409577 (Cameron et al., 2016) and from studies investigating alternatives to the thienopyridone core in A769662 such as pyrrolopyridone derivatives (Mirguet et al., 2013) (reviewed by Cameron and Kurumbail, 2016). Crystallographic studies will provide insight into the molecular mechanism and site of action of these compounds. This knowledge provides a strong foundation for the design and development of isoform-selective AMPK activator.

Atherosclerosis is primarily a disease of large conduit arteries and is initiated when cardiovascular risk factors through chemical, mechanical or immunological insult activate the endothelium. HUVECs are vein ECs derived from immune-privileged foetal tissue (Jaffe et al., 1973). Therefore, a limitation in the current study is that the effects of AMPK on IL-6 signalling have only been studied in HUVECs. Preferentially, human arterial ECs isolated from the coronary artery or aorta would have been used for *in vitro* studies. Unfortunately, the availability of these tissues are limited, however human saphenous vein ECs (HSVEC) are more widely available. HSVECs were shown to be more functionally similar to arterial ECs than HUVECs (Tan et al., 2004). Therefore, future work is required to confirm AMPK-mediated inhibition of IL-6 signalling in HSVECs. Following these experiments, the effects of pharmacological AMPK activation on the development on atherosclerotic lesions and p-STAT3/1 levels in atherosclerotic prone mice are examined. These studies would also focus on determining whether AMPK-mediated phosphorylation of JAK1 or JAK2 is the molecular mechanism underlying AMPK-mediated inhibition of IL-6 signalling *in situ* and *in vivo*. A key tool for this work would be the

generation of phospho-specific antibodies against JAK1 Ser515/518 and JAK2 Ser473 phosphorylation sites and use of these antibodies in immunoblotting, immunoprecipitation and immunohistochemistry applications. Mass spectrometry is another method that could be used to detect AMPK phosphorylation sites in each JAK isoform.

In addition to atherosclerosis, aberrant activation of the JAK-STAT pathway has been reported in a variety of disease states, including autoimmune disease and haematological malignancies (Grote et al., 2005, Thomas et al., 2015, Banerjee et al., 2017). Therefore, the findings of the current study provide a mechanistic rationale for potential repurposing of AMPK activators such as metformin for the management and/or treatment of these diseases. Rheumatoid arthritis (RA), acute lymphoblastic leukaemia (ALL), and myeloproliferative neoplasms (MPNs) are associated with aberrant JAK-STAT signalling and are discussed below. For each disease: the pathological role of JAK-STAT signalling and the future work required to investigate the therapeutic potential of AMPK activators is discussed.

ALL is an aggressive haematological malignancy characterised by the uncontrolled proliferation of lymphoid progenitor cells and classified into B-cell ALL (B-ALL) and T-cell ALL (T-ALL) (Chiaretti et al., 2014). ALL is the most common paediatric cancer, accounting for 26% of all cancer cases in children (Siegel et al, 2015, Siegel et al., 2012). Although T-ALL accounts for only 15% of paediatric ALL cases, T-ALL is generally more clinically aggressive than B-ALL (Chiaretti et al., 2014, You et al., 2015). Currently, patients with ALL receive an intensive combination of cytotoxic chemotherapies and long-term survival in paediatric ALL is currently 85-90% (Schmiegelow et al., 2010, Hunger et al., 2012). However, chemotherapies often induce long-term side-effects, resulting in impairment of vital physiological functions among the survivors (Sioka and Kyritsis, 2009, Krishnan and Rajasekaran, 2014). 20-25% of children with T-ALL experience relapse and are often resistant to further chemotherapy and the outcome at this point is much worse (Nguyen et al., 2008). For patients who relapse allogeneic haematopoietic stem cell transplant (HSCT) therapy is also an option. However, HSCT is associated with high risks of treatment failure and treatment-related mortality (Gupta et al., 2012). The current therapeutic strategy to overcome the long-term side effects and relapse/resistance associated with chemotherapies is to specifically target the

aberrantly activated signalling pathways driving proliferation and survival of cells. Therefore, in order to identify therapeutic targets research has focused on characterising aberrations and molecular signatures of haematological malignancies. Aberrant JAK-STAT signalling is implicated in the pathogenesis of haematological malignancies including MPNs, acute myeloid leukaemia (AML) and ALL (Springuel et al., 2015). Activating mutations of JAK1 have been identified in 6-27% of cases of T-ALL and less frequently in B-ALL (1.5%) (Flex et al., 2008, Jeong et al., 2008, Mullighan et al., 2009, Zhang et al., 2012) The V658F mutation in JAK1 has been identified in T-ALL patients (Jeong et al., 2008, Mullighan et al., 2009). The V658F JAK1 mutation drives the ligand-independent activation of STAT molecules and transformation of Ba/F3 pro-B cells (Hornakova et al., 2011). Therefore, V658F JAK1 is an attractive therapeutic target for treating T-ALL. The current study demonstrated that pharmacological activation of AMPK inhibits constitutively active V658F-mutated JAK1 mediated phosphorylation of STATs via a mechanism requiring Ser515/Ser518 in the SH2 domain (Figure 4.19). Overall, our findings provide a mechanistic rationale for the clinical evaluation of AMPK activators such as metformin, as potential treatment options for ALL associated with constitutive JAK1 signalling. Metformin has previously been investigated as a candidate to target T-ALL through AMPK-mediated inhibition of mTOR (Grimaldi et al., 2012). About 85% of T-ALL patient's display increased PI3K/mTOR activation, and this has a negative prognostic impact (Silva et al., 2008, Cardoso et al., 2009, Jotta et al., 2010). Grimaldi and co-workers demonstrated that metformin activates AMPK in T-ALL cells, leading to mTOR inhibition and induced apoptotic cell death (Grimaldi et al., 2012). Taken together with the current study, these findings suggest that AMPK activators would be most effective in treating T-ALL cases that depend on activation of JAK-STAT and PI3K/mTOR pathways for their proliferation and survival. Overall, these findings provide a strong rationale for the development of AMPK agonists as novel therapeutic agents for T-ALL patients. There is currently a clinical trial recruiting paediatric patients with relapsed ALL for treatment with a combination of metformin and chemotherapy (NCT01324180). Future work would focus on determining whether AMPK activators exert anti-leukemic effects on T-ALL cells and confirming that these effects are via AMPK-mediated inhibition of JAK-STAT signalling. Initial experiments would utilise the BaF3 cells, an IL-3 dependent murine pro B cell line. Previously, it has been confirmed that BaF3 cells transduced with retroviral constructs expressing

V658F JAK1 mutant resulted in constitutive JAK-STAT activation and promoted autonomous cell proliferation (Hornakova et al., 2011). Furthermore, treatment with ruxolitinib (JAK 1/2 inhibitor) completely blocked phosphorylation of JAK1 and STAT5, and autonomous cell proliferation (Hornakova et al., 2011). Therefore, BaF3 cells transduced with V658F JAK1 mutant or V658F/S515A/S518A JAK1 mutant could be used to determine the effects of a panel of AMPK activators on constitutive JAK-STAT signalling and autonomous cell proliferation versus JAK inhibitors. Following these experiments, the therapeutic efficacy of AMPK activators would be tested in T-ALL cell lines and T-ALL primary cells with JAK genomic lesions. Finally, the *in vivo* efficacy of AMPK activators would assessed in murine xenograft models of T-ALL derived from primary human T-ALL samples with JAK genomic lesions. This *in vivo* model will be used to evaluate whether AMPK activators are tolerated, can decrease leukemic burden and prolong survival.

MPNs are a group of haematological malignancies characterised by the uncontrolled proliferation of myeloid progenitor cells such as platelets, erythrocytes, and neutrophils. Aberrant JAK2 signalling plays a key role in the pathogenesis of MPNs. V617F JAK2, which is a mutation analogous to the T-ALL-associated V658F JAK1, is frequently found in patients with classical MPNs: polycythemia vera (PV) (>95%), essential thrombocythemia (ET) (~50%), and primary myelofibrosis (PMF) (~50%) (Baxter et al., 2005, James et al., 2005, Kralovics et al., 2005, Levine et al., 2005). In the current study the effects of AMPK activation on signalling downstream of an endogenous ligand activated JAK2 or a constitutively active V617F mutant JAK2 were not examined. During the completion of this thesis, Kawashima and Kirito reported that metformin treatment of V617F JAK2 positive MPN cell lines induced AMPK activation, leading to decreased levels of STAT5 phosphorylation and induction of apoptotic cell death (Kawashima and Kirito, 2016). In the current study, AMPK was shown to phosphorylate SH2 domain-derived peptides from JAK1 and JAK2 but not JAK3 or Tyk2, and alignment of the primary sequences of JAK1 and JAK2 revealed that Ser473 in JAK2 aligns with Ser518 in JAK1 (Figure 4.11). Taken together, these findings suggest that pharmacological activation of AMPK inhibits constitutively active V617F-mutated JAK2 mediated phosphorylation of STATs via a mechanism requiring Ser473 in the SH2 domain. Therefore, clinical studies evaluating AMPK activators as potential treatment options for T-ALL should be expanded to include

MPNs associated with V617F JAK2. The effectiveness of targeting JAK-STAT signalling has been demonstrated in in patients with myelofibrosis. In 2011, ruxolitinib, a ATP-competitive JAK1/2 inhibitor, was approved by the U.S. Food and Drug Administration (FDA) for the treatment of intermediate/high-risk MF based on the results of two phase III clinical trials for myelofibrosis (COMFORT-I [Verstovsek et al., 2012] and COMFORT-II [Harrison et al., 2012]). Although treatment with ruxolitinib alleviated splenomegaly and other symptoms of MF, allele burden of the V617F JAK2 mutant clone was only minimally decreased (Cervantes et al., 2013, Verstovsek et al., 2013). These observations have prompted efforts to devise combinatorial treatment strategies to improve and extend the benefits of ruxolitinib therapy. Disease-related complications affecting survival in MPN include thrombohaemorrhagic events and disease transformation into AML (Tefferi and Barbuie, 2015). PV and ET are considered relatively benign diseases and thrombohaemorrhagic events are the main cause of morbidity and mortality in patients (Tefferi and Barbuie, 2015). Therefore, these patients require a treatment strategy mainly aimed at preventing thrombotic and bleeding complications. Currently, patients are managed with phlebotomy (PV patients only), lose dose aspirin for its inhibitory effects on platelet function and thrombus formation, and cytoreduction with either hydroxyurea or IFN-α (Tefferi and Barbuie, 2015). New treatment options are urgently required for those patients not adequately managed by current treatments. However, the pathogenesis of thrombosis and dysfunctional haemostasis in MPNs remains elusive. A recent study reported that a subpopulation of MPN patients express V617F JAK2 in ECs (Teofili et al., 2011). Following this report, Etheridge and co-workers utilised mouse models expressing V617F JAK2 specifically in ECs or haematopoietic cells to determine which cells contribute to thrombohaemorrhagic events in MPNs (Etheridge et al., 2014). Mice expressing V617F JAK2 in both endothelial and haematopoietic cells developed a MPN phenotype and these mice showed severely attenuated thrombosis following injury. Restricting V617F JAK2 expression to ECs or haematopoietic cells revealed that both cell types contribute to attenuated thrombosis (Etheridge et al., 2014). Overall, Etheridge and co-workers have identified endothelial cells expressing V617F JAK2 as a potential new cellular target for MPN therapies. Furthermore, the study proposes that the expression of V617F JAK2 in both haematopoietic and endothelial compartments contributes to the bleeding phenotype via dysregulation of von Willebrand factor (a pro-

thrombotic molecule) (Etheridge et al., 2014). Taken together with the current study, these finding suggest AMPK activators could be a new treatment option to manage clotting defects in MPN patients. Thus, in addition to the evaluating the potential anti-proliferative effects of AMPK activators on V617F JAK2 MPNs, the anti-haemorrhagic potential of AMPK activators should also be evaluated in V617F JAK2 positive -MPNs and -endothelial cells. Future work would focus on investigating of anti-haemorrhagic potential of AMPK activators on V617F JAK2 ECs. Lin et al., demonstrated that primary lung V617F JAK2 ECs, isolated from mice expressing V617F JAK2 in both endothelial and haematopoietic cells, proliferated to a greater extent than WT JAK2 ECs (Lin et al., 2016), which was consistent with a previous report on lentiviral-transduced V617F JAK2 HUVECs (Kilani et al., 2014). Therefore, HUVECs transduced with V617F JAK2 or V617F/S473A JAK2 could be used to determine the effects of a panel of AMPK activators on constitutive JAK-STAT signalling and V617F JAK2-mediated cell proliferation versus JAK inhibitors. This experiment would also determine whether Ser473 is required for AMPK-mediated inhibition of constitutively active V617F JAK2 signalling. The endothelium is a primary source of many of the major haemostatic regulatory molecules such as prothrombotic molecules vWF and factor VIII, and antiplatelet molecules prostacyclins and nitric oxide (Verhamme and Hoylaerts, 2006). The expression and secretion of these molecules should be examined in V617F JAK2 ECs treated with or without AMPK activators. Utilising the mouse models expressing V617F JAK2 specifically in ECs, haematopoietic cells, or both compartments (as described by Etheridge et al., 2014), to examine the ability of AMPK activators to prevent dysfunctional haemostasis in these models.

RA is a common autoimmune disease characterised by synovial inflammation and hyperplasia, autoantibody production such as rheumatoid factor and anti-citrullinated protein antibody, cartilage and bone destruction, and systemic features, including cardiovascular, pulmonary, psychological, and skeletal disorders (McInnes and Schett, 2011). Although the etiology of RA is not fully understood, evidence suggests that autoimmunity to citrullinated epitopes predominantly present on matrix proteins plays a central role in the pathology of RA (Wegner et al., 2010). In addition, evidence suggests that IL-6 plays a crucial role in RA pathogenesis, as elevated levels of IL-6 in RA patients' sera and synovial fluid correlate with high disease activity (Madhok et al., 1993). While IL-6 may

perpetuate the inflammatory and degenerative process by inducing the hepatic acute-phase response, directly activating different cells such as B and T lymphocytes, macrophages and osteoclasts, promoting the infiltration of inflammatory cells and production matrix metalloproteinases, it may also play a role in the initiation stage of RA (Srirangan and Choy, 2010). The pathogenic potential of IL-6-STAT3 signalling in initiating RA is illustrated by findings demonstrating that activation of this pathway in CD4 + T cells predicts development of RA in a cohort of undifferentiated early arthritis (Pratt et al., 2012). Interestingly, IL-6-mediated STAT-3 signalling in CD4 + T cells was most prominent in in patients with anti-citrullinated peptide antibody-negative RA (Pratt et al., 2012). Furthermore, using CD4 + T cells isolated from the peripheral blood and synovial fluid of RA patients, Ju et al showed that siRNA mediated knockdown of STAT3 in these cells prevented T helper type 17 (Th17) differentiation but increased the proportion of regulatory T cells (Tregs) (Ju et al., 2012). Evidence suggests that keeping an adequate balance between pathogenic Th17 cells and protective Tregs is critical for preventing the development of RA and IL-6 has been considered a key cytokine that shifts the Th17/Treg balance the toward the pro-inflammatory Th17 phenotype (Pesce et al., 2012, Nistala and Wedderburn, 2009, Bettelli et al., 2006). Therefore, agents targeting IL-6 signalling have attracted significant attention as a promising agent in RA prevention and treatment. The central role of IL-6 in RA pathogenesis has been confirmed by successful therapeutic blockade of membrane and soluble interleukin-6 receptor in RA patients with a humanized anti-IL-6R antibody (tocilizumab) (Mihara et al., 2005, Garnero et al., 2010, Kremer et al., 2011). Most recently, tofacitinib, a ATP-competitive JAK1/3 inhibitor, was approved by the US FDA for RA treatment of patients who are intolerant/resistant to first line therapies such as methotrexate (reviewed by Nakayamada et al., 2016). The current study demonstrated that pharmacological activation of AMPK inhibits sIL-6Rα/IL-6 stimulation of the JAK-STAT pathway via a mechanism requiring Ser515/Ser518 in the JAK1 SH2 domain. Therefore, our findings provide a mechanistic rationale for the clinical evaluation of AMPK activators such as metformin, as a potential treatment option for the management of RA. In fact, a small number of studies have already shown that AMPK activators, metformin and A769662, suppressed inflammatory arthritis in murine models of RA (Kang et al., 2013, Son et al., 2014, Guma et al., 2015). Interestingly, Kang and co-workers

demonstrated that metformin inhibits Th17-cell differentiation both *in vivo* and *ex vivo*, and metformin stimulates AMPK activation and inhibits STAT3 phosphorylation in CD4 + T cells *in vitro* (Kang et al., 2013). Taken together with the current study, the data suggests that metformin suppresses Th17 cell differentiation by inhibiting STAT3 phosphorylation via AMPK-mediated phosphorylation of JAK1. Therefore, these findings provide a mechanistic rationale for targeted activation of AMPK as a therapeutic approach in RA. Future studies would focus on determining that AMPK-mediated phosphorylation of JAK1 is the molecular mechanism underlying AMPK-induced inhibition of Th17-cell differentiation and attenuation of arthritis *in vivo*. A key tool in this study would be the generation of phospho-specific antibodies against JAK1 Ser515/518 and JAK2 Ser473 phosphorylation sites and use of these antibodies in immunoblotting, immunoprecipitation and immunohistochemistry applications.

As described above, pharmacological JAK inhibitors are available; ruxolitinib (a ATP-competitive JAK1/JAK2 inhibitor) approved for use in MF and PV, and tofacitinib (a ATP-competitive JAK1/JAK3 inhibitor) approved for use in RA. By occupying the ATP-binding pocket in the kinase domain, these inhibitors abolish phosphoryl transfer from ATP to the substrate. Given the high sequence and structural identity between the JAK kinase domains, developing specific inhibitors against each JAK member represents a challenge. Thus, alternative and novel approaches to targeting JAK, not involving the ATP-binding pocket are required (reviewed by Leroy and Constantinescu, 2017). An alternative approach that might result in improved specificity would be to target the cytokine receptor - JAK interaction. However, currently there are no JAK inhibitors targeting the cytokine receptor-JAK interaction in development as lack of structural information has hindered this approach. As discussed in chapter 4, the recent advances made by the group of P. Lupardus has provided the first structural understanding of cytokine receptor – JAK association (Lupardus et al., 2014, Ferrao et al., 2016). Surprisingly, it was found that the SH2 domain interacts with the cytokine receptor box 2 motif (Lupardus et al., 2014). Given that Ser518 and Ser515 were found to lie beside this interaction, it was proposed that AMPK phosphorylation of Ser515 and Ser518 of JAK1 disrupts the cytokine receptor box2-JAK1 SH2 binding site to destabilise the JAK1-cytokine receptor complex leading to impaired JAK1 signalling. Therefore, these findings suggest that the receptor box2-JAK1 SH2 interaction is

a potential target for designing small-molecule chemical probes that may induce disruption of the interaction. Crucially, targeting the SH2 domain may produce a small molecule that has selectivity for one specific JAK isoform and given SH2 domains close interaction with the receptor this may also lead to targeting specific JAK isoforms in complex with distinct receptors.

Chapter 6 - Appendices

6.1 AMPK-mediated inhibition of JAK-STAT signalling

Previous unpublished studies in our group have investigated whether AMPK modifies IL-6 stimulation of JAK-STAT signalling in HUVECs (Claire Rutherford, Marie-Ann Ewart, Ian Salt, Tim Palmer, personal communication). Those studies, performed by Dr. Claire Rutherford and Dr. Marie-Ann Ewart (University of Glasgow) are described in more detail in sections 6.1.1-6.1.3 and form the basis of the studies described in this thesis.

6.1.1 Pharmacological activation of AMPK inhibits sIL-6Rα/IL-6 signalling in vascular ECs

Incubation of HUVECs with sIL-6Rα/IL-6 trans-signalling complex for 30 minutes increased STAT3 phosphorylation on Tyr705. Pharmacological activation of AMPK, using two chemically distinct agonists AICAR or A769662, significantly (**p<0.01) inhibited sIL-6Rα/IL-6 stimulation of STAT3 Tyr705 phosphorylation (Figure 6.1). In addition, sIL-6Rα/IL-6 stimulation of STAT3 Tyr705 phosphorylation was significantly (*p<0.05) inhibited in HUVECs pre-treated with a combination of clinically utilized AMPK activators metformin and salicylate (Hawley et al., 2012) (Figure 6.1). Activation of AMPK by each distinct stimulus was assessed by confirming AMPK-mediated ACC phosphorylation on Ser79 (Davies et al., 1992). Furthermore, AMPK activation on its own had no detectable effect on STAT3 phosphorylation (Figure 6.1). Overall, these data demonstrate that pharmacological activators of AMPK inhibit sIL-6Rα/IL-6 signalling in vascular ECs. The data shown in figure 6.1 was generated and analysed by Dr Claire Rutherford, University of Glasgow.

Targeted short interfering RNA (siRNA)-mediated knockdown of AMPKα1 catalytic subunits attenuated the inhibitory effect of A769662 (Figure 6.2A) and AICAR (Figure 6.2B) on STAT3 Tyr705 phosphorylation. Immunoblotting of whole cell extracts with phospho-ACC (Ser79) antibody verified that treatment of cells with AMPK-siRNA inhibits AMPK activity in HUVECs as indicated by reduced phospho-ACC (Ser79) levels relative to HUVECs transfected with the control siRNA (Figures 6.2A and 6.2B). Overall, these data indicate that A769662- and AICAR- mediated inhibition of sIL-6Rα/IL-6 signalling is *via* AMPK activation. The data shown in

figure 6.2 was generated and analysed by Dr Claire Rutherford, University of Glasgow.

6.1.2 Activation of AMPK inhibits induction of STAT3 regulated genes and STAT3-mediated monocyte chemotaxis

It was next sought to determine whether AMPK activation influenced the induction of STAT3 target genes SOCS3 and CCAAT/enhancer-binding protein δ (C/EBPδ) in HUVECs (Cantwell et al., 1998, Yang et al., 2010). Total RNA was extracted from HUVECs incubated with sIL-6Rα/IL-6 in the presence or absence of A769662, and messenger RNA (mRNA) levels were then analysed by quantitative reverse transcription PCR. Incubation of HUVECs with sIL-6Rα/IL-6 in the absence of A769662 caused a significant increase, compared to the basal level, in SOCS3 (**p<0.01) and C/EBPδ (***p<0.001) mRNA expression (Figure 6.3). Preincubation with A769662 inhibited sIL-6Rα/IL-6 stimulation of SOCS3 and C/EBPδ mRNA expression, relative to sIL-6Rα/IL-6 treatment alone (Figure 6.3). Furthermore, treatment of HUVECs with A769662 alone had no significant (p>0.05, NS) effect on SOCS3 and C/EBPδ mRNA levels, compared to basal levels (Figure 6.3). Overall, A769662 reduced sIL-6Rα/IL-6 -stimulated SOCS3 and C/EBPδ mRNA and protein expression. The data shown in figure 6.3 was generated and analysed by Dr Claire Rutherford, University of Glasgow.

The effects of AMPK activation on sIL-6Rα/IL-6 -induced monocyte chemotaxis were also investigated. The ability of IL-6 to induce chemokine expression and thereby increase monocyte chemotaxis is well described (Jougasaki et al., 2010, Ortiz-Muñoz et al., 2009, Romano et al., 1997). Conditioned media was collected from HUVECs following stimulation with or without sIL-6Rα/IL-6 in the presence or absence of A769662. To ensure that sIL-6Rα/IL-6 and A769662 were not present in the conditioned media, HUVEC monolayers were extensively washed prior to incubation and collection of conditioned medium. The capacity of the conditioned media to stimulate monocyte migration was assessed using a trans-well migration assay. It was found that the migration of U937 monocytic cells towards conditioned media from sIL-6Rα/IL-6-stimulated HUVECs was significantly (*p<0.05) increased (Figure 6.4). Conditioned medium from HUVECs pre-treated with A769662 for 30 min prior to cytokine stimulation elicited significantly (*p<0.05) less U937 cell migration compared to conditioned media from sIL-6Rα/IL-6-stimulated HUVECs

(Figure 6.4). The data shown in Figures 6.4 was generated and analysed by Dr Marie-Ann Ewart, University of Glasgow.

6.1.3 Activation of AMPK inhibits sIL-6Rα/IL-6 and IFNα responses in vascular ECs via a common post-receptor intermediate

IFN-α stimulates the JAK-STAT signalling pathway *via* an IFNAR1/IFNAR2 complex which is distinct from the sIL-6Rα/IL-6/gp130 complex (Borden et al., 2007). A769662 significantly (**p<0.01) inhibits both sIL-6Rα/IL-6 and IFN-α stimulation of STAT3 Tyr705 phosphorylation in HUVECs (Figure 6.5A). Furthermore, the inhibitory effect of AMPK on sIL-6Rα/IL-6 responses was not restricted to STAT3, as pre-treatment of HUVECs with A769662 significantly (***p<0.001) inhibited sIL-6Rα/IL-6 stimulated phosphorylation of STAT1 on Tyr701 (Figure 6.5B). The data shown in figures 6.5 was generated and analysed by Dr Claire Rutherford, University of Glasgow.Taken together, these data demonstrated that activation of AMPK by multiple stimuli triggered a rapid and significant reduction in the ability of sIL-6Rα/IL-6 to stimulate STAT3 phosphorylation on Tyr705. AMPK activation reduced sIL-6Rα/IL-6 induction of STAT3 target genes and STAT3-meditated monocyte chemotaxis. These results would suggest that AMPK exerts its inhibitory effects on multiple cytokine-activated signalling pathways at one or more common loci downstream of both IFNAR1/IFNAR2 and gp130-containing cytokine receptor complexes.

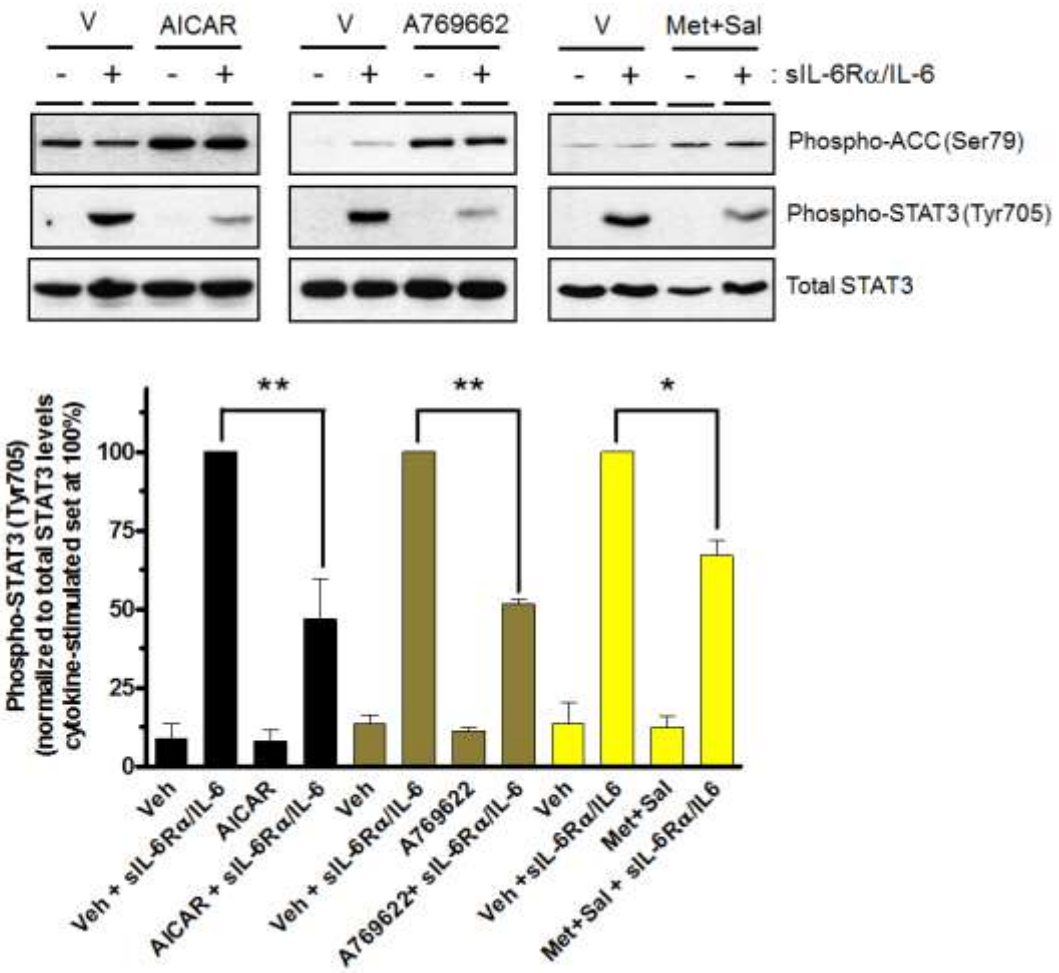

Figure 6.1: Pharmacological activation of AMPK inhibits sIL-6Rα/IL-6 signalling in HUVECs
HUVECs were pre-incubated in the presence or absence of 1 mM AICAR (2 hr), 100 μM A769662 (40 min) or a combination of 3 mM metformin and 5 mM salicylate (Met+Sal, 1 hr) prior to stimulation with sIL-6Rα/IL-6 (25 ng/ml, 5 ng/ml) for a further 30 min as indicated. Protein-equalized cell lysates were then analysed by SDS-PAGE and immunoblotting with the indicated antibodies. Densitometric analysis for STAT3 phosphorylation normalized to respective total levels is shown in each case. Data are shown as mean ±SEM for n=3 independent experiments. *p<0.05, **p<0.01. (Data was generated and analysed by Dr. Claire Rutherford, University of Glasgow.)

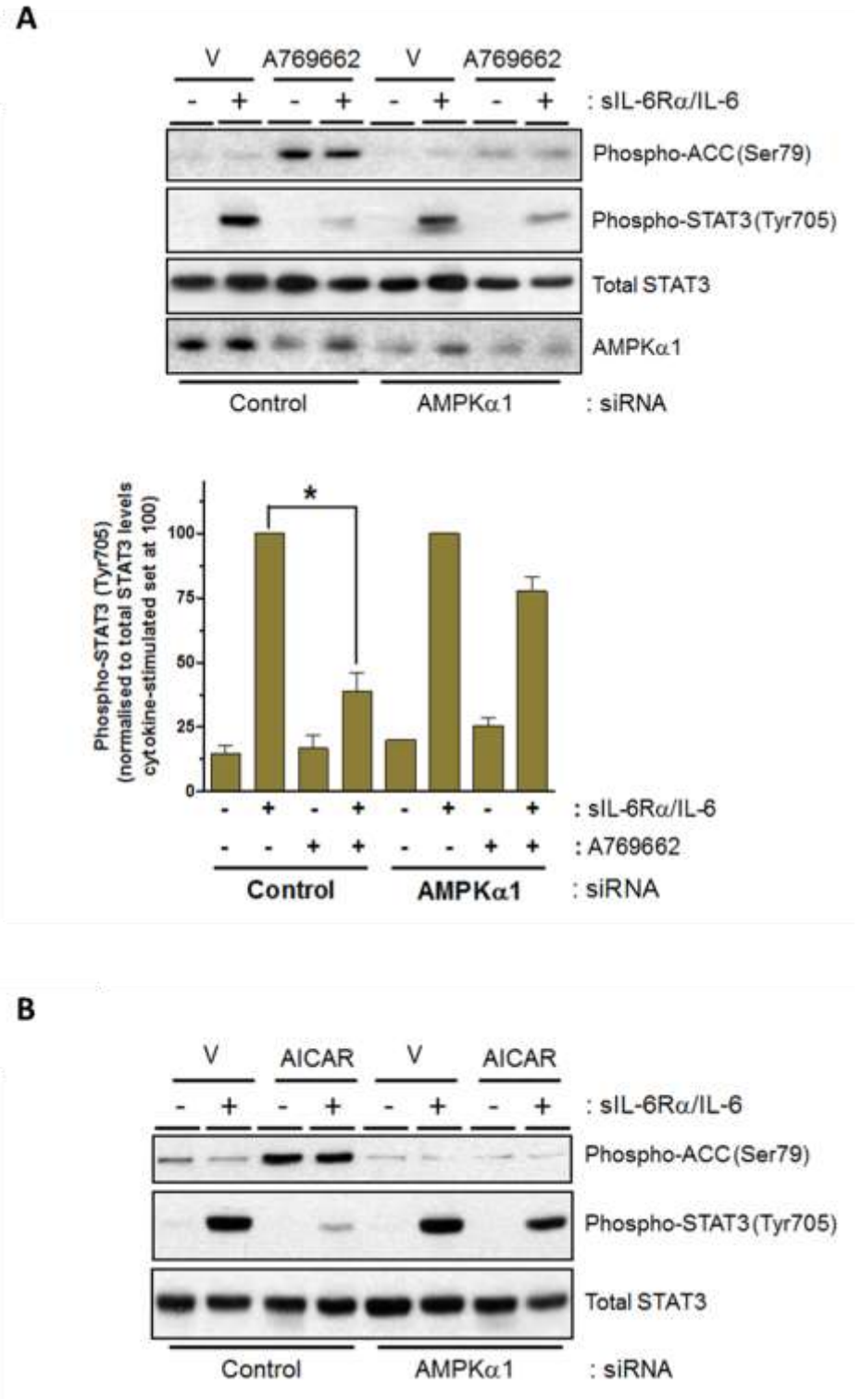

Figure 6.2: AMPK-mediated inhibition of STAT3 Tyr705 phosphorylation in HUVECs.
(A) HUVECs were transfected with either non-targeting control or AMPKα1-specific siRNAs as indicated. Cells were then pre-incubated in the presence or absence of 100 μM A769662 (40 min) prior to stimulation with sIL-6Rα/IL-6 (25 ng/ml, 5 ng/ml) for a further 30 min as indicated. Protein-equalized cell lysates were then analysed by SDS-PAGE and immunoblotting with the indicated antibodies. Densitometric analysis for STAT3 phosphorylation normalized to respective total levels is shown in each case. Data are shown as mean ±SEM for n=3 independent experiments. *p<0.05. **(B)** HUVECs were pre-incubated in the presence or absence of 1 mM AICAR (2 hr) prior to stimulation with sIL-6Rα/IL-6 (25 ng/ml, 5 ng/ml) for a further 30 min as indicated. Protein-equalized cell lysates were then analysed by SDS-PAGE and immunoblotting with the indicated antibodies. The data shown are representative of multiple experiments. (Data was generated and analysed by Dr. Claire Rutherford, University of Glasgow.)

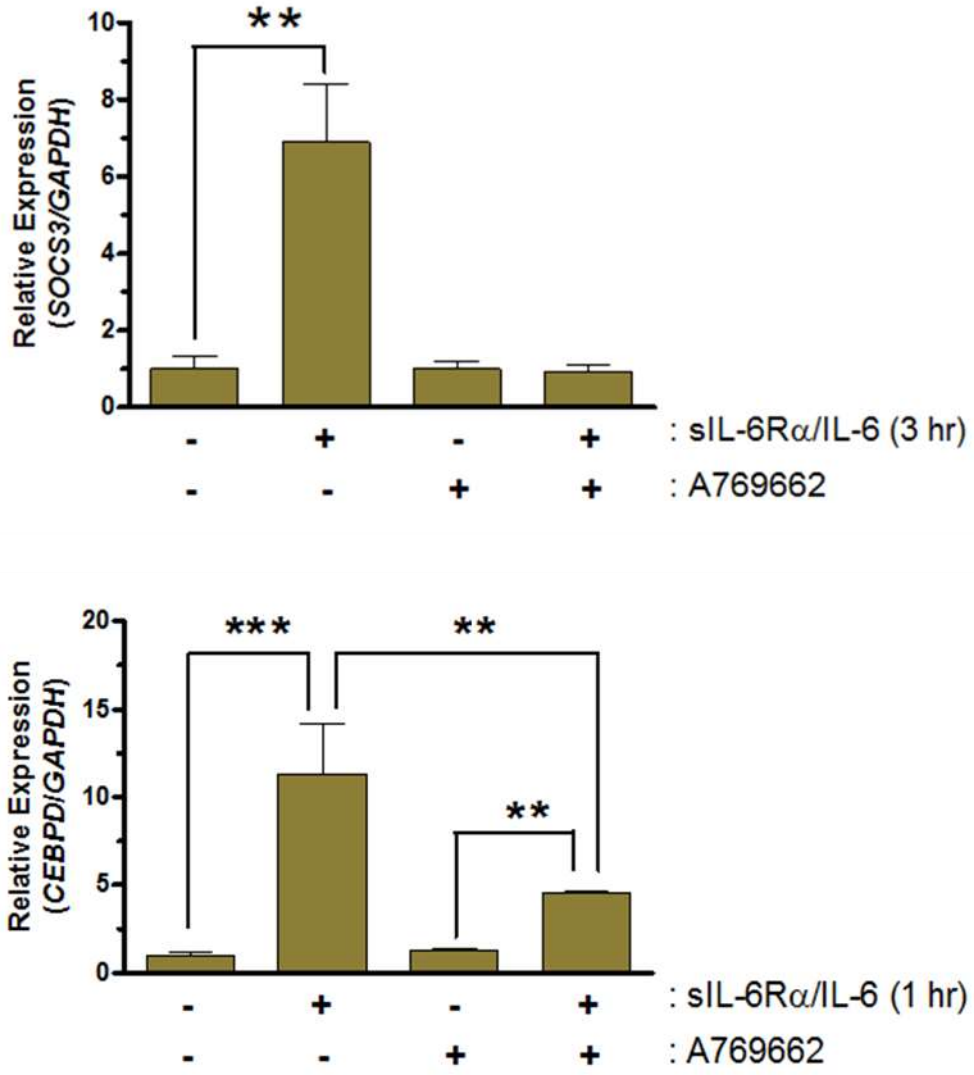

Figure 6.3: A769662 inhibits sIL-6Rα/IL-6-mediated *SOCS3* and *CEBPD* mRNA induction. HUVECs were pre-treated for 30 min with or without A769662 (100 μM) prior to stimulation with sIL-6Rα/IL-6 (25 ng/ml, 5 ng/ml) for either 1 hr (*CEBPD*) or 3 hr (*SOCS3*). Messenger RNA levels were then analyzed by quantitative reverse transcription PCR and normalized to *GAPDH* mRNA. Analysis of n=3 (*CEBPD*) or n=4 (*SOCS3*) independent experiments for *SOCS3* and *CEBPD* normalized to *GAPDH* levels is shown. ***p*<0.01, ****p*<0.001 (Data was generated and analysed by Dr. Claire Rutherford, University of Glasgow.)

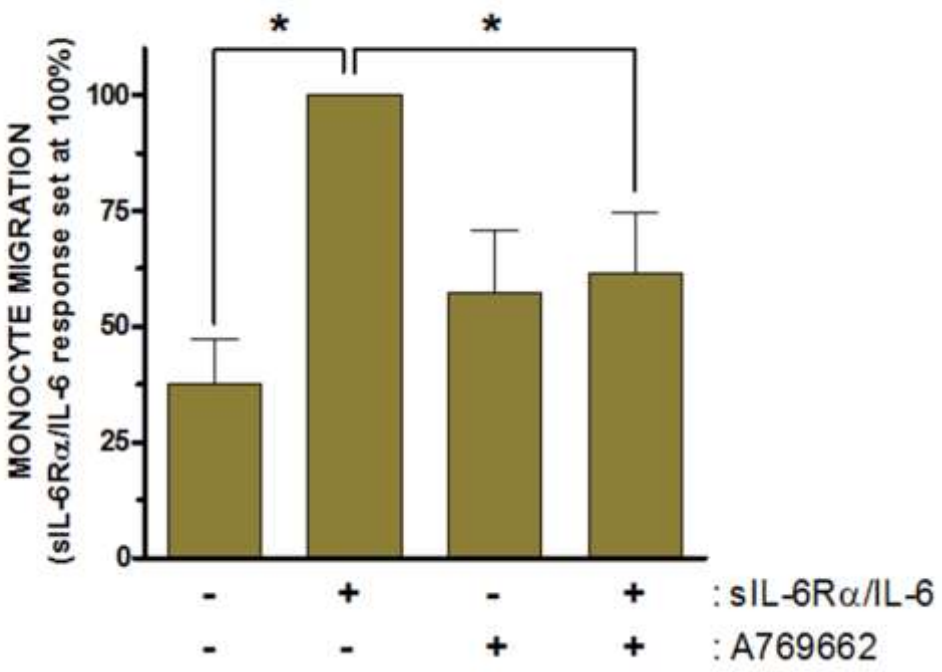

Figure 6.4: A769662 inhibits sIL-6Rα/IL-6-mediated U937 monocytic cell migration induced by conditioned medium from treated HUVECs *in vitro*

HUVECs were pre-treated for 30 min with or without A769662 (100 μM) prior to stimulation with sIL-6Rα/IL-6 (25 ng/ml, 5 ng/ml) for 2 hr. After washing and incubation in fresh medium for a further 1 hr, conditioned medium was removed and used for chemotaxis assays using U937 monocytic cells. Data are shown as mean ±SEM for n = 3 independent experiments. **p*<0.05, (Data was generated and analysed by Dr. Marie-Ann Ewart, University of Glasgow.)

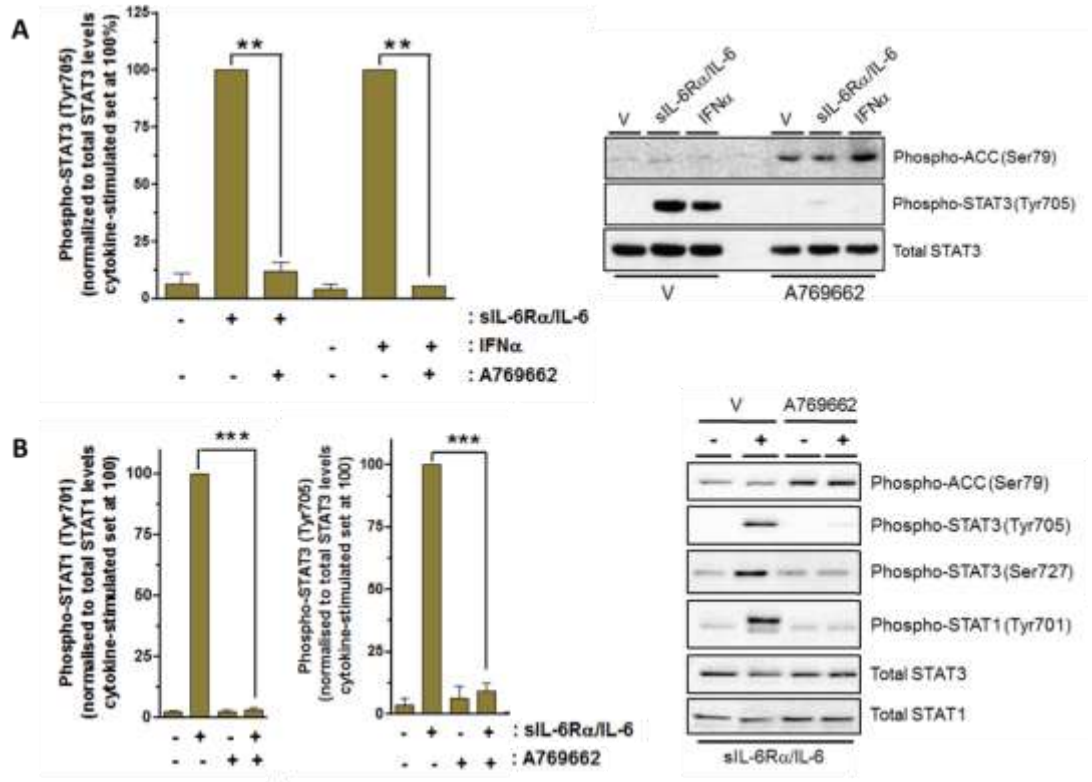

Figure 6.5: AMPK inhibits STAT1 and STAT3 activation by sIL-6Rα/IL-6 and STAT3 by IFNα. (A&B)HUVECs were incubated for 30 min with either vehicle (V) or A769662 (100 μM) prior to stimulation with either vehicle (V), sIL-6Rα/IL-6 (25 ng/ml, 5 ng/ml) for 30 min or IFNα (1000U/ml) for 15 min. Cell lysates were then analyzed by SDS-PAGE and immunoblotting with the indicated antibodies. Densitometric analysis for STAT3 or STAT1 phosphorylation normalized to respective total levels is shown in each case. Data are shown as mean ±SEM for n=3 independent experiments. ** p>0.01, *** p<0.001. Data was generated and analysed by Dr. Claire Rutherford, University of Glasgow.

6.2 Materials

Abcam, Cambridge, UK
Anti-GST antibody

Agilent Technologies, Santa Clara, CA, USA

Quikchange II Site-Directed Mutagenesis kit

BL21 (DE3) Competent Cells

XL10-Gold ultracompetent cells

Cayman Chemicals, Ann Arbor, MI, USA

PP242

Cell Biolabs, Inc., San Diego, CA, USA

Rapid GST Inclusion Body Solubilization and Renaturation Kit

Bio-Rad Laboratories Ltd, Hemel Hempstead, Hertfordshire, UK

Precision Plus Protein Kaleidoscope Standards

Fisher Scientific UK Ltd, Loughborough, Leicestershire, UK

2-[4-(2-hydroxyethyl)-1-piperazine] ethanesuphonic acid (HEPES)

Ammonium Persulphate (APS)

Corning tissue culture T75/T150 flasks, 10 cm plates and 6 well plates

Ethanol

Ethidium Bromide

Glycine

Methanol

Tris base (tris(hydroxymethyl)aminoethane)

Formendium, Hunstanton, Norfolk, UK

Bacterial Agar

Tryptone

Yeast extract powder

GE Healthcare, Little Chalfont, Buckinghamshire, UK

Streptavidin-Sepharose beads, high performance

Whatman Protran Nitrocellulose Membrane

Glutathine-S-Sepharose 4B
Invitrogen (Life Technologies Ltd), Paisley, UK
Dulbecco's Modified Eagle Medium (DMEM)
Endotoxin-free phosphate buffered saline (PBS)
Opti-MEM, reduced serum media

Kodak Company, Hemel Hampstead, Hertfordshire, UK
Medical X-ray Film General Purpose Blue

Lonza, Walkersville, MD, USA
Endothelial Cell Basal Medium-2 (EBM-2)
Endothelial cell growth media kit (EGM-2)
Human umbilical vein endothelial cells (HUVECs)

Merck Millipore, Watford, Hertfordshire, UK
Anti-Phosphotyrosine, clone 4G10
Bugbuster protein extraction reagent

Melford Laboratories Ltd, Chelsworth, Ipswich, Suffolk, UK
Dithiothreitol (DTT)
Isopropyl-β-D-thiogalactopyranoside (IPTG)

New England Bioscience (UK) Ltd, Hitchin, Hertfordshire, UK
100 mM dNTPs (dATP, dTTP, dGTP, dCTG)

Perkin-Elmer Life Sciences, Waltham, MA, USA
Western Lightning Plus Enhanced chemiluminescence (ECL) substrate
ATP, [γ-32P]- 3000Ci/mmol 10mCi/ml Lead

Premier International Foods, Cheshire, UK
Marvel dried skimmed milk

Promega UK Ltd, Southampton, UK
1 kb DNA Ladder
100 bp DNA Ladder

6x DNA Loading Buffer
Acetylated BSA
BamHI
EcoRI
Pfu DNA polymer 10X buffer
Pfu DNA polymerase
Restriction Enzyme 10X Buffer
T4 DNA Ligase
T4 DNA Ligase 10X Buffer

Promega, Madison, WI, USA
Wizard® Plus SV Minipreps Kit

Qiagen, Crawley, West Sussex, UK
Endofree Plasmid Maxi Kit
QIAquick Gel Extraction Kit
Human JAK1 siRNA
Human JAK2 siRNA
Human TYK2 siRNA
Ni-NTA Agarose

R & D Systems, Abingdon Science Park, Abingdon, Oxford, UK
Interleukin-6 (IL-6) (murine/human)
Soluble interleukin-6 receptor-α (sIL-6α) (murine/human)
GF109203X
Recombinant Human 14-3-3 zeta, HRP-conjugated

Roche Diagnostic Ltd, Burgess Hill, UK
Complete, EDTA-free protease inhibitor cocktail tablets

Sigma-Aldrich Ltd, Gillingham, Dorset, UK
(+)-Etomoxir sodium salt hydrate (Etomoxir)
30% (w/v) acrylamide/0.8% (w/v) bis-acrylamide
Ampicillin
Anti-FLAG M2 affinity gel

Benzamidine

Bovine serum albumin

Bovine serum albumin (BSA)

Bromophenol blue

Dimethyl Suphoxide (DMSO)

Ethylenediamine tetraacetic acid (EDTA)

Fetal bovine serum (FBS)

Glycerol

Hydrogen peroxide (H_2O_2)

Imidazole

Interferon-α (IFN-α)

Isopropanol

Kanamycin

L-glutamine

Medium 199 with HEPES modification

Nω-Nitro-D-arginine methyl ester hydrochloride (D-NAME)

Nω-Nitro-L-arginine methyl ester hydrochloride (L-NAME)

Penicillin-Streptomycin

phenylmethylsulphonyl fluoride (PMSF)

Ponceau stain

Potassium Hydroxide

Protein-G-Sepharose4B Fast Flow recombinant protein

Puromycin

Reduced Glutathione

Sodium Dodecyl Sulphate (SDS)

Sodium deoxycholate

Sodium orthovanadate

Soybean trypsin inhibitor

Sterile filtered cell culture water

Triton X-100

Trypsin-EDTA

Trypsin-EDTA for endothelial cells

Tween-20

Sarstedt, Beaumont Leys, Leicester, UK

Tissue culture cell scraper 25 cm

SelleckChem, Houston, TX, USA

EX527 (Selisistat)

ThermoScientific (Thermo), Boston, MA, USA

Human non-targeting siRNA

G418

Tocris Bioscience, Ellisville, MO, USA

A769662 (6,7-Dihydro-4-hydroxy-3-(2′-hydroxy[1,1′-biphenyl]-4-yl)-6-oxo-thieno[2,3-b]pyridine-5-carbonitrile)

VWR International Ltd., Lutterworth, Leicestershire, UK

Glacial Acetic Acid

Disodium hydrogen orthophosphate (Na_2HPO_4)

Potassium Acetate

Potassium Chloride (KCl)

Potassium dihydrogen orthophosphate (KH_2PO_4)

Sodium Carbonate (Na_2CO_3)

Sodium Chloride (NaCl)

6.3 Full length JAK peptide array sequences and layout

Full Length Human JAK1 Peptide Array					
Array Position	Peptide Sequence	Amino Acid Position	Array Position	Peptide Sequence	Amino Acid Position
1	M-Q-Y-L-N-I-K-E-D-C-N-A-M-A-F-C-A-K-M-R-S-S-K-K-T	1 - 25	81	E-A-L-S-F-V-S-L-V-D-G-Y-F-R-L-T-A-D-A-H-H-Y-L-C-T	401 - 425
2	I-K-E-D-C-N-A-M-A-F-C-A-K-M-R-S-S-K-K-T-E-V-N-L-E	6 - 30	82	V-S-L-V-D-G-Y-F-R-L-T-A-D-A-H-H-Y-L-C-T-D-V-A-P-P	406 - 430
3	N-A-M-A-F-C-A-K-M-R-S-S-K-K-T-E-V-N-L-E-A-P-E-P-G	11 - 35	83	G-Y-F-R-L-T-A-D-A-H-H-Y-L-C-T-D-V-A-P-P-L-I-V-H-N	411 - 435
4	C-A-K-M-R-S-S-K-K-T-E-V-N-L-E-A-P-E-P-G-V-E-V-I-F	16 - 40	84	T-A-D-A-H-H-Y-L-C-T-D-V-A-P-P-L-I-V-H-N-I-Q-N-G-C	416 - 440
5	S-S-K-K-T-E-V-N-L-E-A-P-E-P-G-V-E-V-I-F-Y-L-S-D-R	21 - 45	85	H-Y-L-C-T-D-V-A-P-P-L-I-V-H-N-I-Q-N-G-C-H-G-P-I-C	421 - 445
6	E-V-N-L-E-A-P-E-P-G-V-E-V-I-F-Y-L-S-D-R-E-P-L-R-L	26 - 50	86	D-V-A-P-P-L-I-V-H-N-I-Q-N-G-C-H-G-P-I-C-T-E-Y-A-I	426 - 450
7	A-P-E-P-G-V-E-V-I-F-Y-L-S-D-R-E-P-L-R-L-G-S-G-E-Y	31 - 55	87	L-I-V-H-N-I-Q-N-G-C-H-G-P-I-C-T-E-Y-A-I-N-K-L-R-Q	431 - 455
8	V-E-V-I-F-Y-L-S-D-R-E-P-L-R-L-G-S-G-E-Y-T-A-E-E-L	36 - 60	88	I-Q-N-G-C-H-G-P-I-C-T-E-Y-A-I-N-K-L-R-Q-E-G-S-E-E	436 - 460
9	Y-L-S-D-R-E-P-L-R-L-G-S-G-E-Y-T-A-E-E-L-C-I-R-A-A	41 - 65	89	H-G-P-I-C-T-E-Y-A-I-N-K-L-R-Q-E-G-S-E-E-G-M-Y-V-L	441 - 465
10	E-P-L-R-L-G-S-G-E-Y-T-A-E-E-L-C-I-R-A-A-Q-A-C-R-I	46 - 70	90	T-E-Y-A-I-N-K-L-R-Q-E-G-S-E-E-G-M-Y-V-L-R-W-S-C-T	446 - 470
11	G-S-G-E-Y-T-A-E-E-L-C-I-R-A-A-Q-A-C-R-I-S-P-L-C-H	51 - 75	91	N-K-L-R-Q-E-G-S-E-E-G-M-Y-V-L-R-W-S-C-T-D-F-D-N-I	451 - 475
12	T-A-E-E-L-C-I-R-A-A-Q-A-C-R-I-S-P-L-C-H-N-L-F-A-L	56 - 80	92	E-G-S-E-E-G-M-Y-V-L-R-W-S-C-T-D-F-D-N-I-L-M-T-V-T	456 - 480
13	C-I-R-A-A-Q-A-C-R-I-S-P-L-C-H-N-L-F-A-L-Y-D-E-N-T	61 - 85	93	G-M-Y-V-L-R-W-S-C-T-D-F-D-N-I-L-M-T-V-T-C-F-E-K-S	461 - 485
14	Q-A-C-R-I-S-P-L-C-H-N-L-F-A-L-Y-D-E-N-T-K-L-W-Y-A	66 - 90	94	R-W-S-C-T-D-F-D-N-I-L-M-T-V-T-C-F-E-K-S-E-Q-V-Q-G	466 - 490
15	S-P-L-C-H-N-L-F-A-L-Y-D-E-N-T-K-L-W-Y-A-P-N-R-T-I	71 - 95	95	D-F-D-N-I-L-M-T-V-T-C-F-E-K-S-E-Q-V-Q-G-A-Q-K-Q-F	471 - 495
16	N-L-F-A-L-Y-D-E-N-T-K-L-W-Y-A-P-N-R-T-I-T-V-D-D-K	76 - 100	96	L-M-T-V-T-C-F-E-K-S-E-Q-V-Q-G-A-Q-K-Q-F-K-N-F-Q-I	476 - 500
17	Y-D-E-N-T-K-L-W-Y-A-P-N-R-T-I-T-V-D-D-K-M-S-L-R-L	81 - 105	97	C-F-E-K-S-E-Q-V-Q-G-A-Q-K-Q-F-K-N-F-Q-I-E-V-Q-K-G	481 - 505
18	K-L-W-Y-A-P-N-R-T-I-T-V-D-D-K-M-S-L-R-L-H-Y-R-M-R	86 - 110	98	E-Q-V-Q-G-A-Q-K-Q-F-K-N-F-Q-I-E-V-Q-K-G-R-Y-S-L-H	486 - 510
19	P-N-R-T-I-T-V-D-D-K-M-S-L-R-L-H-Y-R-M-R-F-Y-F-T-N	91 - 115	99	A-Q-K-Q-F-K-N-F-Q-I-E-V-Q-K-G-R-Y-S-L-H-G-S-D-R-S	491 - 515
20	T-V-D-D-K-M-S-L-R-L-H-Y-R-M-R-F-Y-F-T-N-W-H-G-T-N	96 - 120	100	K-N-F-Q-I-E-V-Q-K-G-R-Y-S-L-H-G-S-D-R-S-F-P-S-L-G	496 - 520
21	M-S-L-R-L-H-Y-R-M-R-F-Y-F-T-N-W-H-G-T-N-D-N-E-Q-S	101 - 125	101	E-V-Q-K-G-R-Y-S-L-H-G-S-D-R-S-F-P-S-L-G-D-L-M-S-H	501 - 525
22	H-Y-R-M-R-F-Y-F-T-N-W-H-G-T-N-D-N-E-Q-S-V-W-R-H-S	106 - 130	102	R-Y-S-L-H-G-S-D-R-S-F-P-S-L-G-D-L-M-S-H-L-K-K-Q-I	506 - 530
23	F-Y-F-T-N-W-H-G-T-N-D-N-E-Q-S-V-W-R-H-S-P-K-K-Q-K	111 - 135	103	G-S-D-R-S-F-P-S-L-G-D-L-M-S-H-L-K-K-Q-I-L-R-T-D-N	511 - 535
24	W-H-G-T-N-D-N-E-Q-S-V-W-R-H-S-P-K-K-Q-K-N-G-Y-E-K	116 - 140	104	F-P-S-L-G-D-L-M-S-H-L-K-K-Q-I-L-R-T-D-N-I-S-F-M-L	516 - 540
25	D-N-E-Q-S-V-W-R-H-S-P-K-K-Q-K-N-G-Y-E-K-K-K-I-P-D	121 - 145	105	D-L-M-S-H-L-K-K-Q-I-L-R-T-D-N-I-S-F-M-L-K-R-C-C-Q	521 - 545
26	V-W-R-H-S-P-K-K-Q-K-N-G-Y-E-K-K-K-I-P-D-A-T-P-L-L	126 - 150	106	L-K-K-Q-I-L-R-T-D-N-I-S-F-M-L-K-R-C-C-Q-P-K-P-R-E	526 - 550
27	P-K-K-Q-K-N-G-Y-E-K-K-K-I-P-D-A-T-P-L-L-D-A-S-S-L	131 - 155	107	L-R-T-D-N-I-S-F-M-L-K-R-C-C-Q-P-K-P-R-E-I-S-N-L-L	531 - 555
28	N-G-Y-E-K-K-K-I-P-D-A-T-P-L-L-D-A-S-S-L-E-Y-L-F-A	136 - 160	108	I-S-F-M-L-K-R-C-C-Q-P-K-P-R-E-I-S-N-L-L-V-A-T-K-K	536 - 560
29	K-K-I-P-D-A-T-P-L-L-D-A-S-S-L-E-Y-L-F-A-Q-G-Q-Y-D	141 - 165	109	K-R-C-C-Q-P-K-P-R-E-I-S-N-L-L-V-A-T-K-K-A-Q-E-W-Q	541 - 565
30	A-T-P-L-L-D-A-S-S-L-E-Y-L-F-A-Q-G-Q-Y-D-L-V-K-C-L	146 - 170	110	P-K-P-R-E-I-S-N-L-L-V-A-T-K-K-A-Q-E-W-Q-P-V-Y-P-M	546 - 570
31	D-A-S-S-L-E-Y-L-F-A-Q-G-Q-Y-D-L-V-K-C-L-A-P-I-R-D	151 - 175	111	I-S-N-L-L-V-A-T-K-K-A-Q-E-W-Q-P-V-Y-P-M-S-Q-L-S-F	551 - 575
32	E-Y-L-F-A-Q-G-Q-Y-D-L-V-K-C-L-A-P-I-R-D-P-K-T-E-Q	156 - 180	112	V-A-T-K-K-A-Q-E-W-Q-P-V-Y-P-M-S-Q-L-S-F-D-R-I-L-K	556 - 580
33	Q-G-Q-Y-D-L-V-K-C-L-A-P-I-R-D-P-K-T-E-Q-D-G-H-D-I	161 - 185	113	A-Q-E-W-Q-P-V-Y-P-M-S-Q-L-S-F-D-R-I-L-K-K-D-L-V-Q	561 - 585
34	L-V-K-C-L-A-P-I-R-D-P-K-T-E-Q-D-G-H-D-I-E-N-E-C-L	166 - 190	114	P-V-Y-P-M-S-Q-L-S-F-D-R-I-L-K-K-D-L-V-Q-G-E-H-L-G	566 - 590
35	A-P-I-R-D-P-K-T-E-Q-D-G-H-D-I-E-N-E-C-L-G-M-A-V-L	171 - 195	115	S-Q-L-S-F-D-R-I-L-K-K-D-L-V-Q-G-E-H-L-G-R-G-T-R-T	571 - 595
36	P-K-T-E-Q-D-G-H-D-I-E-N-E-C-L-G-M-A-V-L-A-I-S-H-Y	176 - 200	116	D-R-I-L-K-K-D-L-V-Q-G-E-H-L-G-R-G-T-R-T-H-I-Y-S-G	576 - 600
37	D-G-H-D-I-E-N-E-C-L-G-M-A-V-L-A-I-S-H-Y-A-M-M-K-K	181 - 205	117	K-D-L-V-Q-G-E-H-L-G-R-G-T-R-T-H-I-Y-S-G-T-L-M-D-Y	581 - 605
38	E-N-E-C-L-G-M-A-V-L-A-I-S-H-Y-A-M-M-K-K-M-Q-L-P-E	186 - 210	118	G-E-H-L-G-R-G-T-R-T-H-I-Y-S-G-T-L-M-D-Y-K-D-D-E-G	586 - 610
39	G-M-A-V-L-A-I-S-H-Y-A-M-M-K-K-M-Q-L-P-E-L-P-K-D-I	191 - 215	119	R-G-T-R-T-H-I-Y-S-G-T-L-M-D-Y-K-D-D-E-G-T-S-E-E-K	591 - 615
40	A-I-S-H-Y-A-M-M-K-K-M-Q-L-P-E-L-P-K-D-I-S-Y-K-R-Y	196 - 220	120	H-I-Y-S-G-T-L-M-D-Y-K-D-D-E-G-T-S-E-E-K-K-I-K-V-I	596 - 620
41	A-M-M-K-K-M-Q-L-P-E-L-P-K-D-I-S-Y-K-R-Y-I-P-E-T-L	201 - 225	121	T-L-M-D-Y-K-D-D-E-G-T-S-E-E-K-K-I-K-V-I-L-K-V-L-D	601 - 625
42	M-Q-L-P-E-L-P-K-D-I-S-Y-K-R-Y-I-P-E-T-L-N-K-S-I-R	206 - 230	122	K-D-D-E-G-T-S-E-E-K-K-I-K-V-I-L-K-V-L-D-P-S-H-R-D	606 - 630
43	L-P-K-D-I-S-Y-K-R-Y-I-P-E-T-L-N-K-S-I-R-Q-R-N-L-L	211 - 235	123	T-S-E-E-K-K-I-K-V-I-L-K-V-L-D-P-S-H-R-D-I-S-L-A-F	611 - 635
44	S-Y-K-R-Y-I-P-E-T-L-N-K-S-I-R-Q-R-N-L-L-T-R-M-R-I	216 - 240	124	K-I-K-V-I-L-K-V-L-D-P-S-H-R-D-I-S-L-A-F-F-E-A-A-S	616 - 640
45	I-P-E-T-L-N-K-S-I-R-Q-R-N-L-L-T-R-M-R-I-N-N-V-F-K	221 - 245	125	L-K-V-L-D-P-S-H-R-D-I-S-L-A-F-F-E-A-A-S-M-M-R-Q-V	621 - 645
46	N-K-S-I-R-Q-R-N-L-L-T-R-M-R-I-N-N-V-F-K-D-F-L-K-E	226 - 250	126	P-S-H-R-D-I-S-L-A-F-F-E-A-A-S-M-M-R-Q-V-S-H-K-H-I	626 - 650
47	Q-R-N-L-L-T-R-M-R-I-N-N-V-F-K-D-F-L-K-E-F-N-N-K-T	231 - 255	127	I-S-L-A-F-F-E-A-A-S-M-M-R-Q-V-S-H-K-H-I-V-Y-L-Y-G	631 - 655
48	T-R-M-R-I-N-N-V-F-K-D-F-L-K-E-F-N-N-K-T-I-C-D-S-S	236 - 260	128	F-E-A-A-S-M-M-R-Q-V-S-H-K-H-I-V-Y-L-Y-G-V-C-V-R-D	636 - 660
49	N-N-V-F-K-D-F-L-K-E-F-N-N-K-T-I-C-D-S-S-V-S-T-H-D	241 - 265	129	M-M-R-Q-V-S-H-K-H-I-V-Y-L-Y-G-V-C-V-R-D-V-E-N-I-M	641 - 665
50	D-F-L-K-E-F-N-N-K-T-I-C-D-S-S-V-S-T-H-D-L-K-V-K-Y	246 - 270	130	S-H-K-H-I-V-Y-L-Y-G-V-C-V-R-D-V-E-N-I-M-V-E-E-F-V	646 - 670
51	F-N-N-K-T-I-C-D-S-S-V-S-T-H-D-L-K-V-K-Y-L-A-T-L-E	251 - 275	131	V-Y-L-Y-G-V-C-V-R-D-V-E-N-I-M-V-E-E-F-V-E-G-G-P-L	651 - 675
52	I-C-D-S-S-V-S-T-H-D-L-K-V-K-Y-L-A-T-L-E-T-L-T-K-H	256 - 280	132	V-C-V-R-D-V-E-N-I-M-V-E-E-F-V-E-G-G-P-L-D-L-F-M-H	656 - 680
53	V-S-T-H-D-L-K-V-K-Y-L-A-T-L-E-T-L-T-K-H-Y-G-A-E-I	261 - 285	133	V-E-N-I-M-V-E-E-F-V-E-G-G-P-L-D-L-F-M-H-R-K-S-D-V	661 - 685
54	L-K-V-K-Y-L-A-T-L-E-T-L-T-K-H-Y-G-A-E-I-F-E-T-S-M	266 - 290	134	V-E-E-F-V-E-G-G-P-L-D-L-F-M-H-R-K-S-D-V-L-T-T-P-W	666 - 690
55	L-A-T-L-E-T-L-T-K-H-Y-G-A-E-I-F-E-T-S-M-L-L-I-S-S	271 - 295	135	E-G-G-P-L-D-L-F-M-H-R-K-S-D-V-L-T-T-P-W-K-F-K-V-A	671 - 695
56	T-L-T-K-H-Y-G-A-E-I-F-E-T-S-M-L-L-I-S-S-E-N-E-M-N	276 - 300	136	D-L-F-M-H-R-K-S-D-V-L-T-T-P-W-K-F-K-V-A-K-Q-L-A-S	676 - 700
57	Y-G-A-E-I-F-E-T-S-M-L-L-I-S-S-E-N-E-M-N-W-F-H-S-N	281 - 305	137	R-K-S-D-V-L-T-T-P-W-K-F-K-V-A-K-Q-L-A-S-A-L-S-Y-L	681 - 705
58	F-E-T-S-M-L-L-I-S-S-E-N-E-M-N-W-F-H-S-N-D-G-G-N-V	286 - 310	138	L-T-T-P-W-K-F-K-V-A-K-Q-L-A-S-A-L-S-Y-L-E-D-K-D-L	686 - 710
59	L-L-I-S-S-E-N-E-M-N-W-F-H-S-N-D-G-G-N-V-L-Y-Y-E-V	291 - 315	139	K-F-K-V-A-K-Q-L-A-S-A-L-S-Y-L-E-D-K-D-L-V-H-G-N-V	691 - 715
60	E-N-E-M-N-W-F-H-S-N-D-G-G-N-V-L-Y-Y-E-V-M-V-T-G-N	296 - 320	140	K-Q-L-A-S-A-L-S-Y-L-E-D-K-D-L-V-H-G-N-V-C-T-K-N-L	696 - 720
61	W-F-H-S-N-D-G-G-N-V-L-Y-Y-E-V-M-V-T-G-N-L-G-I-Q-W	301 - 325	141	A-L-S-Y-L-E-D-K-D-L-V-H-G-N-V-C-T-K-N-L-L-L-A-R-E	701 - 725
62	D-G-G-N-V-L-Y-Y-E-V-M-V-T-G-N-L-G-I-Q-W-R-H-K-P-N	306 - 330	142	E-D-K-D-L-V-H-G-N-V-C-T-K-N-L-L-L-A-R-E-G-I-D-S-E	706 - 730
63	L-Y-Y-E-V-M-V-T-G-N-L-G-I-Q-W-R-H-K-P-N-V-V-S-V-E	311 - 335	143	V-H-G-N-V-C-T-K-N-L-L-L-A-R-E-G-I-D-S-E-C-G-P-F-I	711 - 735
64	M-V-T-G-N-L-G-I-Q-W-R-H-K-P-N-V-V-S-V-E-K-E-K-N-K	316 - 340	144	C-T-K-N-L-L-L-A-R-E-G-I-D-S-E-C-G-P-F-I-K-L-S-D-P	716 - 740
65	L-G-I-Q-W-R-H-K-P-N-V-V-S-V-E-K-E-K-N-K-L-K-R-K-K	321 - 345	145	L-L-A-R-E-G-I-D-S-E-C-G-P-F-I-K-L-S-D-P-G-I-P-I-T	721 - 745
66	R-H-K-P-N-V-V-S-V-E-K-E-K-N-K-L-K-R-K-K-L-E-N-K-H	326 - 350	146	G-I-D-S-E-C-G-P-F-I-K-L-S-D-P-G-I-P-I-T-V-L-S-R-Q	726 - 750
67	V-V-S-V-E-K-E-K-N-K-L-K-R-K-K-L-E-N-K-H-K-K-D-E-E	331 - 355	147	C-G-P-F-I-K-L-S-D-P-G-I-P-I-T-V-L-S-R-Q-E-C-I-E-R	731 - 755
68	K-E-K-N-K-L-K-R-K-K-L-E-N-K-H-K-K-D-E-E-K-N-K-I-R	336 - 360	148	K-L-S-D-P-G-I-P-I-T-V-L-S-R-Q-E-C-I-E-R-I-P-W-I-A	736 - 760
69	L-K-R-K-K-L-E-N-K-H-K-K-D-E-E-K-N-K-I-R-E-E-W-N-N	341 - 365	149	G-I-P-I-T-V-L-S-R-Q-E-C-I-E-R-I-P-W-I-A-P-E-C-V-E	741 - 765
70	L-E-N-K-H-K-K-D-E-E-K-N-K-I-R-E-E-W-N-N-F-S-Y-F-P	346 - 370	150	V-L-S-R-Q-E-C-I-E-R-I-P-W-I-A-P-E-C-V-E-D-S-K-N-L	746 - 770
71	K-K-D-E-E-K-N-K-I-R-E-E-W-N-N-F-S-Y-F-P-E-I-T-H-I	351 - 375	151	E-C-I-E-R-I-P-W-I-A-P-E-C-V-E-D-S-K-N-L-S-V-A-A-D	751 - 775
72	K-N-K-I-R-E-E-W-N-N-F-S-Y-F-P-E-I-T-H-I-V-I-K-E-S	356 - 380	152	I-P-W-I-A-P-E-C-V-E-D-S-K-N-L-S-V-A-A-D-K-W-S-F-G	756 - 780
73	E-E-W-N-N-F-S-Y-F-P-E-I-T-H-I-V-I-K-E-S-V-V-S-I-N	361 - 385	153	P-E-C-V-E-D-S-K-N-L-S-V-A-A-D-K-W-S-F-G-T-T-L-W-E	761 - 785
74	F-S-Y-F-P-E-I-T-H-I-V-I-K-E-S-V-V-S-I-N-K-Q-D-N-K	366 - 390	154	D-S-K-N-L-S-V-A-A-D-K-W-S-F-G-T-T-L-W-E-I-C-Y-N-G	766 - 790
75	E-I-T-H-I-V-I-K-E-S-V-V-S-I-N-K-Q-D-N-K-K-M-E-L-K	371 - 395	155	S-V-A-A-D-K-W-S-F-G-T-T-L-W-E-I-C-Y-N-G-E-I-P-L-K	771 - 795
76	V-I-K-E-S-V-V-S-I-N-K-Q-D-N-K-K-M-E-L-K-L-S-S-H-E	376 - 400	156	K-W-S-F-G-T-T-L-W-E-I-C-Y-N-G-E-I-P-L-K-D-K-T-L-I	776 - 800
77	V-V-S-I-N-K-Q-D-N-K-K-M-E-L-K-L-S-S-H-E-E-A-L-S-F	381 - 405	157	T-T-L-W-E-I-C-Y-N-G-E-I-P-L-K-D-K-T-L-I-E-K-E-R-F	781 - 805
78	K-Q-D-N-K-K-M-E-L-K-L-S-S-H-E-E-A-L-S-F-V-S-L-V-D	386 - 410	158	I-C-Y-N-G-E-I-P-L-K-D-K-T-L-I-E-K-E-R-F-Y-E-S-R-C	786 - 810
79	K-M-E-L-K-L-S-S-H-E-E-A-L-S-F-V-S-L-V-D-G-Y-F-R-L	391 - 415	159	E-I-P-L-K-D-K-T-L-I-E-K-E-R-F-Y-E-S-R-C-R-P-V-T-P	791 - 815
80	L-S-S-H-E-E-A-L-S-F-V-S-L-V-D-G-Y-F-R-L-T-A-D-A-H	396 - 420	160	D-K-T-L-I-E-K-E-R-F-Y-E-S-R-C-R-P-V-T-P-S-C-K-E-L	796 - 820

Table 6-1: **Peptide array spanning the human JAK1 open reading frame**

(continued overleaf)

Full Length Human JAK1 Peptide Array					
Array Position	Peptide Sequence	Amino Acid Position	Array Position	Peptide Sequence	Amino Acid Position
161	E-K-E-R-F-Y-E-S-R-C-R-P-V-T-P-S-C-K-E-L-A-D-L-M-T	801 - 825	195	N-K-N-K-I-N-L-K-Q-Q-L-K-Y-A-V-Q-I-C-K-G-M-D-Y-L-G	971 - 995
162	Y-E-S-R-C-R-P-V-T-P-S-C-K-E-L-A-D-L-M-T-R-C-M-N-Y	806 - 830	196	N-L-K-Q-Q-L-K-Y-A-V-Q-I-C-K-G-M-D-Y-L-G-S-R-Q-Y-V	976 - 1000
163	R-P-V-T-P-S-C-K-E-L-A-D-L-M-T-R-C-M-N-Y-D-P-N-Q-R	811 - 835	197	L-K-Y-A-V-Q-I-C-K-G-M-D-Y-L-G-S-R-Q-Y-V-H-R-D-L-A	981 - 1005
164	S-C-K-E-L-A-D-L-M-T-R-C-M-N-Y-D-P-N-Q-R-P-F-F-R-A	816 - 840	198	Q-I-C-K-G-M-D-Y-L-G-S-R-Q-Y-V-H-R-D-L-A-A-R-N-V-L	986 - 1010
165	A-D-L-M-T-R-C-M-N-Y-D-P-N-Q-R-P-F-F-R-A-I-M-R-D-I	821 - 845	199	M-D-Y-L-G-S-R-Q-Y-V-H-R-D-L-A-A-R-N-V-L-V-E-S-E-H	991 - 1015
166	R-C-M-N-Y-D-P-N-Q-R-P-F-F-R-A-I-M-R-D-I-N-K-L-E-E	826 - 850	200	S-R-Q-Y-V-H-R-D-L-A-A-R-N-V-L-V-E-S-E-H-Q-V-K-I-G	996 - 1020
167	D-P-N-Q-R-P-F-F-R-A-I-M-R-D-I-N-K-L-E-E-Q-N-P-D-I	831 - 855	201	H-R-D-L-A-A-R-N-V-L-V-E-S-E-H-Q-V-K-I-G-D-F-G-L-T	1001 - 1025
168	P-F-F-R-A-I-M-R-D-I-N-K-L-E-E-Q-N-P-D-I-V-S-E-K-K	836 - 860	202	A-R-N-V-L-V-E-S-E-H-Q-V-K-I-G-D-F-G-L-T-K-A-I-E-T	1006 - 1030
169	I-M-R-D-I-N-K-L-E-E-Q-N-P-D-I-V-S-E-K-K-P-A-T-E-V	841 - 865	203	V-E-S-E-H-Q-V-K-I-G-D-F-G-L-T-K-A-I-E-T-D-K-E-Y-Y	1011 - 1035
170	N-K-L-E-E-Q-N-P-D-I-V-S-E-K-K-P-A-T-E-V-D-P-T-H-F	846 - 870	204	Q-V-K-I-G-D-F-G-L-T-K-A-I-E-T-D-K-E-Y-Y-T-V-K-D-D	1016 - 1040
171	Q-N-P-D-I-V-S-E-K-K-P-A-T-E-V-D-P-T-H-F-E-K-R-F-L	851 - 875	205	D-F-G-L-T-K-A-I-E-T-D-K-E-Y-Y-T-V-K-D-D-R-D-S-P-V	1021 - 1045
172	V-S-E-K-K-P-A-T-E-V-D-P-T-H-F-E-K-R-F-L-K-R-I-R-D	856 - 880	206	K-A-I-E-T-D-K-E-Y-Y-T-V-K-D-D-R-D-S-P-V-F-W-Y-A-P	1026 - 1050
173	P-A-T-E-V-D-P-T-H-F-E-K-R-F-L-K-R-I-R-D-L-G-E-G-H	861 - 885	207	D-K-E-Y-Y-T-V-K-D-D-R-D-S-P-V-F-W-Y-A-P-E-C-L-M-Q	1031 - 1055
174	D-P-T-H-F-E-K-R-F-L-K-R-I-R-D-L-G-E-G-H-F-G-K-V-E	866 - 890	208	T-V-K-D-D-R-D-S-P-V-F-W-Y-A-P-E-C-L-M-Q-S-K-F-Y-I	1036 - 1060
175	E-K-R-F-L-K-R-I-R-D-L-G-E-G-H-F-G-K-V-E-L-C-R-Y-D	871 - 895	209	R-D-S-P-V-F-W-Y-A-P-E-C-L-M-Q-S-K-F-Y-I-A-S-D-V-W	1041 - 1065
176	K-R-I-R-D-L-G-E-G-H-F-G-K-V-E-L-C-R-Y-D-P-E-G-D-N	876 - 900	210	F-W-Y-A-P-E-C-L-M-Q-S-K-F-Y-I-A-S-D-V-W-S-F-G-V-T	1046 - 1070
177	L-G-E-G-H-F-G-K-V-E-L-C-R-Y-D-P-E-G-D-N-T-G-E-Q-V	881 - 905	211	E-C-L-M-Q-S-K-F-Y-I-A-S-D-V-W-S-F-G-V-T-L-H-E-L-L	1051 - 1075
178	F-G-K-V-E-L-C-R-Y-D-P-E-G-D-N-T-G-E-Q-V-A-V-K-S-L	886 - 910	212	S-K-F-Y-I-A-S-D-V-W-S-F-G-V-T-L-H-E-L-L-T-Y-C-D-S	1056 - 1080
179	L-C-R-Y-D-P-E-G-D-N-T-G-E-Q-V-A-V-K-S-L-K-P-E-S-G	891 - 915	213	A-S-D-V-W-S-F-G-V-T-L-H-E-L-L-T-Y-C-D-S-D-S-S-P-M	1061 - 1085
180	P-E-G-D-N-T-G-E-Q-V-A-V-K-S-L-K-P-E-S-G-G-N-H-I-A	896 - 920	214	S-F-G-V-T-L-H-E-L-L-T-Y-C-D-S-D-S-S-P-M-A-L-F-L-K	1066 - 1090
181	T-G-E-Q-V-A-V-K-S-L-K-P-E-S-G-G-N-H-I-A-D-L-K-K-E	901 - 925	215	L-H-E-L-L-T-Y-C-D-S-D-S-S-P-M-A-L-F-L-K-M-I-G-P-T	1071 - 1095
182	A-V-K-S-L-K-P-E-S-G-G-N-H-I-A-D-L-K-K-E-I-E-I-L-R	906 - 930	216	T-Y-C-D-S-D-S-S-P-M-A-L-F-L-K-M-I-G-P-T-H-G-Q-M-T	1076 - 1100
183	K-P-E-S-G-G-N-H-I-A-D-L-K-K-E-I-E-I-L-R-N-L-Y-H-E	911 - 935	217	D-S-S-P-M-A-L-F-L-K-M-I-G-P-T-H-G-Q-M-T-V-T-R-L-V	1081 - 1105
184	G-N-H-I-A-D-L-K-K-E-I-E-I-L-R-N-L-Y-H-E-N-I-V-K-Y	916 - 940	218	A-L-F-L-K-M-I-G-P-T-H-G-Q-M-T-V-T-R-L-V-N-T-L-K-E	1086 - 1110
185	D-L-K-K-E-I-E-I-L-R-N-L-Y-H-E-N-I-V-K-Y-K-G-I-C-T	921 - 945	219	M-I-G-P-T-H-G-Q-M-T-V-T-R-L-V-N-T-L-K-E-G-K-R-L-P	1091 - 1115
186	I-E-I-L-R-N-L-Y-H-E-N-I-V-K-Y-K-G-I-C-T-E-D-G-G-N	926 - 950	220	H-G-Q-M-T-V-T-R-L-V-N-T-L-K-E-G-K-R-L-P-C-P-P-N-C	1096 - 1120
187	N-L-Y-H-E-N-I-V-K-Y-K-G-I-C-T-E-D-G-G-N-G-I-K-L-I	931 - 955	221	V-T-R-L-V-N-T-L-K-E-G-K-R-L-P-C-P-P-N-C-P-D-E-V-Y	1101 - 1125
188	N-I-V-K-Y-K-G-I-C-T-E-D-G-G-N-G-I-K-L-I-M-E-F-L-P	936 - 960	222	N-T-L-K-E-G-K-R-L-P-C-P-P-N-C-P-D-E-V-Y-Q-L-M-R-K	1106 - 1130
189	K-G-I-C-T-E-D-G-G-N-G-I-K-L-I-M-E-F-L-P-S-G-S-L-K	941 - 965	223	G-K-R-L-P-C-P-P-N-C-P-D-E-V-Y-Q-L-M-R-K-C-W-E-F-Q	1111 - 1135
190	E-D-G-G-N-G-I-K-L-I-M-E-F-L-P-S-G-S-L-K-E-Y-L-P-K	946 - 970	224	C-P-P-N-C-P-D-E-V-Y-Q-L-M-R-K-C-W-E-F-Q-P-S-N-R-T	1116 - 1140
191	G-I-K-L-I-M-E-F-L-P-S-G-S-L-K-E-Y-L-P-K-N-K-N-K-I	951 - 975	225	P-D-E-V-Y-Q-L-M-R-K-C-W-E-F-Q-P-S-N-R-T-S-F-Q-N-L	1121 - 1145
192	M-E-F-L-P-S-G-S-L-K-E-Y-L-P-K-N-K-N-K-I-N-L-K-Q-Q	956 - 980	226	Q-L-M-R-K-C-W-E-F-Q-P-S-N-R-T-S-F-Q-N-L-I-E-G-F-E	1126 - 1150
193	S-G-S-L-K-E-Y-L-P-K-N-K-N-K-I-N-L-K-Q-Q-L-K-Y-A-V	961 - 985	227	K-C-W-E-F-Q-P-S-N-R-T-S-F-Q-N-L-I-E-G-F-E-A-L-L-K	1131 - 1155
194	E-Y-L-P-K-N-K-N-K-I-N-L-K-Q-Q-L-K-Y-A-V-Q-I-C-K-G	966 - 990	228	H-M-R-S-A-M-S-G-L-H-L-V-K-R-R	SAMS peptide

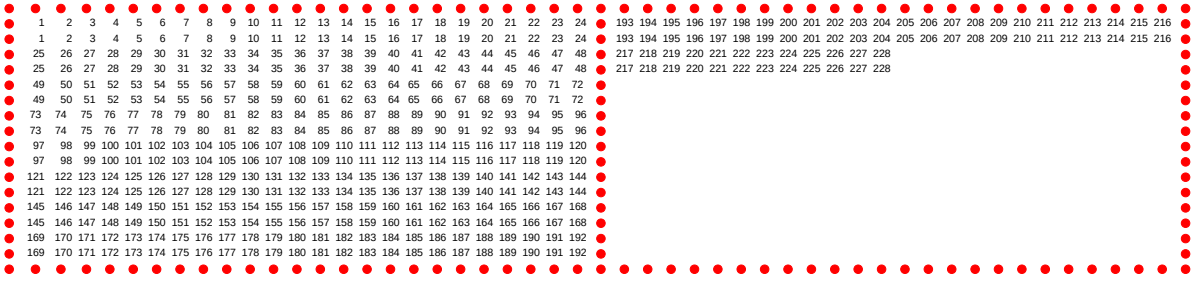

Table 6-1: **Peptide array spanning the human JAK1 open reading frame**

Full length JAK2 Peptide Array					
Array Position	Peptide sequence	Amino Acid Position	Array Position	Peptide sequence	Amino Acid Position
1	M-G-M-A-C-L-T-M-T-E-M-E-G-T-S-T-S-S-I-Y-Q-N-G-D-I	1 - 25	81	H-G-P-I-S-M-D-F-A-I-S-K-L-K-K-A-G-N-Q-T-G-L-Y-V-L	401 - 425
2	L-T-M-T-E-M-E-G-T-S-T-S-S-I-Y-Q-N-G-D-I-S-G-N-A-N	6 - 30	82	M-D-F-A-I-S-K-L-K-K-A-G-N-Q-T-G-L-Y-V-L-R-C-S-P-K	406 - 430
3	M-E-G-T-S-T-S-S-I-Y-Q-N-G-D-I-S-G-N-A-N-S-M-K-Q-I	11 - 35	83	S-K-L-K-K-A-G-N-Q-T-G-L-Y-V-L-R-C-S-P-K-D-F-N-K-Y	411 - 435
4	T-S-S-I-Y-Q-N-G-D-I-S-G-N-A-N-S-M-K-Q-I-D-P-V-L-Q	16 - 40	84	A-G-N-Q-T-G-L-Y-V-L-R-C-S-P-K-D-F-N-K-Y-F-L-T-F-A	416 - 440
5	Q-N-G-D-I-S-G-N-A-N-S-M-K-Q-I-D-P-V-L-Q-V-Y-L-Y-H	21 - 45	85	G-L-Y-V-L-R-C-S-P-K-D-F-N-K-Y-F-L-T-F-A-V-E-R-E-N	421 - 445
6	S-G-N-A-N-S-M-K-Q-I-D-P-V-L-Q-V-Y-L-Y-H-S-L-G-K-S	26 - 50	86	R-C-S-P-K-D-F-N-K-Y-F-L-T-F-A-V-E-R-E-N-V-I-E-Y-K	426 - 450
7	S-M-K-Q-I-D-P-V-L-Q-V-Y-L-Y-H-S-L-G-K-S-E-A-D-Y-L	31 - 55	87	D-F-N-K-Y-F-L-T-F-A-V-E-R-E-N-V-I-E-Y-K-H-C-L-I-T	431 - 455
8	D-P-V-L-Q-V-Y-L-Y-H-S-L-G-K-S-E-A-D-Y-L-T-F-P-S-G	36 - 60	88	F-L-T-F-A-V-E-R-E-N-V-I-E-Y-K-H-C-L-I-T-K-N-E-N-E	436 - 460
9	V-Y-L-Y-H-S-L-G-K-S-E-A-D-Y-L-T-F-P-S-G-E-Y-V-A-E	41 - 65	89	V-E-R-E-N-V-I-E-Y-K-H-C-L-I-T-K-N-E-N-E-E-Y-N-L-S	441 - 465
10	S-L-G-K-S-E-A-D-Y-L-T-F-P-S-G-E-Y-V-A-E-E-I-C-I-A	46 - 70	90	V-I-E-Y-K-H-C-L-I-T-K-N-E-N-E-E-Y-N-L-S-G-T-K-K-N	446 - 470
11	E-A-D-Y-L-T-F-P-S-G-E-Y-V-A-E-E-I-C-I-A-A-S-K-A-C	51 - 75	91	H-C-L-I-T-K-N-E-N-E-E-Y-N-L-S-G-T-K-K-N-F-S-S-L-K	451 - 475
12	T-F-P-S-G-E-Y-V-A-E-E-I-C-I-A-A-S-K-A-C-G-I-T-P-V	56 - 80	92	K-N-E-N-E-E-Y-N-L-S-G-T-K-K-N-F-S-S-L-K-D-L-L-N-C	456 - 480
13	E-Y-V-A-E-E-I-C-I-A-A-S-K-A-C-G-I-T-P-V-Y-H-N-M-F	61 - 85	93	E-Y-N-L-S-G-T-K-K-N-F-S-S-L-K-D-L-L-N-C-Y-Q-M-E-T	461 - 485
14	E-I-C-I-A-A-S-K-A-C-G-I-T-P-V-Y-H-N-M-F-A-L-M-S-E	66 - 90	94	G-T-K-K-N-F-S-S-L-K-D-L-L-N-C-Y-Q-M-E-T-V-R-S-D-N	466 - 490
15	A-S-K-A-C-G-I-T-P-V-Y-H-N-M-F-A-L-M-S-E-T-E-R-I-W	71 - 95	95	F-S-S-L-K-D-L-L-N-C-Y-Q-M-E-T-V-R-S-D-N-I-I-F-Q-F	471 - 495
16	G-I-T-P-V-Y-H-N-M-F-A-L-M-S-E-T-E-R-I-W-Y-P-P-N-H	76 - 100	96	D-L-L-N-C-Y-Q-M-E-T-V-R-S-D-N-I-I-F-Q-F-T-K-C-C-P	476 - 500
17	Y-H-N-M-F-A-L-M-S-E-T-E-R-I-W-Y-P-P-N-H-V-F-H-I-D	81 - 105	97	Y-Q-M-E-T-V-R-S-D-N-I-I-F-Q-F-T-K-C-C-P-P-K-P-K-D	481 - 505
18	A-L-M-S-E-T-E-R-I-W-Y-P-P-N-H-V-F-H-I-D-E-S-T-R-H	86 - 110	98	V-R-S-D-N-I-I-F-Q-F-T-K-C-C-P-P-K-P-K-D-K-S-N-L-L	486 - 510
19	T-E-R-I-W-Y-P-P-N-H-V-F-H-I-D-E-S-T-R-H-N-V-L-Y-R	91 - 115	99	I-I-F-Q-F-T-K-C-C-P-P-K-P-K-D-K-S-N-L-L-V-F-R-T-N	491 - 515
20	Y-P-P-N-H-V-F-H-I-D-E-S-T-R-H-N-V-L-Y-R-I-R-F-Y-F	96 - 120	100	T-K-C-C-P-P-K-P-K-D-K-S-N-L-L-V-F-R-T-N-G-V-S-D-V	496 - 520
21	V-F-H-I-D-E-S-T-R-H-N-V-L-Y-R-I-R-F-Y-F-P-R-W-Y-C	101 - 125	101	P-K-P-K-D-K-S-N-L-L-V-F-R-T-N-G-V-S-D-V-P-T-S-P-T	501 - 525
22	E-S-T-R-H-N-V-L-Y-R-I-R-F-Y-F-P-R-W-Y-C-S-G-S-N-R	106 - 130	102	K-S-N-L-L-V-F-R-T-N-G-V-S-D-V-P-T-S-P-T-L-Q-R-P-T	506 - 530
23	N-V-L-Y-R-I-R-F-Y-F-P-R-W-Y-C-S-G-S-N-R-A-Y-R-H-G	111 - 135	103	V-F-R-T-N-G-V-S-D-V-P-T-S-P-T-L-Q-R-P-T-H-M-N-Q-M	511 - 535
24	I-R-F-Y-F-P-R-W-Y-C-S-G-S-N-R-A-Y-R-H-G-I-S-R-G-A	116 - 140	104	G-V-S-D-V-P-T-S-P-T-L-Q-R-P-T-H-M-N-Q-M-V-F-H-K-I	516 - 540
25	P-R-W-Y-C-S-G-S-N-R-A-Y-R-H-G-I-S-R-G-A-E-A-P-L-L	121 - 145	105	P-T-S-P-T-L-Q-R-P-T-H-M-N-Q-M-V-F-H-K-I-R-N-E-D-L	521 - 545
26	S-G-S-N-R-A-Y-R-H-G-I-S-R-G-A-E-A-P-L-L-D-D-F-V-M	126 - 150	106	L-Q-R-P-T-H-M-N-Q-M-V-F-H-K-I-R-N-E-D-L-I-F-N-E-S	526 - 550
27	A-Y-R-H-G-I-S-R-G-A-E-A-P-L-L-D-D-F-V-M-S-Y-L-F-A	131 - 155	107	H-M-N-Q-M-V-F-H-K-I-R-N-E-D-L-I-F-N-E-S-L-G-Q-G-T	531 - 555
28	I-S-R-G-A-E-A-P-L-L-D-D-F-V-M-S-Y-L-F-A-Q-W-R-H-D	136 - 160	108	V-F-H-K-I-R-N-E-D-L-I-F-N-E-S-L-G-Q-G-T-F-T-K-I-F	536 - 560
29	E-A-P-L-L-D-D-F-V-M-S-Y-L-F-A-Q-W-R-H-D-F-V-H-G-W	141 - 165	109	R-N-E-D-L-I-F-N-E-S-L-G-Q-G-T-F-T-K-I-F-K-G-V-R-R	541 - 565
30	D-D-F-V-M-S-Y-L-F-A-Q-W-R-H-D-F-V-H-G-W-I-K-V-P-V	146 - 170	110	I-F-N-E-S-L-G-Q-G-T-F-T-K-I-F-K-G-V-R-R-E-V-G-D-Y	546 - 570
31	S-Y-L-F-A-Q-W-R-H-D-F-V-H-G-W-I-K-V-P-V-T-H-E-T-Q	151 - 175	111	L-G-Q-G-T-F-T-K-I-F-K-G-V-R-R-E-V-G-D-Y-G-Q-L-H-E	551 - 575
32	Q-W-R-H-D-F-V-H-G-W-I-K-V-P-V-T-H-E-T-Q-E-E-C-L-G	156 - 180	112	F-T-K-I-F-K-G-V-R-R-E-V-G-D-Y-G-Q-L-H-E-T-E-V-L-L	556 - 580
33	F-V-H-G-W-I-K-V-P-V-T-H-E-T-Q-E-E-C-L-G-M-A-V-L-D	161 - 185	113	K-G-V-R-R-E-V-G-D-Y-G-Q-L-H-E-T-E-V-L-L-K-V-L-D-K	561 - 585
34	I-K-V-P-V-T-H-E-T-Q-E-E-C-L-G-M-A-V-L-D-M-M-R-I-A	166 - 190	114	E-V-G-D-Y-G-Q-L-H-E-T-E-V-L-L-K-V-L-D-K-A-H-R-N-Y	566 - 590
35	T-H-E-T-Q-E-E-C-L-G-M-A-V-L-D-M-M-R-I-A-K-E-N-D-Q	171 - 195	115	G-Q-L-H-E-T-E-V-L-L-K-V-L-D-K-A-H-R-N-Y-S-E-S-F-F	571 - 595
36	E-E-C-L-G-M-A-V-L-D-M-M-R-I-A-K-E-N-D-Q-T-P-L-A-I	176 - 200	116	T-E-V-L-L-K-V-L-D-K-A-H-R-N-Y-S-E-S-F-F-E-A-A-S-M	576 - 600
37	M-A-V-L-D-M-M-R-I-A-K-E-N-D-Q-T-P-L-A-I-Y-N-S-I-S	181 - 205	117	K-V-L-D-K-A-H-R-N-Y-S-E-S-F-F-E-A-A-S-M-M-S-K-L-S	581 - 605
38	M-M-R-I-A-K-E-N-D-Q-T-P-L-A-I-Y-N-S-I-S-Y-K-T-F-L	186 - 210	118	A-H-R-N-Y-S-E-S-F-F-E-A-A-S-M-M-S-K-L-S-H-K-H-L-V	586 - 610
39	K-E-N-D-Q-T-P-L-A-I-Y-N-S-I-S-Y-K-T-F-L-P-K-C-I-R	191 - 215	119	S-E-S-F-F-E-A-A-S-M-M-S-K-L-S-H-K-H-L-V-L-N-Y-G-V	591 - 615
40	T-P-L-A-I-Y-N-S-I-S-Y-K-T-F-L-P-K-C-I-R-A-K-I-Q-D	196 - 220	120	E-A-A-S-M-M-S-K-L-S-H-K-H-L-V-L-N-Y-G-V-C-V-C-G-D	596 - 620
41	Y-N-S-I-S-Y-K-T-F-L-P-K-C-I-R-A-K-I-Q-D-Y-H-I-L-T	201 - 225	121	M-S-K-L-S-H-K-H-L-V-L-N-Y-G-V-C-V-C-G-D-E-N-I-L-V	601 - 625
42	Y-K-T-F-L-P-K-C-I-R-A-K-I-Q-D-Y-H-I-L-T-R-K-R-I-R	206 - 230	122	H-K-H-L-V-L-N-Y-G-V-C-V-C-G-D-E-N-I-L-V-Q-E-F-V-K	606 - 630
43	P-K-C-I-R-A-K-I-Q-D-Y-H-I-L-T-R-K-R-I-R-Y-R-F-R-R	211 - 235	123	L-N-Y-G-V-C-V-C-G-D-E-N-I-L-V-Q-E-F-V-K-F-G-S-L-D	611 - 635
44	A-K-I-Q-D-Y-H-I-L-T-R-K-R-I-R-Y-R-F-R-R-F-I-Q-Q-F	216 - 240	124	C-V-C-G-D-E-N-I-L-V-Q-E-F-V-K-F-G-S-L-D-T-Y-L-K-K	616 - 640
45	Y-H-I-L-T-R-K-R-I-R-Y-R-F-R-R-F-I-Q-Q-F-S-Q-C-K-A	221 - 245	125	E-N-I-L-V-Q-E-F-V-K-F-G-S-L-D-T-Y-L-K-K-N-K-N-C-I	621 - 645
46	R-K-R-I-R-Y-R-F-R-R-F-I-Q-Q-F-S-Q-C-K-A-T-A-R-N-L	226 - 250	126	Q-E-F-V-K-F-G-S-L-D-T-Y-L-K-K-N-K-N-C-I-N-I-L-W-K	626 - 650
47	Y-R-F-R-R-F-I-Q-Q-F-S-Q-C-K-A-T-A-R-N-L-K-L-K-Y-L	231 - 255	127	F-G-S-L-D-T-Y-L-K-K-N-K-N-C-I-N-I-L-W-K-L-E-V-A-K	631 - 655
48	F-I-Q-Q-F-S-Q-C-K-A-T-A-R-N-L-K-L-K-Y-L-I-N-L-E-T	236 - 260	128	T-Y-L-K-K-N-K-N-C-I-N-I-L-W-K-L-E-V-A-K-Q-L-A-W-A	636 - 660
49	S-Q-C-K-A-T-A-R-N-L-K-L-K-Y-L-I-N-L-E-T-L-Q-S-A-F	241 - 265	129	N-K-N-C-I-N-I-L-W-K-L-E-V-A-K-Q-L-A-W-A-M-H-F-L-E	641 - 665
50	T-A-R-N-L-K-L-K-Y-L-I-N-L-E-T-L-Q-S-A-F-Y-T-E-K-F	246 - 270	130	N-I-L-W-K-L-E-V-A-K-Q-L-A-W-A-M-H-F-L-E-E-N-T-L-I	646 - 670
51	K-L-K-Y-L-I-N-L-E-T-L-Q-S-A-F-Y-T-E-K-F-E-V-K-E-P	251 - 275	131	L-E-V-A-K-Q-L-A-W-A-M-H-F-L-E-E-N-T-L-I-H-G-N-V-C	651 - 675
52	I-N-L-E-T-L-Q-S-A-F-Y-T-E-K-F-E-V-K-E-P-G-S-G-P-S	256 - 280	132	Q-L-A-W-A-M-H-F-L-E-E-N-T-L-I-H-G-N-V-C-A-K-N-I-L	656 - 680
53	L-Q-S-A-F-Y-T-E-K-F-E-V-K-E-P-G-S-G-P-S-G-E-E-I-F	261 - 285	133	M-H-F-L-E-E-N-T-L-I-H-G-N-V-C-A-K-N-I-L-L-I-R-E-E	661 - 685
54	Y-T-E-K-F-E-V-K-E-P-G-S-G-P-S-G-E-E-I-F-A-T-I-I-I	266 - 290	134	E-N-T-L-I-H-G-N-V-C-A-K-N-I-L-L-I-R-E-E-D-R-K-T-G	666 - 690
55	E-V-K-E-P-G-S-G-P-S-G-E-E-I-F-A-T-I-I-I-T-G-N-G-G	271 - 295	135	H-G-N-V-C-A-K-N-I-L-L-I-R-E-E-D-R-K-T-G-N-P-P-F-I	671 - 695
56	G-S-G-P-S-G-E-E-I-F-A-T-I-I-I-T-G-N-G-G-I-Q-W-S-R	276 - 300	136	A-K-N-I-L-L-I-R-E-E-D-R-K-T-G-N-P-P-F-I-K-L-S-D-P	676 - 700
57	G-E-E-I-F-A-T-I-I-I-T-G-N-G-G-I-Q-W-S-R-G-K-H-K-E	281 - 305	137	L-I-R-E-E-D-R-K-T-G-N-P-P-F-I-K-L-S-D-P-G-I-S-I-T	681 - 705
58	A-T-I-I-I-T-G-N-G-G-I-Q-W-S-R-G-K-H-K-E-S-E-T-L-T	286 - 310	138	D-R-K-T-G-N-P-P-F-I-K-L-S-D-P-G-I-S-I-T-V-L-P-K-D	686 - 710
59	T-G-N-G-G-I-Q-W-S-R-G-K-H-K-E-S-E-T-L-T-E-Q-D-L-Q	291 - 315	139	N-P-P-F-I-K-L-S-D-P-G-I-S-I-T-V-L-P-K-D-I-L-Q-E-R	691 - 715
60	I-Q-W-S-R-G-K-H-K-E-S-E-T-L-T-E-Q-D-L-Q-L-Y-C-D-F	296 - 320	140	K-L-S-D-P-G-I-S-I-T-V-L-P-K-D-I-L-Q-E-R-I-P-W-V-P	696 - 720
61	G-K-H-K-E-S-E-T-L-T-E-Q-D-L-Q-L-Y-C-D-F-P-N-I-I-D	301 - 325	141	G-I-S-I-T-V-L-P-K-D-I-L-Q-E-R-I-P-W-V-P-P-E-C-I-E	701 - 725
62	S-E-T-L-T-E-Q-D-L-Q-L-Y-C-D-F-P-N-I-I-D-V-S-I-K-Q	306 - 330	142	V-L-P-K-D-I-L-Q-E-R-I-P-W-V-P-P-E-C-I-E-N-P-K-N-L	706 - 730
63	E-Q-D-L-Q-L-Y-C-D-F-P-N-I-I-D-V-S-I-K-Q-A-N-Q-E-G	311 - 335	143	I-L-Q-E-R-I-P-W-V-P-P-E-C-I-E-N-P-K-N-L-N-L-A-T-D	711 - 735
64	L-Y-C-D-F-P-N-I-I-D-V-S-I-K-Q-A-N-Q-E-G-S-N-E-S-R	316 - 340	144	I-P-W-V-P-P-E-C-I-E-N-P-K-N-L-N-L-A-T-D-K-W-S-F-G	716 - 740
65	P-N-I-I-D-V-S-I-K-Q-A-N-Q-E-G-S-N-E-S-R-V-V-T-I-H	321 - 345	145	P-E-C-I-E-N-P-K-N-L-N-L-A-T-D-K-W-S-F-G-T-T-L-W-E	721 - 745
66	V-S-I-K-Q-A-N-Q-E-G-S-N-E-S-R-V-V-T-I-H-K-Q-D-G-K	326 - 350	146	N-P-K-N-L-N-L-A-T-D-K-W-S-F-G-T-T-L-W-E-I-C-S-G-G	726 - 750
67	A-N-Q-E-G-S-N-E-S-R-V-V-T-I-H-K-Q-D-G-K-N-L-E-I-E	331 - 355	147	N-L-A-T-D-K-W-S-F-G-T-T-L-W-E-I-C-S-G-G-D-K-P-L-S	731 - 755
68	S-N-E-S-R-V-V-T-I-H-K-Q-D-G-K-N-L-E-I-E-L-S-S-L-R	336 - 360	148	K-W-S-F-G-T-T-L-W-E-I-C-S-G-G-D-K-P-L-S-A-L-D-S-Q	736 - 760
69	V-V-T-I-H-K-Q-D-G-K-N-L-E-I-E-L-S-S-L-R-E-A-L-S-F	341 - 365	149	T-T-L-W-E-I-C-S-G-G-D-K-P-L-S-A-L-D-S-Q-R-K-L-Q-F	741 - 765
70	K-Q-D-G-K-N-L-E-I-E-L-S-S-L-R-E-A-L-S-F-V-S-L-I-D	346 - 370	150	I-C-S-G-G-D-K-P-L-S-A-L-D-S-Q-R-K-L-Q-F-Y-E-D-R-H	746 - 770
71	N-L-E-I-E-L-S-S-L-R-E-A-L-S-F-V-S-L-I-D-G-Y-Y-R-L	351 - 375	151	D-K-P-L-S-A-L-D-S-Q-R-K-L-Q-F-Y-E-D-R-H-Q-L-P-A-P	751 - 775
72	L-S-S-L-R-E-A-L-S-F-V-S-L-I-D-G-Y-Y-R-L-T-A-D-A-H	356 - 380	152	A-L-D-S-Q-R-K-L-Q-F-Y-E-D-R-H-Q-L-P-A-P-K-W-A-E-L	756 - 780
73	E-A-L-S-F-V-S-L-I-D-G-Y-Y-R-L-T-A-D-A-H-H-Y-L-C-K	361 - 385	153	R-K-L-Q-F-Y-E-D-R-H-Q-L-P-A-P-K-W-A-E-L-A-N-L-I-N	761 - 785
74	V-S-L-I-D-G-Y-Y-R-L-T-A-D-A-H-H-Y-L-C-K-E-V-A-P-P	366 - 390	154	Y-E-D-R-H-Q-L-P-A-P-K-W-A-E-L-A-N-L-I-N-N-C-M-D-Y	766 - 790
75	G-Y-Y-R-L-T-A-D-A-H-H-Y-L-C-K-E-V-A-P-P-A-V-L-E-N	371 - 395	155	Q-L-P-A-P-K-W-A-E-L-A-N-L-I-N-N-C-M-D-Y-E-P-D-F-R	771 - 795
76	T-A-D-A-H-H-Y-L-C-K-E-V-A-P-P-A-V-L-E-N-I-Q-S-N-C	376 - 400	156	K-W-A-E-L-A-N-L-I-N-N-C-M-D-Y-E-P-D-F-R-P-S-F-R-A	776 - 800
77	H-Y-L-C-K-E-V-A-P-P-A-V-L-E-N-I-Q-S-N-C-H-G-P-I-S	381 - 405	157	A-N-L-I-N-N-C-M-D-Y-E-P-D-F-R-P-S-F-R-A-I-I-R-D-L	781 - 805
78	E-V-A-P-P-A-V-L-E-N-I-Q-S-N-C-H-G-P-I-S-M-D-F-A-I	386 - 410	158	N-C-M-D-Y-E-P-D-F-R-P-S-F-R-A-I-I-R-D-L-N-S-L-F-T	786 - 810
79	A-V-L-E-N-I-Q-S-N-C-H-G-P-I-S-M-D-F-A-I-S-K-L-K-K	391 - 415	159	E-P-D-F-R-P-S-F-R-A-I-I-R-D-L-N-S-L-F-T-P-D-Y-E-L	791 - 815
80	I-Q-S-N-C-H-G-P-I-S-M-D-F-A-I-S-K-L-K-K-A-G-N-Q-T	396 - 420	160	P-S-F-R-A-I-I-R-D-L-N-S-L-F-T-P-D-Y-E-L-L-T-E-N-D	796 - 820

Table 6-2: **Peptide array spanning the human JAK2 open reading frame**

(continued overleaf)

Full length JAK2 Peptide Array					
Array Position	Peptide sequence	Amino Acid Position	Array Position	Peptide sequence	Amino Acid Position
161	I-I-R-D-L-N-S-L-F-T-P-D-Y-E-L-L-T-E-N-D-M-L-P-N-M	801 - 825	193	C-K-G-M-E-Y-L-G-T-K-R-Y-I-H-R-D-L-A-T-R-N-I-L-V-E	961 - 985
162	N-S-L-F-T-P-D-Y-E-L-L-T-E-N-D-M-L-P-N-M-R-I-G-A-L	806 - 830	194	Y-L-G-T-K-R-Y-I-H-R-D-L-A-T-R-N-I-L-V-E-N-E-N-R-V	966 - 990
163	P-D-Y-E-L-L-T-E-N-D-M-L-P-N-M-R-I-G-A-L-G-F-S-G-A	811 - 835	195	R-Y-I-H-R-D-L-A-T-R-N-I-L-V-E-N-E-N-R-V-K-I-G-D-F	971 - 995
164	L-T-E-N-D-M-L-P-N-M-R-I-G-A-L-G-F-S-G-A-F-E-D-R-D	816 - 840	196	D-L-A-T-R-N-I-L-V-E-N-E-N-R-V-K-I-G-D-F-G-L-T-K-V	976 - 1000
165	M-L-P-N-M-R-I-G-A-L-G-F-S-G-A-F-E-D-R-D-P-T-Q-F-E	821 - 845	197	N-I-L-V-E-N-E-N-R-V-K-I-G-D-F-G-L-T-K-V-L-P-Q-D-K	981 - 1005
166	R-I-G-A-L-G-F-S-G-A-F-E-D-R-D-P-T-Q-F-E-E-R-H-L-K	826 - 850	198	N-E-N-R-V-K-I-G-D-F-G-L-T-K-V-L-P-Q-D-K-E-Y-Y-K-V	986 - 1010
167	G-F-S-G-A-F-E-D-R-D-P-T-Q-F-E-E-R-H-L-K-F-L-Q-Q-L	831 - 855	199	K-I-G-D-F-G-L-T-K-V-L-P-Q-D-K-E-Y-Y-K-V-K-E-P-G-E	991 - 1015
168	F-E-D-R-D-P-T-Q-F-E-E-R-H-L-K-F-L-Q-Q-L-G-K-G-N-F	836 - 860	200	G-L-T-K-V-L-P-Q-D-K-E-Y-Y-K-V-K-E-P-G-E-S-P-I-F-W	996 - 1020
169	P-T-Q-F-E-E-R-H-L-K-F-L-Q-Q-L-G-K-G-N-F-G-S-V-E-M	841 - 865	201	L-P-Q-D-K-E-Y-Y-K-V-K-E-P-G-E-S-P-I-F-W-Y-A-P-E-S	1001 - 1025
170	E-R-H-L-K-F-L-Q-Q-L-G-K-G-N-F-G-S-V-E-M-C-R-Y-D-P	846 - 870	202	E-Y-Y-K-V-K-E-P-G-E-S-P-I-F-W-Y-A-P-E-S-L-T-E-S-K	1006 - 1030
171	F-L-Q-Q-L-G-K-G-N-F-G-S-V-E-M-C-R-Y-D-P-L-Q-D-N-T	851 - 875	203	K-E-P-G-E-S-P-I-F-W-Y-A-P-E-S-L-T-E-S-K-F-S-V-A-S	1011 - 1035
172	G-K-G-N-F-G-S-V-E-M-C-R-Y-D-P-L-Q-D-N-T-G-E-V-V-A	856 - 880	204	S-P-I-F-W-Y-A-P-E-S-L-T-E-S-K-F-S-V-A-S-D-V-W-S-F	1016 - 1040
173	G-S-V-E-M-C-R-Y-D-P-L-Q-D-N-T-G-E-V-V-A-V-K-K-L-Q	861 - 885	205	Y-A-P-E-S-L-T-E-S-K-F-S-V-A-S-D-V-W-S-F-G-V-V-L-Y	1021 - 1045
174	C-R-Y-D-P-L-Q-D-N-T-G-E-V-V-A-V-K-K-L-Q-H-S-T-E-E	866 - 890	206	L-T-E-S-K-F-S-V-A-S-D-V-W-S-F-G-V-V-L-Y-E-L-F-T-Y	1026 - 1050
175	L-Q-D-N-T-G-E-V-V-A-V-K-K-L-Q-H-S-T-E-E-H-L-R-D-F	871 - 895	207	F-S-V-A-S-D-V-W-S-F-G-V-V-L-Y-E-L-F-T-Y-I-E-K-S-K	1031 - 1055
176	G-E-V-V-A-V-K-K-L-Q-H-S-T-E-E-H-L-R-D-F-E-R-E-I-E	876 - 900	208	D-V-W-S-F-G-V-V-L-Y-E-L-F-T-Y-I-E-K-S-K-S-P-P-A-E	1036 - 1060
177	V-K-K-L-Q-H-S-T-E-E-H-L-R-D-F-E-R-E-I-E-I-L-K-S-L	881 - 905	209	G-V-V-L-Y-E-L-F-T-Y-I-E-K-S-K-S-P-P-A-E-F-M-R-M-I	1041 - 1065
178	H-S-T-E-E-H-L-R-D-F-E-R-E-I-E-I-L-K-S-L-Q-H-D-N-I	886 - 910	210	E-L-F-T-Y-I-E-K-S-K-S-P-P-A-E-F-M-R-M-I-G-N-D-K-Q	1046 - 1070
179	H-L-R-D-F-E-R-E-I-E-I-L-K-S-L-Q-H-D-N-I-V-K-Y-K-G	891 - 915	211	I-E-K-S-K-S-P-P-A-E-F-M-R-M-I-G-N-D-K-Q-G-Q-M-I-V	1051 - 1075
180	E-R-E-I-E-I-L-K-S-L-Q-H-D-N-I-V-K-Y-K-G-V-C-Y-S-A	896 - 920	212	S-P-P-A-E-F-M-R-M-I-G-N-D-K-Q-G-Q-M-I-V-F-H-L-I-E	1056 - 1080
181	I-L-K-S-L-Q-H-D-N-I-V-K-Y-K-G-V-C-Y-S-A-G-R-R-N-L	901 - 925	213	F-M-R-M-I-G-N-D-K-Q-G-Q-M-I-V-F-H-L-I-E-L-L-K-N-N	1061 - 1085
182	Q-H-D-N-I-V-K-Y-K-G-V-C-Y-S-A-G-R-R-N-L-K-L-I-M-E	906 - 930	214	G-N-D-K-Q-G-Q-M-I-V-F-H-L-I-E-L-L-K-N-N-G-R-L-P-R	1066 - 1090
183	V-K-Y-K-G-V-C-Y-S-A-G-R-R-N-L-K-L-I-M-E-Y-L-P-Y-G	911 - 935	215	G-Q-M-I-V-F-H-L-I-E-L-L-K-N-N-G-R-L-P-R-P-D-G-C-P	1071 - 1095
184	V-C-Y-S-A-G-R-R-N-L-K-L-I-M-E-Y-L-P-Y-G-S-L-R-D-Y	916 - 940	216	F-H-L-I-E-L-L-K-N-N-G-R-L-P-R-P-D-G-C-P-D-E-I-Y-M	1076 - 1100
185	G-R-R-N-L-K-L-I-M-E-Y-L-P-Y-G-S-L-R-D-Y-L-Q-K-H-K	921 - 945	217	L-L-K-N-N-G-R-L-P-R-P-D-G-C-P-D-E-I-Y-M-I-M-T-E-C	1081 - 1105
186	K-L-I-M-E-Y-L-P-Y-G-S-L-R-D-Y-L-Q-K-H-K-E-R-I-D-H	926 - 950	218	G-R-L-P-R-P-D-G-C-P-D-E-I-Y-M-I-M-T-E-C-W-N-N-N-V	1086 - 1110
187	Y-L-P-Y-G-S-L-R-D-Y-L-Q-K-H-K-E-R-I-D-H-I-K-L-L-Q	931 - 955	219	P-D-G-C-P-D-E-I-Y-M-I-M-T-E-C-W-N-N-N-V-N-Q-R-P-S	1091 - 1115
188	S-L-R-D-Y-L-Q-K-H-K-E-R-I-D-H-I-K-L-L-Q-Y-T-S-Q-I	936 - 960	220	D-E-I-Y-M-I-M-T-E-C-W-N-N-N-V-N-Q-R-P-S-F-R-D-L-A	1096 - 1120
189	L-Q-K-H-K-E-R-I-D-H-I-K-L-L-Q-Y-T-S-Q-I-C-K-G-M-E	941 - 965	221	I-M-T-E-C-W-N-N-N-V-N-Q-R-P-S-F-R-D-L-A-L-R-V-D-Q	1101 - 1125
190	E-R-I-D-H-I-K-L-L-Q-Y-T-S-Q-I-C-K-G-M-E-Y-L-G-T-K	946 - 970	222	W-N-N-N-V-N-Q-R-P-S-F-R-D-L-A-L-R-V-D-Q-I-R-D-N-M	1106 - 1130
191	I-K-L-L-Q-Y-T-S-Q-I-C-K-G-M-E-Y-L-G-T-K-R-Y-I-H-R	951 - 975	223	N-N-V-N-Q-R-P-S-F-R-D-L-A-L-R-V-D-Q-I-R-D-N-M-A-G	1111 - 1135
192	Y-T-S-Q-I-C-K-G-M-E-Y-L-G-T-K-R-Y-I-H-R-D-L-A-T-R	956 - 980	224	H-M-R-S-A-M-S-G-L-H-L-V-K-R-R	SAMS Peptide

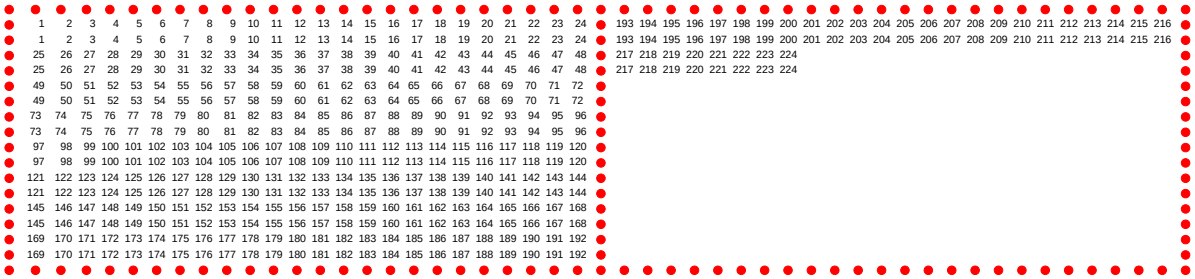

Table 6-2: Peptide array spanning the human JAK2 open reading frame

Array position	JAK Peptide Sequence	Amino Acid position
1	R-Y-S-L-H-G-S-D-R-S-F-P-S-L-G-D-L-M-S-H-L-K-K-Q-I	JAK1 wild type: 506 - 530
2	R-Y-A-L-H-G-A-D-R-A-F-P-A-L-G-D-L-M-A-H-L-K-K-Q-I	JAK1 mutant: S508A, S512A, S515A,
3	R-Y-A-L-H-G-S-D-R-S-F-P-S-L-G-D-L-M-S-H-L-K-K-Q-I	JAK1 mutant: S508A
4	R-Y-S-L-H-G-A-D-R-S-F-P-S-L-G-D-L-M-S-H-L-K-K-Q-I	JAK1 mutant: S512A
5	R-Y-S-L-H-G-S-D-R-A-F-P-S-L-G-D-L-M-S-H-L-K-K-Q-I	JAK1 mutant: S515A
6	R-Y-S-L-H-G-S-D-R-S-F-P-A-L-G-D-L-M-S-H-L-K-K-Q-I	JAK1 mutant: S518A
7	R-Y-S-L-H-G-S-D-R-S-F-P-S-L-G-D-L-M-A-H-L-K-K-Q-I	JAK1 mutant: S524A
8	R-Y-S-L-H-G-S-D-R-A-F-P-A-L-G-D-L-M-S-H-L-K-K-Q-I	JAK1 mutant: S515A and S518A
9	R-Y-A-L-H-G-A-D-R-S-F-P-S-L-G-D-L-M-A-H-L-K-K-Q-I	JAK1 mutant: S508A, S512A and
10	E-Y-N-L-S-G-T-K-K-N-F-S-S-L-K-D-L-L-N-C-Y-Q-M-E-T	JAK2 Wild Type: 461 - 485
11	T-F-L-L-V-G-L-S-R-P-H-S-S-L-R-E-L-L-A-T-C-W-D-G-G	JAK3 Wild Type: 437 - 467
12	A-F-V-L-E-G-W-G-R-S-F-P-S-V-R-E-L-G-A-A-L-Q-G-C-L	TYK2 Wild Type: 513 - 537

Array position	JAK3 Peptide Sequence	Amino Acid position
13	M-A-P-P-S-E-E-T-P-L-I-P-Q-R-S-C-S-L-L-S-T-E-A-G-A	1 - 25
14	E-E-T-P-L-I-P-Q-R-S-C-S-L-L-S-T-E-A-G-A-L-H-V-L-L	6 - 30
15	I-P-Q-R-S-C-S-L-L-S-T-E-A-G-A-L-H-V-L-L-P-A-R-G-P	11 - 35
16	C-S-L-L-S-T-E-A-G-A-L-H-V-L-L-P-A-R-G-P-G-P-P-Q-R	16 - 40
17	T-E-A-G-A-L-H-V-L-L-P-A-R-G-P-G-P-P-Q-R-L-S-F-S-F	21 - 45
18	L-H-V-L-L-P-A-R-G-P-G-P-P-Q-R-L-S-F-S-F-G-D-H-L-A	26 - 50
19	P-A-R-G-P-G-P-P-Q-R-L-S-F-S-F-G-D-H-L-A-E-D-L-C-V	31 - 55
20	G-P-P-Q-R-L-S-F-S-F-G-D-H-L-A-E-D-L-C-V-Q-A-A-K-A	36 - 60
21	L-S-F-S-F-G-D-H-L-A-E-D-L-C-V-Q-A-A-K-A-S-G-I-L-P	41 - 65
22	G-D-H-L-A-E-D-L-C-V-Q-A-A-K-A-S-G-I-L-P-V-Y-H-S-L	46 - 70
23	E-D-L-C-V-Q-A-A-K-A-S-G-I-L-P-V-Y-H-S-L-F-A-L-A-T	51 - 75
24	Q-A-A-K-A-S-G-I-L-P-V-Y-H-S-L-F-A-L-A-T-E-D-L-S-C	56 - 80
25	S-G-I-L-P-V-Y-H-S-L-F-A-L-A-T-E-D-L-S-C-W-F-P-P-S	61 - 85
26	V-Y-H-S-L-F-A-L-A-T-E-D-L-S-C-W-F-P-P-S-H-I-F-S-V	66 - 90
27	F-A-L-A-T-E-D-L-S-C-W-F-P-P-S-H-I-F-S-V-E-D-A-S-T	71 - 95
28	E-D-L-S-C-W-F-P-P-S-H-I-F-S-V-E-D-A-S-T-Q-V-L-L-Y	76 - 100
29	W-F-P-P-S-H-I-F-S-V-E-D-A-S-T-Q-V-L-L-Y-R-I-R-F-Y	81 - 105
30	H-I-F-S-V-E-D-A-S-T-Q-V-L-L-Y-R-I-R-F-Y-F-P-N-W-F	86 - 110
31	E-D-A-S-T-Q-V-L-L-Y-R-I-R-F-Y-F-P-N-W-F-G-L-E-K-C	91 - 115
32	Q-V-L-L-Y-R-I-R-F-Y-F-P-N-W-F-G-L-E-K-C-H-R-F-G-L	96 - 120
33	R-I-R-F-Y-F-P-N-W-F-G-L-E-K-C-H-R-F-G-L-R-K-D-L-A	101 - 125
34	F-P-N-W-F-G-L-E-K-C-H-R-F-G-L-R-K-D-L-A-S-A-I-L-D	106 - 130
35	G-L-E-K-C-H-R-F-G-L-R-K-D-L-A-S-A-I-L-D-L-P-V-L-E	111 - 135
36	H-R-F-G-L-R-K-D-L-A-S-A-I-L-D-L-P-V-L-E-H-L-F-A-Q	116 - 140
37	R-K-D-L-A-S-A-I-L-D-L-P-V-L-E-H-L-F-A-Q-H-R-S-D-L	121 - 145
38	S-A-I-L-D-L-P-V-L-E-H-L-F-A-Q-H-R-S-D-L-V-S-G-R-L	126 - 150
39	L-P-V-L-E-H-L-F-A-Q-H-R-S-D-L-V-S-G-R-L-P-V-G-L-S	131 - 155
40	H-L-F-A-Q-H-R-S-D-L-V-S-G-R-L-P-V-G-L-S-L-K-E-Q-G	136 - 160
41	H-R-S-D-L-V-S-G-R-L-P-V-G-L-S-L-K-E-Q-G-E-C-L-S-L	141 - 165
42	V-S-G-R-L-P-V-G-L-S-L-K-E-Q-G-E-C-L-S-L-A-V-L-D-L	146 - 170
43	P-V-G-L-S-L-K-E-Q-G-E-C-L-S-L-A-V-L-D-L-A-R-M-A-R	151 - 175
44	L-K-E-Q-G-E-C-L-S-L-A-V-L-D-L-A-R-M-A-R-E-Q-A-Q-R	156 - 180
45	E-C-L-S-L-A-V-L-D-L-A-R-M-A-R-E-Q-A-Q-R-P-G-E-L-L	161 - 185
46	A-V-L-D-L-A-R-M-A-R-E-Q-A-Q-R-P-G-E-L-L-K-T-V-S-Y	166 - 190
47	A-R-M-A-R-E-Q-A-Q-R-P-G-E-L-L-K-T-V-S-Y-K-A-C-L-P	171 - 195
48	E-Q-A-Q-R-P-G-E-L-L-K-T-V-S-Y-K-A-C-L-P-P-S-L-R-D	176 - 200
49	P-G-E-L-L-K-T-V-S-Y-K-A-C-L-P-P-S-L-R-D-L-I-Q-G-L	181 - 205
50	K-T-V-S-Y-K-A-C-L-P-P-S-L-R-D-L-I-Q-G-L-S-F-V-T-R	186 - 210
51	K-A-C-L-P-P-S-L-R-D-L-I-Q-G-L-S-F-V-T-R-R-I-R-R	191 - 215
52	P-S-L-R-D-L-I-Q-G-L-S-F-V-T-R-R-R-I-R-R-T-V-R-R-A	196 - 220
53	L-I-Q-G-L-S-F-V-T-R-R-R-I-R-R-T-V-R-R-A-L-R-R-V-A	201 - 225
54	S-F-V-T-R-R-R-I-R-R-T-V-R-R-A-L-R-R-V-A-A-C-Q-A-D	206 - 230
55	R-R-I-R-R-T-V-R-R-A-L-R-R-V-A-A-C-Q-A-D-R-H-S-L-M	211 - 235
56	T-V-R-R-A-L-R-R-V-A-A-C-Q-A-D-R-H-S-L-M-A-K-Y-I-M	216 - 240
57	L-R-R-V-A-A-C-Q-A-D-R-H-S-L-M-A-K-Y-I-M-D-L-E-R-L	221 - 245
58	A-C-Q-A-D-R-H-S-L-M-A-K-Y-I-M-D-L-E-R-L-D-P-A-G-A	226 - 250
59	R-H-S-L-M-A-K-Y-I-M-D-L-E-R-L-D-P-A-G-A-A-E-T-F-H	231 - 255
60	A-K-Y-I-M-D-L-E-R-L-D-P-A-G-A-A-E-T-F-H-V-G-L-P-G	236 - 260

Array position	JAK3 Peptide Sequence	Amino Acid position
61	D-L-E-R-L-D-P-A-G-A-A-E-T-F-H-V-G-L-P-G-A-L-G-G-H	241 - 265
62	D-P-A-G-A-A-E-T-F-H-V-G-L-P-G-A-L-G-G-H-D-G-L-G-L	246 - 270
63	A-E-T-F-H-V-G-L-P-G-A-L-G-G-H-D-G-L-G-L-L-R-V-A-G	251 - 275
64	V-G-L-P-G-A-L-G-G-H-D-G-L-G-L-L-R-V-A-G-D-G-G-I-A	256 - 280
65	A-L-G-G-H-D-G-L-G-L-L-R-V-A-G-D-G-G-I-A-W-T-Q-G-E	261 - 285
66	D-G-L-G-L-L-R-V-A-G-D-G-G-I-A-W-T-Q-G-E-Q-E-V-L-Q	266 - 290
67	L-R-V-A-G-D-G-G-I-A-W-T-Q-G-E-Q-E-V-L-Q-P-F-C-D-F	271 - 295
68	D-G-G-I-A-W-T-Q-G-E-Q-E-V-L-Q-P-F-C-D-F-P-E-I-V-D	276 - 300
69	W-T-Q-G-E-Q-E-V-L-Q-P-F-C-D-F-P-E-I-V-D-I-S-I-K-Q	281 - 305
70	Q-E-V-L-Q-P-F-C-D-F-P-E-I-V-D-I-S-I-K-Q-A-P-R-V-G	286 - 310
71	P-F-C-D-F-P-E-I-V-D-I-S-I-K-Q-A-P-R-V-G-P-A-G-E-H	291 - 315
72	P-E-I-V-D-I-S-I-K-Q-A-P-R-V-G-P-A-G-E-H-R-L-V-T-V	296 - 320
73	I-S-I-K-Q-A-P-R-V-G-P-A-G-E-H-R-L-V-T-V-T-R-T-D-N	301 - 325
74	A-P-R-V-G-P-A-G-E-H-R-L-V-T-V-T-R-T-D-N-Q-I-L-E-A	306 - 330
75	P-A-G-E-H-R-L-V-T-V-T-R-T-D-N-Q-I-L-E-A-E-F-P-G-L	311 - 335
76	R-L-V-T-V-T-R-T-D-N-Q-I-L-E-A-E-F-P-G-L-P-E-A-L-S	316 - 340
77	T-R-T-D-N-Q-I-L-E-A-E-F-P-G-L-P-E-A-L-S-F-V-A-L-V	321 - 345
78	Q-I-L-E-A-E-F-P-G-L-P-E-A-L-S-F-V-A-L-V-D-G-Y-F-R	326 - 350
79	E-F-P-G-L-P-E-A-L-S-F-V-A-L-V-D-G-Y-F-R-L-T-T-D-S	331 - 355
80	P-E-A-L-S-F-V-A-L-V-D-G-Y-F-R-L-T-T-D-S-Q-H-F-F-C	336 - 360
81	F-V-A-L-V-D-G-Y-F-R-L-T-T-D-S-Q-H-F-F-C-K-E-V-A-P	341 - 365
82	D-G-Y-F-R-L-T-T-D-S-Q-H-F-F-C-K-E-V-A-P-P-R-L-L-E	346 - 370
83	L-T-T-D-S-Q-H-F-F-C-K-E-V-A-P-P-R-L-L-E-E-V-A-E-Q	351 - 375
84	Q-H-F-F-C-K-E-V-A-P-P-R-L-L-E-E-V-A-E-Q-C-H-G-P-I	356 - 380
85	K-E-V-A-P-P-R-L-L-E-E-V-A-E-Q-C-H-G-P-I-T-L-D-F-A	361 - 385
86	P-R-L-L-E-E-V-A-E-Q-C-H-G-P-I-T-L-D-F-A-I-N-K-L-K	366 - 390
87	E-V-A-E-Q-C-H-G-P-I-T-L-D-F-A-I-N-K-L-K-T-G-G-S-R	371 - 395
88	C-H-G-P-I-T-L-D-F-A-I-N-K-L-K-T-G-G-S-R-P-G-S-Y-V	376 - 400
89	T-L-D-F-A-I-N-K-L-K-T-G-G-S-R-P-G-S-Y-V-L-R-R-S-P	381 - 405
90	I-N-K-L-K-T-G-G-S-R-P-G-S-Y-V-L-R-R-S-P-Q-D-F-D-S	386 - 410
91	T-G-G-S-R-P-G-S-Y-V-L-R-R-S-P-Q-D-F-D-S-F-L-L-T-V	391 - 415
92	P-G-S-Y-V-L-R-R-S-P-Q-D-F-D-S-F-L-L-T-V-C-V-Q-N-P	396 - 420
93	L-R-R-S-P-Q-D-F-D-S-F-L-L-T-V-C-V-Q-N-P-L-G-P-D-Y	401 - 425
94	Q-D-F-D-S-F-L-L-T-V-C-V-Q-N-P-L-G-P-D-Y-K-G-C-L-I	406 - 430
95	F-L-L-T-V-C-V-Q-N-P-L-G-P-D-Y-K-G-C-L-I-R-R-S-P-T	411 - 435
96	C-V-Q-N-P-L-G-P-D-Y-K-G-C-L-I-R-R-S-P-T-G-T-F-L-L	416 - 440
97	L-G-P-D-Y-K-G-C-L-I-R-R-S-P-T-G-T-F-L-L-V-G-L-S-R	421 - 445
98	K-G-C-L-I-R-R-S-P-T-G-T-F-L-L-V-G-L-S-R-P-H-S-S-L	426 - 450
99	R-R-S-P-T-G-T-F-L-L-V-G-L-S-R-P-H-S-S-L-R-E-L-L-A	431 - 455
100	G-T-F-L-L-V-G-L-S-R-P-H-S-S-L-R-E-L-L-A-T-C-W-D-G	436 - 460
101	V-G-L-S-R-P-H-S-S-L-R-E-L-L-A-T-C-W-D-G-G-L-H-V-D	441 - 465
102	P-H-S-S-L-R-E-L-L-A-T-C-W-D-G-G-L-H-V-D-G-V-A-V-T	446 - 470
103	R-E-L-L-A-T-C-W-D-G-G-L-H-V-D-G-V-A-V-T-L-T-S-C-C	451 - 475
104	T-C-W-D-G-G-L-H-V-D-G-V-A-V-T-L-T-S-C-C-I-P-R-P-K	456 - 480
105	G-L-H-V-D-G-V-A-V-T-L-T-S-C-C-I-P-R-P-K-E-K-S-N-L	461 - 485
106	G-V-A-V-T-L-T-S-C-C-I-P-R-P-K-E-K-S-N-L-I-V-V-Q-R	466 - 490
107	L-T-S-C-C-I-P-R-P-K-E-K-S-N-L-I-V-V-Q-R-G-H-S-P-P	471 - 495
108	I-P-R-P-K-E-K-S-N-L-I-V-V-Q-R-G-H-S-P-P-T-S-S-L-V	476 - 500
109	E-K-S-N-L-I-V-V-Q-R-G-H-S-P-P-T-S-S-L-V-Q-P-Q-S-Q	481 - 505
110	I-V-V-Q-R-G-H-S-P-P-T-S-S-L-V-Q-P-Q-S-Q-Y-Q-L-S-Q	486 - 510
111	G-H-S-P-P-T-S-S-L-V-Q-P-Q-S-Q-Y-Q-L-S-Q-M-T-F-H-K	491 - 515
112	T-S-S-L-V-Q-P-Q-S-Q-Y-Q-L-S-Q-M-T-F-H-K-I-P-A-D-S	496 - 520
113	Q-P-Q-S-Q-Y-Q-L-S-Q-M-T-F-H-K-I-P-A-D-S-L-E-W-H-E	501 - 525
114	Y-Q-L-S-Q-M-T-F-H-K-I-P-A-D-S-L-E-W-H-E-N-L-G-H-G	506 - 530
115	M-T-F-H-K-I-P-A-D-S-L-E-W-H-E-N-L-G-H-G-S-F-T-K-I	511 - 535
116	I-P-A-D-S-L-E-W-H-E-N-L-G-H-G-S-F-T-K-I-Y-R-G-C-R	516 - 540
117	L-E-W-H-E-N-L-G-H-G-S-F-T-K-I-Y-R-G-C-R-H-E-V-V-D	521 - 545
118	N-L-G-H-G-S-F-T-K-I-Y-R-G-C-R-H-E-V-V-D-G-E-A-R-K	526 - 550
119	S-F-T-K-I-Y-R-G-C-R-H-E-V-V-D-G-E-A-R-K-T-E-V-L-L	531 - 555
120	Y-R-G-C-R-H-E-V-V-D-G-E-A-R-K-T-E-V-L-L-K-V-M-D-A	536 - 560
121	H-E-V-V-D-G-E-A-R-K-T-E-V-L-L-K-V-M-D-A-K-H-K-N-C	541 - 565

Table 6-3: Peptide array spanning the human JAK3 open reading frame
(continued overleaf)

Array position	JAK3 Peptide Sequence	Amino Acid position
122	G-E-A-R-K-T-E-V-L-L-K-V-M-D-A-K-H-K-N-C-M-E-S-F-L	546 - 570
123	T-E-V-L-L-K-V-M-D-A-K-H-K-N-C-M-E-S-F-L-E-A-A-S-L	551 - 575
124	K-V-M-D-A-K-H-K-N-C-M-E-S-F-L-E-A-A-S-L-M-S-Q-V-S	556 - 580
125	K-H-K-N-C-M-E-S-F-L-E-A-A-S-L-M-S-Q-V-S-Y-R-H-L-V	561 - 585
126	M-E-S-F-L-E-A-A-S-L-M-S-Q-V-S-Y-R-H-L-V-L-L-H-G-V	566 - 590
127	E-A-A-S-L-M-S-Q-V-S-Y-R-H-L-V-L-L-H-G-V-C-M-A-G-D	571 - 595
128	M-S-Q-V-S-Y-R-H-L-V-L-L-H-G-V-C-M-A-G-D-S-T-M-V-Q	576 - 600
129	Y-R-H-L-V-L-L-H-G-V-C-M-A-G-D-S-T-M-V-Q-E-F-V-H-L	581 - 605
130	L-L-H-G-V-C-M-A-G-D-S-T-M-V-Q-E-F-V-H-L-G-A-I-D-M	586 - 610
131	C-M-A-G-D-S-T-M-V-Q-E-F-V-H-L-G-A-I-D-M-Y-L-R-K-R	591 - 615
132	S-T-M-V-Q-E-F-V-H-L-G-A-I-D-M-Y-L-R-K-R-G-H-L-V-P	596 - 620
133	E-F-V-H-L-G-A-I-D-M-Y-L-R-K-R-G-H-L-V-P-A-S-W-K-L	601 - 625
134	G-A-I-D-M-Y-L-R-K-R-G-H-L-V-P-A-S-W-K-L-Q-V-V-K-Q	606 - 630
135	Y-L-R-K-R-G-H-L-V-P-A-S-W-K-L-Q-V-V-K-Q-L-A-Y-A-L	611 - 635
136	G-H-L-V-P-A-S-W-K-L-Q-V-V-K-Q-L-A-Y-A-L-N-Y-L-E-D	616 - 640
137	A-S-W-K-L-Q-V-V-K-Q-L-A-Y-A-L-N-Y-L-E-D-K-G-L-P-H	621 - 645
138	Q-V-V-K-Q-L-A-Y-A-L-N-Y-L-E-D-K-G-L-P-H-G-N-V-S-A	626 - 650
139	L-A-Y-A-L-N-Y-L-E-D-K-G-L-P-H-G-N-V-S-A-R-K-V-L-L	631 - 655
140	N-Y-L-E-D-K-G-L-P-H-G-N-V-S-A-R-K-V-L-L-A-R-E-G-A	636 - 660
141	K-G-L-P-H-G-N-V-S-A-R-K-V-L-L-A-R-E-G-A-D-G-S-P-P	641 - 665
142	G-N-V-S-A-R-K-V-L-L-A-R-E-G-A-D-G-S-P-P-F-I-K-L-S	646 - 670
143	R-K-V-L-L-A-R-E-G-A-D-G-S-P-P-F-I-K-L-S-D-P-G-V-S	651 - 675
144	A-R-E-G-A-D-G-S-P-P-F-I-K-L-S-D-P-G-V-S-P-A-V-L-S	656 - 680
145	D-G-S-P-P-F-I-K-L-S-D-P-G-V-S-P-A-V-L-S-L-E-M-L-T	661 - 685
146	F-I-K-L-S-D-P-G-V-S-P-A-V-L-S-L-E-M-L-T-D-R-I-P-W	666 - 690
147	D-P-G-V-S-P-A-V-L-S-L-E-M-L-T-D-R-I-P-W-V-A-P-E-C	671 - 695
148	P-A-V-L-S-L-E-M-L-T-D-R-I-P-W-V-A-P-E-C-L-R-E-A-Q	676 - 700
149	L-E-M-L-T-D-R-I-P-W-V-A-P-E-C-L-R-E-A-Q-T-L-S-L-E	681 - 705
150	D-R-I-P-W-V-A-P-E-C-L-R-E-A-Q-T-L-S-L-E-A-D-K-W-G	686 - 710
151	V-A-P-E-C-L-R-E-A-Q-T-L-S-L-E-A-D-K-W-G-F-G-A-T-V	691 - 715
152	L-R-E-A-Q-T-L-S-L-E-A-D-K-W-G-F-G-A-T-V-W-E-V-F-S	696 - 720
153	T-L-S-L-E-A-D-K-W-G-F-G-A-T-V-W-E-V-F-S-G-V-T-M-P	701 - 725
154	A-D-K-W-G-F-G-A-T-V-W-E-V-F-S-G-V-T-M-P-I-S-A-L-D	706 - 730
155	F-G-A-T-V-W-E-V-F-S-G-V-T-M-P-I-S-A-L-D-P-A-K-K-L	711 - 735
156	W-E-V-F-S-G-V-T-M-P-I-S-A-L-D-P-A-K-K-L-Q-F-Y-E-D	716 - 740
157	G-V-T-M-P-I-S-A-L-D-P-A-K-K-L-Q-F-Y-E-D-R-Q-Q-L-P	721 - 745
158	I-S-A-L-D-P-A-K-K-L-Q-F-Y-E-D-R-Q-Q-L-P-A-P-K-W-T	726 - 750
159	P-A-K-K-L-Q-F-Y-E-D-R-Q-Q-L-P-A-P-K-W-T-E-L-A-L-L	731 - 755
160	Q-F-Y-E-D-R-Q-Q-L-P-A-P-K-W-T-E-L-A-L-L-I-Q-Q-C-M	736 - 760
161	R-Q-Q-L-P-A-P-K-W-T-E-L-A-L-L-I-Q-Q-C-M-A-Y-E-P-V	741 - 765
162	A-P-K-W-T-E-L-A-L-L-I-Q-Q-C-M-A-Y-E-P-V-Q-R-P-S-F	746 - 770
163	E-L-A-L-L-I-Q-Q-C-M-A-Y-E-P-V-Q-R-P-S-F-R-A-V-I-R	751 - 775
164	I-Q-Q-C-M-A-Y-E-P-V-Q-R-P-S-F-R-A-V-I-R-D-L-N-S-L	756 - 780
165	A-Y-E-P-V-Q-R-P-S-F-R-A-V-I-R-D-L-N-S-L-I-S-S-D-Y	761 - 785
166	Q-R-P-S-F-R-A-V-I-R-D-L-N-S-L-I-S-S-D-Y-E-L-L-S-D	766 - 790
167	R-A-V-I-R-D-L-N-S-L-I-S-S-D-Y-E-L-L-S-D-P-T-P-G-A	771 - 795
168	D-L-N-S-L-I-S-S-D-Y-E-L-L-S-D-P-T-P-G-A-L-A-P-R-D	776 - 800
169	I-S-S-D-Y-E-L-L-S-D-P-T-P-G-A-L-A-P-R-D-G-L-W-N-G	781 - 805
170	E-L-L-S-D-P-T-P-G-A-L-A-P-R-D-G-L-W-N-G-A-Q-L-Y-A	786 - 810
171	P-T-P-G-A-L-A-P-R-D-G-L-W-N-G-A-Q-L-Y-A-C-Q-D-P-T	791 - 815
172	L-A-P-R-D-G-L-W-N-G-A-Q-L-Y-A-C-Q-D-P-T-I-F-E-E-R	796 - 820
173	G-L-W-N-G-A-Q-L-Y-A-C-Q-D-P-T-I-F-E-E-R-H-L-K-Y-I	801 - 825
174	A-Q-L-Y-A-C-Q-D-P-T-I-F-E-E-R-H-L-K-Y-I-S-Q-L-G-K	806 - 830
175	C-Q-D-P-T-I-F-E-E-R-H-L-K-Y-I-S-Q-L-G-K-G-N-F-G-S	811 - 835
176	I-F-E-E-R-H-L-K-Y-I-S-Q-L-G-K-G-N-F-G-S-V-E-L-C-R	816 - 840
177	H-L-K-Y-I-S-Q-L-G-K-G-N-F-G-S-V-E-L-C-R-Y-D-P-L-G	821 - 845

Array position	JAK3 Peptide Sequence	Amino Acid position
178	S-Q-L-G-K-G-N-F-G-S-V-E-L-C-R-Y-D-P-L-G-D-N-T-G-A	826 - 850
179	G-N-F-G-S-V-E-L-C-R-Y-D-P-L-G-D-N-T-G-A-L-V-A-V-K	831 - 855
180	V-E-L-C-R-Y-D-P-L-G-D-N-T-G-A-L-V-A-V-K-Q-L-Q-H-S	836 - 860
181	Y-D-P-L-G-D-N-T-G-A-L-V-A-V-K-Q-L-Q-H-S-G-P-D-Q-Q	841 - 865
182	D-N-T-G-A-L-V-A-V-K-Q-L-Q-H-S-G-P-D-Q-Q-R-D-F-Q-R	846 - 870
183	L-V-A-V-K-Q-L-Q-H-S-G-P-D-Q-Q-R-D-F-Q-R-E-I-Q-I-L	851 - 875
184	Q-L-Q-H-S-G-P-D-Q-Q-R-D-F-Q-R-E-I-Q-I-L-K-A-L-H-S	856 - 880
185	G-P-D-Q-Q-R-D-F-Q-R-E-I-Q-I-L-K-A-L-H-S-D-F-I-V-K	861 - 885
186	R-D-F-Q-R-E-I-Q-I-L-K-A-L-H-S-D-F-I-V-K-Y-R-G-V-S	866 - 890
187	E-I-Q-I-L-K-A-L-H-S-D-F-I-V-K-Y-R-G-V-S-Y-G-P-G-R	871 - 895
188	K-A-L-H-S-D-F-I-V-K-Y-R-G-V-S-Y-G-P-G-R-Q-S-L-R-L	876 - 900
189	D-F-I-V-K-Y-R-G-V-S-Y-G-P-G-R-Q-S-L-R-L-V-M-E-Y-L	881 - 905
190	Y-R-G-V-S-Y-G-P-G-R-Q-S-L-R-L-V-M-E-Y-L-P-S-G-C-L	886 - 910
191	Y-G-P-G-R-Q-S-L-R-L-V-M-E-Y-L-P-S-G-C-L-R-D-F-L-Q	891 - 915
192	Q-S-L-R-L-V-M-E-Y-L-P-S-G-C-L-R-D-F-L-Q-R-H-R-A-R	896 - 920
193	V-M-E-Y-L-P-S-G-C-L-R-D-F-L-Q-R-H-R-A-R-L-D-A-S-R	901 - 925
194	P-S-G-C-L-R-D-F-L-Q-R-H-R-A-R-L-D-A-S-R-L-L-L-Y-S	906 - 930
195	R-D-F-L-Q-R-H-R-A-R-L-D-A-S-R-L-L-L-Y-S-S-Q-I-C-K	911 - 935
196	R-H-R-A-R-L-D-A-S-R-L-L-L-Y-S-S-Q-I-C-K-G-M-E-Y-L	916 - 940
197	L-D-A-S-R-L-L-L-Y-S-S-Q-I-C-K-G-M-E-Y-L-G-S-R-R-C	921 - 945
198	L-L-L-Y-S-S-Q-I-C-K-G-M-E-Y-L-G-S-R-R-C-V-H-R-D-L	926 - 950
199	S-Q-I-C-K-G-M-E-Y-L-G-S-R-R-C-V-H-R-D-L-A-A-R-N-I	931 - 955
200	G-M-E-Y-L-G-S-R-R-C-V-H-R-D-L-A-A-R-N-I-L-V-E-S-E	936 - 960
201	G-S-R-R-C-V-H-R-D-L-A-A-R-N-I-L-V-E-S-E-A-H-V-K-I	941 - 965
202	V-H-R-D-L-A-A-R-N-I-L-V-E-S-E-A-H-V-K-I-A-D-F-G-L	946 - 970
203	A-A-R-N-I-L-V-E-S-E-A-H-V-K-I-A-D-F-G-L-A-K-L-L-P	951 - 975
204	L-V-E-S-E-A-H-V-K-I-A-D-F-G-L-A-K-L-L-P-L-D-K-D-Y	956 - 980
205	A-H-V-K-I-A-D-F-G-L-A-K-L-L-P-L-D-K-D-Y-Y-V-V-R-E	961 - 985
206	A-D-F-G-L-A-K-L-L-P-L-D-K-D-Y-Y-V-V-R-E-P-G-Q-S-P	966 - 990
207	A-K-L-L-P-L-D-K-D-Y-Y-V-V-R-E-P-G-Q-S-P-I-F-W-Y-A	971 - 995
208	L-D-K-D-Y-Y-V-V-R-E-P-G-Q-S-P-I-F-W-Y-A-P-E-S-L-S	976 - 1000
209	Y-V-V-R-E-P-G-Q-S-P-I-F-W-Y-A-P-E-S-L-S-D-N-I-F-S	981 - 1005
210	P-G-Q-S-P-I-F-W-Y-A-P-E-S-L-S-D-N-I-F-S-R-Q-S-D-V	986 - 1010
211	I-F-W-Y-A-P-E-S-L-S-D-N-I-F-S-R-Q-S-D-V-W-S-F-G-V	991 - 1015
212	P-E-S-L-S-D-N-I-F-S-R-Q-S-D-V-W-S-F-G-V-V-L-Y-E-L	996 - 1020
213	D-N-I-F-S-R-Q-S-D-V-W-S-F-G-V-V-L-Y-E-L-F-T-Y-C-D	1001 - 1025
214	R-Q-S-D-V-W-S-F-G-V-V-L-Y-E-L-F-T-Y-C-D-K-S-C-S-P	1006 - 1030
215	W-S-F-G-V-V-L-Y-E-L-F-T-Y-C-D-K-S-C-S-P-S-A-E-F-L	1011 - 1035
216	V-L-Y-E-L-F-T-Y-C-D-K-S-C-S-P-S-A-E-F-L-R-M-M-G-C	1016 - 1040
217	F-T-Y-C-D-K-S-C-S-P-S-A-E-F-L-R-M-M-G-C-E-R-D-V-P	1021 - 1045
218	K-S-C-S-P-S-A-E-F-L-R-M-M-G-C-E-R-D-V-P-A-L-C-R-L	1026 - 1050
219	S-A-E-F-L-R-M-M-G-C-E-R-D-V-P-A-L-C-R-L-L-E-L-L-E	1031 - 1055
220	R-M-M-G-C-E-R-D-V-P-A-L-C-R-L-L-E-L-L-E-E-G-Q-R-L	1036 - 1060
221	E-R-D-V-P-A-L-C-R-L-L-E-L-L-E-E-G-Q-R-L-P-A-P-P-A	1041 - 1065
222	A-L-C-R-L-L-E-L-L-E-E-G-Q-R-L-P-A-P-P-A-C-P-A-E-V	1046 - 1070
223	L-E-L-L-E-E-G-Q-R-L-P-A-P-P-A-C-P-A-E-V-H-E-L-M-K	1051 - 1075
224	E-G-Q-R-L-P-A-P-P-A-C-P-A-E-V-H-E-L-M-K-L-C-W-A-P	1056 - 1080
225	P-A-P-P-A-C-P-A-E-V-H-E-L-M-K-L-C-W-A-P-S-P-Q-D-R	1061 - 1085
226	C-P-A-E-V-H-E-L-M-K-L-C-W-A-P-S-P-Q-D-R-P-S-F-S-A	1066 - 1090
227	H-E-L-M-K-L-C-W-A-P-S-P-Q-D-R-P-S-F-S-A-L-G-P-Q-L	1071 - 1095
228	L-C-W-A-P-S-P-Q-D-R-P-S-F-S-A-L-G-P-Q-L-D-M-L-W-S	1076 - 1100
229	S-P-Q-D-R-P-S-F-S-A-L-G-P-Q-L-D-M-L-W-S-G-S-R-G-C	1081 - 1105
230	P-S-F-S-A-L-G-P-Q-L-D-M-L-W-S-G-S-R-G-C-E-T-H-A-F	1086 - 1110
231	L-G-P-Q-L-D-M-L-W-S-G-S-R-G-C-E-T-H-A-F-T-A-H-P-E	1091 - 1115
232	D-M-L-W-S-G-S-R-G-C-E-T-H-A-F-T-A-H-P-E-G-K-H-H-S	1096 - 1120
233	S-G-S-R-G-C-E-T-H-A-F-T-A-H-P-E-G-K-H-H-S-L-S-F-S	1101 - 1125
234	H-M-R-S-A-M-S-G-L-H-L-V-K-R-R	SAMS Peptide

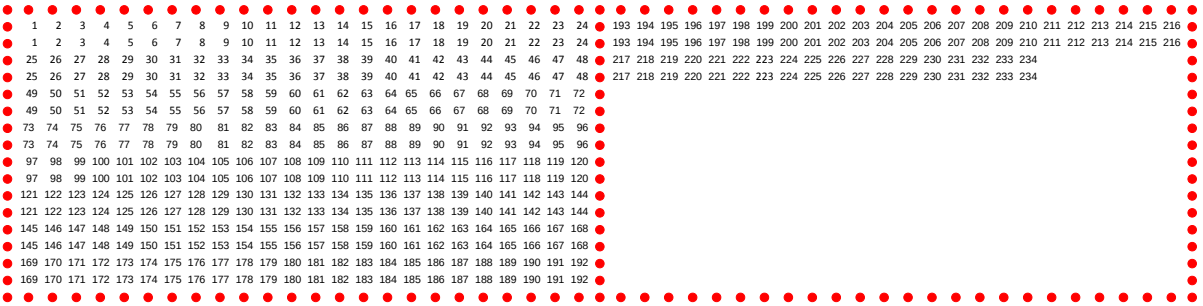

Table 6-3: Peptide array spanning the human JAK3 open reading frame

Array Position	JAK Peptide Sequence	Amino Acid Position	Array Position	TYK2 Peptide Sequence	Amino Acid Position
1	R-Y-S-L-H-G-S-D-R-S-F-P-S-L-G-D-L-M-S-H-L-K-K-Q-I	JAK1 Wild Type: 506 - 530	61	F-L-R-D-F-Q-P-G-R-L-S-Q-Q-M-V-M-V-K-Y-L-A-T-L-E-R	241 - 265
2	R-Y-A-L-H-G-A-D-R-A-F-P-A-L-G-D-L-M-A-H-L-K-K-Q-I	JAK1 mutant: S508A, S512A, S515A, S518A and S524A	62	Q-P-G-R-L-S-Q-Q-M-V-M-V-K-Y-L-A-T-L-E-R-L-A-P-R-F	246 - 270
3	R-Y-A-L-H-G-S-D-R-S-F-P-S-L-G-D-L-M-S-H-L-K-K-Q-I	JAK1 mutant: S508A	63	S-Q-Q-M-V-M-V-K-Y-L-A-T-L-E-R-L-A-P-R-F-G-T-E-R-V	251 - 275
4	R-Y-S-L-H-G-A-D-R-S-F-P-S-L-G-D-L-M-S-H-L-K-K-Q-I	JAK1 mutant: S512A	64	M-V-K-Y-L-A-T-L-E-R-L-A-P-R-F-G-T-E-R-V-P-V-C-H-L	256 - 280
5	R-Y-S-L-H-G-S-D-R-A-F-P-S-L-G-D-L-M-S-H-L-K-K-Q-I	JAK1 mutant: S515A	65	A-T-L-E-R-L-A-P-R-F-G-T-E-R-V-P-V-C-H-L-R-L-L-A-Q	261 - 285
6	R-Y-S-L-H-G-S-D-R-S-F-P-A-L-G-D-L-M-S-H-L-K-K-Q-I	JAK1 mutant: S518A	66	L-A-P-R-F-G-T-E-R-V-P-V-C-H-L-R-L-L-A-Q-A-E-G-E-P	266 - 290
7	R-Y-S-L-H-G-S-D-R-S-F-P-S-L-G-D-L-M-A-H-L-K-K-Q-I	JAK1 mutant: S524A	67	G-T-E-R-V-P-V-C-H-L-R-L-L-A-Q-A-E-G-E-P-C-Y-I-R-D	271 - 295
8	R-Y-S-L-H-G-S-D-R-A-F-P-A-L-G-D-L-M-S-H-L-K-K-Q-I	JAK1 mutant: S515A and S518A	68	P-V-C-H-L-R-L-L-A-Q-A-E-G-E-P-C-Y-I-R-D-S-G-V-A-P	276 - 300
9	R-Y-A-L-H-G-A-D-R-S-F-P-S-L-G-D-L-M-A-H-L-K-K-Q-I	JAK1 mutant: S508A, S512A and S5124A	69	R-L-L-A-Q-A-E-G-E-P-C-Y-I-R-D-S-G-V-A-P-T-D-P-G-P	281 - 305
10	E-Y-N-L-S-G-T-K-K-N-F-S-S-L-K-D-L-L-N-C-Y-Q-M-E-T	JAK2 Wild Type: 461 - 485	70	A-E-G-E-P-C-Y-I-R-D-S-G-V-A-P-T-D-P-G-P-E-S-A-A-G	286 - 310
11	T-F-L-L-V-G-L-S-R-P-H-S-S-L-R-E-L-L-A-T-C-W-D-G-G	JAK3 Wild Type: 437 - 467	71	C-Y-I-R-D-S-G-V-A-P-T-D-P-G-P-E-S-A-A-G-P-P-T-H-E	291 - 315
12	A-F-V-L-E-G-W-G-R-S-F-P-S-V-R-E-L-G-A-A-L-Q-G-C-L	TYK2 Wild Type: 513 - 537	72	S-G-V-A-P-T-D-P-G-P-E-S-A-A-G-P-P-T-H-E-V-L-V-T-G	296 - 320
Array Position	**TYK2 Peptide Sequence**	**Amino Acid Position**	73	T-D-P-G-P-E-S-A-A-G-P-P-T-H-E-V-L-V-T-G-T-G-G-I-Q	301 - 325
13	M-P-L-R-H-W-G-M-A-R-G-S-K-P-V-G-D-G-A-Q-P-M-A-A-M	1 - 25	74	E-S-A-A-G-P-P-T-H-E-V-L-V-T-G-T-G-G-I-Q-W-W-P-V-E	306 - 330
14	W-G-M-A-R-G-S-K-P-V-G-D-G-A-Q-P-M-A-A-M-G-G-L-K-V	6 - 30	75	P-P-T-H-E-V-L-V-T-G-T-G-G-I-Q-W-W-P-V-E-E-E-V-N-K	311 - 335
15	G-S-K-P-V-G-D-G-A-Q-P-M-A-A-M-G-G-L-K-V-L-L-H-W-A	11 - 35	76	V-L-V-T-G-T-G-G-I-Q-W-W-P-V-E-E-E-V-N-K-E-E-G-S-S	316 - 340
16	G-D-G-A-Q-P-M-A-A-M-G-G-L-K-V-L-L-H-W-A-G-P-G-G-G	16 - 40	77	T-G-G-I-Q-W-W-P-V-E-E-E-V-N-K-E-E-G-S-S-G-S-S-G-R	321 - 345
17	P-M-A-A-M-G-G-L-K-V-L-L-H-W-A-G-P-G-G-G-E-P-W-V-T	21 - 45	78	W-W-P-V-E-E-E-V-N-K-E-E-G-S-S-G-S-S-G-R-N-P-Q-A-S	326 - 350
18	G-G-L-K-V-L-L-H-W-A-G-P-G-G-G-E-P-W-V-T-F-S-E-S-S	26 - 50	79	E-E-V-N-K-E-E-G-S-S-G-S-S-G-R-N-P-Q-A-S-L-F-G-K-K	331 - 355
19	L-L-H-W-A-G-P-G-G-G-E-P-W-V-T-F-S-E-S-S-L-T-A-E-E	31 - 55	80	E-E-G-S-S-G-S-S-G-R-N-P-Q-A-S-L-F-G-K-K-A-K-A-H-K	336 - 360
20	G-P-G-G-G-E-P-W-V-T-F-S-E-S-S-L-T-A-E-E-V-C-I-H-I	36 - 60	81	G-S-S-G-R-N-P-Q-A-S-L-F-G-K-K-A-K-A-H-K-A-V-G-Q-P	341 - 365
21	E-P-W-V-T-F-S-E-S-S-L-T-A-E-E-V-C-I-H-I-A-H-K-V-G	41 - 65	82	N-P-Q-A-S-L-F-G-K-K-A-K-A-H-K-A-V-G-Q-P-A-D-R-P-R	346 - 370
22	F-S-E-S-S-L-T-A-E-E-V-C-I-H-I-A-H-K-V-G-I-T-P-P-C	46 - 70	83	L-F-G-K-K-A-K-A-H-K-A-V-G-Q-P-A-D-R-P-R-E-P-L-W-A	351 - 375
23	L-T-A-E-E-V-C-I-H-I-A-H-K-V-G-I-T-P-P-C-F-N-L-F-A	51 - 75	84	A-K-A-H-K-A-V-G-Q-P-A-D-R-P-R-E-P-L-W-A-Y-F-C-D-F	356 - 380
24	V-C-I-H-I-A-H-K-V-G-I-T-P-P-C-F-N-L-F-A-L-F-D-A-Q	56 - 80	85	A-V-G-Q-P-A-D-R-P-R-E-P-L-W-A-Y-F-C-D-F-R-D-I-T-H	361 - 385
25	A-H-K-V-G-I-T-P-P-C-F-N-L-F-A-L-F-D-A-Q-A-Q-V-W-L	61 - 85	86	A-D-R-P-R-E-P-L-W-A-Y-F-C-D-F-R-D-I-T-H-V-V-L-K-E	366 - 390
26	I-T-P-P-C-F-N-L-F-A-L-F-D-A-Q-A-Q-V-W-L-P-P-N-H-I	66 - 90	87	E-P-L-W-A-Y-F-C-D-F-R-D-I-T-H-V-V-L-K-E-H-C-V-S-I	371 - 395
27	F-N-L-F-A-L-F-D-A-Q-A-Q-V-W-L-P-P-N-H-I-L-E-I-P-R	71 - 95	88	Y-F-C-D-F-R-D-I-T-H-V-V-L-K-E-H-C-V-S-I-H-R-Q-D-N	376 - 400
28	L-F-D-A-Q-A-Q-V-W-L-P-P-N-H-I-L-E-I-P-R-D-A-S-L-M	76 - 100	89	R-D-I-T-H-V-V-L-K-E-H-C-V-S-I-H-R-Q-D-N-K-C-L-E-L	381 - 405
29	A-Q-V-W-L-P-P-N-H-I-L-E-I-P-R-D-A-S-L-M-L-Y-F-R-I	81 - 105	90	V-V-L-K-E-H-C-V-S-I-H-R-Q-D-N-K-C-L-E-L-S-L-P-S-R	386 - 410
30	P-P-N-H-I-L-E-I-P-R-D-A-S-L-M-L-Y-F-R-I-R-F-Y-F-R	86 - 110	91	H-C-V-S-I-H-R-Q-D-N-K-C-L-E-L-S-L-P-S-R-A-A-A-L-S	391 - 415
31	L-E-I-P-R-D-A-S-L-M-L-Y-F-R-I-R-F-Y-F-R-N-W-H-G-M	91 - 115	92	H-R-Q-D-N-K-C-L-E-L-S-L-P-S-R-A-A-A-L-S-F-V-S-L-V	396 - 420
32	D-A-S-L-M-L-Y-F-R-I-R-F-Y-F-R-N-W-H-G-M-N-P-R-E-P	96 - 120	93	K-C-L-E-L-S-L-P-S-R-A-A-A-L-S-F-V-S-L-V-D-G-Y-F-R	401 - 425
33	L-Y-F-R-I-R-F-Y-F-R-N-W-H-G-M-N-P-R-E-P-A-V-Y-R-C	101 - 125	94	S-L-P-S-R-A-A-A-L-S-F-V-S-L-V-D-G-Y-F-R-L-T-A-D-S	406 - 430
34	R-F-Y-F-R-N-W-H-G-M-N-P-R-E-P-A-V-Y-R-C-G-P-P-G-T	106 - 130	95	A-A-A-L-S-F-V-S-L-V-D-G-Y-F-R-L-T-A-D-S-S-H-Y-L-C	411 - 435
35	N-W-H-G-M-N-P-R-E-P-A-V-Y-R-C-G-P-P-G-T-E-A-S-S-D	111 - 135	96	F-V-S-L-V-D-G-Y-F-R-L-T-A-D-S-S-H-Y-L-C-H-E-V-A-P	416 - 440
36	N-P-R-E-P-A-V-Y-R-C-G-P-P-G-T-E-A-S-S-D-Q-T-A-Q-G	116 - 140	97	D-G-Y-F-R-L-T-A-D-S-S-H-Y-L-C-H-E-V-A-P-P-R-L-V-M	421 - 445
37	A-V-Y-R-C-G-P-P-G-T-E-A-S-S-D-Q-T-A-Q-G-M-Q-L-L-D	121 - 145	98	L-T-A-D-S-S-H-Y-L-C-H-E-V-A-P-P-R-L-V-M-S-I-R-D-G	426 - 450
38	G-P-P-G-T-E-A-S-S-D-Q-T-A-Q-G-M-Q-L-L-D-P-A-S-F-E	126 - 150	99	S-H-Y-L-C-H-E-V-A-P-P-R-L-V-M-S-I-R-D-G-I-H-G-P-L	431 - 455
39	E-A-S-S-D-Q-T-A-Q-G-M-Q-L-L-D-P-A-S-F-E-Y-L-F-E-Q	131 - 155	100	H-E-V-A-P-P-R-L-V-M-S-I-R-D-G-I-H-G-P-L-L-E-P-F-V	436 - 460
40	Q-T-A-Q-G-M-Q-L-L-D-P-A-S-F-E-Y-L-F-E-Q-G-K-H-E-F	136 - 160	101	P-R-L-V-M-S-I-R-D-G-I-H-G-P-L-L-E-P-F-V-Q-A-K-L-R	441 - 465
41	M-Q-L-L-D-P-A-S-F-E-Y-L-F-E-Q-G-K-H-E-F-V-N-D-V-A	141 - 165	102	S-I-R-D-G-I-H-G-P-L-L-E-P-F-V-Q-A-K-L-R-P-E-D-G-L	446 - 470
42	P-A-S-F-E-Y-L-F-E-Q-G-K-H-E-F-V-N-D-V-A-S-L-W-E-L	146 - 170	103	I-H-G-P-L-L-E-P-F-V-Q-A-K-L-R-P-E-D-G-L-Y-L-I-H-W	451 - 475
43	Y-L-F-E-Q-G-K-H-E-F-V-N-D-V-A-S-L-W-E-L-S-T-E-E-E	151 - 175	104	L-E-P-F-V-Q-A-K-L-R-P-E-D-G-L-Y-L-I-H-W-S-T-S-H-P	456 - 480
44	G-K-H-E-F-V-N-D-V-A-S-L-W-E-L-S-T-E-E-E-I-H-H-F-K	156 - 180	105	Q-A-K-L-R-P-E-D-G-L-Y-L-I-H-W-S-T-S-H-P-Y-R-L-I-L	461 - 485
45	V-N-D-V-A-S-L-W-E-L-S-T-E-E-E-I-H-H-F-K-N-E-S-L-G	161 - 185	106	P-E-D-G-L-Y-L-I-H-W-S-T-S-H-P-Y-R-L-I-L-T-V-A-Q-R	466 - 490
46	S-L-W-E-L-S-T-E-E-E-I-H-H-F-K-N-E-S-L-G-M-A-F-L-H	166 - 190	107	Y-L-I-H-W-S-T-S-H-P-Y-R-L-I-L-T-V-A-Q-R-S-Q-A-P-D	471 - 495
47	S-T-E-E-E-I-H-H-F-K-N-E-S-L-G-M-A-F-L-H-L-C-H-L-A	171 - 195	108	S-T-S-H-P-Y-R-L-I-L-T-V-A-Q-R-S-Q-A-P-D-G-M-Q-S-L	476 - 500
48	I-H-H-F-K-N-E-S-L-G-M-A-F-L-H-L-C-H-L-A-L-R-H-G-I	176 - 200	109	Y-R-L-I-L-T-V-A-Q-R-S-Q-A-P-D-G-M-Q-S-L-R-L-R-K-F	481 - 505
49	N-E-S-L-G-M-A-F-L-H-L-C-H-L-A-L-R-H-G-I-P-L-E-E-V	181 - 205	110	T-V-A-Q-R-S-Q-A-P-D-G-M-Q-S-L-R-L-R-K-F-P-I-E-Q-Q	486 - 510
50	M-A-F-L-H-L-C-H-L-A-L-R-H-G-I-P-L-E-E-V-A-K-K-T-S	186 - 210	111	S-Q-A-P-D-G-M-Q-S-L-R-L-R-K-F-P-I-E-Q-Q-D-G-A-F-V	491 - 515
51	L-C-H-L-A-L-R-H-G-I-P-L-E-E-V-A-K-K-T-S-F-K-D-C-I	191 - 215	112	G-M-Q-S-L-R-L-R-K-F-P-I-E-Q-Q-D-G-A-F-V-L-E-G-W-G	496 - 520
52	L-R-H-G-I-P-L-E-E-V-A-K-K-T-S-F-K-D-C-I-P-R-S-F-R	196 - 220	113	R-L-R-K-F-P-I-E-Q-Q-D-G-A-F-V-L-E-G-W-G-R-S-F-P-S	501 - 525
53	P-L-E-E-V-A-K-K-T-S-F-K-D-C-I-P-R-S-F-R-R-H-I-R-Q	201 - 225	114	P-I-E-Q-Q-D-G-A-F-V-L-E-G-W-G-R-S-F-P-S-V-R-E-L-G	506 - 530
54	A-K-K-T-S-F-K-D-C-I-P-R-S-F-R-R-H-I-R-Q-H-S-A-L-T	206 - 230	115	D-G-A-F-V-L-E-G-W-G-R-S-F-P-S-V-R-E-L-G-A-A-L-Q-G	511 - 535
55	F-K-D-C-I-P-R-S-F-R-R-H-I-R-Q-H-S-A-L-T-R-L-R-L-R	211 - 235	116	L-E-G-W-G-R-S-F-P-S-V-R-E-L-G-A-A-L-Q-G-C-L-L-R-A	516 - 540
56	P-R-S-F-R-R-H-I-R-Q-H-S-A-L-T-R-L-R-L-R-N-V-F-R-R	216 - 240	117	R-S-F-P-S-V-R-E-L-G-A-A-L-Q-G-C-L-L-R-A-G-D-D-C-F	521 - 545
57	R-H-I-R-Q-H-S-A-L-T-R-L-R-L-R-N-V-F-R-R-F-L-R-D-F	221 - 245	118	V-R-E-L-G-A-A-L-Q-G-C-L-L-R-A-G-D-D-C-F-S-L-R-R-C	526 - 550
58	H-S-A-L-T-R-L-R-L-R-N-V-F-R-R-F-L-R-D-F-Q-P-G-R-L	226 - 250	119	A-A-L-Q-G-C-L-L-R-A-G-D-D-C-F-S-L-R-R-C-C-L-P-Q-P	531 - 555
59	R-L-R-L-R-N-V-F-R-R-F-L-R-D-F-Q-P-G-R-L-S-Q-Q-M-V	231 - 255	120	C-L-L-R-A-G-D-D-C-F-S-L-R-R-C-C-L-P-Q-P-G-E-T-S-N	536 - 560
60	N-V-F-R-R-F-L-R-D-F-Q-P-G-R-L-S-Q-Q-M-V-M-V-K-Y-L	236 - 260	121	G-D-D-C-F-S-L-R-R-C-C-L-P-Q-P-G-E-T-S-N-L-I-I-M-R	541 - 565

Table 6-4: Peptide array spanning the human TYK2 open reading frame

(continued overleaf)

Array Position	TYK2 Peptide Sequence	Amino Acid Position	Array Position	TYK2 Peptide Sequence	Amino Acid Position
122	S-L-R-R-C-C-L-P-Q-P-G-E-T-S-N-L-I-I-M-R-G-A-R-A-S	546 - 570	185	T-I-L-R-D-L-T-R-L-Q-P-H-N-L-A-D-V-L-T-V-N-P-D-S-P	861 - 885
123	C-L-P-Q-P-G-E-T-S-N-L-I-I-M-R-G-A-R-A-S-P-R-T-L-N	551 - 575	186	L-T-R-L-Q-P-H-N-L-A-D-V-L-T-V-N-P-D-S-P-A-S-D-P-T	866 - 890
124	G-E-T-S-N-L-I-I-M-R-G-A-R-A-S-P-R-T-L-N-L-S-Q-L-S	556 - 580	187	P-H-N-L-A-D-V-L-T-V-N-P-D-S-P-A-S-D-P-T-V-F-H-K-R	871 - 895
125	L-I-I-M-R-G-A-R-A-S-P-R-T-L-N-L-S-Q-L-S-F-H-R-V-D	561 - 585	188	D-V-L-T-V-N-P-D-S-P-A-S-D-P-T-V-F-H-K-R-Y-L-K-K-I	876 - 900
126	G-A-R-A-S-P-R-T-L-N-L-S-Q-L-S-F-H-R-V-D-Q-K-E-I-T	566 - 590	189	N-P-D-S-P-A-S-D-P-T-V-F-H-K-R-Y-L-K-K-I-R-D-L-G-E	881 - 905
127	P-R-T-L-N-L-S-Q-L-S-F-H-R-V-D-Q-K-E-I-T-Q-L-S-H-L	571 - 595	190	A-S-D-P-T-V-F-H-K-R-Y-L-K-K-I-R-D-L-G-E-G-H-F-G-K	886 - 910
128	L-S-Q-L-S-F-H-R-V-D-Q-K-E-I-T-Q-L-S-H-L-G-Q-G-T-R	576 - 600	191	V-F-H-K-R-Y-L-K-K-I-R-D-L-G-E-G-H-F-G-K-V-S-L-Y-C	891 - 915
129	F-H-R-V-D-Q-K-E-I-T-Q-L-S-H-L-G-Q-G-T-R-T-N-V-Y-E	581 - 605	192	Y-L-K-K-I-R-D-L-G-E-G-H-F-G-K-V-S-L-Y-C-Y-D-P-T-N	896 - 920
130	Q-K-E-I-T-Q-L-S-H-L-G-Q-G-T-R-T-N-V-Y-E-G-R-L-R-V	586 - 610	193	R-D-L-G-E-G-H-F-G-K-V-S-L-Y-C-Y-D-P-T-N-D-G-T-G-E	901 - 925
131	Q-L-S-H-L-G-Q-G-T-R-T-N-V-Y-E-G-R-L-R-V-E-G-S-G-D	591 - 615	194	G-H-F-G-K-V-S-L-Y-C-Y-D-P-T-N-D-G-T-G-E-M-V-A-V-K	906 - 930
132	G-Q-G-T-R-T-N-V-Y-E-G-R-L-R-V-E-G-S-G-D-P-E-E-G-K	596 - 620	195	V-S-L-Y-C-Y-D-P-T-N-D-G-T-G-E-M-V-A-V-K-A-L-K-A-D	911 - 935
133	T-N-V-Y-E-G-R-L-R-V-E-G-S-G-D-P-E-E-G-K-M-D-D-E-D	601 - 625	196	Y-D-P-T-N-D-G-T-G-E-M-V-A-V-K-A-L-K-A-D-C-G-P-Q-H	916 - 940
134	G-R-L-R-V-E-G-S-G-D-P-E-E-G-K-M-D-D-E-D-P-L-V-P-G	606 - 630	197	D-G-T-G-E-M-V-A-V-K-A-L-K-A-D-C-G-P-Q-H-R-S-G-W-K	921 - 945
135	E-G-S-G-D-P-E-E-G-K-M-D-D-E-D-P-L-V-P-G-R-D-R-G-Q	611 - 635	198	M-V-A-V-K-A-L-K-A-D-C-G-P-Q-H-R-S-G-W-K-Q-E-I-D-I	926 - 950
136	P-E-E-G-K-M-D-D-E-D-P-L-V-P-G-R-D-R-G-Q-E-L-R-V-V	616 - 640	199	A-L-K-A-D-C-G-P-Q-H-R-S-G-W-K-Q-E-I-D-I-L-R-T-L-Y	931 - 955
137	M-D-D-E-D-P-L-V-P-G-R-D-R-G-Q-E-L-R-V-V-L-K-V-L-D	621 - 645	200	C-G-P-Q-H-R-S-G-W-K-Q-E-I-D-I-L-R-T-L-Y-H-E-H-I-I	936 - 960
138	P-L-V-P-G-R-D-R-G-Q-E-L-R-V-V-L-K-V-L-D-P-S-H-H-D	626 - 650	201	R-S-G-W-K-Q-E-I-D-I-L-R-T-L-Y-H-E-H-I-I-K-Y-K-G-C	941 - 965
139	R-D-R-G-Q-E-L-R-V-V-L-K-V-L-D-P-S-H-H-D-I-A-L-A-F	631 - 655	202	Q-E-I-D-I-L-R-T-L-Y-H-E-H-I-I-K-Y-K-G-C-C-E-D-Q-G	946 - 970
140	E-L-R-V-V-L-K-V-L-D-P-S-H-H-D-I-A-L-A-F-Y-E-T-A-S	636 - 660	203	L-R-T-L-Y-H-E-H-I-I-K-Y-K-G-C-C-E-D-Q-G-E-K-S-L-Q	951 - 975
141	L-K-V-L-D-P-S-H-H-D-I-A-L-A-F-Y-E-T-A-S-L-M-S-Q-V	641 - 665	204	H-E-H-I-I-K-Y-K-G-C-C-E-D-Q-G-E-K-S-L-Q-L-V-M-E-Y	956 - 980
142	P-S-H-H-D-I-A-L-A-F-Y-E-T-A-S-L-M-S-Q-V-S-H-T-H-L	646 - 670	205	K-Y-K-G-C-C-E-D-Q-G-E-K-S-L-Q-L-V-M-E-Y-V-P-L-G-S	961 - 985
143	I-A-L-A-F-Y-E-T-A-S-L-M-S-Q-V-S-H-T-H-L-A-F-V-H-G	651 - 675	206	C-E-D-Q-G-E-K-S-L-Q-L-V-M-E-Y-V-P-L-G-S-L-R-D-Y-L	966 - 990
144	Y-E-T-A-S-L-M-S-Q-V-S-H-T-H-L-A-F-V-H-G-V-C-V-R-G	656 - 680	207	E-K-S-L-Q-L-V-M-E-Y-V-P-L-G-S-L-R-D-Y-L-P-R-H-S-I	971 - 995
145	L-M-S-Q-V-S-H-T-H-L-A-F-V-H-G-V-C-V-R-G-P-E-N-I-M	661 - 685	208	L-V-M-E-Y-V-P-L-G-S-L-R-D-Y-L-P-R-H-S-I-G-L-A-Q-L	976 - 1000
146	S-H-T-H-L-A-F-V-H-G-V-C-V-R-G-P-E-N-I-M-V-T-E-Y-V	666 - 690	209	V-P-L-G-S-L-R-D-Y-L-P-R-H-S-I-G-L-A-Q-L-L-L-F-A-Q	981 - 1005
147	A-F-V-H-G-V-C-V-R-G-P-E-N-I-M-V-T-E-Y-V-E-H-G-P-L	671 - 695	210	L-R-D-Y-L-P-R-H-S-I-G-L-A-Q-L-L-L-F-A-Q-Q-I-C-E-G	986 - 1010
148	V-C-V-R-G-P-E-N-I-M-V-T-E-Y-V-E-H-G-P-L-D-V-W-L-R	676 - 700	211	P-R-H-S-I-G-L-A-Q-L-L-L-F-A-Q-Q-I-C-E-G-M-A-Y-L-H	991 - 1015
149	P-E-N-I-M-V-T-E-Y-V-E-H-G-P-L-D-V-W-L-R-R-E-R-G-H	681 - 705	212	G-L-A-Q-L-L-L-F-A-Q-Q-I-C-E-G-M-A-Y-L-H-A-Q-H-Y-I	996 - 1020
150	V-T-E-Y-V-E-H-G-P-L-D-V-W-L-R-R-E-R-G-H-V-P-M-A-W	686 - 710	213	L-L-F-A-Q-Q-I-C-E-G-M-A-Y-L-H-A-Q-H-Y-I-H-R-D-L-A	1001 - 1025
151	E-H-G-P-L-D-V-W-L-R-R-E-R-G-H-V-P-M-A-W-K-M-V-V-A	691 - 715	214	Q-I-C-E-G-M-A-Y-L-H-A-Q-H-Y-I-H-R-D-L-A-A-R-N-V-L	1006 - 1030
152	D-V-W-L-R-R-E-R-G-H-V-P-M-A-W-K-M-V-V-A-Q-Q-L-A-S	696 - 720	215	M-A-Y-L-H-A-Q-H-Y-I-H-R-D-L-A-A-R-N-V-L-L-D-N-D-R	1011 - 1035
153	R-E-R-G-H-V-P-M-A-W-K-M-V-V-A-Q-Q-L-A-S-A-L-S-Y-L	701 - 725	216	A-Q-H-Y-I-H-R-D-L-A-A-R-N-V-L-L-D-N-D-R-L-V-K-I-G	1016 - 1040
154	V-P-M-A-W-K-M-V-V-A-Q-Q-L-A-S-A-L-S-Y-L-E-N-K-N-L	706 - 730	217	H-R-D-L-A-A-R-N-V-L-L-D-N-D-R-L-V-K-I-G-D-F-G-L-A	1021 - 1045
155	K-M-V-V-A-Q-Q-L-A-S-A-L-S-Y-L-E-N-K-N-L-V-H-G-N-V	711 - 735	218	A-R-N-V-L-L-D-N-D-R-L-V-K-I-G-D-F-G-L-A-K-A-V-P-E	1026 - 1050
156	Q-Q-L-A-S-A-L-S-Y-L-E-N-K-N-L-V-H-G-N-V-C-G-R-N-I	716 - 740	219	L-D-N-D-R-L-V-K-I-G-D-F-G-L-A-K-A-V-P-E-G-H-E-Y-Y	1031 - 1055
157	A-L-S-Y-L-E-N-K-N-L-V-H-G-N-V-C-G-R-N-I-L-L-A-R-L	721 - 745	220	L-V-K-I-G-D-F-G-L-A-K-A-V-P-E-G-H-E-Y-Y-R-V-R-E-D	1036 - 1060
158	E-N-K-N-L-V-H-G-N-V-C-G-R-N-I-L-L-A-R-L-G-L-A-E-G	726 - 750	221	D-F-G-L-A-K-A-V-P-E-G-H-E-Y-Y-R-V-R-E-D-G-D-S-P-V	1041 - 1065
159	V-H-G-N-V-C-G-R-N-I-L-L-A-R-L-G-L-A-E-G-T-S-P-F-I	731 - 755	222	K-A-V-P-E-G-H-E-Y-Y-R-V-R-E-D-G-D-S-P-V-F-W-Y-A-P	1046 - 1070
160	C-G-R-N-I-L-L-A-R-L-G-L-A-E-G-T-S-P-F-I-K-L-S-D-P	736 - 760	223	G-H-E-Y-Y-R-V-R-E-D-G-D-S-P-V-F-W-Y-A-P-E-C-L-K-E	1051 - 1075
161	L-L-A-R-L-G-L-A-E-G-T-S-P-F-I-K-L-S-D-P-G-V-G-L-G	741 - 765	224	R-V-R-E-D-G-D-S-P-V-F-W-Y-A-P-E-C-L-K-E-Y-K-F-Y-Y	1056 - 1080
162	G-L-A-E-G-T-S-P-F-I-K-L-S-D-P-G-V-G-L-G-A-L-S-R-E	746 - 770	225	G-D-S-P-V-F-W-Y-A-P-E-C-L-K-E-Y-K-F-Y-Y-A-S-D-V-W	1061 - 1085
163	T-S-P-F-I-K-L-S-D-P-G-V-G-L-G-A-L-S-R-E-E-R-V-E-R	751 - 775	226	F-W-Y-A-P-E-C-L-K-E-Y-K-F-Y-Y-A-S-D-V-W-S-F-G-V-T	1066 - 1090
164	K-L-S-D-P-G-V-G-L-G-A-L-S-R-E-E-R-V-E-R-I-P-W-L-A	756 - 780	227	E-C-L-K-E-Y-K-F-Y-Y-A-S-D-V-W-S-F-G-V-T-L-Y-E-L-L	1071 - 1095
165	G-V-G-L-G-A-L-S-R-E-E-R-V-E-R-I-P-W-L-A-P-E-C-L-P	761 - 785	228	Y-K-F-Y-Y-A-S-D-V-W-S-F-G-V-T-L-Y-E-L-L-T-H-C-D-S	1076 - 1100
166	A-L-S-R-E-E-R-V-E-R-I-P-W-L-A-P-E-C-L-P-G-G-A-N-S	766 - 790	229	A-S-D-V-W-S-F-G-V-T-L-Y-E-L-L-T-H-C-D-S-S-Q-S-P-P	1081 - 1105
167	E-R-V-E-R-I-P-W-L-A-P-E-C-L-P-G-G-A-N-S-L-S-T-A-M	771 - 795	230	S-F-G-V-T-L-Y-E-L-L-T-H-C-D-S-S-Q-S-P-P-T-K-F-L-E	1086 - 1110
168	I-P-W-L-A-P-E-C-L-P-G-G-A-N-S-L-S-T-A-M-D-K-W-G-F	776 - 800	231	L-Y-E-L-L-T-H-C-D-S-S-Q-S-P-P-T-K-F-L-E-L-I-G-I-A	1091 - 1115
169	P-E-C-L-P-G-G-A-N-S-L-S-T-A-M-D-K-W-G-F-G-A-T-L-L	781 - 805	232	T-H-C-D-S-S-Q-S-P-P-T-K-F-L-E-L-I-G-I-A-Q-G-Q-M-T	1096 - 1120
170	G-G-A-N-S-L-S-T-A-M-D-K-W-G-F-G-A-T-L-L-E-I-C-F-D	786 - 810	233	S-Q-S-P-P-T-K-F-L-E-L-I-G-I-A-Q-G-Q-M-T-V-L-R-L-T	1101 - 1125
171	L-S-T-A-M-D-K-W-G-F-G-A-T-L-L-E-I-C-F-D-G-E-A-P-L	791 - 815	234	T-K-F-L-E-L-I-G-I-A-Q-G-Q-M-T-V-L-R-L-T-E-L-L-E-R	1106 - 1130
172	D-K-W-G-F-G-A-T-L-L-E-I-C-F-D-G-E-A-P-L-Q-S-R-S-P	796 - 820	235	L-I-G-I-A-Q-G-Q-M-T-V-L-R-L-T-E-L-L-E-R-G-E-R-L-P	1111 - 1135
173	G-A-T-L-L-E-I-C-F-D-G-E-A-P-L-Q-S-R-S-P-S-E-K-E-H	801 - 825	236	Q-G-Q-M-T-V-L-R-L-T-E-L-L-E-R-G-E-R-L-P-R-P-D-K-C	1116 - 1140
174	E-I-C-F-D-G-E-A-P-L-Q-S-R-S-P-S-E-K-E-H-F-Y-Q-R-Q	806 - 830	237	V-L-R-L-T-E-L-L-E-R-G-E-R-L-P-R-P-D-K-C-P-C-E-V-Y	1121 - 1145
175	G-E-A-P-L-Q-S-R-S-P-S-E-K-E-H-F-Y-Q-R-Q-H-R-L-P-E	811 - 835	238	E-L-L-E-R-G-E-R-L-P-R-P-D-K-C-P-C-E-V-Y-H-L-M-K-N	1126 - 1150
176	Q-S-R-S-P-S-E-K-E-H-F-Y-Q-R-Q-H-R-L-P-E-P-S-C-P-Q	816 - 840	239	G-E-R-L-P-R-P-D-K-C-P-C-E-V-Y-H-L-M-K-N-C-W-E-T-E	1131 - 1155
177	S-E-K-E-H-F-Y-Q-R-Q-H-R-L-P-E-P-S-C-P-Q-L-A-T-L-T	821 - 845	240	R-P-D-K-C-P-C-E-V-Y-H-L-M-K-N-C-W-E-T-E-A-S-F-R-P	1136 - 1160
178	F-Y-Q-R-Q-H-R-L-P-E-P-S-C-P-Q-L-A-T-L-T-S-Q-C-L-T	826 - 850	241	P-C-E-V-Y-H-L-M-K-N-C-W-E-T-E-A-S-F-R-P-T-F-E-N-L	1141 - 1165
179	H-R-L-P-E-P-S-C-P-Q-L-A-T-L-T-S-Q-C-L-T-Y-E-P-T-Q	831 - 855	242	H-L-M-K-N-C-W-E-T-E-A-S-F-R-P-T-F-E-N-L-I-P-I-L-K	1146 - 1170
180	P-S-C-P-Q-L-A-T-L-T-S-Q-C-L-T-Y-E-P-T-Q-R-P-S-F-R	836 - 860	243	C-W-E-T-E-A-S-F-R-P-T-F-E-N-L-I-P-I-L-K-T-V-H-E-K	1151 - 1175
181	L-A-T-L-T-S-Q-C-L-T-Y-E-P-T-Q-R-P-S-F-R-T-I-L-R-D	841 - 865	244	A-S-F-R-P-T-F-E-N-L-I-P-I-L-K-T-V-H-E-K-Y-Q-G-Q-A	1156 - 1180
182	S-Q-C-L-T-Y-E-P-T-Q-R-P-S-F-R-T-I-L-R-D-L-T-R-L-Q	846 - 870	245	T-F-E-N-L-I-P-I-L-K-T-V-H-E-K-Y-Q-G-Q-A-P-S-V-F-S	1161 - 1185
183	Y-E-P-T-Q-R-P-S-F-R-T-I-L-R-D-L-T-R-L-Q-P-H-N-L-A	851 - 875	246	E-N-L-I-P-I-L-K-T-V-H-E-K-Y-Q-G-Q-A-P-S-V-F-S-V-C	1166 - 1190
184	R-P-S-F-R-T-I-L-R-D-L-T-R-L-Q-P-H-N-L-A-D-V-L-T-V	856 - 880	247	H-M-R-S-A-M-S-G-L-H-L-V-K-R-R	SAMS peptide

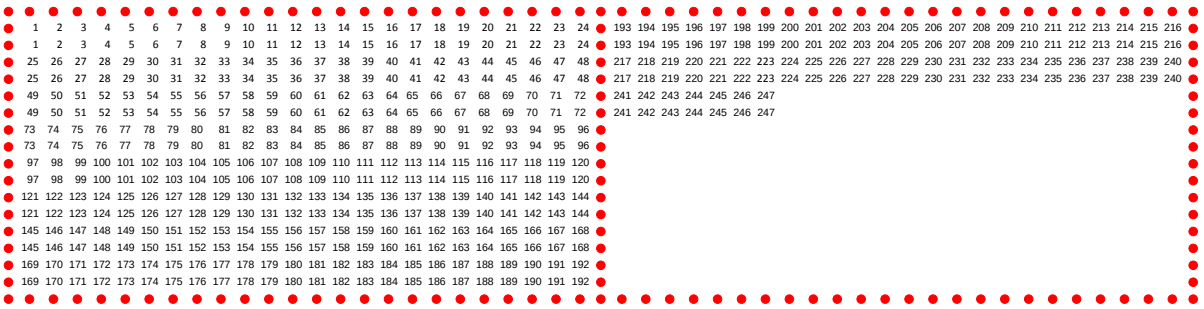

Table 6-4: Peptide array spanning the human TYK2 open reading frame

References

Kinase Profiling Inhibitor Database: GF109203X [Online]. Available: http://www.kinase-screen.mrc.ac.uk/screening-compounds/341060 [Accessed 01 May 2017].

ABDEL-ALEEM, S., LI, X., ANSTADT, M., PEREZ-TAMAYO, R. & LOWE, J. 1994. Regulation of glucose utilization during the inhibition of fatty acid oxidation in rat myocytes. *Horm Metab Res* 26**,** 88 –91.

AHMED, A. U. 2011. An overview of inflammation: mechanism and consequences. *Frontiers in Biology,* 6**,** 274.

ANDERSON, T. J. 1999. Assessment and treatment of endothelial dysfunction in humans. *J Am Coll Cardiol,* 34**,** 631-8.

AUTIERI, M. V. 2012. Pro- and Anti-Inflammatory Cytokine Networks in Atherosclerosis. *ISRN Vascular Medicine,* 2012**,** 17.

BABON, J. J., KERSHAW, N. J., MURPHY, J. M., VARGHESE, L. N., LAKTYUSHIN, A., YOUNG, S. N., LUCET, I. S., NORTON, R. S. & NICOLA, N. A. 2012. Suppression of cytokine signaling by SOCS3: characterization of the mode of inhibition and the basis of its specificity. *Immunity,* 36**,** 239-50.

BABON, J. J., LUCET, I. S., MURPHY, J. M., NICOLA, N. A. & VARGHESE, L. N. 2014. The molecular regulation of Janus kinase (JAK) activation. *Biochem J,* 462**,** 1-13.

BABON, J. J., SABO, J. K., ZHANG, J. G., NICOLA, N. A. & NORTON, R. S. 2009. The SOCS box encodes a hierarchy of affinities for Cullin5: implications for ubiquitin ligase formation and cytokine signalling suppression. *J Mol Biol,* 387**,** 162-74.

BAI, A., YONG, M., MA, A. G., MA, Y., WEISS, C. R., GUAN, Q., BERNSTEIN, C. N. & PENG, Z. 2010. Novel Anti-Inflammatory Action of 5-Aminoimidazole-4-carboxamide Ribonucleoside with Protective Effect in Dextran Sulfate Sodium-Induced Acute and Chronic Colitis. *Journal of Pharmacology and Experimental Therapeutics,* 333**,** 717-725.

BANERJEE, S., BIEHL, A., GADINA, M., HASNI, S. & SCHWARTZ, D. M. 2017. JAK–STAT Signaling as a Target for Inflammatory and Autoimmune Diseases: Current and Future Prospects. *Drugs,* 77**,** 521-546.

BARATH, P., FISHBEIN, M. C., CAO, J., BERENSON, J., HELFANT, R. H. & FORRESTER, J. S. 1990. Tumor necrosis factor gene expression in human vascular intimal smooth muscle cells detected by in situ hybridization. *Am J Pathol,* 137**,** 503-9.

BATEMAN, A. 1997. The structure of a domain common to archaebacteria and the homocystinuria disease protein. *Trends in Biochemical Sciences,* 22**,** 12-13.

BAXTER, E. J., SCOTT, L. M., CAMPBELL, P. J., EAST, C., FOUROUCLAS, N., SWANTON, S., VASSILIOU, G. S., BENCH, A. J., BOYD, E. M., CURTIN, N., SCOTT, M. A., ERBER, W. N. & GREEN, A. R. 2005. Acquired mutation of the tyrosine kinase JAK2 in human myeloproliferative disorders. *Lancet,* 365**,** 1054-61.

BECKER, S., GRONER, B. & MULLER, C. W. 1998. Three-dimensional structure of the Stat3beta homodimer bound to DNA. *Nature,* 394**,** 145-51.

BESS, E., FISSLTHALER, B., FROMEL, T. & FLEMING, I. 2011. Nitric oxide-induced activation of the AMP-activated protein kinase alpha2 subunit attenuates IkappaB kinase activity and inflammatory responses in endothelial cells. *PLoS One,* 6**,** e20848.

BETTELLI, E., CARRIER, Y., GAO, W., KORN, T., STROM, T. B., OUKKA, M., WEINER, H. L. & KUCHROO, V. K. 2006. Reciprocal developmental pathways for the generation of pathogenic effector TH17 and regulatory T cells. *Nature,* 441**,** 235-8.

BEVILACQUA, M. P., POBER, J. S., MENDRICK, D. L., COTRAN, R. S. & GIMBRONE, M. A. 1987. Identification of an inducible endothelial-leukocyte adhesion molecule. *Proceedings of the National Academy of Sciences of the United States of America,* 84**,** 9238-9242.

BEVILACQUA, M. P., POBER, J. S., WHEELER, M. E., COTRAN, R. S. & GIMBRONE, M. A., JR. 1985. Interleukin 1 acts on cultured human vascular endothelium to increase the adhesion of polymorphonuclear leukocytes, monocytes, and related leukocyte cell lines. *J Clin Invest,* 76**,** 2003-11.

BONE, H., DECHERT, U., JIRIK, F., SCHRADER, J. W. & WELHAM, M. J. 1997. SHP1 and SHP2 protein-tyrosine phosphatases associate with betac after interleukin-3-induced receptor tyrosine phosphorylation. Identification of potential binding sites and substrates. *J Biol Chem,* 272**,** 14470-6.

BORDEN, E. C., SEN, G. C., UZE, G., SILVERMAN, R. H., RANSOHOFF, R. M., FOSTER, G. R. & STARK, G. R. 2007. Interferons at age 50: past, current and future impact on biomedicine. *Nat Rev Drug Discov,* 6**,** 975-90.

BOTTO, S., STREBLOW, D. N., DEFILIPPIS, V., WHITE, L., KREKLYWICH, C. N., SMITH, P. P. & CAPOSIO, P. 2011. IL-6 in human cytomegalovirus secretome promotes angiogenesis and survival of endothelial cells through the stimulation of survivin. *Blood,* 117**,** 352.

BRIDGES, D. & MOORHEAD, G. B. 2005. 14-3-3 proteins: a number of functions for a numbered protein. *Sci STKE,* 2005**,** re10.

BRUNMAIR, B., STANIEK, K., GRAS, F., SCHARF, N., ALTHAYM, A., CLARA, R., RODEN, M., GNAIGER, E., NOHL, H., WALDHÄUSL, W. & FÜRNSINN, C. 2004. Thiazolidinediones, Like Metformin, Inhibit Respiratory Complex I. *A Common Mechanism Contributing to Their Antidiabetic Actions?,* 53**,** 1052-1059.

CACICEDO, J. M., YAGIHASHI, N., KEANEY JR, J. F., RUDERMAN, N. B. & IDO, Y. 2004. AMPK inhibits fatty acid-induced increases in NF-κB transactivation in cultured human umbilical vein endothelial cells. *Biochemical and Biophysical Research Communications,* 324**,** 1204-1209.

CAMERON, K. O., KUNG, D. W., KALGUTKAR, A. S., KURUMBAIL, R. G., MILLER, R., SALATTO, C. T., WARD, J., WITHKA, J. M., BHATTACHARYA, S. K., BOEHM, M., BORZILLERI, K. A., BROWN, J. A., CALABRESE, M., CASPERS, N. L., COKORINOS, E., CONN, E. L., DOWLING, M. S., EDMONDS, D. J., ENG, H., FERNANDO, D. P., FRISBIE, R., HEPWORTH, D., LANDRO, J., MAO, Y., RAJAMOHAN, F., REYES, A. R., ROSE, C. R., RYDER, T., SHAVNYA, A., SMITH, A. C., TU, M., WOLFORD, A. C. & XIAO, J. 2016. Discovery and Preclinical Characterization of 6-Chloro-5-[4-(1-hydroxycyclobutyl)phenyl]-1H-indole-3-carboxylic Acid (PF-06409577), a Direct Activator of Adenosine Monophosphate-activated Protein Kinase (AMPK), for the Potential Treatment of Diabetic Nephropathy. *Journal of Medicinal Chemistry,* 59**,** 8068-8081.

CAMERON, K. O. & KURUMBAIL, R. G. 2016. Recent progress in the identification of adenosine monophosphate-activated protein kinase (AMPK) activators. *Bioorganic & Medicinal Chemistry Letters,* 26**,** 5139-5148.

CANSBY, E., NERSTEDT, A., AMRUTKAR, M., DURAN, E. N., SMITH, U. & MAHLAPUU, M. 2014. Partial hepatic resistance to IL-6-induced inflammation develops in type 2 diabetic mice, while the anti-inflammatory effect of AMPK is maintained. *Mol Cell Endocrinol,* 393**,** 143-51.

CANTÓ, C. & AUWERX, J. 2009. PGC-1alpha, SIRT1 and AMPK, an energy sensing network that controls energy expenditure. *Current opinion in lipidology,* 20**,** 98-105.

CANTWELL, C. A., STERNECK, E. & JOHNSON, P. F. 1998. Interleukin-6-Specific Activation of the C/EBPδ Gene in Hepatocytes Is Mediated by Stat3 and Sp1. *Molecular and Cellular Biology,* 18**,** 2108-2117.

CERVANTES, F., VANNUCCHI, A. M., KILADJIAN, J. J., AL-ALI, H. K., SIRULNIK, A., STALBOVSKAYA, V., MCQUITTY, M., HUNTER, D. S., LEVY, R. S., PASSAMONTI, F., BARBUI, T., BAROSI, G., HARRISON, C. N., KNOOPS, L. & GISSLINGER, H. 2013. Three-year efficacy, safety, and survival findings from COMFORT-II, a phase 3 study comparing ruxolitinib with best available therapy for myelofibrosis. *Blood,* 122**,** 4047-53.

CHATTERJEE, P. K., AL-ABED, Y., SHERRY, B. & METZ, C. N. 2009. Cholinergic agonists regulate JAK2/STAT3 signaling to suppress endothelial cell activation. *American Journal of Physiology - Cell Physiology,* 297**,** C1294-C1306.

CHEN, L., JIAO, Z.-H., ZHENG, L.-S., ZHANG, Y.-Y., XIE, S.-T., WANG, Z.-X. & WU, J.-W. 2009a. Structural insight into the autoinhibition mechanism of AMP-activated protein kinase. *Nature,* 459**,** 1146-1149.

CHEN, W., DAINES, M. O. & KHURANA HERSHEY, G. K. 2004. Turning off signal transducer and activator of transcription (STAT): the negative regulation of STAT signaling. *J Allergy Clin Immunol,* 114**,** 476-89; quiz 490.

CHEN, W., MA, T., SHEN, X.-N., XIA, X.-F., XU, G.-D., BAI, X.-L. & LIANG, T.-B. 2012. Macrophage-Induced Tumor Angiogenesis Is Regulated by the TSC2–mTOR Pathway. *Cancer Research,* 72**,** 1363-1372.

CHEN, X., VINKEMEIER, U., ZHAO, Y., JERUZALMI, D., DARNELL, J. E., JR. & KURIYAN, J. 1998. Crystal structure of a tyrosine phosphorylated STAT-1 dimer bound to DNA. *Cell,* 93**,** 827-39.

CHEN, Z.-P., MCCONELL, G. K., MICHELL, B. J., SNOW, R. J., CANNY, B. J. & KEMP, B. E. 2000. AMPK signaling in contracting human skeletal muscle: acetyl-CoA carboxylase and NO synthase phosphorylation. *American Journal of Physiology - Endocrinology And Metabolism,* 279**,** E1202-E1206.

CHEN, Z., PENG, I. C., SUN, W., SU, M.-I., HSU, P.-H., FU, Y., ZHU, Y., DEFEA, K., PAN, S., TSAI, M.-D. & SHYY, J. Y. J. 2009b. AMP-Activated Protein Kinase Functionally Phosphorylates Endothelial Nitric Oxide Synthase Ser633. *Circulation research,* 104**,** 496-505.

CHERANOV, S. Y., KARPURAPU, M., WANG, D., ZHANG, B., VENEMA, R. C. & RAO, G. N. 2008. An essential role for SRC-activated STAT-3 in 14,15-EET–induced VEGF expression and angiogenesis. *Blood,* 111**,** 5581.

CHEUNG, P. C., SALT, I. P., DAVIES, S. P., HARDIE, D. G. & CARLING, D. 2000. Characterization of AMP-activated protein kinase gamma-subunit isoforms and their role in AMP binding. *Biochemical Journal,* 346**,** 659-669.

CHIARETTI, S., ZINI, G. & BASSAN, R. 2014. Diagnosis and Subclassification of Acute Lymphoblastic Leukemia. *Mediterranean Journal of Hematology and Infectious Diseases,* 6**,** e2014073.

COLLABORATION, I. R. G. C. E. R. F. 2012. Interleukin-6 receptor pathways in coronary heart disease: a collaborative meta-analysis of 82 studies. *Lancet,* 379**,** 1205-1213.

COOL, B., ZINKER, B., CHIOU, W., KIFLE, L., CAO, N., PERHAM, M., DICKINSON, R., ADLER, A., GAGNE, G., IYENGAR, R., ZHAO, G., MARSH, K., KYM, P., JUNG, P., CAMP, H. S. & FREVERT, E. 2006. Identification and characterization of a small molecule AMPK activator that treats key components of type 2 diabetes and the metabolic syndrome. *Cell Metabolism,* 3**,** 403-416.

CORTON, J. M., GILLESPIE, J. G., HAWLEY, S. A. & HARDIE, D. G. 1995. 5-Aminoimidazole-4-Carboxamide Ribonucleoside. *European Journal of Biochemistry,* 229**,** 558-565.

CROKER, B. A., KREBS, D. L., ZHANG, J. G., WORMALD, S., WILLSON, T. A., STANLEY, E. G., ROBB, L., GREENHALGH, C. J., FORSTER, I., CLAUSEN, B. E., NICOLA, N. A., METCALF, D., HILTON, D. J., ROBERTS, A. W. & ALEXANDER, W. S. 2003. SOCS3 negatively regulates IL-6 signaling in vivo. *Nat Immunol,* 4**,** 540-5.

CRUTE, B. E., SEEFELD, K., GAMBLE, J., KEMP, B. E. & WITTERS, L. A. 1998. Functional Domains of the α1 Catalytic Subunit of the AMP-activated Protein Kinase. *Journal of Biological Chemistry,* 273**,** 35347-35354.

DAGHER, Z., RUDERMAN, N., TORNHEIM, K. & IDO, Y. 2001. Acute Regulation of Fatty Acid Oxidation and AMP-Activated Protein Kinase in Human Umbilical Vein Endothelial Cells. *Circulation Research,* 88**,** 1276-1282.

DANIEL, J.-M., DUTZMANN, J., BIELENBERG, W., WIDMER-TESKE, R., GÜNDÜZ, D., HAMM, C. W. & SEDDING, D. G. 2012. Inhibition of STAT3 signaling prevents vascular smooth muscle cell proliferation and neointima formation. *Basic Research in Cardiology,* 107**,** 261.

DARNELL, J. E., KERR, I. M. & STARK, G. R. 1994. Jak-STAT pathways and transcriptional activation in response to IFNs and other extracellular signaling proteins. *Science,* 264**,** 1415.

DAVID, M., CHEN, H. E., GOELZ, S., LARNER, A. C. & NEEL, B. G. 1995. Differential regulation of the alpha/beta interferon-stimulated Jak/Stat pathway by the SH2 domain-containing tyrosine phosphatase SHPTP1. *Molecular and Cellular Biology,* 15**,** 7050-7058.

DAVIES, S. P., CARLING, D. & HARDIE, D. G. 1989. Tissue distribution of the AMP-activated protein kinase, and lack of activation by cyclic-AMP-dependent protein kinase, studied using a specific and sensitive peptide assay. *European Journal of Biochemistry,* 186**,** 123-128.

DAVIES, S. P., CARLING, D., MUNDAY, M. R. & HARDIE, D. G. 1992. Diurnal rhythm of phosphorylation of rat liver acetyl – CoA carboxylase by the AMP-activated protein kinase, demonstrated using freeze-clamping. *European Journal of Biochemistry,* 203**,** 615-623.

DAVIGNON, J. & GANZ, P. 2004. Role of endothelial dysfunction in atherosclerosis. *Circulation,* 109**,** Iii27-32.

DE JAGER, J., KOOY, A., LEHERT, P., BETS, D., WULFFELÉ, M. G., TEERLINK, T., SCHEFFER, P. G., SCHALKWIJK, C. G., DONKER, A. J. M. & STEHOUWER, C. D. A. 2005. Effects of short-term treatment with metformin on markers of endothelial function and inflammatory activity in type 2 diabetes mellitus: a randomized, placebo-controlled trial. *Journal of Internal Medicine,* 257**,** 100-109.

DE VRIES, M. R. & QUAX, P. H. 2016. Plaque angiogenesis and its relation to inflammation and atherosclerotic plaque destabilization. *Curr Opin Lipidol,* 27**,** 499-506.

DECKER, T. & KOVARIK, P. 2000. Serine phosphorylation of STATs. *Oncogene,* 19**,** 2628-37.

DONG, Y., ZHANG, M., LIANG, B., XIE, Z., ZHAO, Z., ASFA, S., CHOI, H. C. & ZOU, M.-H. 2010. Reduction of AMP-activated Protein Kinase Alpha 2 Increases Endoplasmic Reticulum Stress and Atherosclerosis In Vivo. *Circulation,* 121**,** 792-803.

DOS, D. S., ALI, S. M., KIM, D.-H., GUERTIN, D. A., LATEK, R. R., ERDJUMENT-BROMAGE, H., TEMPST, P. & SABATINI, D. M. 2004. Rictor, a Novel Binding Partner of mTOR, Defines a Rapamycin-Insensitive and Raptor-Independent Pathway that Regulates the Cytoskeleton. *Current Biology,* 14**,** 1296-1302.

EGAN, B. M., LU, G. & GREENE, E. L. 1999. Vascular effects of non-esterified fatty acids: implications for the cardiovascular risk factor cluster. *Prostaglandins Leukot Essent Fatty Acids,* 60**,** 411-20.

ENDO, T. A., MASUHARA, M., YOKOUCHI, M., SUZUKI, R., SAKAMOTO, H., MITSUI, K., MATSUMOTO, A., TANIMURA, S., OHTSUBO, M., MISAWA, H., MIYAZAKI, T., LEONOR, N., TANIGUCHI, T., FUJITA, T., KANAKURA, Y., KOMIYA, S. & YOSHIMURA, A. 1997. A new protein containing an SH2 domain that inhibits JAK kinases. *Nature,* 387**,** 921-4.

ETHERIDGE, S. L., ROH, M. E., COSGROVE, M. E., SANGKHAE, V., FOX, N. E., CHEN, J., LÓPEZ, J. A., KAUSHANSKY, K. & HITCHCOCK, I. S. 2014. JAK2V(617)F-positive endothelial cells contribute to clotting abnormalities in myeloproliferative neoplasms. *Proceedings of the National Academy of Sciences of the United States of America,* 111**,** 2295-2300.

EUFEMI, M., COCCHIOLA, R., ROMANIELLO, D., CORREANI, V., DI FRANCESCO, L., FABRIZI, C., MARAS, B. & SCHININA, M. E. 2015. Acetylation and phosphorylation of STAT3 are involved in the responsiveness of microglia to beta amyloid. *Neurochem Int,* 81**,** 48-56.

EWART, M.-A. & KENNEDY, S. 2011. AMPK and vasculoprotection. *Pharmacology & Therapeutics,* 131**,** 242-253.

EWART, M.-A., KOHLHAAS, C. F. & SALT, I. P. 2008. Inhibition of Tumor Necrosis Factor α–Stimulated Monocyte Adhesion to Human Aortic Endothelial Cells by AMP-Activated Protein Kinase. *Arteriosclerosis, Thrombosis, and Vascular Biology,* 28**,** 2255-2257.

FELDMAN, M. E., APSEL, B., UOTILA, A., LOEWITH, R., KNIGHT, Z. A., RUGGERO, D. & SHOKAT, K. M. 2009. Active-Site Inhibitors of mTOR Target Rapamycin-Resistant Outputs of mTORC1 and mTORC2. *PLoS Biology,* 7**,** e1000038.

FENG, J., WITTHUHN, B. A., MATSUDA, T., KOHLHUBER, F., KERR, I. M. & IHLE, J. N. 1997. Activation of Jak2 catalytic activity requires phosphorylation of Y1007 in the kinase activation loop. *Molecular and Cellular Biology,* 17**,** 2497-2501.

FERRAO, R., WALLWEBER, H. J., HO, H., TAM, C., FRANKE, Y., QUINN, J. & LUPARDUS, P. J. 2016. The Structural Basis for Class II Cytokine Receptor Recognition by JAK1. *Structure,* 24**,** 897-905.

FLEX, E., PETRANGELI, V., STELLA, L., CHIARETTI, S., HORNAKOVA, T., KNOOPS, L., ARIOLA, C., FODALE, V., CLAPPIER, E., PAOLONI, F., MARTINELLI, S., FRAGALE, A., SANCHEZ, M., TAVOLARO, S., MESSINA, M., CAZZANIGA, G., CAMERA, A., PIZZOLO, G., TORNESELLO, A., VIGNETTI, M., BATTISTINI, A., CAVE, H., GELB, B. D., RENAULD, J. C., BIONDI, A., CONSTANTINESCU, S. N., FOA, R. & TARTAGLIA, M. 2008. Somatically acquired JAK1 mutations in adult acute lymphoblastic leukemia. *J Exp Med,* 205**,** 751-8.

FORD, R. J., FULLERTON, M. D., PINKOSKY, S. L., DAY, E. A., SCOTT, J. W., OAKHILL, J. S., BUJAK, A. L., SMITH, B. K., CRANE, J. D., BLUMER, R. M., MARCINKO, K., KEMP, B. E., GERSTEIN, H. C. & STEINBERG, G. R. 2015. Metformin and salicylate synergistically activate liver AMPK, inhibit lipogenesis and improve insulin sensitivity. *Biochem J,* 468**,** 125-32.

FORETZ, M., GUIGAS, B., BERTRAND, L., POLLAK, M. & VIOLLET, B. 2014. Metformin: From Mechanisms of Action to Therapies. *Cell Metabolism,* 20**,** 953-966.

FOX, C. S., COADY, S., SORLIE, P. D., D'AGOSTINO, R. B., SR., PENCINA, M. J., VASAN, R. S., MEIGS, J. B., LEVY, D. & SAVAGE, P. J. 2007. Increasing cardiovascular disease burden due to diabetes mellitus: the Framingham Heart Study. *Circulation,* 115**,** 1544-50.

FRANK, R. 2002. The SPOT-synthesis technique: Synthetic peptide arrays on membrane supports—principles and applications. *Journal of Immunological Methods,* 267**,** 13-26.

FROSTEGARD, J., ULFGREN, A. K., NYBERG, P., HEDIN, U., SWEDENBORG, J., ANDERSSON, U. & HANSSON, G. K. 1999. Cytokine expression in advanced human atherosclerotic plaques: dominance of pro-inflammatory (Th1) and macrophage-stimulating cytokines. *Atherosclerosis,* 145**,** 33-43.

FUKADA, T., HIBI, M., YAMANAKA, Y., TAKAHASHI-TEZUKA, M., FUJITANI, Y., YAMAGUCHI, T., NAKAJIMA, K. & HIRANO, T. 1996. Two Signals Are Necessary for Cell Proliferation Induced by a Cytokine Receptor gp130: Involvement of STAT3 in Anti-Apoptosis. *Immunity,* 5**,** 449-460.

GALIS, Z. S., MUSZYNSKI, M., SUKHOVA, G. K., SIMON-MORRISSEY, E. & LIBBY, P. 1995. Enhanced expression of vascular matrix metalloproteinases induced in vitro by cytokines and in regions of human atherosclerotic lesions. *Ann N Y Acad Sci,* 748**,** 501-7.

GARNERO, P., THOMPSON, E., WOODWORTH, T. & SMOLEN, J. S. 2010. Rapid and sustained improvement in bone and cartilage turnover markers with the anti-interleukin-6 receptor inhibitor tocilizumab plus methotrexate in rheumatoid arthritis patients with an inadequate response to methotrexate: results from a substudy of the multicenter double-blind, placebo-controlled trial of tocilizumab in inadequate responders to methotrexate alone. *Arthritis Rheum,* 62**,** 33-43.

GARTON, A. J., FLINT, A. J. & TONKS, N. K. 1996. Identification of p130(cas) as a substrate for the cytosolic protein tyrosine phosphatase PTP-PEST. *Molecular and Cellular Biology,* 16**,** 6408-6418.

GASKIN, F. S., KAMADA, K., ZUIDEMA, M. Y., JONES, A. W., RUBIN, L. J. & KORTHUIS, R. J. 2011. Isoform-selective 5'-AMP-activated protein kinase-dependent preconditioning mechanisms to prevent postischemic leukocyte-endothelial cell adhesive interactions. *Am J Physiol Heart Circ Physiol,* 300**,** H1352-60.

GAUZZI, M. C., VELAZQUEZ, L., MCKENDRY, R., MOGENSEN, K. E., FELLOUS, M. & PELLEGRINI, S. 1996. Interferon-α-dependent Activation of Tyk2 Requires Phosphorylation of Positive Regulatory Tyrosines by Another Kinase. *Journal of Biological Chemistry,* 271**,** 20494-20500.

GERHARTZ, C., HEESEL, B., SASSE, J., HEMMANN, U., LANDGRAF, C., SCHNEIDER-MERGENER, J., HORN, F., HEINRICH, P. C. & GRAEVE, L. 1996. Differential activation of acute phase response factor/STAT3 and STAT1 via the cytoplasmic domain of the interleukin 6 signal transducer gp130. I. Definition of a novel phosphotyrosine motif mediating STAT1 activation. *J Biol Chem,* 271**,** 12991-8.

GERTZ, M., FISCHER, F., NGUYEN, G. T., LAKSHMINARASIMHAN, M., SCHUTKOWSKI, M., WEYAND, M. & STEEGBORN, C. 2013. Ex-527 inhibits Sirtuins by exploiting their unique NAD+-dependent deacetylation mechanism. *Proc Natl Acad Sci U S A,* 110**,** E2772-81.

GHARAVI, N. M., ALVA, J. A., MOUILLESSEAUX, K. P., LAI, C., YEH, M., YEUNG, W., JOHNSON, J., SZETO, W. L., HONG, L., FISHBEIN, M., WEI, L., PFEFFER, L. M. & BERLINER, J. A. 2007. Role of the JAK/STAT Pathway in the Regulation of Interleukin-8 Transcription by Oxidized Phospholipids in Vitro and in Atherosclerosis in Vivo. *Journal of Biological Chemistry,* 282**,** 31460-31468.

GIRAULT, J. A., LABESSE, G., MORNON, J. P. & CALLEBAUT, I. 1998. Janus kinases and focal adhesion kinases play in the 4.1 band: a superfamily of band 4.1 domains important for cell structure and signal transduction. *Mol Med,* 4**,** 751-69.

GIRI, S., NATH, N., SMITH, B., VIOLLET, B., SINGH, A. K. & SINGH, I. 2004. 5-Aminoimidazole-4-Carboxamide-1-β-4-Ribofuranoside Inhibits Proinflammatory Response in Glial Cells: A Possible Role of AMP-Activated Protein Kinase. *The Journal of Neuroscience,* 24**,** 479-487.

GLASS, C. K. & WITZTUM, J. L. 2001. Atherosclerosis. the road ahead. *Cell,* 104**,** 503-16.

GÓMEZ-GALENO, J. E., DANG, Q., NGUYEN, T. H., BOYER, S. H., GROTE, M. P., SUN, Z., CHEN, M., CRAIGO, W. A., VAN POELJE, P. D., MACKENNA, D. A., CABLE, E. E., ROLZIN, P. A., FINN, P. D., CHI, B., LINEMEYER, D. L., HECKER, S. J. & ERION, M. D. 2010. A Potent and Selective AMPK Activator That Inhibits de Novo Lipogenesis. *ACS Medicinal Chemistry Letters,* 1**,** 478-482.

GONCHAROVA, E. A., GONCHAROV, D. A., DAMERA, G., TLIBA, O., AMRANI, Y., PANETTIERI, R. A. & KRYMSKAYA, V. P. 2009. Signal Transducer and Activator of Transcription 3 Is Required for Abnormal Proliferation and Survival of TSC2-Deficient Cells: Relevance to Pulmonary Lymphangioleiomyomatosis. *Molecular Pharmacology,* 76**,** 766-777.

GÖRANSSON, O., MCBRIDE, A., HAWLEY, S. A., ROSS, F. A., SHPIRO, N., FORETZ, M., VIOLLET, B., HARDIE, D. G. & SAKAMOTO, K. 2007. MECHANISM OF ACTION OF A-769662, A VALUABLE TOOL FOR ACTIVATION OF AMP-ACTIVATED PROTEIN KINASE. *The Journal of biological chemistry,* 282**,** 32549-32560.

GORANTLA, S. P., DECHOW, T. N., GRUNDLER, R., ILLERT, A. L., ZUM BUSCHENFELDE, C. M., KREMER, M., PESCHEL, C. & DUYSTER, J. 2010. Oncogenic JAK2V617F requires an intact SH2-like domain for constitutive activation and induction of a myeloproliferative disease in mice. *Blood,* 116**,** 4600-11.

GOWANS, GRAEME J., HAWLEY, SIMON A., ROSS, FIONA A. & HARDIE, D G. 2013. AMP Is a True Physiological Regulator of AMP-Activated Protein Kinase by Both Allosteric Activation and Enhancing Net Phosphorylation. *Cell Metabolism,* 18**,** 556-566.

GREENLUND, A. C., FARRAR, M. A., VIVIANO, B. L. & SCHREIBER, R. D. 1994. Ligand-induced IFN gamma receptor tyrosine phosphorylation couples the receptor to its signal transduction system (p91). *The EMBO Journal,* 13**,** 1591-1600.

GREER, E. L., OSKOUI, P. R., BANKO, M. R., MANIAR, J. M., GYGI, M. P., GYGI, S. P. & BRUNET, A. 2007. The Energy Sensor AMP-activated Protein Kinase Directly Regulates the Mammalian FOXO3 Transcription Factor. *Journal of Biological Chemistry,* 282**,** 30107-30119.

GRIMALDI, C., CHIARINI, F., TABELLINI, G., RICCI, F., TAZZARI, P. L., BATTISTELLI, M., FALCIERI, E., BORTUL, R., MELCHIONDA, F., IACOBUCCI, I., PAGLIARO, P., MARTINELLI, G., PESSION, A., BARATA, J. T., MCCUBREY, J. A. & MARTELLI, A. M. 2012. AMP-dependent kinase/mammalian target of rapamycin complex 1 signaling in T-cell acute lymphoblastic leukemia: therapeutic implications. *Leukemia,* 26**,** 91-100.

GROTE, K., LUCHTEFELD, M. & SCHIEFFER, B. 2005. JANUS under stress--role of JAK/STAT signaling pathway in vascular diseases. *Vascul Pharmacol,* 43**,** 357-63.

GUMA, M., WANG, Y., VIOLLET, B. & LIU-BRYAN, R. 2015. AMPK Activation by A-769662 Controls IL-6 Expression in Inflammatory Arthritis. *PLoS ONE,* 10**,** e0140452.

GUPTA, V., HARI, P. & HOFFMAN, R. 2012. Allogeneic hematopoietic cell transplantation for myelofibrosis in the era of JAK inhibitors. *Blood,* 120**,** 1367-79.

GUSCHIN, D., ROGERS, N., BRISCOE, J., WITTHUHN, B., WATLING, D., HORN, F., PELLEGRINI, S., YASUKAWA, K., HEINRICH, P., STARK, G. R. & ET AL. 1995. A major role for the protein tyrosine kinase JAK1 in the JAK/STAT signal transduction pathway in response to interleukin-6. *EMBO J,* 14**,** 1421-9.

GWINN, D. M., SHACKELFORD, D. B., EGAN, D. F., MIHAYLOVA, M. M., MERY, A., VASQUEZ, D. S., TURK, B. E. & SHAW, R. J. 2008. AMPK phosphorylation of raptor mediates a metabolic checkpoint. *Mol Cell,* 30**,** 214-26.

HAAN, C., BEHRMANN, I. & HAAN, S. 2010. Perspectives for the use of structural information and chemical genetics to develop inhibitors of Janus kinases. *J Cell Mol Med,* 14**,** 504-27.

HAAN, C., HEINRICH, P. C. & BEHRMANN, I. 2002. Structural requirements of the interleukin-6 signal transducer gp130 for its interaction with Janus kinase 1: the receptor is crucial for kinase activation. *Biochemical Journal,* 361**,** 105-111.

HAAN, C., IS'HARC, H., HERMANNS, H. M., SCHMITZ-VAN DE LEUR, H., KERR, I. M., HEINRICH, P. C., GROTZINGER, J. & BEHRMANN, I. 2001. Mapping of a region within the N terminus of Jak1 involved in cytokine receptor interaction. *J Biol Chem,* 276**,** 37451-8.

HAAN, C., KREIS, S., MARGUE, C. & BEHRMANN, I. 2006. Jaks and cytokine receptors--an intimate relationship. *Biochem Pharmacol,* 72**,** 1538-46.

HAAN, S., MARGUE, C., ENGRAND, A., ROLVERING, C., SCHMITZ-VAN DE LEUR, H., HEINRICH, P. C., BEHRMANN, I. & HAAN, C. 2008. Dual role of the Jak1 FERM and kinase domains in cytokine receptor binding and in stimulation-dependent Jak activation. *J Immunol,* 180**,** 998-1007.

HADI, H. A. R., CARR, C. S. & AL SUWAIDI, J. 2005. Endothelial Dysfunction: Cardiovascular Risk Factors, Therapy, and Outcome. *Vascular Health and Risk Management,* 1**,** 183-198.

HAMILTON, T. A., MA, G. P. & CHISOLM, G. M. 1990. Oxidized low density lipoprotein suppresses the expression of tumor necrosis factor-alpha mRNA in stimulated murine peritoneal macrophages. *J Immunol,* 144**,** 2343-50.

HANDY, J. A., SAXENA, N. K., FU, P., LIN, S., MELLS, J. E., GUPTA, N. A. & ANANIA, F. A. 2010. Adiponectin activation of AMPK disrupts leptin-mediated hepatic fibrosis via Suppressors of Cytokine signaling (SOCS-3). *Journal of cellular biochemistry,* 110**,** 1195-1207.

HANSSON, G. K., LIBBY, P., SCHONBECK, U. & YAN, Z. Q. 2002. Innate and adaptive immunity in the pathogenesis of atherosclerosis. *Circ Res,* 91**,** 281-91.

HARA, K., MARUKI, Y., LONG, X., YOSHINO, K.-I., OSHIRO, N., HIDAYAT, S., TOKUNAGA, C., AVRUCH, J. & YONEZAWA, K. 2002. Raptor, a Binding Partner of Target of Rapamycin (TOR), Mediates TOR Action. *Cell,* 110**,** 177-189.

HARDIE, D. G. 2011. Sensing of energy and nutrients by AMP-activated protein kinase. *The American Journal of Clinical Nutrition,* 93**,** 891S-896S.

HARDIE, D. G. 2014. AMP-activated protein kinase: a key regulator of energy balance with many roles in human disease. *Journal of Internal Medicine,* 276**,** 543-559.

HARDIE, D. G. & ASHFORD, M. L. J. 2014. AMPK: Regulating Energy Balance at the Cellular and Whole Body Levels. *Physiology,* 29**,** 99-107.

HARDIE, D. G., ROSS, FIONA A. & HAWLEY, SIMON A. 2012a. AMP-Activated Protein Kinase: A Target for Drugs both Ancient and Modern. *Chemistry & Biology,* 19**,** 1222-1236.

HARDIE, D. G., ROSS, F. A. & HAWLEY, S. A. 2012b. AMPK: a nutrient and energy sensor that maintains energy homeostasis. *Nat Rev Mol Cell Biol,* 13**,** 251-262.

HARDIE, D. G., SCHAFFER, B. E. & BRUNET, A. 2016. AMPK: An Energy-Sensing Pathway with Multiple Inputs and Outputs. *Trends in Cell Biology,* 26**,** 190-201.

HARRISON, C., KILADJIAN, J.-J., AL-ALI, H. K., GISSLINGER, H., WALTZMAN, R., STALBOVSKAYA, V., MCQUITTY, M., HUNTER, D. S., LEVY, R., KNOOPS, L., CERVANTES, F., VANNUCCHI, A. M., BARBUI, T. & BAROSI, G. 2012. JAK Inhibition with Ruxolitinib versus Best Available Therapy for Myelofibrosis. *New England Journal of Medicine,* 366**,** 787-798.

HATTORI, Y., NAKANO, Y., HATTORI, S., TOMIZAWA, A., INUKAI, K. & KASAI, K. 2008. High molecular weight adiponectin activates AMPK and suppresses cytokine-induced NF-κB activation in vascular endothelial cells. *FEBS Letters,* 582**,** 1719-1724.

HAWLEY, S. A., BOUDEAU, J., REID, J. L., MUSTARD, K. J., UDD, L., MÄKELÄ, T. P., ALESSI, D. R. & HARDIE, D. G. 2003. Complexes between the LKB1 tumor suppressor, STRADα/β and MO25α/β are upstream kinases in the AMP-activated protein kinase cascade. *Journal of Biology,* 2**,** 28-28.

HAWLEY, S. A., DAVISON, M., WOODS, A., DAVIES, S. P., BERI, R. K., CARLING, D. & HARDIE, D. G. 1996. Characterization of the AMP-activated Protein Kinase Kinase from Rat Liver and Identification of Threonine 172 as the Major Site at Which It Phosphorylates AMP-activated Protein Kinase. *Journal of Biological Chemistry,* 271**,** 27879-27887.

HAWLEY, S. A., FULLERTON, M. D., ROSS, F. A., SCHERTZER, J. D., CHEVTZOFF, C., WALKER, K. J., PEGGIE, M. W., ZIBROVA, D., GREEN, K. A., MUSTARD, K. J., KEMP, B. E., SAKAMOTO, K.,

STEINBERG, G. R. & HARDIE, D. G. 2012. The ancient drug salicylate directly activates AMP-activated protein kinase. *Science (New York, N.Y.),* 336**,** 918-922.

HAWLEY, S. A., PAN, D. A., MUSTARD, K. J., ROSS, L., BAIN, J., EDELMAN, A. M., FRENGUELLI, B. G. & HARDIE, D. G. 2005. Calmodulin-dependent protein kinase kinase-β is an alternative upstream kinase for AMP-activated protein kinase. *Cell Metabolism,* 2**,** 9-19.

HAWLEY, S. A., ROSS, F. A., CHEVTZOFF, C., GREEN, K. A., EVANS, A., FOGARTY, S., TOWLER, M. C., BROWN, L. J., OGUNBAYO, O. A., EVANS, A. M. & HARDIE, D. G. 2010. Use of Cells Expressing γ Subunit Variants to Identify Diverse Mechanisms of AMPK Activation. *Cell Metabolism,* 11**,** 554-565.

HE, C., LI, H., VIOLLET, B., ZOU, M.-H. & XIE, Z. 2015. AMPK Suppresses Vascular Inflammation In Vivo by Inhibiting Signal Transducer and Activator of Transcription-1. *Diabetes,* 64**,** 4285-4297.

HECHT, D. & ZICK, Y. 1992. Selective inhibition of protein tyrosine phosphatase activities by H2O2 and vanadate In vitro. *Biochemical and Biophysical Research Communications,* 188**,** 773-779.

HEIM, M. H., KERR, I. M., STARK, G. R. & DARNELL, J. E., JR. 1995. Contribution of STAT SH2 groups to specific interferon signaling by the Jak-STAT pathway. *Science,* 267**,** 1347-9.

HEINRICH, P. C., BEHRMANN, I., HAAN, S., HERMANNS, H. M., MULLER-NEWEN, G. & SCHAPER, F. 2003. Principles of interleukin (IL)-6-type cytokine signalling and its regulation. *Biochem J,* 374**,** 1-20.

HENNEKENS, C. H. & DALEN, J. E. 2013. Aspirin in the treatment and prevention of cardiovascular disease: past and current perspectives and future directions. *Am J Med,* 126**,** 373-8.

HIGGS, G. A., SALMON, J. A., HENDERSON, B. & VANE, J. R. 1987. Pharmacokinetics of aspirin and salicylate in relation to inhibition of arachidonate cyclooxygenase and antiinflammatory activity. *Proc Natl Acad Sci U S A,* 84**,** 1417-20.

HILKENS, C. M., IS'HARC, H., LILLEMEIER, B. F., STROBL, B., BATES, P. A., BEHRMANN, I. & KERR, I. M. 2001. A region encompassing the FERM domain of Jak1 is necessary for binding to the cytokine receptor gp130. *FEBS Lett,* 505**,** 87-91.

HILTON, D. J., RICHARDSON, R. T., ALEXANDER, W. S., VINEY, E. M., WILLSON, T. A., SPRIGG, N. S., STARR, R., NICHOLSON, S. E., METCALF, D. & NICOLA, N. A. 1998. Twenty proteins containing a C-terminal SOCS box form five structural classes. *Proc Natl Acad Sci U S A,* 95**,** 114-9.

HO, H. H. & IVASHKIV, L. B. 2006. Role of STAT3 in type I interferon responses. Negative regulation of STAT1-dependent inflammatory gene activation. *J Biol Chem,* 281**,** 14111-8.

HOLMAN , R. R., PAUL , S. K., BETHEL , M. A., MATTHEWS , D. R. & NEIL , H. A. W. 2008. 10-Year Follow-up of Intensive Glucose Control in Type 2 Diabetes. *New England Journal of Medicine,* 359**,** 1577-1589.

HORNAKOVA, T., SPRINGUEL, L., DEVREUX, J., DUSA, A., CONSTANTINESCU, S. N., KNOOPS, L. & RENAULD, J.-C. 2011. Oncogenic JAK1 and JAK2-activating mutations resistant to ATP-competitive inhibitors. *Haematologica,* 96**,** 845-853.

HORVATH, C. M. 2000. STAT proteins and transcriptional responses to extracellular signals. *Trends Biochem Sci,* 25**,** 496-502.

HSU, M.-F. & MENG, T.-C. 2010. Enhancement of Insulin Responsiveness by Nitric Oxide-mediated Inactivation of Protein-tyrosine Phosphatases. *The Journal of Biological Chemistry,* 285**,** 7919-7928.

HUBER, S. A., SAKKINEN, P., CONZE, D., HARDIN, N. & TRACY, R. 1999. Interleukin-6 Exacerbates Early Atherosclerosis in Mice. *Arteriosclerosis, Thrombosis, and Vascular Biology,* 19**,** 2364.

HUDSON, E. R., PAN, D. A., JAMES, J., LUCOCQ, J. M., HAWLEY, S. A., GREEN, K. A., BABA, O., TERASHIMA, T. & HARDIE, D. G. 2003. A Novel Domain in AMP-Activated Protein Kinase Causes Glycogen Storage Bodies Similar to Those Seen in Hereditary Cardiac Arrhythmias. *Current Biology,* 13**,** 861-866.

HUNGER, S. P., LU, X., DEVIDAS, M., CAMITTA, B. M., GAYNON, P. S., WINICK, N. J., REAMAN, G. H. & CARROLL, W. L. 2012. Improved survival for children and adolescents with acute

lymphoblastic leukemia between 1990 and 2005: a report from the children's oncology group. *J Clin Oncol,* 30**,** 1663-9.

HUNTER, ROGER W., FORETZ, M., BULTOT, L., FULLERTON, MORGAN D., DEAK, M., ROSS, FIONA A., HAWLEY, SIMON A., SHPIRO, N., VIOLLET, B., BARRON, D., KEMP, BRUCE E., STEINBERG, GREGORY R., HARDIE, D. G. & SAKAMOTO, K. 2014. Mechanism of Action of Compound-13: An α1-Selective Small Molecule Activator of AMPK. *Chemistry & Biology,* 21**,** 866-879.

HURLEY, R. L., ANDERSON, K. A., FRANZONE, J. M., KEMP, B. E., MEANS, A. R. & WITTERS, L. A. 2005. The Ca2+/Calmodulin-dependent Protein Kinase Kinases Are AMP-activated Protein Kinase Kinases. *Journal of Biological Chemistry,* 280**,** 29060-29066.

IGLESIAS, M. A., YE, J. M., FRANGIOUDAKIS, G., SAHA, A. K., TOMAS, E., RUDERMAN, N. B., COONEY, G. J. & KRAEGEN, E. W. 2002. AICAR administration causes an apparent enhancement of muscle and liver insulin action in insulin-resistant high-fat-fed rats. *Diabetes,* 51**,** 2886-94.

IHLE, J. N., WITTHUHN, B. A., QUELLE, F. W., YAMAMOTO, K., THIERFELDER, W. E., KREIDER, B. & SILVENNOINEN, O. 1994. Signaling by the cytokine receptor superfamily: JAKs and STATs. *Trends Biochem Sci,* 19**,** 222-7.

IL6R MR, C. 2012. The interleukin-6 receptor as a target for prevention of coronary heart disease: a mendelian randomisation analysis. *Lancet,* 379**,** 1214-1224.

INOKI, K., ZHU, T. & GUAN, K. L. 2003. TSC2 mediates cellular energy response to control cell growth and survival. *Cell,* 115**,** 577-90.

INZUCCHI, S. E., BERGENSTAL, R. M., BUSE, J. B., DIAMANT, M., FERRANNINI, E., NAUCK, M., PETERS, A. L., TSAPAS, A., WENDER, R. & MATTHEWS, D. R. 2015. Management of hyperglycaemia in type 2 diabetes, 2015: a patient-centred approach. Update to a position statement of the American Diabetes Association and the European Association for the Study of Diabetes. *Diabetologia,* 58**,** 429-42.

JACINTO, E., LOEWITH, R., SCHMIDT, A., LIN, S., RUEGG, M. A., HALL, A. & HALL, M. N. 2004. Mammalian TOR complex 2 controls the actin cytoskeleton and is rapamycin insensitive. *Nat Cell Biol,* 6**,** 1122-1128.

JAFFE, E. A., NACHMAN, R. L., BECKER, C. G. & MINICK, C. R. 1973. Culture of human endothelial cells derived from umbilical veins. Identification by morphologic and immunologic criteria. *J Clin Invest,* 52**,** 2745-56.

JAMES, C., UGO, V., LE COUEDIC, J. P., STAERK, J., DELHOMMEAU, F., LACOUT, C., GARCON, L., RASLOVA, H., BERGER, R., BENNACEUR-GRISCELLI, A., VILLEVAL, J. L., CONSTANTINESCU, S. N., CASADEVALL, N. & VAINCHENKER, W. 2005. A unique clonal JAK2 mutation leading to constitutive signalling causes polycythaemia vera. *Nature,* 434**,** 1144-8.

JEONG, E. G., KIM, M. S., NAM, H. K., MIN, C. K., LEE, S., CHUNG, Y. J., YOO, N. J. & LEE, S. H. 2008. Somatic mutations of JAK1 and JAK3 in acute leukemias and solid cancers. *Clin Cancer Res,* 14**,** 3716-21.

JEONG, H. W., HSU, K. C., LEE, J.-W., HAM, M., HUH, J. Y., SHIN, H. J., KIM, W. S. & KIM, J. B. 2009. Berberine suppresses proinflammatory responses through AMPK activation in macrophages. *American Journal of Physiology - Endocrinology And Metabolism,* 296**,** E955-E964.

JOHNSON, J. A., SIMPSON, S. H., TOTH, E. L. & MAJUMDAR, S. R. 2005. Reduced cardiovascular morbidity and mortality associated with metformin use in subjects with Type 2 diabetes. *Diabet Med,* 22**,** 497-502.

JOTTA, P. Y., GANAZZA, M. A., SILVA, A., VIANA, M. B., DA SILVA, M. J., ZAMBALDI, L. J., BARATA, J. T., BRANDALISE, S. R. & YUNES, J. A. 2010. Negative prognostic impact of PTEN mutation in pediatric T-cell acute lymphoblastic leukemia. *Leukemia,* 24**,** 239-42.

JOUGASAKI, M., ICHIKI, T., TAKENOSHITA, Y. & SETOGUCHI, M. 2010. Statins suppress interleukin-6-induced monocyte chemo-attractant protein-1 by inhibiting Janus kinase/signal transducers and activators of transcription pathways in human vascular endothelial cells. *British Journal of Pharmacology,* 159**,** 1294-1303.

JU, J. H., HEO, Y. J., CHO, M. L., JHUN, J. Y., PARK, J. S., LEE, S. Y., OH, H. J., MOON, S. J., KWOK, S. K., PARK, K. S., PARK, S. H. & KIM, H. Y. 2012. Modulation of STAT-3 in rheumatoid synovial T cells suppresses Th17 differentiation and increases the proportion of Treg cells. *Arthritis Rheum,* 64**,** 3543-52.

KAHN, B. B., ALQUIER, T., CARLING, D. & HARDIE, D. G. 2005. AMP-activated protein kinase: Ancient energy gauge provides clues to modern understanding of metabolism. *Cell Metabolism,* 1**,** 15-25.

KAMURA, T., SATO, S., HAQUE, D., LIU, L., KAELIN, W. G., CONAWAY, R. C. & CONAWAY, J. W. 1998. The Elongin BC complex interacts with the conserved SOCS-box motif present in members of the SOCS, ras, WD-40 repeat, and ankyrin repeat families. *Genes & Development,* 12**,** 3872-3881.

KANG, K. Y., KIM, Y. K., YI, H., KIM, J., JUNG, H. R., KIM, I. J., CHO, J. H., PARK, S. H., KIM, H. Y. & JU, J. H. 2013. Metformin downregulates Th17 cells differentiation and attenuates murine autoimmune arthritis. *Int Immunopharmacol,* 16**,** 85-92.

KAPTEIN, A., PAILLARD, V. & SAUNDERS, M. 1996. Dominant negative stat3 mutant inhibits interleukin-6-induced Jak-STAT signal transduction. *J Biol Chem,* 271**,** 5961-4.

KAWASHIMA, I. & KIRITO, K. 2016. Metformin inhibits JAK2V617F activity in MPN cells by activating AMPK and PP2A complexes containing the B56alpha subunit. *Exp Hematol,* 44**,** 1156-1165.e4.

KELLY, S. M., JESS, T. J. & PRICE, N. C. 2005. How to study proteins by circular dichroism. *Biochim Biophys Acta,* 1751**,** 119-39.

KEMP, B. E. 2004. Bateman domains and adenosine derivatives form a binding contract. *Journal of Clinical Investigation,* 113**,** 182-184.

KERSHAW, N. J., MURPHY, J. M., LIAU, N. P., VARGHESE, L. N., LAKTYUSHIN, A., WHITLOCK, E. L., LUCET, I. S., NICOLA, N. A. & BABON, J. J. 2013. SOCS3 binds specific receptor-JAK complexes to control cytokine signaling by direct kinase inhibition. *Nat Struct Mol Biol,* 20**,** 469-76.

KILANI, B., VIEIRA DIAS, J., GOURDOU-LATYSZENOK, V., LIPPERT, E., SEWDUTH, R., DUPLAA, C., VILLEVAL, J.-L., COUFFINHAL, T. & JAMES, C. 2014. Consequences of the Presence of the JAK2V617F Mutation in Endothelial Cells: Towards a Better Understanding of the Increased Angiogenesis in Myeloproliferative Neoplasms. *Blood,* 124**,** 102.

KIM, J., WON, J.-S., SINGH, A. K., SHARMA, A. K. & SINGH, I. 2014. STAT3 Regulation by S-Nitrosylation: Implication for Inflammatory Disease. *Antioxidants & Redox Signaling,* 20**,** 2514-2527.

KIM, Y. D., KIM, Y. H., CHO, Y. M., KIM, D. K., AHN, S. W., LEE, J. M., CHANDA, D., SHONG, M., LEE, C. H. & CHOI, H. S. 2012. Metformin ameliorates IL-6-induced hepatic insulin resistance via induction of orphan nuclear receptor small heterodimer partner (SHP) in mouse models. *Diabetologia,* 55**,** 1482-1494.

KIMURA, N., TOKUNAGA, C., DALAL, S., RICHARDSON, C., YOSHINO, K.-I., HARA, K., KEMP, B. E., WITTERS, L. A., MIMURA, O. & YONEZAWA, K. 2003. A possible linkage between AMP-activated protein kinase (AMPK) and mammalian target of rapamycin (mTOR) signalling pathway. *Genes to Cells,* 8**,** 65-79.

KIRII, H., NIWA, T., YAMADA, Y., WADA, H., SAITO, K., IWAKURA, Y., ASANO, M., MORIWAKI, H. & SEISHIMA, M. 2003. Lack of interleukin-1beta decreases the severity of atherosclerosis in ApoE-deficient mice. *Arterioscler Thromb Vasc Biol,* 23**,** 656-60.

KISSELEVA, T., BHATTACHARYA, S., BRAUNSTEIN, J. & SCHINDLER, C. W. 2002. Signaling through the JAK/STAT pathway, recent advances and future challenges. *Gene,* 285**,** 1-24.

KLINGMULLER, U., LORENZ, U., CANTLEY, L. C., NEEL, B. G. & LODISH, H. F. 1995. Specific recruitment of SH-PTP1 to the erythropoietin receptor causes inactivation of JAK2 and termination of proliferative signals. *Cell,* 80**,** 729-38.

KLOUCHE, M., BHAKDI, S., HEMMES, M. & ROSE-JOHN, S. 1999. Novel Path to Activation of Vascular Smooth Muscle Cells: Up-Regulation of gp130 Creates an Autocrine Activation Loop by IL-6 and Its Soluble Receptor. *The Journal of Immunology,* 163**,** 4583.

KOGA, M., KAI, H., YASUKAWA, H., YAMAMOTO, T., KAWAI, Y., KATO, S., KUSABA, K., KAI, M., EGASHIRA, K., KATAOKA, Y. & IMAIZUMI, T. 2007. Inhibition of Progression and Stabilization of Plaques by Postnatal Interferon-γ Function Blocking in ApoE-Knockout Mice. *Circulation Research,* 101**,** 348-356.

KOJIMA, H., SASAKI, T., ISHITANI, T., IEMURA, S.-I., ZHAO, H., KANEKO, S., KUNIMOTO, H., NATSUME, T., MATSUMOTO, K. & NAKAJIMA, K. 2005. STAT3 regulates Nemo-like kinase by mediating its interaction with IL-6-stimulated TGFβ-activated kinase 1 for STAT3 Ser-727 phosphorylation. *Proceedings of the National Academy of Sciences of the United States of America,* 102**,** 4524-4529.

KOVACIC, J. C., GUPTA, R., LEE, A. C., MA, M., FANG, F., TOLBERT, C. N., WALTS, A. D., BELTRAN, L. E., SAN, H., CHEN, G., ST. HILAIRE, C. & BOEHM, M. 2010. Stat3-dependent acute Rantes production in vascular smooth muscle cells modulates inflammation following arterial injury in mice. *The Journal of Clinical Investigation,* 120**,** 303-314.

KOVARIK, P., MANGOLD, M., RAMSAUER, K., HEIDARI, H., STEINBORN, R., ZOTTER, A., LEVY, D. E., MÜLLER, M. & DECKER, T. 2001. Specificity of signaling by STAT1 depends on SH2 and C-terminal domains that regulate Ser727 phosphorylation, differentially affecting specific target gene expression. *The EMBO Journal,* 20**,** 91-100.

KRALOVICS , R., PASSAMONTI , F., BUSER , A. S., TEO , S.-S., TIEDT , R., PASSWEG , J. R., TICHELLI , A., CAZZOLA , M. & SKODA , R. C. 2005. A Gain-of-Function Mutation of JAK2 in Myeloproliferative Disorders. *New England Journal of Medicine,* 352**,** 1779-1790.

KRAMER, O. H., KNAUER, S. K., GREINER, G., JANDT, E., REICHARDT, S., GUHRS, K. H., STAUBER, R. H., BOHMER, F. D. & HEINZEL, T. 2009. A phosphorylation-acetylation switch regulates STAT1 signaling. *Genes Dev,* 23**,** 223-35.

KRISHNAN, V. & RAJASEKARAN, A. K. 2014. Clinical nanomedicine: a solution to the chemotherapy conundrum in pediatric leukemia therapy. *Clin Pharmacol Ther,* 95**,** 168-78.

LAM, M. H. C., MICHELL, B. J., FODERO-TAVOLETTI, M. T., KEMP, B. E., TONKS, N. K. & TIGANIS, T. 2001. Cellular Stress Regulates the Nucleocytoplasmic Distribution of the Protein-tyrosine Phosphatase TCPTP. *Journal of Biological Chemistry,* 276**,** 37700-37707.

LANG, R., PAULEAU, A. L., PARGANAS, E., TAKAHASHI, Y., MAGES, J., IHLE, J. N., RUTSCHMAN, R. & MURRAY, P. J. 2003. SOCS3 regulates the plasticity of gp130 signaling. *Nat Immunol,* 4**,** 546-50.

LANGENDORF, C. G., NGOEI, K. R. W., SCOTT, J. W., LING, N. X. Y., ISSA, S. M. A., GORMAN, M. A., PARKER, M. W., SAKAMOTO, K., OAKHILL, J. S. & KEMP, B. E. 2016. Structural basis of allosteric and synergistic activation of AMPK by furan-2-phosphonic derivative C2 binding. *Nature Communications,* 7**,** 10912.

LANGHEINRICH, A. C. & BOHLE, R. M. 2005. Atherosclerosis: humoral and cellular factors of inflammation. *Virchows Arch,* 446**,** 101-11.

LAU, A. W., LIU, P., INUZUKA, H. & GAO, D. 2014. SIRT1 phosphorylation by AMP-activated protein kinase regulates p53 acetylation. *American Journal of Cancer Research,* 4**,** 245-255.

LEBRUN, J. J., ALI, S., ULLRICH, A. & KELLY, P. A. 1995. Proline-rich sequence-mediated Jak2 association to the prolactin receptor is required but not sufficient for signal transduction. *J Biol Chem,* 270**,** 10664-70.

LEE, C.-W., WONG, L. L.-Y., TSE, E. Y.-T., LIU, H.-F., LEONG, V. Y.-L., MAN-FONG, J., HARDIE, D. G., NG, I. O.-L. & CHING, Y.-P. 2012. AMPK promotes p53 acetylation via phosphorylation and inactivation of SIRT1 in liver cancer cells. *Cancer research,* 72**,** 4394-4404.

LEE, Y. W., HENNIG, B. & TOBOREK, M. 2003. Redox-regulated mechanisms of IL-4-induced MCP-1 expression in human vascular endothelial cells. *American Journal of Physiology - Heart and Circulatory Physiology,* 284**,** H185.

LEHMANN, U., SCHMITZ, J., WEISSENBACH, M., SOBOTA, R. M., HÖRTNER, M., FRIEDERICHS, K., BEHRMANN, I., TSIARIS, W., SASAKI, A., SCHNEIDER-MERGENER, J., YOSHIMURA, A., NEEL, B. G., HEINRICH, P. C. & SCHAPER, F. 2003. SHP2 and SOCS3 Contribute to Tyr-759-dependent Attenuation of Interleukin-6 Signaling through gp130. *Journal of Biological Chemistry,* 278**,** 661-671.

LEONARD, W. J. & O'SHEA, J. J. 1998. Jaks and STATs: biological implications. *Annu Rev Immunol,* 16**,** 293-322.

LEROY, E. & CONSTANTINESCU, S. N. 2017. Rethinking JAK2 inhibition: towards novel strategies of more specific and versatile janus kinase inhibition. *Leukemia*.

LEVINE, R. L., WADLEIGH, M., COOLS, J., EBERT, B. L., WERNIG, G., HUNTLY, B. J., BOGGON, T. J., WLODARSKA, I., CLARK, J. J., MOORE, S., ADELSPERGER, J., KOO, S., LEE, J. C., GABRIEL, S., MERCHER, T., D'ANDREA, A., FROHLING, S., DOHNER, K., MARYNEN, P., VANDENBERGHE, P., MESA, R. A., TEFFERI, A., GRIFFIN, J. D., ECK, M. J., SELLERS, W. R., MEYERSON, M., GOLUB, T. R., LEE, S. J. & GILLILAND, D. G. 2005. Activating mutation in the tyrosine kinase JAK2 in polycythemia vera, essential thrombocythemia, and myeloid metaplasia with myelofibrosis. *Cancer Cell,* 7**,** 387-97.

LEXIS, C. P. H., VAN DER HORST, I. C. C., LIPSIC, E., VAN DER HARST, P., VAN DER HORST-SCHRIVERS, A. N. A., WOLFFENBUTTEL, B. H. R., DE BOER, R. A., VAN ROSSUM, A. C., VAN VELDHUISEN, D. J., DE SMET, B. J. G. L. & FOR THE, G.-I. I. I. I. 2012. Metformin in non-Diabetic Patients Presenting with ST Elevation Myocardial Infarction: Rationale and Design of the Glycometabolic Intervention as Adjunct to Primary Percutaneous Intervention in ST Elevation Myocardial Infarction (GIPS)-III Trial. *Cardiovascular Drugs and Therapy,* 26**,** 417-426.

LIANG, H., VENEMA, V. J., WANG, X., JU, H., VENEMA, R. C. & MARRERO, M. B. 1999. Regulation of Angiotensin II-induced Phosphorylation of STAT3 in Vascular Smooth Muscle Cells. *Journal of Biological Chemistry,* 274**,** 19846-19851.

LIBBY, P. 2002. Inflammation in atherosclerosis. *Nature,* 420**,** 868-74.

LIBBY, P., ORDOVAS, J. M., AUGER, K. R., ROBBINS, A. H., BIRINYI, L. K. & DINARELLO, C. A. 1986. Endotoxin and tumor necrosis factor induce interleukin-1 gene expression in adult human vascular endothelial cells. *Am J Pathol,* 124**,** 179-85.

LIN, C. H., KAUSHANSKY, K. & ZHAN, H. 2016. JAK2V617F-mutant vascular niche contributes to JAK2V617F clonal expansion in myeloproliferative neoplasms. *Blood Cells Mol Dis,* 62**,** 42-48.

LIU, B. A., ENGELMANN, B. W. & NASH, P. D. 2012. The language of SH2 domain interactions defines phosphotyrosine-mediated signal transduction. *FEBS Lett,* 586**,** 2597-605.

LIU, K. D., GAFFEN, S. L., GOLDSMITH, M. A. & GREENE, W. C. 1997. Janus kinases in interleukin-2-mediated signaling: JAK1 and JAK3 are differentially regulated by tyrosine phosphorylation. *Curr Biol,* 7**,** 817-26.

LUPARDUS, P. J., ULTSCH, M., WALLWEBER, H., BIR KOHLI, P., JOHNSON, A. R. & EIGENBROT, C. 2014. Structure of the pseudokinase-kinase domains from protein kinase TYK2 reveals a mechanism for Janus kinase (JAK) autoinhibition. *Proc Natl Acad Sci U S A,* 111**,** 8025-30.

LUST, J. A., DONOVAN, K. A., KLINE, M. P., GREIPP, P. R., KYLE, R. A. & MAIHLE, N. J. 1992. Isolation of an mRNA encoding a soluble form of the human interleukin-6 receptor. *Cytokine,* 4**,** 96-100.

MACK, H. I., ZHENG, B., ASARA, J. M. & THOMAS, S. M. 2012. AMPK-dependent phosphorylation of ULK1 regulates ATG9 localization. *Autophagy,* 8**,** 1197-214.

MADHOK, R., CRILLY, A., WATSON, J. & CAPELL, H. A. 1993. Serum interleukin 6 levels in rheumatoid arthritis: correlations with clinical and laboratory indices of disease activity. *Ann Rheum Dis,* 52**,** 232-4.

MAHBOUBI, K., LI, F., PLESCIA, J., KIRKILES-SMITH, N. C., MESRI, M., DU, Y., CARROLL, J. M., ELIAS, J. A., ALTIERI, D. C. & POBER, J. S. 2001. Interleukin-11 up-regulates survivin expression in endothelial cells through a signal transducer and activator of transcription-3 pathway. *Lab Invest,* 81**,** 327-34.

MAINI, R. N., ELLIOTT, M. J., BRENNAN, F. M. & FELDMANN, M. 1995. Beneficial effects of tumour necrosis factor-alpha (TNF-alpha) blockade in rheumatoid arthritis (RA). *Clin Exp Immunol,* 101**,** 207-12.

MALDEN, L. T., CHAIT, A., RAINES, E. W. & ROSS, R. 1991. The influence of oxidatively modified low density lipoproteins on expression of platelet-derived growth factor by human monocyte-derived macrophages. *J Biol Chem,* 266**,** 13901-7.

MANCINI, S. J., WHITE, A. D., BIJLAND, S., RUTHERFORD, C., GRAHAM, D., RICHTER, E. A., VIOLLET, B., TOUYZ, R. M., PALMER, T. M. & SALT, I. P. 2017. Activation of AMP-activated protein kinase rapidly suppresses multiple pro-inflammatory pathways in adipocytes including IL-1 receptor-associated kinase-4 phosphorylation. *Mol Cell Endocrinol,* 440**,** 44-56.

MANEA, S.-A., MANEA, A. & HELTIANU, C. 2010. Inhibition of JAK/STAT signaling pathway prevents high-glucose-induced increase in endothelin-1 synthesis in human endothelial cells. *Cell and Tissue Research,* 340**,** 71-79.

MATTHEWS, V., SCHUSTER, B., SCHUTZE, S., BUSSMEYER, I., LUDWIG, A., HUNDHAUSEN, C., SADOWSKI, T., SAFTIG, P., HARTMANN, D., KALLEN, K. J. & ROSE-JOHN, S. 2003. Cellular cholesterol depletion triggers shedding of the human interleukin-6 receptor by ADAM10 and ADAM17 (TACE). *J Biol Chem,* 278**,** 38829-39.

MCBRIDE, A., GHILAGABER, S., NIKOLAEV, A. & HARDIE, D. G. 2009. The Glycogen-Binding Domain on the AMPK β Subunit Allows the Kinase to Act as a Glycogen Sensor. *Cell Metabolism,* 9**,** 23-34.

MCGARRY, J. D. & BROWN, N. F. 1997. The Mitochondrial Carnitine Palmitoyltransferase System — From Concept to Molecular Analysis. *European Journal of Biochemistry,* 244**,** 1-14.

MCINNES, I. B. & SCHETT, G. 2011. The pathogenesis of rheumatoid arthritis. *N Engl J Med,* 365**,** 2205-19.

MEDZHITOV, R. 2008. Origin and physiological roles of inflammation. *Nature,* 454**,** 428-435.

MELLBIN, L. G., MALMBERG, K., NORHAMMAR, A., WEDEL, H. & RYDEN, L. 2011. Prognostic implications of glucose-lowering treatment in patients with acute myocardial infarction and diabetes: experiences from an extended follow-up of the Diabetes Mellitus Insulin-Glucose Infusion in Acute Myocardial Infarction (DIGAMI) 2 Study. *Diabetologia,* 54**,** 1308-17.

MIHARA, M., HASHIZUME, M., YOSHIDA, H., SUZUKI, M. & SHIINA, M. 2012. IL-6/IL-6 receptor system and its role in physiological and pathological conditions. *Clin Sci (Lond),* 122**,** 143-59.

MIHARA, M., KASUTANI, K., OKAZAKI, M., NAKAMURA, A., KAWAI, S., SUGIMOTO, M., MATSUMOTO, Y. & OHSUGI, Y. 2005. Tocilizumab inhibits signal transduction mediated by both mIL-6R and sIL-6R, but not by the receptors of other members of IL-6 cytokine family. *Int Immunopharmacol,* 5**,** 1731-40.

MING, W. J., BERSANI, L. & MANTOVANI, A. 1987. Tumor necrosis factor is chemotactic for monocytes and polymorphonuclear leukocytes. *J Immunol,* 138**,** 1469-74.

MIRGUET, O., SAUTET, S., CLÉMENT, C.-A., TOUM, J., DONCHE, F., MARQUES, C., RONDET, E., PIZZONERO, M., BEAUFILS, B., DUDIT, Y., HUET, P., TROTTET, L., GRONDIN, P., BRUSQ, J.-M., BOURSIER, E., SAINTILLAN, Y. & NICODEME, E. 2013. Discovery of Pyridones As Oral AMPK Direct Activators. *ACS Medicinal Chemistry Letters,* 4**,** 632-636.

MODUR, V., LI, Y., ZIMMERMAN, G. A., PRESCOTT, S. M. & MCINTYRE, T. M. 1997. Retrograde inflammatory signaling from neutrophils to endothelial cells by soluble interleukin-6 receptor alpha. *Journal of Clinical Investigation,* 100**,** 2752-2756.

MORROW, V. A., FOUFELLE, F., CONNELL, J. M. C., PETRIE, J. R., GOULD, G. W. & SALT, I. P. 2003. Direct Activation of AMP-activated Protein Kinase Stimulates Nitric-oxide Synthesis in Human Aortic Endothelial Cells. *Journal of Biological Chemistry,* 278**,** 31629-31639.

MUGABO, Y., MUKANEZA, Y. & RENIER, G. 2011. Palmitate induces C-reactive protein expression in human aortic endothelial cells. Relevance to fatty acid–induced endothelial dysfunction. *Metabolism,* 60**,** 640-648.

MULLBERG, J., SCHOOLTINK, H., STOYAN, T., GUNTHER, M., GRAEVE, L., BUSE, G., MACKIEWICZ, A., HEINRICH, P. C. & ROSE-JOHN, S. 1993. The soluble interleukin-6 receptor is generated by shedding. *Eur J Immunol,* 23**,** 473-80.

MULLER-NEWEN, G., KOHNE, C., KEUL, R., HEMMANN, U., MULLER-ESTERL, W., WIJDENES, J., BRAKENHOFF, J. P., HART, M. H. & HEINRICH, P. C. 1996. Purification and characterization of the soluble interleukin-6 receptor from human plasma and identification of an isoform generated through alternative splicing. *Eur J Biochem,* 236**,** 837-42.

MULLER, A. M., HERMANNS, M. I., SKRZYNSKI, C., NESSLINGER, M., MULLER, K. M. & KIRKPATRICK, C. J. 2002. Expression of the endothelial markers PECAM-1, vWf, and CD34 in vivo and in vitro. *Exp Mol Pathol,* 72**,** 221-9.

MULLER, M., BRISCOE, J., LAXTON, C., GUSCHIN, D., ZIEMIECKI, A., SILVENNOINEN, O., HARPUR, A. G., BARBIERI, G., WITTHUHN, B. A., SCHINDLER, C. & ET AL. 1993. The protein tyrosine kinase JAK1 complements defects in interferon-alpha/beta and -gamma signal transduction. *Nature,* 366**,** 129-35.

MULLIGHAN, C. G., ZHANG, J., HARVEY, R. C., COLLINS-UNDERWOOD, J. R., SCHULMAN, B. A., PHILLIPS, L. A., TASIAN, S. K., LOH, M. L., SU, X., LIU, W., DEVIDAS, M., ATLAS, S. R., CHEN, I. M., CLIFFORD, R. J., GERHARD, D. S., CARROLL, W. L., REAMAN, G. H., SMITH, M., DOWNING, J. R., HUNGER, S. P. & WILLMAN, C. L. 2009. JAK mutations in high-risk childhood acute lymphoblastic leukemia. *Proc Natl Acad Sci U S A,* 106**,** 9414-8.

MURAKAMI, M., HIBI, M., NAKAGAWA, N., NAKAGAWA, T., YASUKAWA, K., YAMANISHI, K., TAGA, T. & KISHIMOTO, T. 1993. IL-6-induced homodimerization of gp130 and associated activation of a tyrosine kinase. *Science,* 260**,** 1808-10.

MURAKAMI, M., NARAZAKI, M., HIBI, M., YAWATA, H., YASUKAWA, K., HAMAGUCHI, M., TAGA, T. & KISHIMOTO, T. 1991. Critical cytoplasmic region of the interleukin 6 signal transducer gp130 is conserved in the cytokine receptor family. *Proc Natl Acad Sci U S A,* 88**,** 11349-53.

MURRAY, P. J. 2007. The JAK-STAT Signaling Pathway: Input and Output Integration. *The Journal of Immunology,* 178**,** 2623-2629.

MUSLIN, A. J. 2008. MAPK signalling in cardiovascular health and disease: molecular mechanisms and therapeutic targets. *Clin Sci (Lond),* 115**,** 203-18.

NAKA, T., NARAZAKI, M., HIRATA, M., MATSUMOTO, T., MINAMOTO, S., AONO, A., NISHIMOTO, N., KAJITA, T., TAGA, T., YOSHIZAKI, K., AKIRA, S. & KISHIMOTO, T. 1997. Structure and function of a new STAT-induced STAT inhibitor. *Nature,* 387**,** 924-9.

NAKAYAMADA, S., KUBO, S., IWATA, S. & TANAKA, Y. 2016. Recent Progress in JAK Inhibitors for the Treatment of Rheumatoid Arthritis. *BioDrugs,* 30**,** 407-419.

NAPPER, A. D., HIXON, J., MCDONAGH, T., KEAVEY, K., PONS, J. F., BARKER, J., YAU, W. T., AMOUZEGH, P., FLEGG, A., HAMELIN, E., THOMAS, R. J., KATES, M., JONES, S., NAVIA, M. A., SAUNDERS, J. O., DISTEFANO, P. S. & CURTIS, R. 2005. Discovery of indoles as potent and selective inhibitors of the deacetylase SIRT1. *J Med Chem,* 48**,** 8045-54.

NATALI, A. & FERRANNINI, E. 2006. Effects of metformin and thiazolidinediones on suppression of hepatic glucose production and stimulation of glucose uptake in type 2 diabetes: a systematic review. *Diabetologia,* 49**,** 434-41.

NEEL, B. G. & TONKS, N. K. 1997. Protein tyrosine phosphatases in signal transduction. *Current Opinion in Cell Biology,* 9**,** 193-204.

NERSTEDT, A., CANSBY, E., AMRUTKAR, M., SMITH, U. & MAHLAPUU, M. 2013. Pharmacological activation of AMPK suppresses inflammatory response evoked by IL-6 signalling in mouse liver and in human hepatocytes. *Molecular and Cellular Endocrinology,* 375**,** 68-78.

NERSTEDT, A., JOHANSSON, A., ANDERSSON, C. X., CANSBY, E., SMITH, U. & MAHLAPUU, M. 2010. AMP-activated protein kinase inhibits IL-6-stimulated inflammatory response in human liver cells by suppressing phosphorylation of signal transducer and activator of transcription 3 (STAT3). *Diabetologia,* 53**,** 2406-2416.

NEWTON, K. & DIXIT, V. M. 2012. Signaling in Innate Immunity and Inflammation. *Cold Spring Harbor Perspectives in Biology,* 4**,** a006049-a006049.

NGUYEN, K., DEVIDAS, M., CHENG, S. C., LA, M., RAETZ, E. A., CARROLL, W. L., WINICK, N. J., HUNGER, S. P., GAYNON, P. S. & LOH, M. L. 2008. Factors influencing survival after relapse from acute lymphoblastic leukemia: a Children's Oncology Group study. *Leukemia,* 22**,** 2142-50.

NI, C.-W., HSIEH, H.-J., CHAO, Y.-J. & WANG, D. L. 2004. Interleukin-6-induced JAK2/STAT3 signaling pathway in endothelial cells is suppressed by hemodynamic flow. *American Journal of Physiology - Cell Physiology,* 287**,** C771-C780.

NICHOLLS, S. J., TUZCU, E. M., KALIDINDI, S., WOLSKI, K., MOON, K. W., SIPAHI, I., SCHOENHAGEN, P. & NISSEN, S. E. 2008. Effect of diabetes on progression of coronary atherosclerosis and arterial remodeling: a pooled analysis of 5 intravascular ultrasound trials. *J Am Coll Cardiol,* 52**,** 255-62.

NICHOLSON, S. E., DE SOUZA, D., FABRI, L. J., CORBIN, J., WILLSON, T. A., ZHANG, J. G., SILVA, A., ASIMAKIS, M., FARLEY, A., NASH, A. D., METCALF, D., HILTON, D. J., NICOLA, N. A. & BACA, M. 2000. Suppressor of cytokine signaling-3 preferentially binds to the SHP-2-binding site on the shared cytokine receptor subunit gp130. *Proc Natl Acad Sci U S A,* 97**,** 6493-8.

NIE, Y., ERION, D. M., YUAN, Z., DIETRICH, M., SHULMAN, G. I., HORVATH, T. L. & GAO, Q. 2009. STAT3 inhibition of gluconeogenesis is downregulated by SirT1. *Nature cell biology,* 11**,** 492-500.

NIN, V., ESCANDE, C., CHINI, C. C., GIRI, S., CAMACHO-PEREIRA, J., MATALONGA, J., LOU, Z. & CHINI, E. N. 2012. Role of Deleted in Breast Cancer 1 (DBC1) Protein in SIRT1 Deacetylase Activation Induced by Protein Kinase A and AMP-activated Protein Kinase. *The Journal of Biological Chemistry,* 287**,** 23489-23501.

NISTALA, K. & WEDDERBURN, L. R. 2009. Th17 and regulatory T cells: rebalancing pro- and anti-inflammatory forces in autoimmune arthritis. *Rheumatology (Oxford),* 48**,** 602-6.

O'SHEA, J. J., GADINA, M. & SCHREIBER, R. D. 2002. Cytokine signaling in 2002: new surprises in the Jak/Stat pathway. *Cell,* 109 Suppl**,** S121-31.

OAKHILL, J. S., STEEL, R., CHEN, Z.-P., SCOTT, J. W., LING, N., TAM, S. & KEMP, B. E. 2011. AMPK Is a Direct Adenylate Charge-Regulated Protein Kinase. *Science,* 332**,** 1433-1435.

OHTA, H., WADA, H., NIWA, T., KIRII, H., IWAMOTO, N., FUJII, H., SAITO, K., SEKIKAWA, K. & SEISHIMA, M. 2005. Disruption of tumor necrosis factor-alpha gene diminishes the development of atherosclerosis in ApoE-deficient mice. *Atherosclerosis,* 180**,** 11-7.

OHTANI, T., ISHIHARA, K., ATSUMI, T., NISHIDA, K., KANEKO, Y., MIYATA, T., ITOH, S., NARIMATSU, M., MAEDA, H., FUKADA, T., ITOH, M., OKANO, H., HIBI, M. & HIRANO, T. 2000. Dissection of Signaling Cascades through gp130 In Vivo: Reciprocal Roles for STAT3-and SHP2-Mediated Signals in Immune Responses. *Immunity,* 12**,** 95-105.

ONDA, H., CRINO, P. B., ZHANG, H., MURPHEY, R. D., RASTELLI, L., GOULD ROTHBERG, B. E. & KWIATKOWSKI, D. J. 2002. Tsc2 Null Murine Neuroepithelial Cells Are a Model for Human Tuber Giant Cells, and Show Activation of an mTOR Pathway. *Molecular and Cellular Neuroscience,* 21**,** 561-574.

ORTIZ-MUÑOZ, G., MARTIN-VENTURA, J. L., HERNANDEZ-VARGAS, P., MALLAVIA, B., LOPEZ-PARRA, V., LOPEZ-FRANCO, O., MUÑOZ-GARCIA, B., FERNANDEZ-VIZARRA, P., ORTEGA, L., EGIDO, J. & GOMEZ-GUERRERO, C. 2009. Suppressors of Cytokine Signaling Modulate JAK/STAT-Mediated Cell Responses During Atherosclerosis. *Arteriosclerosis, Thrombosis, and Vascular Biology,* 29**,** 525.

OSBORN, L., HESSION, C., TIZARD, R., VASSALLO, C., LUHOWSKYJ, S., CHI-ROSSO, G. & LOBB, R. 1989. Direct expression cloning of vascular cell adhesion molecule 1, a cytokine-induced endothelial protein that binds to lymphocytes. *Cell,* 59**,** 1203-11.

PALING, N. R. D. & WELHAM, M. J. 2002. Role of the protein tyrosine phosphatase SHP-1 (Src homology phosphatase-1) in the regulation of interleukin-3-induced survival, proliferation and signalling. *Biochemical Journal,* 368**,** 885-894.

PALMER, R. M. J., ASHTON, D. S. & MONCADA, S. 1988. Vascular endothelial cells synthesize nitric oxide from L-arginine. *Nature,* 333**,** 664-666.

PAMUKCU, B., LIP, G. Y. & SHANTSILA, E. 2011. The nuclear factor--kappa B pathway in atherosclerosis: a potential therapeutic target for atherothrombotic vascular disease. *Thromb Res,* 128**,** 117-23.

PANG, T., XIONG, B., LI, J.-Y., QIU, B.-Y., JIN, G.-Z., SHEN, J.-K. & LI, J. 2007. Conserved α-Helix Acts as Autoinhibitory Sequence in AMP-activated Protein Kinase α Subunits. *Journal of Biological Chemistry,* 282**,** 495-506.

PELLETIER, S., GINGRAS, S., FUNAKOSHI-TAGO, M., HOWELL, S. & IHLE, J. N. 2006. Two domains of the erythropoietin receptor are sufficient for Jak2 binding/activation and function. *Mol Cell Biol,* 26**,** 8527-38.

PESCE, B., SOTO, L., SABUGO, F., WURMANN, P., CUCHACOVICH, M., LOPEZ, M. N., SOTELO, P. H., MOLINA, M. C., AGUILLON, J. C. & CATALAN, D. 2013. Effect of interleukin-6 receptor blockade on the balance between regulatory T cells and T helper type 17 cells in rheumatoid arthritis patients. *Clin Exp Immunol,* 171**,** 237-42.

PFEIFFER, S., LEOPOLD, E., SCHMIDT, K., BRUNNER, F. & MAYER, B. 1996. Inhibition of nitric oxide synthesis by NG-nitro-L-arginine methyl ester (L-NAME): requirement for bioactivation to the free acid, NG-nitro-L-arginine. *British Journal of Pharmacology,* 118**,** 1433-1440.

PLOTNIKOV, A., ZEHORAI, E., PROCACCIA, S. & SEGER, R. 2011. The MAPK cascades: signaling components, nuclear roles and mechanisms of nuclear translocation. *Biochim Biophys Acta,* 1813**,** 1619-33.

POBER, J. S. & SESSA, W. C. 2007. Evolving functions of endothelial cells in inflammation. *Nat Rev Immunol,* 7**,** 803-15.

POLEKHINA, G., GUPTA, A., MICHELL, B. J., VAN DENDEREN, B., MURTHY, S., FEIL, S. C., JENNINGS, I. G., CAMPBELL, D. J., WITTERS, L. A., PARKER, M. W., KEMP, B. E. & STAPLETON, D. 2003. AMPK β Subunit Targets Metabolic Stress Sensing to Glycogen. *Current Biology,* 13**,** 867-871.

POTULA, H. S. K., WANG, D., VAN QUYEN, D., SINGH, N. K., KUNDUMANI-SRIDHARAN, V., KARPURAPU, M., PARK, E. A., GLASGOW, W. C. & RAO, G. N. 2009. Src-dependent STAT-3-mediated Expression of Monocyte Chemoattractant Protein-1 Is Required for 15(S)-Hydroxyeicosatetraenoic Acid-induced Vascular Smooth Muscle Cell Migration. *The Journal of Biological Chemistry,* 284**,** 31142-31155.

PRASAD, R., GIRI, S., NATH, N., SINGH, I. & SINGH, A. K. 2006. 5-aminoimidazole-4-carboxamide-1-beta-4-ribofuranoside attenuates experimental autoimmune encephalomyelitis via modulation of endothelial–monocyte interaction. *Journal of Neuroscience Research,* 84**,** 614-625.

PRATT, A. G., SWAN, D. C., RICHARDSON, S., WILSON, G., HILKENS, C. M. U., YOUNG, D. A. & ISAACS, J. D. 2012. A CD4 T cell gene signature for early rheumatoid arthritis implicates interleukin 6-mediated STAT3 signalling, particularly in anti-citrullinated peptide antibody-negative disease. *Annals of the Rheumatic Diseases,* 71**,** 1374.

PREISS, D., LLOYD, S. M., FORD, I., MCMURRAY, J. J., HOLMAN, R. R., WELSH, P., FISHER, M., PACKARD, C. J. & SATTAR, N. 2014. Metformin for non-diabetic patients with coronary heart disease (the CAMERA study): a randomised controlled trial. *The Lancet Diabetes & Endocrinology,* 2**,** 116-124.

RADTKE, S., HAAN, S., JORISSEN, A., HERMANNS, H. M., DIEFENBACH, S., SMYCZEK, T., SCHMITZ-VANDELEUR, H., HEINRICH, P. C., BEHRMANN, I. & HAAN, C. 2005. The Jak1 SH2 domain does not fulfill a classical SH2 function in Jak/STAT signaling but plays a structural role for receptor interaction and up-regulation of receptor surface expression. *J Biol Chem,* 280**,** 25760-8.

RAMANA, C. V., CHATTERJEE-KISHORE, M., NGUYEN, H. & STARK, G. R. 2000. Complex roles of Stat1 in regulating gene expression. *Oncogene,* 19**,** 2619-27.

RAMJI, D. P. & DAVIES, T. S. 2015. Cytokines in atherosclerosis: Key players in all stages of disease and promising therapeutic targets. *Cytokine Growth Factor Rev,* 26**,** 673-85.

RAWLINGS, J. S., ROSLER, K. M. & HARRISON, D. A. 2004. The JAK/STAT signaling pathway. *Journal of Cell Science,* 117**,** 1281.

RECINOS, A., LEJEUNE, W. S., SUN, H., LEE, C. Y., TIEU, B. C., LU, M., HOU, T., BOLDOGH, I., TILTON, R. G. & BRASIER, A. R. 2007. Angiotensin II induces IL-6 expression and the Jak-STAT3 pathway in aortic adventitia of LDL receptor-deficient mice. *Atherosclerosis,* 194**,** 125-133.

RECIO, C., OGUIZA, A., MALLAVIA, B., LAZARO, I., ORTIZ-MUÑOZ, G., LOPEZ-FRANCO, O., EGIDO, J. & GOMEZ-GUERRERO, C. 2015. Gene delivery of suppressors of cytokine signaling (SOCS) inhibits inflammation and atherosclerosis development in mice. *Basic Research in Cardiology,* 110**,** 8.

REMY, I., WILSON, I. A. & MICHNICK, S. W. 1999. Erythropoietin receptor activation by a ligand-induced conformation change. *Science,* 283**,** 990-3.

REYNOLDS, A., ANDERSON, E. M., VERMEULEN, A., FEDOROV, Y., ROBINSON, K., LEAKE, D., KARPILOW, J., MARSHALL, W. S. & KHVOROVA, A. 2006. Induction of the interferon response by siRNA is cell type- and duplex length-dependent. *Rna,* 12**,** 988-93.

RIDKER, P. M., RIFAI, N., STAMPFER, M. J. & HENNEKENS, C. H. 2000. Plasma Concentration of Interleukin-6 and the Risk of Future Myocardial Infarction Among Apparently Healthy Men. *Circulation,* 101**,** 1767.

ROLLINS, B. J., YOSHIMURA, T., LEONARD, E. J. & POBER, J. S. 1990. Cytokine-activated human endothelial cells synthesize and secrete a monocyte chemoattractant, MCP-1/JE. *The American Journal of Pathology,* 136**,** 1229-1233.

ROMANO, M., SIRONI, M., TONIATTI, C., POLENTARUTTI, N., FRUSCELLA, P., GHEZZI, P., FAGGIONI, R., LUINI, W., VAN HINSBERGH, V., SOZZANI, S., BUSSOLINO, F., POLI, V., CILIBERTO, G. & MANTOVANI, A. 1997. Role of IL-6 and its soluble receptor in induction of chemokines and leukocyte recruitment. *Immunity,* 6**,** 315-25.

ROSANO, G. L. & CECCARELLI, E. A. 2014. Recombinant protein expression in Escherichia coli: advances and challenges. *Frontiers in Microbiology,* 5**,** 172.

ROSE-JOHN, S. 2012. IL-6 Trans-Signaling via the Soluble IL-6 Receptor: Importance for the Pro-Inflammatory Activities of IL-6. *International Journal of Biological Sciences,* 8**,** 1237-1247.

ROSS, F. A., MACKINTOSH, C. & HARDIE, D. G. 2016. AMP‐activated protein kinase: a cellular energy sensor that comes in 12 flavours. *The Febs Journal,* 283**,** 2987-3001.

ROSS, R. 1999. Atherosclerosis--an inflammatory disease. *N Engl J Med,* 340**,** 115-26.

ROUSSEL, R., TRAVERT, F., PASQUET, B., WILSON, P. W., SMITH, S. C., JR., GOTO, S., RAVAUD, P., MARRE, M., PORATH, A., BHATT, D. L. & STEG, P. G. 2010. Metformin use and mortality among patients with diabetes and atherothrombosis. *Arch Intern Med,* 170**,** 1892-9.

ROYER, Y., STAERK, J., COSTULEANU, M., COURTOY, P. J. & CONSTANTINESCU, S. N. 2005. Janus kinases affect thrombopoietin receptor cell surface localization and stability. *J Biol Chem,* 280**,** 27251-61.

RUTHERFORD, C., WOOLSON, H. & PALMER, T. 2012. Cross-Regulation of JAK-STAT Signaling: Implications for Approaches to Combat Chronic Inflammatory Diseases and Cancers. *Advances in Protein Kinases,* Dr. Gabriela Da Silva Xavier (Ed.), InTech**,** https://www.intechopen.com/books/advances-in-protein-kinases/cross-regulation-of-jak-stat-signalling-implications-for-approaches-to-combat-chronic-inflammato.

SAKAMOTO, K., GÖRANSSON, O., HARDIE, D. G. & ALESSI, D. R. 2004. Activity of LKB1 and AMPK-related kinases in skeletal muscle: effects of contraction, phenformin, and AICAR. *American Journal of Physiology - Endocrinology And Metabolism,* 287**,** E310-E317.

SALMOND, R. J. & ALEXANDER, D. R. 2006. SHP2 forecast for the immune system: fog gradually clearing. *Trends in Immunology,* 27**,** 154-160.

SALT, I. P. & PALMER, T. M. 2012. Exploiting the anti-inflammatory effects of AMP-activated protein kinase activation. *Expert Opinion on Investigational Drugs,* 21**,** 1155-1167.

SANDERS, M. J., ALI, Z. S., HEGARTY, B. D., HEATH, R., SNOWDEN, M. A. & CARLING, D. 2007. Defining the Mechanism of Activation of AMP-activated Protein Kinase by the Small Molecule A-769662, a Member of the Thienopyridone Family. *Journal of Biological Chemistry,* 282**,** 32539-32548.

SASAKI, A., YASUKAWA, H., SUZUKI, A., KAMIZONO, S., SYODA, T., KINJYO, I., SASAKI, M., JOHNSTON, J. A. & YOSHIMURA, A. 1999. Cytokine-inducible SH2 protein-3 (CIS3/SOCS3) inhibits Janus tyrosine kinase by binding through the N-terminal kinase inhibitory region as well as SH2 domain. *Genes Cells,* 4**,** 339-51.

SATOH, J. & TABUNOKI, H. 2013. A Comprehensive Profile of ChIP-Seq-Based STAT1 Target Genes Suggests the Complexity of STAT1-Mediated Gene Regulatory Mechanisms. *Gene Regul Syst Bio,* 7**,** 41-56.

SAUVE, A. A., WOLBERGER, C., SCHRAMM, V. L. & BOEKE, J. D. 2006. The biochemistry of sirtuins. *Annu Rev Biochem,* 75**,** 435-65.

SAXTON, T. M., HENKEMEYER, M., GASCA, S., SHEN, R., ROSSI, D. J., SHALABY, F., FENG, G. S. & PAWSON, T. 1997. Abnormal mesoderm patterning in mouse embryos mutant for the SH2 tyrosine phosphatase Shp-2. *The EMBO Journal,* 16**,** 2352-2364.

SCHAFFER, B. E., LEVIN, R. S., HERTZ, N. T., MAURES, T. J., SCHOOF, M. L., HOLLSTEIN, P. E., BENAYOUN, B. A., BANKO, M. R., SHAW, R. J., SHOKAT, K. M. & BRUNET, A. 2015. Identification of AMPK phosphorylation sites reveals a network of proteins involved in cell invasion and facilitates large-scale substrate prediction. *Cell metabolism,* 22**,** 907-921.

SCHAPER, F., GENDO, C., ECK, M., SCHMITZ, J., GRIMM, C., ANHUF, D., KERR, I. M. & HEINRICH, P. C. 1998. Activation of the protein tyrosine phosphatase SHP2 via the interleukin-6 signal transducing receptor protein gp130 requires tyrosine kinase Jak1 and limits acute-phase protein expression. *Biochem J,* 335 (Pt 3)**,** 557-65.

SCHAPER, F. & ROSE-JOHN, S. 2015. Interleukin-6: Biology, signaling and strategies of blockade. *Cytokine Growth Factor Rev,* 26**,** 475-87.

SCHELLER, J., CHALARIS, A., SCHMIDT-ARRAS, D. & ROSE-JOHN, S. 2011. The pro- and anti-inflammatory properties of the cytokine interleukin-6. *Biochim Biophys Acta,* 1813**,** 878-88.

SCHIEFFER, B., SCHIEFFER, E., HILFIKER-KLEINER, D., HILFIKER, A., KOVANEN, P. T., KAARTINEN, M., NUSSBERGER, J., HARRINGER, W. & DREXLER, H. 2000. Expression of Angiotensin II and Interleukin 6 in Human Coronary Atherosclerotic Plaques. *Circulation,* 101**,** 1372.

SCHINDLER, C., FU, X. Y., IMPROTA, T., AEBERSOLD, R. & DARNELL, J. E., JR. 1992a. Proteins of transcription factor ISGF-3: one gene encodes the 91-and 84-kDa ISGF-3 proteins that are activated by interferon alpha. *Proc Natl Acad Sci U S A,* 89**,** 7836-9.

SCHINDLER, C., SHUAI, K., PREZIOSO, V. R. & DARNELL, J. E., JR. 1992b. Interferon-dependent tyrosine phosphorylation of a latent cytoplasmic transcription factor. *Science,* 257**,** 809-13.

SCHMIEGELOW, K., FORESTIER, E., HELLEBOSTAD, M., HEYMAN, M., KRISTINSSON, J., SODERHALL, S. & TASKINEN, M. 2010. Long-term results of NOPHO ALL-92 and ALL-2000 studies of childhood acute lymphoblastic leukemia. *Leukemia,* 24**,** 345-54.

SCHMITZ, J., WEISSENBACH, M., HAAN, S., HEINRICH, P. C. & SCHAPER, F. 2000. SOCS3 exerts its inhibitory function on interleukin-6 signal transduction through the SHP2 recruitment site of gp130. *J Biol Chem,* 275**,** 12848-56.

SCHUETT, H., OESTREICH, R., WAETZIG, G. H., ANNEMA, W., LUCHTEFELD, M., HILLMER, A., BAVENDIEK, U., VON FELDEN, J., DIVCHEV, D., KEMPF, T., WOLLERT, K. C., SEEGERT, D., ROSE-JOHN, S., TIETGE, U. J. F., SCHIEFFER, B. & GROTE, K. 2012. Transsignaling of Interleukin-6 Crucially Contributes to Atherosclerosis in Mice. *Arteriosclerosis, Thrombosis, and Vascular Biology,* 32**,** 281.

SCHUHMACHER, S., FORETZ, M., KNORR, M., JANSEN, T., HORTMANN, M., WENZEL, P., OELZE, M., KLESCHYOV, A. L., DAIBER, A., KEANEY, J. F., WEGENER, G., LACKNER, K., MÜNZEL, T., VIOLLET, B. & SCHULZ, E. 2011. α1AMP-activated protein kinase preserves endothelial function during chronic angiotensin II treatment by limiting Nox2 upregulation. *Arteriosclerosis, thrombosis, and vascular biology,* 31**,** 560-566.

SCHULZ, E., DOPHEIDE, J., SCHUHMACHER, S., THOMAS, S. R., CHEN, K., DAIBER, A., WENZEL, P., MÜNZEL, T. & KEANEY, J. F. 2008. Suppression of the JNK Pathway by Induction of a Metabolic Stress Response Prevents Vascular Injury and Dysfunction. *Circulation,* 118**,** 1347-1357.

SCOTT, J. W., NORMAN, D. G., HAWLEY, S. A., KONTOGIANNIS, L. & HARDIE, D. G. 2002. Protein kinase substrate recognition studied using the recombinant catalytic domain of AMP-activated protein kinase and a model substrate1. *Journal of Molecular Biology,* 317**,** 309-323.

SCOTT, J. W., VAN DENDEREN, B. J. W., JORGENSEN, S. B., HONEYMAN, J. E., STEINBERG, G. R., OAKHILL, J. S., ISELI, T. J., KOAY, A., GOOLEY, P. R., STAPLETON, D. & KEMP, B. E. 2008. Thienopyridone Drugs Are Selective Activators of AMP-Activated Protein Kinase β1-Containing Complexes. *Chemistry & Biology,* 15**,** 1220-1230.

SHAN, Y., GNANASAMBANDAN, K., UNGUREANU, D., KIM, E. T., HAMMAREN, H., YAMASHITA, K., SILVENNOINEN, O., SHAW, D. E. & HUBBARD, S. R. 2014. Molecular basis for pseudokinase-dependent autoinhibition of JAK2 tyrosine kinase. *Nat Struct Mol Biol,* 21**,** 579-84.

SHAW, R. J., KOSMATKA, M., BARDEESY, N., HURLEY, R. L., WITTERS, L. A., DEPINHO, R. A. & CANTLEY, L. C. 2004. The tumor suppressor LKB1 kinase directly activates AMP-activated kinase and regulates apoptosis in response to energy stress. *Proc Natl Acad Sci U S A,* 101**,** 3329-35.

SHAW, R. J., LAMIA, K. A., VASQUEZ, D., KOO, S.-H., BARDEESY, N., DEPINHO, R. A., MONTMINY, M. & CANTLEY, L. C. 2005. The Kinase LKB1 Mediates Glucose Homeostasis in Liver and Therapeutic Effects of Metformin. *Science (New York, N.Y.),* 310**,** 1642-1646.

SHEN, C. H., YUAN, P., PEREZ-LORENZO, R., ZHANG, Y., LEE, S. X., OU, Y., ASARA, J. M., CANTLEY, L. C. & ZHENG, B. 2013. Phosphorylation of BRAF by AMPK impairs BRAF-KSR1 association and cell proliferation. *Mol Cell,* 52**,** 161-72.

SHI, Z.-Q., YU, D.-H., PARK, M., MARSHALL, M. & FENG, G.-S. 2000. Molecular Mechanism for the Shp-2 Tyrosine Phosphatase Function in Promoting Growth Factor Stimulation of Erk Activity. *Molecular and Cellular Biology,* 20**,** 1526-1536.

SHUAI, K., HORVATH, C. M., HUANG, L. H., QURESHI, S. A., COWBURN, D. & DARNELL, J. E., JR. 1994. Interferon activation of the transcription factor Stat91 involves dimerization through SH2-phosphotyrosyl peptide interactions. *Cell,* 76**,** 821-8.

SHUAI, K. & LIU, B. 2003. Regulation of JAK-STAT signalling in the immune system. *Nat Rev Immunol,* 3**,** 900-911.

SHUAI, K., SCHINDLER, C., PREZIOSO, V. R. & DARNELL, J. E., JR. 1992. Activation of transcription by IFN-gamma: tyrosine phosphorylation of a 91-kD DNA binding protein. *Science,* 258**,** 1808-12.

SIEGEL, R., NAISHADHAM, D. & JEMAL, A. 2012. Cancer statistics, 2012. *CA Cancer J Clin,* 62**,** 10-29.

SIEGEL, R. L., MILLER, K. D. & JEMAL, A. 2015. Cancer statistics, 2015. *CA Cancer J Clin,* 65**,** 5-29.

SIKORSKI, K., CHMIELEWSKI, S., PRZYBYL, L., HEEMANN, U., WESOLY, J., BAUMANN, M. & BLUYSSEN, H. A. R. 2011. STAT1-mediated signal integration between IFNγ and LPS leads to increased EC and SMC activation and monocyte adhesion. *American Journal of Physiology - Cell Physiology,* 300**,** C1337-C1344.

SIMONCIC, P. D., LEE-LOY, A., BARBER, D. L., TREMBLAY, M. L. & MCGLADE, C. J. 2002. The T cell protein tyrosine phosphatase is a negative regulator of janus family kinases 1 and 3. *Curr Biol,* 12**,** 446-53.

SINGH, N. K., WANG, D., KUNDUMANI-SRIDHARAN, V., VAN QUYEN, D., NIU, J. & RAO, G. N. 2011. 15-Lipoxygenase-1-enhanced Src-Janus Kinase 2-Signal Transducer and Activator of Transcription 3 Stimulation and Monocyte Chemoattractant Protein-1 Expression Require Redox-sensitive Activation of Epidermal Growth Factor Receptor in Vascular Wall Remodeling. *The Journal of Biological Chemistry,* 286**,** 22478-22488.

SINGH, S. M. & PANDA, A. K. 2005. Solubilization and refolding of bacterial inclusion body proteins. *J Biosci Bioeng,* 99**,** 303-10.

SIOKA, C. & KYRITSIS, A. P. 2009. Central and peripheral nervous system toxicity of common chemotherapeutic agents. *Cancer Chemotherapy and Pharmacology,* 63**,** 761-767.

SKOOG, T., DICHTL, W., BOQUIST, S., SKOGLUND-ANDERSSON, C., KARPE, F., TANG, R., BOND, M. G., DE FAIRE, U., NILSSON, J., ERIKSSON, P. & HAMSTEN, A. 2002. Plasma tumour necrosis factor-alpha and early carotid atherosclerosis in healthy middle-aged men. *Eur Heart J,* 23**,** 376-83.

SOLOMON, J. M., PASUPULETI, R., XU, L., MCDONAGH, T., CURTIS, R., DISTEFANO, P. S. & HUBER, L. J. 2006. Inhibition of SIRT1 Catalytic Activity Increases p53 Acetylation but Does Not Alter Cell Survival following DNA Damage. *Molecular and Cellular Biology,* 26**,** 28-38.

SON, H.-J., LEE, J., LEE, S.-Y., KIM, E.-K., PARK, M.-J., KIM, K.-W., PARK, S.-H. & CHO, M.-L. 2014. Metformin Attenuates Experimental Autoimmune Arthritis through Reciprocal Regulation of Th17/Treg Balance and Osteoclastogenesis. *Mediators of Inflammation,* 2014**,** 13.

SONG, X. M., FIEDLER, M., GALUSKA, D., RYDER, J. W., FERNSTROM, M., CHIBALIN, A. V., WALLBERG-HENRIKSSON, H. & ZIERATH, J. R. 2002. 5-Aminoimidazole-4-carboxamide ribonucleoside treatment improves glucose homeostasis in insulin-resistant diabetic (ob/ob) mice. *Diabetologia,* 45**,** 56-65.

SPRINGUEL, L., RENAULD, J.-C. & KNOOPS, L. 2015. JAK kinase targeting in hematologic malignancies: a sinuous pathway from identification of genetic alterations towards clinical indications. *Haematologica,* 100**,** 1240-1253.

SRIRANGAN, S. & CHOY, E. H. 2010. The Role of Interleukin 6 in the Pathophysiology of Rheumatoid Arthritis. *Therapeutic Advances in Musculoskeletal Disease,* 2**,** 247-256.

STAERK, J., KALLIN, A., DEMOULIN, J. B., VAINCHENKER, W. & CONSTANTINESCU, S. N. 2005. JAK1 and Tyk2 activation by the homologous polycythemia vera JAK2 V617F mutation: cross-talk with IGF1 receptor. *J Biol Chem,* 280**,** 41893-9.

STAHL, N., BOULTON, T. G., FARRUGGELLA, T., IP, N. Y., DAVIS, S., WITTHUHN, B. A., QUELLE, F. W., SILVENNOINEN, O., BARBIERI, G., PELLEGRINI, S. & ET AL. 1994. Association and activation of Jak-Tyk kinases by CNTF-LIF-OSM-IL-6 beta receptor components. *Science,* 263**,** 92-5.

STAHL, N., FARRUGGELLA, T. J., BOULTON, T. G., ZHONG, Z., DARNELL, J. E., JR. & YANCOPOULOS, G. D. 1995. Choice of STATs and other substrates specified by modular tyrosine-based motifs in cytokine receptors. *Science,* 267**,** 1349-53.

STARR, R., WILLSON, T. A., VINEY, E. M., MURRAY, L. J., RAYNER, J. R., JENKINS, B. J., GONDA, T. J., ALEXANDER, W. S., METCALF, D., NICOLA, N. A. & HILTON, D. J. 1997. A family of cytokine-inducible inhibitors of signalling. *Nature,* 387**,** 917-21.

STEPHEN, S. L., FREESTONE, K., DUNN, S., TWIGG, M. W., HOMER-VANNIASINKAM, S., WALKER, J. H., WHEATCROFT, S. B. & PONNAMBALAM, S. 2010. Scavenger Receptors and Their Potential as Therapeutic Targets in the Treatment of Cardiovascular Disease. *International Journal of Hypertension,* 2010.

SUN, H., CHARLES, C. H., LAU, L. F. & TONKS, N. K. 1993. MKP-1 (3CH134), an immediate early gene product, is a dual specificity phosphatase that dephosphorylates MAP kinase in vivo. *Cell,* 75**,** 487-493.

SUZUKI, H., SHIBANO, K., OKANE, M., KONO, I., MATSUI, Y., YAMANE, K. & KASHIWAGI, H. 1989. Interferon-gamma modulates messenger RNA levels of c-sis (PDGF-B chain), PDGF-A chain, and IL-1 beta genes in human vascular endothelial cells. *Am J Pathol,* 134**,** 35-43.

TABAS, I., WILLIAMS, K. J. & BOREN, J. 2007. Subendothelial lipoprotein retention as the initiating process in atherosclerosis: update and therapeutic implications. *Circulation,* 116**,** 1832-44.

TAN, P. H., CHAN, C., XUE, S. A., DONG, R., ANANTHESAYANAN, B., MANUNTA, M., KEROUEDAN, C., CHESHIRE, N. J., WOLFE, J. H., HASKARD, D. O., TAYLOR, K. M. & GEORGE, A. J. 2004. Phenotypic and functional differences between human saphenous vein (HSVEC) and umbilical vein (HUVEC) endothelial cells. *Atherosclerosis,* 173**,** 171-83.

TANNER, J. W., CHEN, W., YOUNG, R. L., LONGMORE, G. D. & SHAW, A. S. 1995. The conserved box 1 motif of cytokine receptors is required for association with JAK kinases. *J Biol Chem,* 270**,** 6523-30.

TEFFERI, A. & BARBUI, T. 2015. Polycythemia vera and essential thrombocythemia: 2015 update on diagnosis, risk-stratification and management. *Am J Hematol,* 90**,** 162-73.

TEN HOEVE, J., DE JESUS IBARRA-SANCHEZ, M., FU, Y., ZHU, W., TREMBLAY, M., DAVID, M. & SHUAI, K. 2002. Identification of a nuclear Stat1 protein tyrosine phosphatase. *Mol Cell Biol,* 22**,** 5662-8.

TEOFILI, L., MARTINI, M., IACHININOTO, M. G., CAPODIMONTI, S., NUZZOLO, E. R., TORTI, L., CENCI, T., LAROCCA, L. M. & LEONE, G. 2011. Endothelial progenitor cells are clonal and exhibit the JAK2(V617F) mutation in a subset of thrombotic patients with Ph-negative myeloproliferative neoplasms. *Blood,* 117**,** 2700-7.

THOMAS, S. J., SNOWDEN, J. A., ZEIDLER, M. P. & DANSON, S. J. 2015. The role of JAK/STAT signalling in the pathogenesis, prognosis and treatment of solid tumours. *Br J Cancer,* 113**,** 365-71.

THORNTON, C., SNOWDEN, M. A. & CARLING, D. 1998. Identification of a Novel AMP-activated Protein Kinase β Subunit Isoform That Is Highly Expressed in Skeletal Muscle. *Journal of Biological Chemistry,* 273**,** 12443-12450.

TOMS, A. V., DESHPANDE, A., MCNALLY, R., JEONG, Y., ROGERS, J. M., KIM, C. U., GRUNER, S. M., FICARRO, S. B., MARTO, J. A., SATTLER, M., GRIFFIN, J. D. & ECK, M. J. 2013. Structure of a

pseudokinase-domain switch that controls oncogenic activation of Jak kinases. *Nat Struct Mol Biol,* 20**,** 1221-3.

TONKS, N. K. & NEEL, B. G. 2001. Combinatorial control of the specificity of protein tyrosine phosphatases. *Current Opinion in Cell Biology,* 13**,** 182-195.

TORELLA, D., CURCIO, A., GASPARRI, C., GALUPPO, V., SERIO, D. D., SURACE, F. C., CAVALIERE, A. L., LEONE, A., COPPOLA, C., ELLISON, G. M. & INDOLFI, C. 2007. Fludarabine prevents smooth muscle proliferation in vitro and neointimal hyperplasia in vivo through specific inhibition of STAT-1 activation. *American Journal of Physiology - Heart and Circulatory Physiology,* 292**,** H2935.

TORZEWSKI, M., RIST, C., MORTENSEN, R. F., ZWAKA, T. P., BIENEK, M., WALTENBERGER, J., KOENIG, W., SCHMITZ, G., HOMBACH, V. & TORZEWSKI, J. 2000. C-Reactive Protein in the Arterial Intima. *Arteriosclerosis, Thrombosis, and Vascular Biology,* 20**,** 2094.

TOULLEC, D., PIANETTI, P., COSTE, H., BELLEVERGUE, P., GRAND-PERRET, T., AJAKANE, M., BAUDET, V., BOISSIN, P., BOURSIER, E. & LORIOLLE, F. 1991. The bisindolylmaleimide GF 109203X is a potent and selective inhibitor of protein kinase C. *Journal of Biological Chemistry,* 266**,** 15771-15781.

TOWNSEND, N., BHATNAGAR, P., WILKINS, E., WICKRAMASINGHE, K. & RAYNER, M. 2015. Cardiovascular disease statistics, 2015. *British Heart Foundation: London*.

TZOULAKI, I., MURRAY, G. D., LEE, A. J., RUMLEY, A., LOWE, G. D. O. & FOWKES, F. G. R. 2005. C-Reactive Protein, Interleukin-6, and Soluble Adhesion Molecules as Predictors of Progressive Peripheral Atherosclerosis in the General Population. *Circulation,* 112**,** 976.

UNGUREANU, D., WU, J., PEKKALA, T., NIRANJAN, Y., YOUNG, C., JENSEN, O. N., XU, C. F., NEUBERT, T. A., SKODA, R. C., HUBBARD, S. R. & SILVENNOINEN, O. 2011. The pseudokinase domain of JAK2 is a dual-specificity protein kinase that negatively regulates cytokine signaling. *Nat Struct Mol Biol,* 18**,** 971-6.

USACHEVA, A., SANDOVAL, R., DOMANSKI, P., KOTENKO, S. V., NELMS, K., GOLDSMITH, M. A. & COLAMONICI, O. R. 2002. Contribution of the Box 1 and Box 2 motifs of cytokine receptors to Jak1 association and activation. *J Biol Chem,* 277**,** 48220-6.

VANE, J. R., BAKHLE, Y. S. & BOTTING, R. M. 1998. Cyclooxygenases 1 and 2. *Annu Rev Pharmacol Toxicol,* 38**,** 97-120.

VARINOU, L., RAMSAUER, K., KARAGHIOSOFF, M., KOLBE, T., PFEFFER, K., MULLER, M. & DECKER, T. 2003. Phosphorylation of the Stat1 transactivation domain is required for full-fledged IFN-gamma-dependent innate immunity. *Immunity,* 19**,** 793-802.

VASAMSETTI, S. B., KARNEWAR, S., KANUGULA, A. K., THATIPALLI, A. R., KUMAR, J. M. & KOTAMRAJU, S. 2015. Metformin inhibits monocyte-to-macrophage differentiation via AMPK-mediated inhibition of STAT3 activation: potential role in atherosclerosis. *Diabetes,* 64**,** 2028-41.

VAVVAS, D., APAZIDIS, A., SAHA, A. K., GAMBLE, J., PATEL, A., KEMP, B. E., WITTERS, L. A. & RUDERMAN, N. B. 1997. Contraction-induced Changes in Acetyl-CoA Carboxylase and 5′-AMP-activated Kinase in Skeletal Muscle. *Journal of Biological Chemistry,* 272**,** 13255-13261.

VAZIRI, H., DESSAIN, S. K., EATON, E. N., IMAI, S.-I., FRYE, R. A., PANDITA, T. K., GUARENTE, L. & WEINBERG, R. A. 2001. hSIR2SIRT1 Functions as an NAD-Dependent p53 Deacetylase. *Cell,* 107**,** 149-159.

VENEMA, R. C., VENEMA, V. J., EATON, D. C. & MARRERO, M. B. 1998. Angiotensin II-induced tyrosine phosphorylation of signal transducers and activators of transcription 1 is regulated by Janus-activated kinase 2 and Fyn kinases and mitogen-activated protein kinase phosphatase 1. *J Biol Chem,* 273**,** 30795-800.

VERBSKY, J. W., BACH, E. A., FANG, Y. F., YANG, L., RANDOLPH, D. A. & FIELDS, L. E. 1996. Expression of Janus kinase 3 in human endothelial and other non-lymphoid and non-myeloid cells. *J Biol Chem,* 271**,** 13976-80.

VERHAMME, P. & HOYLAERTS, M. F. 2006. THE PIVOTAL ROLE OF THE ENDOTHELIUM IN HAEMOSTASIS AND THROMBOSIS. *Acta Clinica Belgica,* 61**,** 213-219.

VERHOEVEN, A. J. M., WOODS, A., BRENNAN, C. H., HAWLEY, S. A., HARDIE, D. G., SCOTT, J., BERI, R. K. & CARLING, D. 1995. The AMP-activated Protein Kinase Gene is Highly Expressed in Rat Skeletal Muscle. *European Journal of Biochemistry,* 228**,** 236-243.

VERSTOVSEK, S., MESA, R. A., GOTLIB, J., LEVY, R. S., GUPTA, V., DIPERSIO, J. F., CATALANO, J. V., DEININGER, M., MILLER, C., SILVER, R. T., TALPAZ, M., WINTON, E. F., HARVEY, J. H., ARCASOY, M. O., HEXNER, E., LYONS, R. M., PAQUETTE, R., RAZA, A., VADDI, K., ERICKSON-VIITANEN, S., KOUMENIS, I. L., SUN, W., SANDOR, V. & KANTARJIAN, H. M. 2012. A Double-Blind, Placebo-Controlled Trial of Ruxolitinib for Myelofibrosis. *New England Journal of Medicine,* 366**,** 799-807.

VERSTOVSEK, S., MESA, R. A., GOTLIB, J., LEVY, R. S., GUPTA, V., DIPERSIO, J. F., CATALANO, J. V., DEININGER, M. W., MILLER, C. B., SILVER, R. T., TALPAZ, M., WINTON, E. F., HARVEY, J. H., JR., ARCASOY, M. O., HEXNER, E. O., LYONS, R. M., PAQUETTE, R., RAZA, A., VADDI, K., ERICKSON-VIITANEN, S., SUN, W., SANDOR, V. & KANTARJIAN, H. M. 2013. Efficacy, safety and survival with ruxolitinib in patients with myelofibrosis: results of a median 2-year follow-up of COMFORT-I. *Haematologica,* 98**,** 1865-71.

VINCENT, M. F., MARANGOS, P. J., GRUBER, H. E. & VAN DEN BERGHE, G. 1991. Inhibition by AICA Riboside of Gluconeogenesis in Isolated Rat Hepatocytes. *Diabetes,* 40**,** 1259-1266.

VINKEMEIER, U., MOAREFI, I., DARNELL, J. E., JR. & KURIYAN, J. 1998. Structure of the amino-terminal protein interaction domain of STAT-4. *Science,* 279**,** 1048-52.

WALDMAN, W. J., SNEDDON, J. M., STEPHENS, R. E. & ROBERTS, W. H. 1989. Enhanced endothelial cytopathogenicity induced by a cytomegalovirus strain propagated in endothelial cells. *J Med Virol,* 28**,** 223-30.

WANG, R., CHERUKURI, P. & LUO, J. 2005. Activation of Stat3 sequence-specific DNA binding and transcription by p300/CREB-binding protein-mediated acetylation. *J Biol Chem,* 280**,** 11528-34.

WATT, M. J., STEINBERG, G. R., CHEN, Z.-P., KEMP, B. E. & FEBBRAIO, M. A. 2006. Fatty acids stimulate AMP-activated protein kinase and enhance fatty acid oxidation in L6 myotubes. *The Journal of Physiology,* 574**,** 139-147.

WEERASEKARA, V. K., PANEK, D. J., BROADBENT, D. G., MORTENSON, J. B., MATHIS, A. D., LOGAN, G. N., PRINCE, J. T., THOMSON, D. M., THOMPSON, J. W. & ANDERSEN, J. L. 2014. Metabolic-stress-induced rearrangement of the 14-3-3zeta interactome promotes autophagy via a ULK1- and AMPK-regulated 14-3-3zeta interaction with phosphorylated Atg9. *Mol Cell Biol,* 34**,** 4379-88.

WEGNER, N., LUNDBERG, K., KINLOCH, A., FISHER, B., MALMSTROM, V., FELDMANN, M. & VENABLES, P. J. 2010. Autoimmunity to specific citrullinated proteins gives the first clues to the etiology of rheumatoid arthritis. *Immunol Rev,* 233**,** 34-54.

WEICHHART, T., COSTANTINO, G., POGLITSCH, M., ROSNER, M., ZEYDA, M., STUHLMEIER, K. M., KOLBE, T., STULNIG, T. M., HÖRL, W. H., HENGSTSCHLÄGER, M., MÜLLER, M. & SÄEMANN, M. D. 2008. The TSC-mTOR Signaling Pathway Regulates the Innate Inflammatory Response. *Immunity,* 29**,** 565-577.

WHITEHEAD, K. A., DAHLMAN, J. E., LANGER, R. S. & ANDERSON, D. G. 2011. Silencing or stimulation? siRNA delivery and the immune system. *Annu Rev Chem Biomol Eng,* 2**,** 77-96.

WITTERS, L. A. 2001. The blooming of the French lilac. *Journal of Clinical Investigation,* 108**,** 1105-1107.

WOODS, A., DICKERSON, K., HEATH, R., HONG, S.-P., MOMCILOVIC, M., JOHNSTONE, S. R., CARLSON, M. & CARLING, D. 2005. Ca2+/calmodulin-dependent protein kinase kinase-β acts upstream of AMP-activated protein kinase in mammalian cells. *Cell Metabolism,* 2**,** 21-33.

WOODS, A., JOHNSTONE, S. R., DICKERSON, K., LEIPER, F. C., FRYER, L. G. D., NEUMANN, D., SCHLATTNER, U., WALLIMANN, T., CARLSON, M. & CARLING, D. 2003. LKB1 Is the Upstream Kinase in the AMP-Activated Protein Kinase Cascade. *Current Biology,* 13**,** 2004-2008.

WOODS, A., MUNDAY, M. R., SCOTT, J., YANG, X., CARLSON, M. & CARLING, D. 1994. Yeast SNF1 is functionally related to mammalian AMP-activated protein kinase and regulates acetyl-CoA carboxylase in vivo. *Journal of Biological Chemistry,* 269**,** 19509-19515.

WU, T. R., HONG, Y. K., WANG, X.-D., LING, M. Y., DRAGOI, A. M., CHUNG, A. S., CAMPBELL, A. G., HAN, Z.-Y., FENG, G.-S. & CHIN, Y. E. 2002. SHP-2 Is a Dual-specificity Phosphatase Involved in Stat1 Dephosphorylation at Both Tyrosine and Serine Residues in Nuclei. *Journal of Biological Chemistry,* 277**,** 47572-47580.

XIAO, B., HEATH, R., SAIU, P., LEIPER, F. C., LEONE, P., JING, C., WALKER, P. A., HAIRE, L., ECCLESTON, J. F., DAVIS, C. T., MARTIN, S. R., CARLING, D. & GAMBLIN, S. J. 2007. Structural basis for AMP binding to mammalian AMP-activated protein kinase. *Nature,* 449**,** 496-500.

XIAO, B., SANDERS, M. J., UNDERWOOD, E., HEATH, R., MAYER, F. V., CARMENA, D., JING, C., WALKER, P. A., ECCLESTON, J. F., HAIRE, L. F., SAIU, P., HOWELL, S. A., AASLAND, R., MARTIN, S. R., CARLING, D. & GAMBLIN, S. J. 2011. Structure of mammalian AMPK and its regulation by ADP. *Nature,* 472**,** 230-233.

XU, D. & QU, C. K. 2008. Protein tyrosine phosphatases in the JAK/STAT pathway. *Front Biosci,* 13**,** 4925-32.

YAFFE, M. B. 2002. How do 14-3-3 proteins work?-- Gatekeeper phosphorylation and the molecular anvil hypothesis. *FEBS Lett,* 513**,** 53-7.

YAFFE, M. B., RITTINGER, K., VOLINIA, S., CARON, P. R., AITKEN, A., LEFFERS, H., GAMBLIN, S. J., SMERDON, S. J. & CANTLEY, L. C. 1997. The structural basis for 14-3-3:phosphopeptide binding specificity. *Cell,* 91**,** 961-71.

YAHATA, Y., SHIRAKATA, Y., TOKUMARU, S., YAMASAKI, K., SAYAMA, K., HANAKAWA, Y., DETMAR, M. & HASHIMOTO, K. 2003. Nuclear Translocation of Phosphorylated STAT3 Is Essential for Vascular Endothelial Growth Factor-induced Human Dermal Microvascular Endothelial Cell Migration and Tube Formation. *Journal of Biological Chemistry,* 278**,** 40026-40031.

YAMAMOTO, T., SEKINE, Y., KASHIMA, K., KUBOTA, A., SATO, N., AOKI, N. & MATSUDA, T. 2002. The nuclear isoform of protein-tyrosine phosphatase TC-PTP regulates interleukin-6-mediated signaling pathway through STAT3 dephosphorylation. *Biochem Biophys Res Commun,* 297**,** 811-7.

YAMAOKA, K., SAHARINEN, P., PESU, M., HOLT, V. E. T., SILVENNOINEN, O. & O'SHEA, J. J. 2004. The Janus kinases (Jaks). *Genome Biology,* 5**,** 253-253.

YAN, H., KRISHNAN, K., LIM, J. T., CONTILLO, L. G. & KROLEWSKI, J. J. 1996. Molecular characterization of an alpha interferon receptor 1 subunit (IFNaR1) domain required for TYK2 binding and signal transduction. *Molecular and Cellular Biology,* 16**,** 2074-2082.

YANG, Z., KAHN, B. B., SHI, H. & XUE, B.-Z. 2010. Macrophage α1 AMP-activated Protein Kinase (α1AMPK) Antagonizes Fatty Acid-induced Inflammation through SIRT1. *The Journal of Biological Chemistry,* 285**,** 19051-19059.

YOU, M., YU, D.-H. & FENG, G.-S. 1999. Shp-2 Tyrosine Phosphatase Functions as a Negative Regulator of the Interferon-Stimulated Jak/STAT Pathway. *Molecular and Cellular Biology,* 19**,** 2416-2424.

YUAN, S., ZHANG, S., ZHUANG, Y., ZHANG, H., BAI, J. & HOU, Q. 2015. Interleukin-17 Stimulates STAT3-Mediated Endothelial Cell Activation for Neutrophil Recruitment. *Cellular Physiology and Biochemistry,* 36**,** 2340-2356.

ZHANG, D., SUN, M., SAMOLS, D. & KUSHNER, I. 1996. STAT3 Participates in Transcriptional Activation of the C-reactive Protein Gene by Interleukin-6. *Journal of Biological Chemistry,* 271**,** 9503-9509.

ZHANG, J., DING, L., HOLMFELDT, L., WU, G., HEATLEY, S. L., PAYNE-TURNER, D., EASTON, J., CHEN, X., WANG, J., RUSCH, M., LU, C., CHEN, S. C., WEI, L., COLLINS-UNDERWOOD, J. R., MA, J., ROBERTS, K. G., POUNDS, S. B., ULYANOV, A., BECKSFORT, J., GUPTA, P., HUETHER, R., KRIWACKI, R. W., PARKER, M., MCGOLDRICK, D. J., ZHAO, D., ALFORD, D., ESPY, S., BOBBA, K. C., SONG, G., PEI, D., CHENG, C., ROBERTS, S., BARBATO, M. I., CAMPANA, D., COUSTAN-SMITH, E., SHURTLEFF, S. A., RAIMONDI, S. C., KLEPPE, M., COOLS, J., SHIMANO, K. A., HERMISTON, M. L., DOULATOV, S., EPPERT, K., LAURENTI, E., NOTTA, F., DICK, J. E.,

BASSO, G., HUNGER, S. P., LOH, M. L., DEVIDAS, M., WOOD, B., WINTER, S., DUNSMORE, K. P., FULTON, R. S., FULTON, L. L., HONG, X., HARRIS, C. C., DOOLING, D. J., OCHOA, K., JOHNSON, K. J., OBENAUER, J. C., EVANS, W. E., PUI, C. H., NAEVE, C. W., LEY, T. J., MARDIS, E. R., WILSON, R. K., DOWNING, J. R. & MULLIGHAN, C. G. 2012. The genetic basis of early T-cell precursor acute lymphoblastic leukaemia. *Nature,* 481**,** 157-63.

ZHANG, J. G., METCALF, D., RAKAR, S., ASIMAKIS, M., GREENHALGH, C. J., WILLSON, T. A., STARR, R., NICHOLSON, S. E., CARTER, W., ALEXANDER, W. S., HILTON, D. J. & NICOLA, N. A. 2001. The SOCS box of suppressor of cytokine signaling-1 is important for inhibition of cytokine action in vivo. *Proc Natl Acad Sci U S A,* 98**,** 13261-5.

ZHANG, Y., LEE, T.-S., KOLB, E. M., SUN, K., LU, X., SLADEK, F. M., KASSAB, G. S., GARLAND, T. & SHYY, J. Y.-J. 2006. AMP-Activated Protein Kinase Is Involved in Endothelial NO Synthase Activation in Response to Shear Stress. *Arteriosclerosis, Thrombosis, and Vascular Biology,* 26**,** 1281-1287.

ZHANG, Y., QIU, J., WANG, X., ZHANG, Y. & XIA, M. 2011. AMP-Activated Protein Kinase Suppresses Endothelial Cell Inflammation Through Phosphorylation of Transcriptional Coactivator p300. *Arteriosclerosis, Thrombosis, and Vascular Biology,* 31**,** 2897-2908.

ZHAO, L., DONG, H., ZHANG, C. C., KINCH, L., OSAWA, M., IACOVINO, M., GRISHIN, N. V., KYBA, M. & HUANG, L. J. 2009. A JAK2 interdomain linker relays Epo receptor engagement signals to kinase activation. *J Biol Chem,* 284**,** 26988-98.

ZHAO, L., MA, Y., SEEMANN, J. & HUANG, L. J. 2010. A regulating role of the JAK2 FERM domain in hyperactivation of JAK2(V617F). *Biochem J,* 426**,** 91-8.

ZHONG, Z., WEN, Z. & DARNELL, J. E., JR. 1994. Stat3 and Stat4: members of the family of signal transducers and activators of transcription. *Proc Natl Acad Sci U S A,* 91**,** 4806-10.

ZHOU, G., MYERS, R., LI, Y., CHEN, Y., SHEN, X., FENYK-MELODY, J., WU, M., VENTRE, J., DOEBBER, T., FUJII, N., MUSI, N., HIRSHMAN, M. F., GOODYEAR, L. J. & MOLLER, D. E. 2001. Role of AMP-activated protein kinase in mechanism of metformin action. *Journal of Clinical Investigation,* 108**,** 1167-1174.

ZHUANG, S. 2013. Regulation of STAT signaling by acetylation. *Cell Signal,* 25**,** 1924-31.